The role of the HIF-PHD pathway in carotid body Type I cell proliferation

James W. Fielding, Linacre College, Oxford.



Supervisors: Dr Tammie Bishop and Professor Sir Peter Ratcliffe

A thesis submitted for examination to the degree of Doctor of Philosophy

Trinity term 201

The role of the HIF-PHD pathway in Carotid Body Type I Cell proliferation

James W. Fielding, Linacre College, Oxford.

A thesis submitted for examination to the degree of Doctor of Philosophy

Trinity term 2019

Abstract:

The carotid body is an important peripheral chemoreceptor in adult mammalian physiology. A small, paired neuroendocrine tissue located at the carotid bifurcation in the neck, the carotid body is a polymodal chemoreceptor which detects fluctuations of a number of substances in arterial blood, most notably oxygen. In response to low oxygen levels (hypoxia), the Type I cells of the carotid body release neurotransmitters onto afferent nerves to stimulate a rapid adaptive hyperventilatory response. In addition to this acute response, sustained hypoxia results in a substantial increase in the size of the carotid body, known as carotid body hyperplasia. It has been proposed that this proliferative response qualifies the carotid body as a stem cell niche, and characterizing the mechanisms behind this proliferation is of significance for understanding both the specialist function of the carotid body and the wider influence of hypoxia on cellular proliferation. Previous work in this field has implicated the hypoxia-inducible factor (HIF) transcription factors and the regulatory prolyl hydroxylase family (PHD) as master regulators of the responses to hypoxia across the organism, and in the carotid body specifically.

The work contained in this thesis seeks to characterize the proliferative and functional responses of the carotid body and related tissues to hypoxia. In particular, it employs

lineage tracing with fluorescent markers to characterize the specific cellular populations which contribute to carotid body hyperplasia, most notably identifying the Type I cells of the carotid body as a major proliferative population. Subsequently, this thesis uses genetic and pharmacological inactivation of the components of the HIF-PHD pathway to identify their role in carotid body function and pathology. This thesis demonstrates that sustained hypoxia drives a substantial proliferation of the Type I cell lineage in the carotid body, and that this proliferation is dependent on the expression of a single HIF transcription factor, HIF-2α. Type I cell specific genetic inactivation of HIF-2α was shown to greatly reduce hypoxia-induced proliferation across the entire organ. These results were replicated by systemic administration of a pharmacological HIF-2α antagonist, PT2385, highlighting the potential uses of these novel compounds for the treatment of carotid body pathologies such as carotid paraganglioma.

This thesis also establishes that pseudohypoxic stimulation of the carotid body Type I cells *via* genetic inactivation of the HIF prolyl hydroxylase PHD2 is sufficient to drive a multilineage expansion of the carotid body. The resulting pseudohypoxic carotid bodies were grossly enlarged, highly vascular and contained multiple ultrastructural abnormalities. An exciting implication of this is that this mouse line may represent the first mouse model for carotid paraganglioma, a subtype of paraganglioma derived from the carotid body. In addition to the effects on proliferation, ultrastructural changes were observed in the signalling vesicles of the Type I cells, suggesting a functional link between the HIF-PHD pathway and the acute signalling function of the organ. Taken together, these results demonstrate an essential role for the HIF-2α-PHD2 couple in the function of Type I cells in the carotid body.

Table of Contents

Abstract: i

Table of Contents iii

Acknowledgements: ix

Abbreviations: xi

Introduction: 1

Hypoxia and oxygen sensing 2

The carotid body: 6

Type I cells 8

Type II cells 11

The carotid body in acute oxygen sensing: 11

The carotid body in acclimatisation: 13

Carotid body hyperplasia 15

The carotid body – a stem cell niche? 16

The HIF-PHD pathway: 19

The HIF pathway in the carotid body: 24

The HIF pathway in carotid body paraganglioma 27

Conclusion: 29

Results Chapter 1: Hypoxia-induced proliferation in neural stem cell niches 31

Introduction: 31

Results:.....35

Characterisation of two lineage tracer lines in neural stem cell populations in the central nervous system.....35

The effect of chronic hypoxia on lineage labelled populations in the subventricular zone. 41

The effect of chronic hypoxia on proliferation in lineage labelled populations in the subventricular zone. 44

The effect of PHD2 inactivation on lineage labelled populations in the subventricular zone. 46

Discussion:.....49

Results Chapter 2: Hypoxia induced proliferation in the carotid body: Type I and Type II cells.....53

Introduction:.....53

Characterisation of Type I and Type II cell specific lineage tracers in the carotid body.55

The effect of chronic hypoxia on lineage labelled carotid body Type I and Type II cells. 59

The effect of chronic hypoxia on proliferation in lineage labelled carotid body cells. ...62

The effect of chronic hypoxia on carotid body ultrastructure.....65

The effect of chronic hypoxia on carotid body gene expression. 68

Characterisation of the THCreER lineage tracer line in other tissues. 72

Discussion:.....74

Results Chapter 3: Genetic manipulation of HIF-2α in carotid body Type I cells.....78

Introduction:.....78

Results:.....80

Expression and inactivation of *Hif-2α* mRNA in carotid body Type I and Type II cells. 80

The effects of HIF-2α inactivation in carotid body Type I and Type II cells on carotid body morphology.....82

The effects of HIF-2α inactivation in carotid body Type I cells on carotid body vascularization and gene expression.....84

The effects of HIF-2α inactivation in carotid body Type I and Type II cells upon hypoxia-induced erythropoiesis.....88

The effects of HIF-2α inactivation in carotid body Type I and Type II cells upon ventilatory acclimatisation in response to chronic hypoxia.....88

The effects of HIF-2α inactivation on carotid body Type I cell ultrastructure.....94

Discussion:.....97

Results Chapter 4: Pharmacological manipulation of HIF-2a in the carotid body.....104

Introduction:.....104

Results:.....106

Experimental design: Chronic hypoxia exposure with PT2385 treatment. 106

The effect of a pharmacological HIF-2α inhibitor upon carotid body gene expression. 108

The effect of varying dosage of pharmacological HIF-2α inhibitors upon carotid body morphology and gene expression.....109

The effect of varying dosage of pharmacological HIF-2α inhibitors upon carotid body morphology and gene expression.....112

The effect of a pharmacological HIF-2α inhibitor upon hypoxia-induced polycythaemia. 114

The effect of a pharmacological HIF-2α inhibitor upon ventilatory acclimatisation to hypoxia.....115

The effect of a pharmacological HIF-2α inhibitor upon carotid body Type I cell ultrastructure. 121

Discussion:.....123

Results Chapter 5: The Effect of PHD2 inactivation in the carotid body Type I cells 128

Introduction:.....128

Results:.....129

The effect of constitutive 'pseudohypoxic' PHD2 inactivation in Type I cells. 129

The effect of constitutive 'pseudohypoxic' PHD2 inactivation in Type I cells upon carotid body gene expression.....133

The role of HIF-1α and HIF-2α in 'pseudohypoxia'-driven carotid body hyperplasia. 136

The effect of 'pseudohypoxic' PHD2 inactivation in Type I cells upon Type I cell ultrastructure. 142

The effect of inducible 'pseudohypoxic' PHD2 inactivation in Type I cells 144

Discussion:.....148

Chapter 6: Thesis Discussion 153

What is the nature of carotid body proliferation? 154

A reassessment of the Stem Cell theory of the carotid body 155
Carotid body Type I cell proliferation: an autonomous HIF-2α dependent stem cell? .157
The paracrine nature of carotid body Type I cell-dependent proliferation 159
Carotid body Type I cell proliferation: developmental vs adult effects of HIF pathway manipulation.....164
What is the role of HIF-2α in acute oxygen sensing?.....167
What are the implications of small molecule inhibitors of HIF-2α for the carotid body? 171
What is the effect of HIF-PHD pathway manipulation on other tissues?.....174
The adrenal medulla.....175
The lung.....178
Summary and Conclusions 180
Chapter 7: Methods 181
Ethical approval 181
Animals.....181
Genotyping.....182
Drug administration 185
Chronic hypoxic exposure of mice 186
Plethysmography 186
Blood measurements.....187
Tissue Preparation.....187
Immunohistochemistry 188

In situ hybridisation 192

Microscopy 193

Electron microscopy 194

RT-PCR 195

Statistical methods 195

References: 196

Acknowledgements:

My life in Oxford, and the work presented in this thesis, would not have been possible without the support of many wonderful people who are too numerous to name. I would like to thank you all for your generosity and support. Nevertheless, I am particularly indebted to several specific individuals, who I would like to thank here.

First, I would like to thank my supervisors, Dr Tammie Bishop and Professor Sir Peter Ratcliffe, for their help and guidance throughout my DPhil. Tammie has been a fantastic supervisor and role model. I have never met someone with a more phenomenal work ethic or dedication to research, and she has always been on hand to provide advice and encouragement. Peter is a remarkable scientist, with a knack for identifying the core elements of a problem that I hope to emulate in my future career. Thank you both.

I would like to extend my thanks to all past and current members of the Ratcliffe-Pugh Group who have taught and supported me for the last four years. In particular, I would like to thank Dr Xiaotong Cheng, Dr Emma Hodson, Luise Eckardt and Maria Prange-Barczynska. All four of these colleagues have not only contributed significantly to the program of work as described in this thesis, but have been good scientists, gracious colleagues, and great friends. Xiaotong has been an unflagging source of good cheer and hard work in the lab, and has put up with more than her share of requests from me. Emma was the senior DPhil student as I began my studies, and much of what I know is directly to her credit. Maria and Luise have been excellent friends and co-workers, and I thank them for many lovely memories.

In addition, I could not have completed my work without the contributions of many skilled

collaborators. These include Professor Francis Szele, whose expertise in the SVZ was invaluable; Dr Keith Buckler, who contributed closely to the academic content and direction of my project; Professor David Ferguson, Dr Lucy Collinson and Alana Burrell, who worked closely with me and provided fantastic technical and academic insights into the field of electron microscopy; and Dr Indrika Ratnayaka, who provided superb technical and moral support in the field of histology.

My thanks also go to the many students who have worked with me throughout my DPhil, for their assistance and good cheer: Isobel Argles, Sharon Christensen, Joanna Lima, Felipe Santella, Ronan Lyr, Dr Matthew Maton-Howarth, Jesus Ortiz, Tamsin Brown and Philomena Lip. I would also like to thank the staff at the Functional Genomics Facility, particularly Douglas Dos Santos Passos.

I would like to express my appreciation and gratitude for the funding I have received from Ludwig Cancer Research, which has enabled me to conduct my studies and perform my research at the highest level.

Finally, I wish to thank my parents, Professor Susan Llewelyn and Dr Guy Fielding, as well as my sister, Dr Josephine Fielding, for their tireless support, unyielding sympathy and ever ready supplies of coffee!

Thank you all.

Abbreviations:

AM, adrenal medulla;

BrdU, 5-bromo-2'-deoxyuridine;

CB, carotid body;

CH, chronic hypoxia;

COPD, chronic obstructive pulmonary disease;

CNS, central nervous system;

ccRCC, clear cell renal cell carcinoma;

DG, dentate gyrus;

DCV, dense core vesicle;

EM, electron microscopy;

EPAS-1, endothelial PAS protein 1;

EPO, erythropoietin;

FIH, factor inhibiting HIF;

GFAP, glial fibrillary acidic protein;

HIF, hypoxia-inducible factor;

HRE, hypoxia-response element;

HVR, hypoxic ventilatory response;

PAS, per-arnt-sim domain;

PCC, phaeochromocytoma;

PGL, paraganglioma;

PHD, prolyl hydroxylase domain-containing protein;

PNS, peripheral nervous system;

NSC, neural stem cell;

NSPCs, neural stem and progenitor cells;

ROS, reactive oxygen species;

SCG, superior cervical ganglion;

SGZ, subgranular zone;

TEM, transmission electron microscope;

TH, tyrosine hydroxylase;

SVZ, subventricular zone;

VAH, ventilatory acclimatisation to hypoxia;

VEGFA, vascular endothelial growth factor A;

VHL, von Hippel-Lindau.

Introduction:

This thesis focuses on the carotid body, a peripheral chemoreceptor, and the central role of the oxygen sensitive Type I cells of this organ. Since the early-20th century, the carotid body has been understood to play a vital role in maintaining mammalian oxygen homeostasis. In response to acute arterial hypoxia, the oxygen sensitive Type I cells of the carotid body depolarize, releasing neurotransmitters which stimulate an adaptive hyperventilatory response. In response to sustained hypoxia, the carotid body undergoes an unusual proliferative hyperplasia, expanding in size, vascularity and in the number of Type I cells. It has been proposed that this carotid body hyperplasia is mediated by the proliferation and differentiation of a stem cell-like subpopulation of a second carotid body cell type, the astrocytic Type II cells. If so, the carotid body represents the first and only example of a proliferating peripheral nervous system (PNS) neural stem cell niche, and may be of clinical and therapeutic use as a source of induced pluripotent stem cells. Mechanistically, previous work by our group has shown that both the ventilatory and proliferative responses of the carotid body to hypoxia are dependent on the expression of hypoxia inducible factor-2 alpha (HIF-2α). However, the cell type(s) in which HIF-2α is acting remain unknown, and the underlying mechanism of carotid body proliferation is likely a complex and multicellular process.

To address this, this thesis will use inducible and constitutive Cre constructs under the control of cell-specific promoters to target the individual cell types of the carotid body parenchyma: the Type I and Type II cells. First, this thesis will combine these cell-specific promoters with fluorescent lineage reporters, allowing this study to characterize the proliferative response to chronic hypoxia and to identify the contributions of each cell type

to carotid body hyperplasia. Secondly, this thesis will use these promoters to inactivate key elements of the HIF-pathway in each carotid body cell population and assess the effect on normal and hypoxic carotid body physiology. In particular, due to their central role in the acute oxygen sensitive response of the niche, this thesis will focus on the oxygen sensitive Type I cells of the carotid body and the function of HIF-2α and the regulatory prolyl hydroxylase PHD2 in these cells. This introduction will cover topics important to the understanding of this work: the nature of hypoxia, the structure and physiology of the carotid body, and the function of the regulatory HIF family of transcription factors.

Hypoxia and oxygen sensing

This thesis stands in the context of more than a century of work demonstrating the fundamental importance of oxygen sensing in mammalian species. The cornerstone of this work began in 1874, when a French physiologist, Paul Bert, published a seminal study demonstrating that the deleterious effects of altitude were due to low oxygen availability in the air (Bert, 1874). Today, we understand that this requirement for oxygen is due to its role as the final electron acceptor in mitochondrial respiration in all metazoan species (Rich, 2003). Since Bert's seminal work, research by physiologists and others has demonstrated that aerobic organisms are capable of sensing and responding to low oxygen levels, enacting adaptive responses which match oxygen demand to supply and promote survival. The study of these homeostatic mechanisms has led to considerable advances in our understanding of altitude physiology and the underlying molecular pathways involved.

Oxygen levels vary, both in the environment as a consequence of altitude and in the organism as a consequence of physiology or pathology, and low physiological oxygen availability is referred to as hypoxia. Hypoxia may refer to low levels of oxygen in an

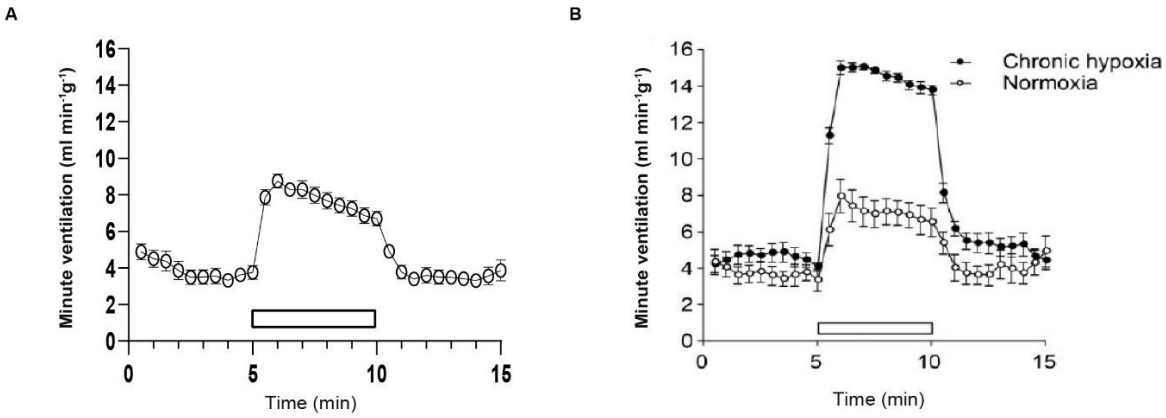
absolute sense (physiological hypoxia) or may refer to oxygen levels being low relative to the level required for optimal physiological function (patho-physiological hypoxia) (Bishop & Ratcliffe, 2014). Optimal physiological oxygen levels have no exact correlate in terms of O_2 concentration or oxygen tension, assessed as partial pressure (PO_2). For example, physiological oxygen tensions in human tissues can range from 100-120 mmHg (~14-15% O_2) in the lung alveoli to 40-55 mmHg (~5-7% O_2) in the liver and can drop lower than 20 mmHg (~2.5% O_2) in the renal medulla (Dirken & Heemstra, 1948; P. Leichtweiss *et al.*, 1969; Brezis & Rosen, 1995; Leary *et al.*, 2002; Carreau *et al.*, 2011). In the blood, physiological oxygen tensions range from 75-100 mmHg (~10-14% O_2) in the arterial blood to 40 mmHg (~5% O_2) in venous blood (Malatesha *et al.*, 2007). If oxygen tension falls below too far below these physiologically appropriate levels in tissues, patho-physiological hypoxia may occur.

Patho-physiological hypoxia may arise from pathological conditions, with hypoxia being a frequent symptom and component of many disease states such as chronic lung disease, sleep apnoea, myocardial infarction and cancer (Lopez-Barneo *et al.*, 2001). However, changes in altitude also significantly affect available oxygen levels: at sea level the barometric pressure of O_2 is 760 mmHg but this steadily declines with altitude, reaching levels as low as 253 mmHg at the summit of Mt. Everest (Grocott *et al.*, 2009). In these conditions, the oxygen available for alveolar diffusion is markedly reduced. This will in turn reduce the oxygenation of blood and the delivery of oxygen to individual organs, in particular causing disruption to the function of organs with high oxygen requirements, such as the brain. The impaired function of these organs results in many of the features of altitude sickness: fatigue, nausea, confusion and dizziness (Hackett & Roach, 2001). In order to cope with these deleterious effects of hypoxia, metazoan organisms sense oxygen

and enact a variety of responses to hypoxia.

These responses to hypoxia can be acute (occurring over a time course of seconds to minutes) or chronic (occurring over hours to days). In mammals, acute responses to hypoxia include hyperventilation, pulmonary vasoconstriction, systemic vasodilation and sympathetic activation (Weir *et al.*, 2005). In particular, acute hypoxic exposure results in an immediate increase in ventilatory activity over seconds to minutes (hyperventilation) at the onset of hypoxia, known as known as the hypoxic ventilatory response (HVR) (Introduction Figure 1A) (Powell *et al.*, 1998; Lopez-Barneo *et al.*, 2008). This HVR is matched by a decrease in ventilatory activity after a return to normoxic conditions (Powell *et al.*, 1998). Other ventilatory responses include hypoxic ventilatory decline, the "roll off" /decrease in ventilation relative to the acute response which occurs after the initial minutes of hypoxic exposure (Introduction Figure 1A) (Powell *et al.*, 1998).

In humans, the chronic responses to altitude were characterized by the work of Haldane, Douglas and Fitzgerald in a rigorous series of experiments performed at sea level and altitude during an Anglo-American expedition to Pike's Peak (Douglas *et al.*, 1913; West, 2012). Haldane and Douglas demonstrated many of the canonical features of altitude sickness, occurring upon rapid ascent to a height of 4300 meters, including fatigue, headaches, loss of appetite, nausea, hyperventilation, cyanosis and periodic breathing, and showed that many of these symptoms disappeared or were ameliorated after 2-3 days of residence at high altitude (Douglas *et al.*, 1913; Haldane *et al.*, 1919). Crucially, this expedition described two long term responses to chronic hypoxia which occurred over a period of 5 weeks of residence at high altitude.



Introduction Figure 1. The hypoxic ventilatory response (HVR) and ventilatory acclimatisation to hypoxia (VAH).

A) The hypoxic ventilatory response (HVR). Minute ventilation of wild-type mice before, during (white bar), and after a 5-minute exposure to 10% oxygen /3% carbon dioxide /balance nitrogen. Minute ventilation is calculated from the respiratory rate and tidal volume of mice, measured *via* plethysmography. Hypoxic ventilatory decline is visible in the slight reduction in minute ventilation during the 5-minute exposure.

B) Mice acclimatised to 7 days of 10% oxygen display a significantly enhanced ventilatory response to acute hypoxic exposure (black line), indicating that ventilatory acclimatisation to hypoxia (VAH) has occurred. 3% carbon dioxide was included in the ventilatory stimulus to buffer against respiratory alkalosis and thus prevent ventilatory depression. Values shown are mean ± SEM. (data reproduced from (Bishop *et al.*, 2013).

First, Haldane and Douglas described an increase in the oxygen capacity of the blood, which was matched by an increased concentration of haemoglobin. Today, the cardiovascular responses to chronic hypoxia are understood to include the formation of new blood vessels in hypoxic tissue regions (angiogenesis) and increased red blood cell production (erythropoiesis) (Hultgren & Grover, 1968). However, prolonged hypoxic exposure can result in polycythaemia, tachycardia, hypertension and cardiac disease, placing a potential disease burden on individuals residing at high altitude (Hultgren & Grover, 1968; Naeije, 2010).

A second set of chronic responses was concerned with the ventilatory responses to hypoxia. Haldane and Douglas demonstrated that acclimatised individuals experience a steady increase in resting ventilation, now referred to as ventilatory acclimatisation to hypoxia (VAH) (Douglas *et al.*, 1913; Barer *et al.*, 1976; Sato *et al.*, 1992; Powell *et al.*, 2000a). In addition to this increase in resting ventilation at altitude, VAH also results in an increase in the magnitude of the hypoxic ventilatory response to acute hypoxia (Introduction Figure 1B), and this adaptation persists for a period of days to weeks after return to normoxic conditions (Powell *et al.*, 1998; Bishop *et al.*, 2013). Although Haldane and others initially attributed these ventilatory changes to changes in $PaCO_2$ modulating central nervous system control of ventilation (Powell *et al.*, 2000a; West, 2012), subsequent work has demonstrated that many aspects of the ventilatory response to hypoxia are instead mediated by a peripheral chemoreceptor: the carotid body.

The carotid body:

The carotid body (CB) is a small paired neuroendocrine organ located either side of the neck at the carotid bifurcation. The earliest predictions of a chemoreceptive function for the carotid body were made by Fernando de Castro, who noted the highly irrigated nature of the carotid body and its afferent innervation by the carotid sinus nerve, a branch of the glossopharyngeal /IX^{th} Cranial nerve (De Castro, 1926, 2009). Based on these purely anatomical and histological observations, De Castro astutely posited that the carotid body has a chemoreceptive function and was “tasting the blood.” In support of this, the carotid body has been shown to be a highly vascular and irrigated tissue with a close association to the carotid artery, receiving a greater blood flow per unit weight than any other tissue in the body (~ 2000 $ml.min.^{-1}.g^{-1}$) (De Burgh Daly *et al.*, 1954; De Castro & Rubio, 1968).

De Castro's hypothesis was vindicated across the subsequent half century, as pioneers in the electrophysiological and histological fields demonstrated the acute oxygen sensitive functions of the tissue (De Castro, 2009). Notable amongst this work was the demonstration that isolated perfusion of vascularly isolated carotid bodies induces respiratory responses in dogs (Heymans & Heymans, 1927) and the demonstration that destruction of the carotid body eliminates the ventilatory response to hypoxia in both rabbits (Verna *et al.*, 1975) and cats (Nishi *et al.*, 1981; Monti-Bloch *et al.*, 1983). Subsequent work has demonstrated that, in response to hypoxia, oxygen sensitive Type I cells within the carotid body depolarise and release neurotransmitters, increasing action potential frequency at the carotid sinus nerve which in turn stimulates the hypoxic ventilatory response (HVR) (Euler *et al.*, 1940; Biscoe & Duchen, 1990b; Lopez-Barneo *et al.*, 2008). The intensity of this reflex ventilatory response follows a hyperbolic relationship between falling oxygen tensions and minute ventilation (Bisgard, 1995), which in turn correlates directly with the release of neurotransmitters from the carotid body (Montoro *et al.*, 1996) and subsequent carotid sinus nerve activity (Vidruk *et al.*, 2001). In addition to oxygen, the carotid body has also been demonstrated to respond to fluctuations in body temperature, pH, glucose, osmolarity, pCO_2 and blood catecholamine content (Eyzaguirre & Koyano, 1965; Gallego & Belmonte, 1979; Heeringa *et al.*, 1979; Alcayaga *et al.*, 1993; Garcia-Fernandez *et al.*, 2007b; Thompson *et al.*, 2016), suggesting that it may possess a broader function as a polymodal chemoreceptor (Kumar & Bin-Jaliah, 2007).

In development, the carotid body derives from the neural crest after the migration of neural crest precursors to the mesenchyme of the third branchial arch (Pearse *et al.*, 1973), and the carotid body therefore has parallels with other neural crest derived tissues such as the

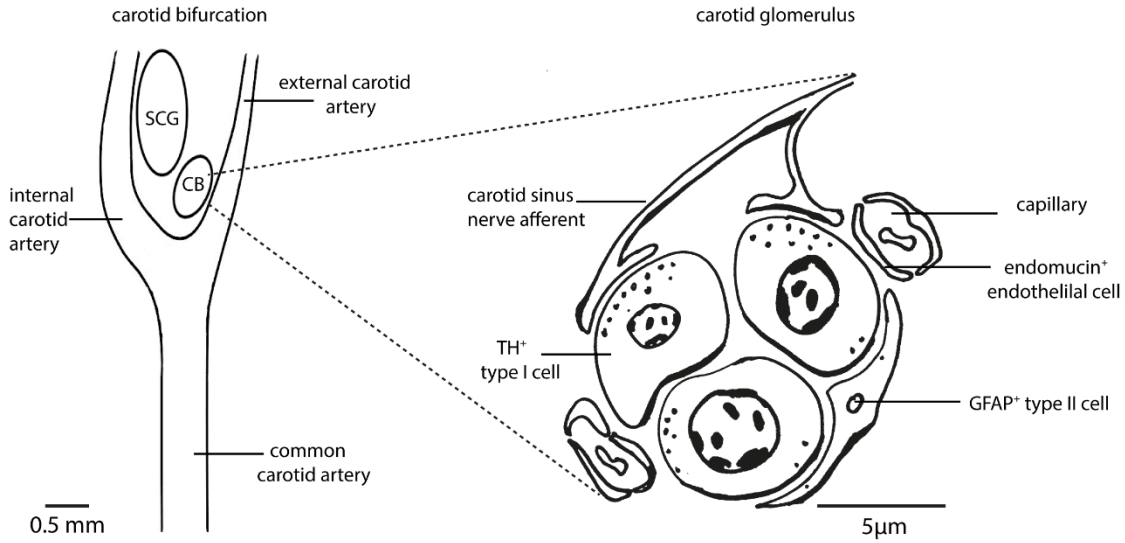
chromaffin cells of the adrenal medulla and the aortic bodies (Kumar & Prabhakar, 2012; Sobrino *et al.*, 2019). Structurally, the carotid body is a conglomerate organ composed of multiple cell types, including endothelial cells, Type I cells, known as glomus cells, and Type II cells, referred to as glial cells (Introduction Figure 2) (De Kock, 1951). The Type I cells of the CB are arranged into clusters or nests of 3-8 (commonly 4-5) cells known as glomeruli. Each glomerulus is enveloped by the cytoplasmic process of a single Type II cell, establishing a roughly 4:1 ratio of Type I to Type II cells in the carotid body (Biscoe, 1971). Each glomerulus is individually enervated by the carotid sinus nerve, making the glomeruli the functional unit of the carotid body (Seidl, 1975). The remaining mass of the carotid body is composed of small blood vessels, which occupy a consistent 5-7% of the total CB mass across multiple species (Verna, 1979; Kumar & Prabhakar, 2012). Histological and physiological analysis has defined distinct roles for the Type I and Type II cells of the carotid body:

Type I cells

The Type I glomus cells are considered to be the oxygen sensitive cells of the carotid body, and they have been shown to be exquisitely sensitive to hypoxia both in culture and in the intact carotid body (Biscoe & Duchen, 1990b; Buckler & Vaughan-Jones, 1994). These glomus cells, also known as chief cells, have a distinctive large, oval appearance and measure between 8 and 15 μm in rat carotid bodies (McDonald & Mitchell, 1975b). Ultrastructurally, these cells contain large nuclei and possess a characteristic complement of secretory vesicles which contain neurotransmitters and other signalling peptides (Ross, 1959; Blumcke *et al.*, 1967; McDonald & Mitchell, 1975a). These vesicles include small clear core vesicles and larger, dense core vesicles (DCVs) which contain densely packaged neuropeptides. These DCVs are reported to contain a number of substances, including

ATP, acetylcholine, dopamine, endothelin-1, VEGFA, serotonin, noradrenaline, enkephalin and neuropeptide Y (Chiocchio *et al.*, 1966; Oomori *et al.*, 1994; Vicario *et al.*, 2000; Kameda, 2005).

Upon exposure to acute hypoxia, Type I cells depolarise and mount an exocytotic response, releasing neurotransmitters which stimulate the carotid sinus nerve (Kumar & Prabhakar, 2012). The release of neurotransmitters from carotid body Type I cells has been shown to have a hyperbolic relationship with oxygen levels (Montoro *et al.*, 1996), and acetylcholine and ATP released from these cells are believed to be the main excitatory agents responsible for the afferent response to acute hypoxia (Zhang *et al.*, 2000; Kumar & Prabhakar, 2012), with a simultaneous release of dopamine possibly playing a modulatory or even inhibitory role depending on the species examined (Czyzyk-Krzeska *et al.*, 1992b; Kumar & Prabhakar, 2012). Carotid body Type I cells can be identified immunohistochemically by their high levels of tyrosine hydroxylase (TH), a rate limiting enzyme in the catecholamine synthesis pathway which is also induced by chronic hypoxic exposure (Introduction Figure 2) (Czyzyk-Krzeska *et al.*, 1992a; Czyzyk-Krzeska *et al.*, 1994).



Introduction Figure 2. Carotid body structure.

Illustrated diagram of carotid body (CB) structure and cell types. The carotid body is a paired organ, located bilaterally in the carotid bifurcation adjacent to the larger superior cervical ganglion (SCG). Within the carotid body the oxygen sensitive TH^+ Type I cells are arranged into clusters (glomeruli) innervated by the carotid sinus nerve. Type I cells are closely associated with astrocytic $GFAP^+$ Type II cells. The carotid body is highly vascular, with a network of capillaries and $endomucin^+$ endothelial cells.
(figure modified from work by Dr Emma Hodson). Scale bars are included for approximate size comparisons (in the mouse).

Type II cells

Fewer in number than the Type I cells, the glial-like astrocytic Type II cells of the carotid body have a characteristic flattened, sickle-like appearance (Introduction Figure 2) (De Kock, 1951; De Kock & Dunn, 1966). These cells can be identified immunohistochemically through the presence of the astrocytic marker glial fibrillary acidic protein (GFAP) (Nurse & Fearon, 2002; Kameda, 2005), as well as the markers vimentin and S-100 (Kondo *et al.*, 1982; Kameda, 1996). Type II cells lack the secretory vesicle content of the Type I cells and do not appear to contain sodium or calcium channels or to generate action potentials when depolarized (Duchen *et al.*, 1988; Xu *et al.*, 2003). As such, Type II cells have historically been assigned a structural, supportive function, although it has been proposed that they may play a role in maintaining ionic balance within the glomeruli, as intracellular levels of Ca^{2+}, K^+ and pH become elevated in Type I cells cultured in the absence of Type II cells (Pang & Eyzaguirre, 1993; Zhang *et al.*, 1995; Jiang & Eyzaguirre, 2004).

The carotid body in acute oxygen sensing:

In response to acute hypoxia, the Type I cells of the carotid body mount a rapid exocytotic response, releasing neurotransmitters such as ATP and acetylcholine which stimulate the carotid sinus nerve and thus respiration (Euler *et al.*, 1940; Biscoe & Duchen, 1990b; Weir *et al.*, 2005). This response requires the presence of an oxygen sensor capable of rapidly transducing oxygen levels into a neurosecretory response. Studies of the Type I cells have suggested that the initial membrane depolarisation is due to the inhibition of a K^+ current (Buckler, 2015). The inhibition of this oxygen sensitive K^+ current results in depolarisation and an influx of Ca^{2+} through voltage-gated Ca^{2+} channels, which in turn drives neurosecretion (Buckler, 1997; Weir *et al.*, 2005). This K^+ current has been identified as

being mediated by the TASK subfamily of K^+ channels, including the TASK-1 and TASK-3 channels (Buckler *et al.*, 2000; Buckler, 2015). The "Membrane Hypothesis" of oxygen sensing proposes that components of the Type I cell membrane, particularly the TASK channels, provide oxygen sensitivity. Competing hypotheses include the "Mitochondrial Theory" of oxygen sensing, which proposes that Type I cell mitochondria possess a unique sensitivity to hypoxia (Wyatt & Buckler, 2004; Buckler & Turner, 2013; Fernandez-Aguera *et al.*, 2015; Waypa *et al.*, 2016). In support of this, almost all mitochondrial inhibitors have been shown to excite Type I cells and thus induce a ventilatory response (Krylov & Anichkov, 1968; Mulligan *et al.*, 1981; Wyatt & Buckler, 2004; Holmes *et al.*, 2016; Holmes *et al.*, 2018). Current evidence strongly supports the mitochondrial theory, but the exact underlying mechanisms remain unclear and multiple competing theories have been proposed (Holmes *et al.*, 2018). Hypoxic inhibition of mitochondria is proposed to result in increased reactive oxygen species (ROS) production (Fernandez-Aguera *et al.*, 2015), reduced ATP synthesis (Buckler & Turner, 2013), an accumulation of lactate, which in turn leads to the activation of an Olfr78 receptor (Chang *et al.*, 2015) and the stimulation of AMP-activated protein kinase (Wyatt *et al.*, 2007; Mahmoud *et al.*, 2016), each of which may contribute to the overall sensitivity of the Type I cells to hypoxia. However, other groups have failed to replicate the results and predictions of the Olfr78 theory using $Olfr78^{-/-}$ mice (Chang *et al.*, 2018; Torres-Torrelo *et al.*, 2018). Given the experimental support for multiple theories of carotid body oxygen sensing, it is possible that multiple, redundant methods of oxygen sensing operate in the carotid body.

The oxygen sensitive properties of these cells may not be a unique feature of the carotid body. It has been shown that some species (although not humans) are capable of recovering sensitivity to hypoxia after carotid body denervation, and this has been

attributed to a slow increase of the sensitivity of the aortic bodies to blood gas concentration in cats, goats and pigs (Kumar & Prabhakar, 2012). Another neural crest-derived cellular population, the chromaffin cells of the adrenal medulla, has been shown to be oxygen sensitive during development (Rychkov *et al.*, 1998). This sensitivity is reduced in adulthood, although a small proportion of cells (~25%) continue to secrete in response to hypoxia (Garcia-Fernandez *et al.*, 2007a) However, when the oxygen sensitive Type I cell TASK K^+ channel was expressed in the adult chromaffin cell population, the TASK channels lost oxygen sensitivity, suggesting a requirement for other CB-intrinsic factors to maintain oxygen sensitivity (Johnson *et al.*, 2004). A third population, the pulmonary neuroendocrine cells (PNECs) of the lung, has also been demonstrated to depolarise and secrete in response to acute hypoxia (Livermore *et al.*, 2015). Other potentially O_2 sensitive populations include the cells of the pulmonary vasculature and the ductus arteriosus (Weir *et al.*, 2005).

The carotid body in acclimatisation:

In addition to its prominent role in mediating the acute ventilatory response to hypoxia, the carotid body is also involved in the acute acclimatization to sustained (chronic) hypoxia. In particular, the carotid body mediates ventilatory acclimatization to hypoxia (VAH). VAH is defined as a time dependent increase in the ventilation which results from prolonged chronic hypoxic exposures of hours to days to weeks (Bisgard, 1995), and can also be defined as the increase in the hypoxic ventilatory response (HVR) to acute hypoxic exposure in acclimatised animals (Vizek *et al.*, 1987; Powell *et al.*, 1998). This increase in ventilation is accompanied by an increase in arterial oxygen tension and a fall in arterial PCO_2 (Bisgard, 2000). The time course over which VAH occurs varies from species to species, with different onset and completion times. For example, VAH is evident within 8

hours in humans (Tansley *et al.*, 1997) but takes 10 or more days to occur fully (Bisgard, 1995, 2000), whereas VAH may completely occur within 6 hours in in goats (Bisgard, 1995, 2000). VAH acts to directly increase the intake of oxygen, ensuring adequate oxygen supply. VAH can be measured experimentally as the difference in HVR between acclimatised and non-acclimatised animals, as in (Bishop *et al.*, 2013; Hodson *et al.*, 2016).

Although initially thought to be mediated by the changes in central chemoreceptor function, a considerable body of evidence has emerged demonstrating that VAH is mediated by the carotid body (Powell *et al.*, 1998). VAH has been shown to be blocked in carotid body denervated animals exposed to systemic hypoxia (Bisgard, 2000) and can be induced in isolated goat carotid bodies perfused with hypoxia for 4-6 h (Bisgard, 1995). Moreover, VAH is also blocked in animals exposed to systemic hypoxia if the carotids are isolated and perfused with normoxic air (Nielsen *et al.*, 1988). The carotid body has also been shown to progressively increase afferent discharge during chronic hypoxia (Nielsen *et al.*, 1988). A simple explanation of VAH in the carotid body is that prolonged hypoxic exposure leads to hypersensitivity of the carotid body to acute hypoxia, and the resulting increase in afferent nerve activity leads to an increased stimulation of respiration (Bisgard, 1995, 2000). This increase in hypoxic sensitivity may be accomplished at multiple levels in the oxygen sensitive machinery of the carotid body, from changes in gene expression to proliferative production of additional oxygen sensitive Type I cells (Bisgard, 2000). For example, chronic hypoxic exposure has been demonstrated to induce Ca^{2+} channel expression and reduce the expression and sensitivity of the carotid body TASK-1 K^+ channel discussed above as a potential mediator of the oxygen sensitive response (Del Toro *et al.*, 2003; Caceres *et al.*, 2007), whilst decreased dopaminergic inhibition at D_2

receptors at the carotid sinus has been reported to largely account for VAH in cats (Tatsumi *et al.*, 1991). Finally, some authors have suggested that VAH may be linked to the proliferative expansion of the carotid body in response to sustained hypoxia, referred to as carotid body hyperplasia.

Carotid body hyperplasia

The carotid body responds to chronic hypoxia by undergoing a proliferative hyperplasia in the days and weeks after the onset of hypoxic exposure. This 2-3 fold increase in carotid body size is attributed to an increase in the number and size of the carotid body Type I cells as well as an associated neovascularisation of the carotid body (Edwards *et al.*, 1971; Arias-Stella & Valcarcel, 1973; Laidler & Kay, 1975; Arias-Stella & Valcarcel, 1976; Kay & Laidler, 1977). Incorporation of nucleoside analogues such as BrdU as well as immunohistochemical and ultrastructural analysis has demonstrated that the proliferation of Type I cells is a component of this response (Paciga *et al.*, 1999; Wang & Bisgard, 2002; Wang *et al.*, 2008; Platero-Luengo *et al.*, 2014). The expression of vascular endothelial growth factor (VEGFA) and platelet-derived endothelial cell growth factor (PDECGF) increases in the carotid body with chronic hypoxic exposure, and these factors may act to drive part of this proliferative response (Jyung *et al.*, 2000; Chen *et al.*, 2003). Other authors have highlighted the potential of other signalling molecules such as endothelin-1 (Paciga *et al.*, 1999; Platero-Luengo *et al.*, 2014). Carotid body hyperplasia has been shown to be reversible upon return to normoxic conditions, with a reduction in vasculature visible within two weeks of a return to normoxia, and a regression in overall size occurring over two to eight weeks (Kusakabe *et al.*, 2004). This carotid body hyperplasia may be linked to the increased risk of carotid body tumours (carotid paraganglioma /chemodectoma) at altitude (Saldana *et al.*, 1973; Astrom *et al.*, 2003),

which in turn may mean that understanding the origin and underlying mechanisms of this hyperplasia may be important for the treatment and prevention of this condition. Surgical resection of carotid paraganglioma /chemodectoma carries considerable risk, but current alternate treatment options (like drugs) are limited. This thesis will investigate this hyperplastic response and attempt to identify the cellular population from which this expansion in cell numbers originates.

The carotid body – a stem cell niche?

The carotid body's proliferative response to hypoxia is highly unusual for a mature tissue, marking the carotid body as a uniquely plastic component of the peripheral nervous system. It has been recently proposed that the carotid body qualifies as a stem cell niche, with this hypoxia-induced increase in Type I cells resulting from the proliferation of a stem cell-like subpopulation of the astrocytic Type II cell population (Kokovay & Temple, 2007; Pardal *et al.*, 2007). This Stem Cell theory of the carotid body proposes that, in response to chronic hypoxia, a subpopulation of $GFAP^+$ pluripotent Type II cells proliferate to give rise to a rapidly proliferating intermediate population of $nestin^+$ precursors, which in turn differentiate to give rise to the expanded population of TH^+ Type I cells (Pardal *et al.*, 2007). In support of this theory, Pardal *et al*., and others have demonstrated that $GFAP^+$ astrocytes can give rise to multiple other carotid body cell types in *in vitro* neurosphere stem cell culture, and that lineage labelled Type II cells proliferate and give rise to TH^+ cells in response to sustained hypoxia *in vivo* (Pardal *et al.*, 2007; Annese *et al.*, 2017). If this Stem Cell theory is correct, this study represents the first demonstration of pluripotent neural stem cell activity in a peripheral stem cell niche, and the carotid body can be viewed as the only neural stem cell niche in the peripheral nervous system (Kokovay & Temple, 2007; Kumar & Prabhakar, 2012). A stem cell function of the

carotid body may have useful implications for the understanding of carotid body related diseases, and the culture and transplantation of carotid body stem cells has been highlighted as a potential treatment for Parkinson's disease due to the highly dopaminergic nature of the mature carotid body Type I cells (Espejo *et al.*, 1998; Arjona *et al.*, 2003; Villadiego *et al.*, 2005).

The majority of evidence advanced in support of the Stem Cell theory of the carotid body has relied on *in vitro* neurosphere culture. The *in vivo* lineage tracing work of Pardal *et al.* that demonstrates the contribution of the Type II population to other cell populations does not present quantitative data on the extent of this contribution. Moreover, the lineage tracer used by these studies relies on a pre-exposure to chronic hypoxia in order to ensure recombination (Pardal *et al.*, 2007). As such, these results may be confounded by the processes of pre-acclimatisation or de-acclimatisation, and may not represent the true function of the niche in the normal physiology of acute acclimatisation. Understanding which cell(s) mediate the proliferative responses to hypoxia is important for understanding the carotid body niche and its potential therapeutic applications. Therefore, further investigation is warranted to confirm whether the Type I cells or Type II cells are the primary proliferative cell type of the carotid body *in vivo*.

If the Stem Cell theory is correct, the carotid body may be viewed as a peripheral neural stem cell niche (Kokovay & Temple, 2007). A stem cell niche is an anatomical compartment containing a stem cell population, distinguished by a closely controlled and specialized microenvironment which helps maintain the stem cell population and regulates how the population participates in tissue generation, maintenance and repair (Scadden, 2006). Intriguingly, proliferating stem cell populations are consistently located in regions

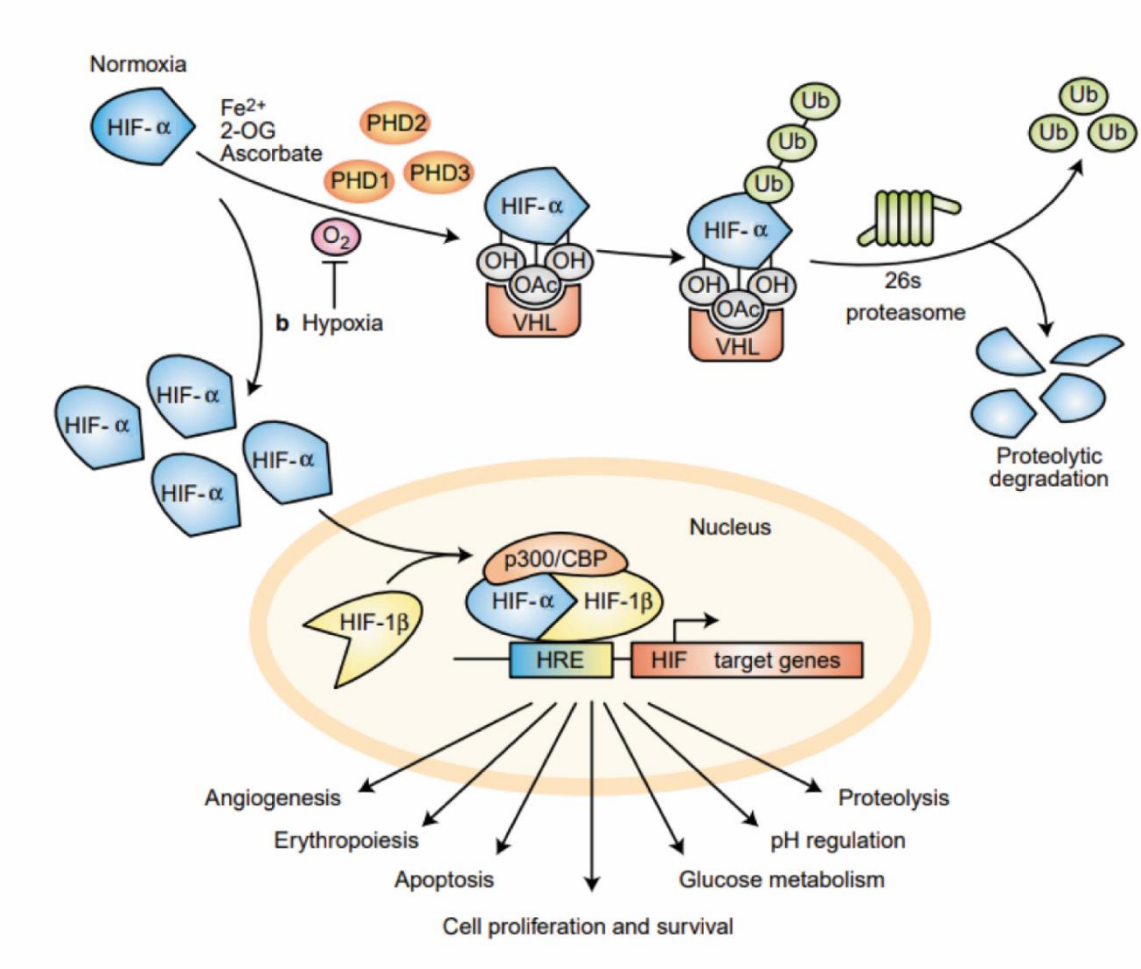
with low physiological oxygen tensions in both development and adulthood (Mitchell & Yochim, 1968; Cipolleschi *et al.*, 1993; Dings *et al.*, 1998; Braun *et al.*, 2001; Erecinska & Silver, 2001; Harrison *et al.*, 2002) suggesting that physiological hypoxia may be an adaptive component of these niches: a hypoxic microenvironment minimizes levels of oxidative aerobic respiration and thus reduces ROS production and the associated mutagenic burden upon the quiescent stem cell population. Hypoxia has also been implicated in maintaining undifferentiated states in embryonic, haematopoietic, mesenchymal and neural stem cells (Morrison *et al.*, 2000; Gustafsson *et al.*, 2005; D'Ippolito *et al.*, 2006; Fehrer *et al.*, 2007). Of particular relevance to this thesis are the neural stem cell niches: the subgranular zone (SGZ) of the dentate gyrus and the subventricular zone (SVZ) of the lateral ventricles (Alvarez-Buylla & Garcia-Verdugo, 2002). These stem cell niches contain astrocytic stem cells which, if the CB Stem Cell theory is correct, are a parallel population to the carotid body stem cells (Kokovay & Temple, 2007; Pardal *et al.*, 2007). Intriguingly, it has been suggested that the microenvironment of the SVZ and SGZ is adapted to maintain astrocytes in a stem cell-like state (Alvarez-Buylla & Lim, 2004), and it is therefore possible that the same environmental and signalling cues play a role in the maintenance of the carotid body. However, if this is the case, hypoxia is acting to maintain a quiescent, pluripotent state in most stem cell niches, a distinctly different phenomenon from the hypoxia-induced hyperplasia reported in the carotid body.

Studies into the behaviour of these stem cell niches, including the carotid body, have suggested that many of these hypoxia sensitive responses are regulated by a single pathway: the hypoxia inducible factor (HIF) signalling pathway (Gustafsson *et al.*, 2005; Malladi *et al.*, 2007; Mohyeldin *et al.*, 2010; Cunningham *et al.*, 2012; Li *et al.*, 2014). In

particular, the HIF pathway has been implicated in mediating both acute and chronic responses to hypoxia in the carotid body (Bishop *et al.*, 2013; Hodson *et al.*, 2016).

The HIF-PHD pathway:

The hypoxia inducible factor (HIF) pathway was initially discovered as a regulator of the erythropoietin (EPO) gene in the kidney, but has since been understood to operate across the organism (Semenza & Wang, 1992; Maxwell *et al.*, 1993). Today, the HIF isoforms are understood to be a family of transcription factors which integrate the physiological responses to hypoxia, ensuring a close matching of oxygen supply to consumption on the systemic and cellular level (Kaelin & Ratcliffe, 2008; Bishop & Ratcliffe, 2014). HIF is an α/β heterodimer consisting of a constitutively expressed HIF-1β (also known as ARNT) subunit and a regulated HIFα subunit (see Introduction Figure 3). The HIFα subunit contains a Per-ARNT-Sim (PAS) binding domain which binds to the HIF-1β to from a stable heterodimer (Erbel *et al.*, 2003). In normoxic conditions, HIFα is hydroxylated at a prolyl residue by a family of 2-oxyglutarate dependent enzymes, the HIF prolyl hydroxylases (PHD1, PHD2 or PHD3) which require oxygen as a co-factor. Hydroxylated HIF is then ubiquitinated by von Hippel-Lindau tumour suppressor (pVHL), which targets it for degradation by the proteasome (Maxwell *et al.*, 1999; Kaelin, 2017). In hypoxia, oxygen becomes rate limiting for the function of the PHD enzymes, resulting in the accumulation of HIF-α, which stabilizes and dimerises with HIF-β. The HIF heterodimer then translocates to the nucleus, where it binds to hypoxic response elements (HREs) at target gene loci and regulates the expression of several hundred target genes (Schofield & Ratcliffe, 2004). HRE gene loci include genes linked to angiogenesis, erythropoiesis, apoptosis, cell proliferation, cell migration, glucose metabolism, pH regulation and proteolysis (Schofield & Ratcliffe, 2004). Of relevance to the processes of acclimatisation,



Introduction Figure 3. The hypoxia inducible factor (HIF) pathway.

The Hypoxia Inducible Factor (HIF) family is a family of transcription factors that mediate the cellular response to hypoxia. HIF is a heterodimer composed of two subunits: a stable HIF-1β subunit, and a regulated HIFα subunit. The HIFα family contains two main isoforms: HIF-1α and HIF-2α. In normoxic conditions, HIFα is hydroxylated at a prolyl residue by the PHD enzymes (PHD1, PHD2 or PHD3) and then ubiquitinated by pVHL targeting it for degradation by the proteasome. The activity of the PHD isoforms is dependent on the presence of oxygen as a co-factor. Consequently, in low oxygen conditions (hypoxia) PHD activity is reduced and stable HIFα accumulates in the cell. Stable HIFα dimerizes with HIF-1β and translocates to the nucleus, where it acts as a transcription factor, binding to hypoxic response elements (HREs) in the genome and controlling the expression of hundreds of genes linked to hypoxic acclimatisation (modified from (Carroll & Ashcroft, 2005)).

HIF has been demonstrated to regulate the expression of erythropoietin (EPO) which mediates the erythropoietic response to hypoxia (Semenza & Wang, 1992; Maxwell *et al.*, 1993) and genes mediating angiogenesis, including vascular endothelial growth factor, VEGFA (Liu *et al.*, 1995; Forsythe *et al.*, 1996), and VEGF receptor 1, also known as Flt-1 (Gerber *et al.*, 1997).

The mammalian HIFα family contains two major isoforms, HIF-1α and HIF-2α (also referred to as endothelial PAS domain-containing protein, EPAS1). These isoforms regulate an overlapping, but distinct, subset of genes: transcriptional studies have identified exclusive targets for HIF-1α and HIF-2α, as well as genes which respond to both isoforms (Hu *et al.*, 2003; Raval *et al.*, 2005; Rankin *et al.*, 2007; Arsenault *et al.*, 2013). Although both HIF isoforms have a high sequence similarity, structurally the PAS B domain of HIF-2α contains a 290Å hydrophobic pocket, which is present but much smaller in the HIF-1α isoform (Scheuermann *et al.*, 2009; Rogers *et al.*, 2013).

HIF-1α is ubiquitously expressed in all cells, and is highly conserved across all multi-cellular organisms (Wiener *et al.*, 1996; Rytkonen *et al.*, 2011). HIF-2α, by contrast, is the more evolutionary "modern" isoform present only in vertebrates (Rytkonen *et al.*, 2011) and although it is near-ubiquitous, its expression is much more highly restricted to specific tissues and cell populations, where it appears to have a more dominant role in regulating respiratory and cardiovascular responses to hypoxia (Schofield & Ratcliffe, 2004). In particular, HIF-2α seems to have a unique role in regulating erythropoiesis *via* upregulating the EPO gene *in vivo* (Rankin *et al.*, 2007; Arsenault *et al.*, 2013; Franke *et al.*, 2013), although both HIF isoforms are capable of binding to the EPO HRE *in vitro* (Arsenault *et al.*, 2013). Intriguingly, experimental evidence suggests a degree of negative

regulation between the HIF isoforms, with HIF-2α appearing to be inactivated or repressed in cells which strongly express HIF-1α (Park *et al.*, 2003; Raval *et al.*, 2005; Hu *et al.*, 2006).

The oxygen sensitivity of the HIF pathway is conferred by the requirement of the prolyl hydroxylase domain-containing protein (PHD) enzymes for oxygen as a co-factor (Schofield & Ratcliffe, 2004). In mammals, the PHD family is composed of three isoforms, PHD1, PHD2 and PHD3. Of these, PHD2 (also known as Egln-9 Family Hypoxia Inducible Factor 1, EGLN1) is the most widely and strongly expressed and is believed to be the primary regulator of the HIF family, whilst PHD1 and PHD3 have more tissue specific expression patterns (Berra *et al.*, 2003; Appelhoff *et al.*, 2004; Kaelin & Ratcliffe, 2008). *In situ* hybridisation and immunohistochemistry has shown that all three isoforms are present in the heart, liver, kidney, brain, testis and lung, with high levels of PHD2 across the body, whilst the highest levels of PHD1 and PHD3 were in the testes and heart myocardium respectively (Lieb *et al.*, 2002; Willam *et al.*, 2006). The importance of PHD2 is highlighted by the embryonic lethality of homozygous $PHD2^{-/-}$ inactivation in mice, which develop placental and heart defects before death, whereas $PHD1^{-/-}$ and $PHD3^{-/-}$ mice developed normally (Takeda *et al.*, 2006).

Defects in the HIF pathway have been linked to a range of conditions and pathologies, particularly cancer. Dysregulation of the HIF pathway has been linked to the formation and progression of cancers, particularly pseudohypoxic cancers including clear cell carcinoma (ccRCC), pheochromocytoma and carotid paraganglioma (Maxwell *et al.*, 2001) and several familial conditions with elevated cancer rates involve mutations in HIF pathway genes, including VHL syndrome (Kaelin, 2002, 2007) and Pacak-Zhuang

syndrome (Zhuang *et al.*, 2012; Pacak *et al.*, 2013). In humans, low levels of HIF-2α mRNA in lung tissue has been linked to chronic obstructive pulmonary disease (COPD) (Yoo *et al.*, 2015) whilst overexpression of HIF-2α is linked to elevated resting ventilation, pulmonary hypertension, polycythaemia and the formation of somatostatinomas and paragangliomas (Formenti *et al.*, 2011; Zhuang *et al.*, 2012; Pacak *et al.*, 2013; Yang *et al.*, 2013). Inactivation of the regulators of the HIF isoforms (such as PHD2 and VHL) can also lead to the stabilization of HIF in the absence of hypoxia, inducing a state of "pseudohypoxia" (Bratslavsky *et al.*, 2007). In line with this, hypomorphic mutations in PHD2 can lead to the development of polycythaemia in humans, and this is replicated by the heterozygous inactivation of PHD2 in mice (Percy *et al.*, 2006; Takeda *et al.*, 2006; Minamishima *et al.*, 2008) whilst a survey of human patients with Chuvash polycythaemia, an inherited syndrome caused by a VHL mutation, found that these individuals had an enhanced ventilatory response to hypoxia (Smith *et al.*, 2006). Notably for the work presented in this thesis, it is possible that these ventilatory phenotypes are induced by pseudohypoxic HIF-mediated effects on the carotid body.

The association of the HIF-PHD pathway with a range of diseases has led to extensive biomedical interest in the therapeutic regulation of the HIF pathway, and recent years have seen the development of several pharmacological methods of intervening in this pathway (Myllyharju, 2009; Harten *et al.*, 2010). Pharmacological inhibitors of 2-oxoglutarate dependent enzymes, such as DMOG and IOX3, are commercially available and affect the PHDs (Bishop *et al.*, 2013). PHD inhibitors including roxadustat and molidustat have potential applications in the treatment of kidney disease and anaemia and are in late stage clinical trials (Besarab *et al.*, 2015; Joharapurkar *et al.*, 2018; Macdougall *et al.*, 2019; Sakashita *et al.*, 2019) or being licensed for use (Dhillon, 2019). In addition to these PHD

inhibitors, small molecule antagonists of HIF-2α have also been recently developed. These small molecule inhibitors take advantage of the structural difference between HIF-2α and HIF-1α, targeting the 290Å hydrophobic pocket within the PAS B domain of HIF-2α (Rogers *et al.*, 2013). These inhibitors bind to the PAS B domain and allosterically disrupt its binding to HIF-1β (ARNT), in turn reducing the formation of the HIF heterodimer and its transcriptional activity without disrupting the function of HIF-1α (Wallace *et al.*, 2016). These initial studies of HIF-2α inhibitors have highlighted their potential for the treatment of HIF-2α-driven conditions in the kidney (Chen *et al.*, 2016), but they have not addressed their potential applications (or side effects) in another tissue with a strong functional role of HIF-2α: the carotid body.

The HIF pathway in the carotid body:

Recent studies have implicated the HIF-PHD signalling pathway as a major regulator of both normal carotid body physiology and its acute and chronic responses to hypoxia. Although $PHD2^{-/-}$ is embryonic lethal, "pseudohypoxic" heterozygous inactivation of PHD2 ($PHD2^{+/-}$) has been shown to result in carotid body hyperplasia, which was accompanied by an enhanced sensitivity to acute hypoxia that resembles ventilatory acclimatisation (Bishop *et al.*, 2013). Mice with a Chuvash VHL mutation displayed a similar phenotype, with enhanced ventilatory sensitivity and hyperplastic carotid bodies (Slingo *et al.*, 2014). PHD2 or VHL inactivation will result in the increasing stabilization of the HIF isoforms, suggesting that these isoforms play an important role in both carotid body size and ventilatory control. In support of this hypothesis, HIF-upregulated genes such as VEGFA (Liu *et al.*, 1995; Forsythe *et al.*, 1996) and endothelin-1 (Hu *et al.*, 1998) have been strongly implicated in carotid body function and development: VEGFA and endothelin-1 have been implicated in the angiogenic /vascular component of hypoxia-

induced carotid body hyperplasia, carotid body Type I cell signalling, and in the formation of carotid paragangliomas (Jyung *et al.*, 2000; Platero-Luengo *et al.*, 2014). Other important HIF regulated genes include tyrosine hydroxylase (TH) (Millhorn *et al.*, 1997; Lim *et al.*, 2015), which catalyses the rate limiting step in the synthesis of catecholamines, such as dopamine, and is strongly expressed in the oxygen sensitive carotid body Type I cells (Izal-Azcarate *et al.*, 2008).

However, early work on knockout mice has shown mixed results with regards to the carotid body. Due to the embryonic lethality of homozygous knockouts of HIF-1α and HIF-2α, these studies employed hemizygous inactivations. HIF-1$\alpha^{+/-}$ mice have been shown to have a delayed or impaired response to chronic hypoxia, showing delayed polycythaemia, pulmonary hypertension and greater weight loss relative to littermates (Yu *et al.*, 1999) but further study has shown that although HIF-1$\alpha^{+/-}$ mice demonstrate minor impairments in carotid body ventilatory control, these mice were able mount a normal ventilatory response to hypoxia through compensation *via* vagal afferents (Kline *et al.*, 2002). Morphologically, these mice showed no differences in carotid body morphology relative to controls (Kline *et al.*, 2002). Conversely, HIF-2$\alpha^{+/-}$ mice present with heightened carotid body sensitivity to hypoxia, hypertension and apnoeas, although acclimatisation was not assessed in these mice (Peng *et al.*, 2011). Although informative, due to the constitutive nature of these inactivations, it is likely the developmental effects of HIF-1α and HIF-2α may confound or overshadow the functions of the HIF-PHD pathway in the adult.

In recent years, advances in inducible and cell specific knockdown models have allowed the assessment of the function of the HIF-PHD pathway in the adult carotid body.

Significantly, our laboratory has demonstrated that inducible inactivation of HIF-2α under the ubiquitous RosaCreER driver abrogated ventilatory acclimatisation to hypoxia and almost totally ablated the carotid body proliferative response to 7 days of chronic hypoxic exposure (Hodson *et al.*, 2016). By contrast, *Hif-1α$^{f/f}$;RosaCreER* mice displayed no statistically significant ventilatory or proliferative abnormalities (Hodson *et al.*, 2016). The RosaCreER driver employed in this study enables the inducible and temporally controlled inactivation of HIF-2α in all cells of an adult organism. Thus, Hodson *et al.* have shown a requirement for HIF-2α, and not HIF-1α, for ventilatory acclimatisation and CB proliferation in the adult carotid body without confounding developmental effects (Hodson *et al.*, 2016). However, the ubiquitous nature of this inactivation means that the cell(s) in which HIF-2α is necessary to mediate the hypoxic response is unknown.

In this context, a major role is likely played by the oxygen sensitive Type I cells of the carotid body. Work which inactivated HIF-2α through the expression of β-gal in exon 2 of the EPAS1 gene demonstrated that β-gal (and therefore HIF-2α) expression is tightly restricted to the Type I cells of the carotid body (Tian *et al.*, 1998). Despite this restricted expression, transcriptional analysis has indicated that HIF-2α is strongly expressed in whole homogenised carotid bodies (Gao *et al.*, 2017), and in Type I cells specifically (Zhou *et al.*, 2016). Moreover, Type I cells contain and secrete growth factors such as VEGFA and platelet-derived endothelial cell growth factor (PDECG), the expression and release of which is induced by hypoxia (Jyung *et al.*, 2000; Chen *et al.*, 2003). Neuroendocrine tissues, including the Type I cell population of the carotid body, can be specifically targeted with a constitutive tyrosine hydroxylase (TH) Cre promoter. Overexpression of HIF-2α using this THCre driver has been demonstrated to result in carotid body hyperplasia, suggesting that pseudohypoxic stimulation of the carotid body

can drive the expansion of the niche (Macias *et al.*, 2014). These studies suggest that the HIF-2α dependence of the carotid body ventilatory and proliferative responses could be mediated by its expression and function in the carotid body Type I cells. This thesis will investigate this hypothesis using inducible inactivation of HIF-2α in both Type I and Type II cell populations.

The HIF pathway in carotid body paraganglioma

The dependence of carotid body cellular proliferation on HIF-2α and the Type I cell population may provide insights into the formation of carotid body tumours (carotid paraganglioma (PGL)). These tumours are a rare tumour type at sea level (occurring at a rate of 1:1000,000 (Dua *et al.*, 2014)), but have a 10-fold higher incidence in high altitude dwellers (Saldana *et al.*, 1973), suggesting that hypoxia-induced growth of the carotid body and its upregulation of mitogenic genes such as VEGFA may increase the risk of tumorigenesis. Carotid tumours are part of a class of tumours of the autonomic ganglia which include paraganglioma and adrenal medulla phaeochromocytomas (PGL /PCC). Unusually for most cancers, paragangliomas and phaeochromocytomas are highly heritable. 40% of these tumours are germline tumours, and roughly a third of the remaining 60% of sporadic tumours are thought to involve a mosaicism or pre-disposing somatic mutation (Favier *et al.*, 2015). Transcriptomic studies have identified that PGL & PCC associate strongly with ~20 genes (Lussey Lepoutre *et al.*, 2018; Pang *et al.*, 2019). These genes fall into two main clusters (1 & 2), of which Cluster 1 genes are "pseudohypoxic" mutations. These include genes implicated in metabolism (SDHx, FH) and in the HIF-pathway (VHL, PHD1, EGLN1 (PHD2) and EPAS1 (HIF-2α)) (Zhuang *et al.*, 2012; Yang *et al.*, 2013; Buffet *et al.*, 2014; Favier *et al.*, 2015; Yang *et al.*, 2015; Lussey Lepoutre *et al.*, 2018). Somatic gain-of-function mutations in HIF-2α, but not HIF-

1α, have also been recently described in human paraganglioma (Toledo *et al.*, 2013; Toledo, 2017). Novel somatic gain-of-function mutations in HIF-2α have been identified in patients with Pacak-Zhuang syndrome, in which individuals develop paraganglioma in addition to duodenal somatostatinomas and polycythaemia (Zhuang *et al.*, 2012; Pacak *et al.*, 2013). Intriguingly, overexpression of HIF-2α has also been demonstrated to be a major driver of brain tumour stem cell proliferation in gliomas (Li *et al.*, 2009) which derive from the neural stem cell populations which have been argued to parallel the stem cell-like cells of the carotid body (Kokovay & Temple, 2007). This suggests that manipulation of HIF-2α may also drive the parallel carotid proliferation, and that manipulation of the HIF pathway may be a component of multiple neural-derived tumours.

A mechanistic explanation for the formation of these cancers is that inactivation of regulatory components of the HIF pathway results in 'pseudohypoxic' HIF stabilization and subsequent upregulation of genes such as EPO, VEGFA and CCND1 which drive angiogenesis and tumour growth. The specific role played by HIF-2α in the carotid body and its capabilities as an oxygen-sensitive niche may make the carotid particularly sensitive to pseudohypoxic stimulation. However, a direct link has yet to be demonstrated, and the underlying cell types involved are unknown. If the Stem Cell theory of the carotid body is correct, it is likely that carotid body stem cells (the Type II cells of the carotid body) contribute to tumorigenesis. Conversely, the oxygen sensitive Type I cells of the carotid express VEGFA and platelet-derived endothelial cell growth factor (PDECGF), have been linked to tumour progression in the carotid body (Jyung *et al.*, 2000; Chen *et al.*, 2003). To investigate this, this thesis will examine whether pseudohypoxia is sufficient to drive carotid body hyperplasia and other PGL-like phenotypes through inducible and constitutive inactivation of PHD2 in the Type I cells of the carotid body.

Conclusion:

This introduction has shown that the carotid body responds to chronic hypoxia with a marked hyperplasia which includes a significant expansion in the number of the oxygen sensitive Type I cells of the carotid body. The Stem Cell theory of the carotid body has proposed that this hyperplasia originates from the activity of a pluripotent stem cell-like subpopulation of Type II cells. Hodson *et al*. have shown that this proliferative response to chronic hypoxia is dependent on the integrity of HIF-2α (Hodson *et al.*, 2016), but this work employed a ubiquitous inactivation across the entire organism. Therefore, it is currently unknown which cells in the carotid body mediate the HIF-2α-dependent response, and how this drives the proliferative and ventilatory responses of the carotid body. Due to their high expression of HIF-2α and mitogenic growth factors such as VEGFA, we hypothesize that the Type I cells of the carotid body may play a major role in mediating this response, although how this interacts with the purported stem cell-like Type II cells is unknown. Thus, there is a need to investigate the specific cell types involved in the carotid body proliferative response, both to test the predictions of the Stem Cell theory and to characterize the precise mechanistic role of HIF-2α in regulating the niche.

To test this, this thesis will investigate the proliferative responses of the Type I and Type II cells of the carotid body by labelling these populations with fluorescent lineage tracers under the control of cell type specific promoters. To fully characterize the response of these cell types to chronic hypoxia, this lineage tracer analysis will be combined with standard immunohistochemistry, plethysmography analysis of ventilation and a novel *in situ* hybridisation approach to imaging the expression of mRNA. Subsequently, these cell type specific promoters will be combined with genetic inactivation of key genes in the HIF-PHD pathway, to confirm and characterize the function of HIF-2α and PHD2 in these cells.

Therefore, in its 5 chapters, this thesis aims to undertake the following:

1) Test whether hypoxia induces proliferation of other neural stem cell niches in the CNS.

2) Characterize the carotid body's proliferative response to hypoxia and identify the main cell types contributing to carotid body hyperplasia.

3) Identify which of these cell types is sensitive to hypoxia and HIF-2α using cell specific genetic inactivation of HIF-2α.

4) Test whether pharmacological inhibition of HIF-2α replicates the effects of genetic HIF-2α inactivation.

5) Demonstrate whether pseudohypoxic stimulation of HIF-2α-sensitive carotid body cells is sufficient to replicate hypoxia-induced carotid hyperplasia.

Results Chapter 1: Hypoxia-induced proliferation in neural stem cell niches

Introduction:

In recent years, many studies have investigated the role of adult neural stem cells (NSCs) and neurogenesis in tumorigenesis, neuroplasticity and the response to injury. Neurogenesis is a rare process in adult mammalian tissue, being tightly restricted to a few specialised microenvironments. In the mammalian central nervous system (CNS), these stem cell 'niches' are the subventricular zone (SVZ) of the lateral ventricles and the subgranular zone (SGZ) of the dentate gyrus (Doetsch *et al.*, 1999; Doetsch, 2003; Alvarez-Buylla & Lim, 2004; Zhao *et al.*, 2008; Benarroch, 2013). The subventricular zone contains NSCs, a sub population of the B1 astrocytic cell population. These $GFAP^+$ B1 pluripotent stem cells continually give rise to $nestin^+$ Type C transit-amplifying progenitors, which in turn differentiate to Type A neuroblasts which migrate along the rostral migratory stream to the olfactory bulb (Kriegstein & Alvarez-Buylla, 2009; Ihrie & Alvarez-Buylla, 2011; Lim & Alvarez-Buylla, 2016) (Fig. 1.1). NSCs are also present in dentate gyrus: in the subgranular zone (SGZ), immature radial glia-like $GFAP^+$ cells divide and differentiate to give rise to neural progenitor cells, neurons and astrocytes which are then integrated into the local network of the dentate gyrus (Benarroch, 2013).

The proliferation and differentiation of these stem cells depends on a complex balance of cellular and environmental signals which, if dysregulated, can lead to the formation of tumours such as gliomas, whilst manipulation of these signals can improve response to brain injury and other conditions. It has been proposed that hypoxia is one of the most important environmental signals for maintaining stem cell populations across multiple

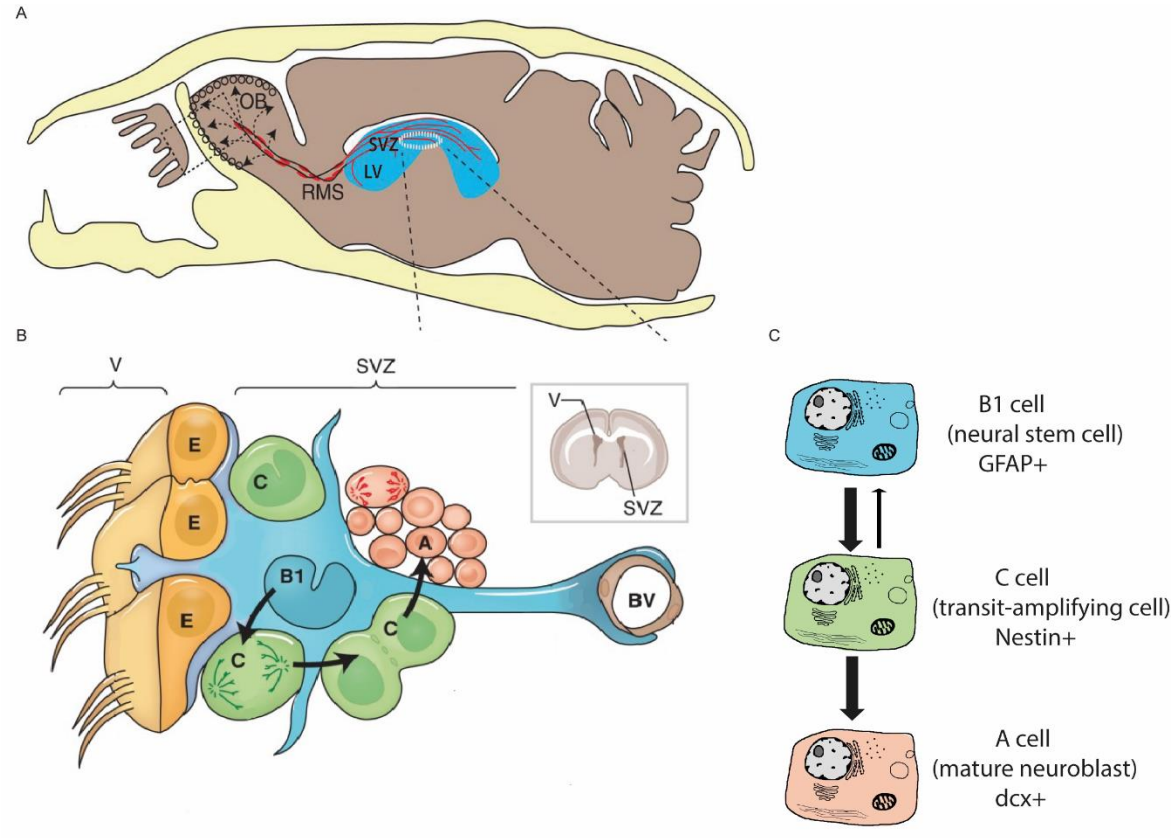


Figure 1.1. Neurogenesis in the SVZ.

A) Sagittal section through a rodent brain (calvarium is yellow). Neuroblasts form in the subventricular zone (SVZ), adjacent to the lateral ventricles (LV). These cells migrate along the rostral migratory stream (RMS) to the olfactory bulb (OB).

B) Cellular composition of the subventricular zone (SVZ). Coronal section of adult mouse brain shown, with the SVZ region indicated by a black arrow. Astrocytic Type B1 cells (blue) function as stem cells. The apical surface of type B1 cells has a primary cilium and makes contact with the ventricle (V). These cells divide and give rise to type C cells (green), which are rapidly dividing, transit amplifying cells. Type C cells give rise to type A cells (red), the migratory neuroblasts which move down the rostral migratory stream (RMS) to the olfactory bulb. The niche is irrigated by blood vessels (BV).

C) Histological characteristics of the SVZ lineage. Astrocytic B1 cells are positive for astrocytic markers including glial fibrillary acidic protein (GFAP). The rapidly amplifying Type C cells are distinguished by expression of dlx2, epidermal growth factor receptor (EGFR) and Nestin. The maturing Type A migratory neuroblasts are positive for doublecortin (dcx).

(figure modified from (Lim & Alvarez-Buylla, 2016))

stem cell niches, including haematopoietic, mesenchymal and neurogenic niches (Mohyeldin *et al.*, 2010). In line with this, there is considerable evidence to suggest that hypoxia plays a role in the function of the SVZ and SGZ stem cell niches. Stem cell culture studies have shown that hypoxia is a key regulator of neurogenesis *in vitro*: SVZ and SGZ derived NSCs proliferate more rapidly in hypoxic conditions (Erecinska & Silver, 2001; Mohyeldin *et al.*, 2010; Ihrie & Alvarez-Buylla, 2011; Ross *et al.*, 2012). However, *in vivo* studies have focused on combined ischaemic /hypoxic insult, rather than hypoxia *per se*. In the intact SVZ, combined hypoxic /ischaemic insult has been shown to stimulate the expansion of neural stem cells and increased BrdU uptake in the SVZ, whilst focal cerebral ischemia induces ipsilateral expansion of the SVZ stem cell population and its migration towards the injury site across multiple species (Kokaia *et al.*, 2006; Yamashita *et al.*, 2006; Li *et al.*, 2010; Cunningham *et al.*, 2012). Together, this suggests that hypoxic /ischemic injury is capable of inducing a proliferative response, but the effect of continuous chronic hypoxia alone has not been tested in the SVZ.

A possible proliferative response to hypoxia in the NSC niches of the CNS is particularly interesting in light of recent studies suggesting the NSC populations of these niches share major parallels with the carotid body, a peripheral stem cell niche. (Fig. 1.2.) (Kokovay & Temple, 2007; Pardal *et al.*, 2007). The carotid body responds to chronic hypoxic exposure with a marked hyperplasic and proliferative response, expanding 2-3 fold in size over a period of days to weeks (Arias-Stella & Valcarcel, 1976). Different carotid body cell populations have been proposed to mediate this response. A recent study by Pardal *et al*. has suggested that a subpopulation of carotid body cells, Type II, $GFAP^+$ glia-like astrocytes, are capable of acting as stem cells and respond to hypoxia by differentiating *via*

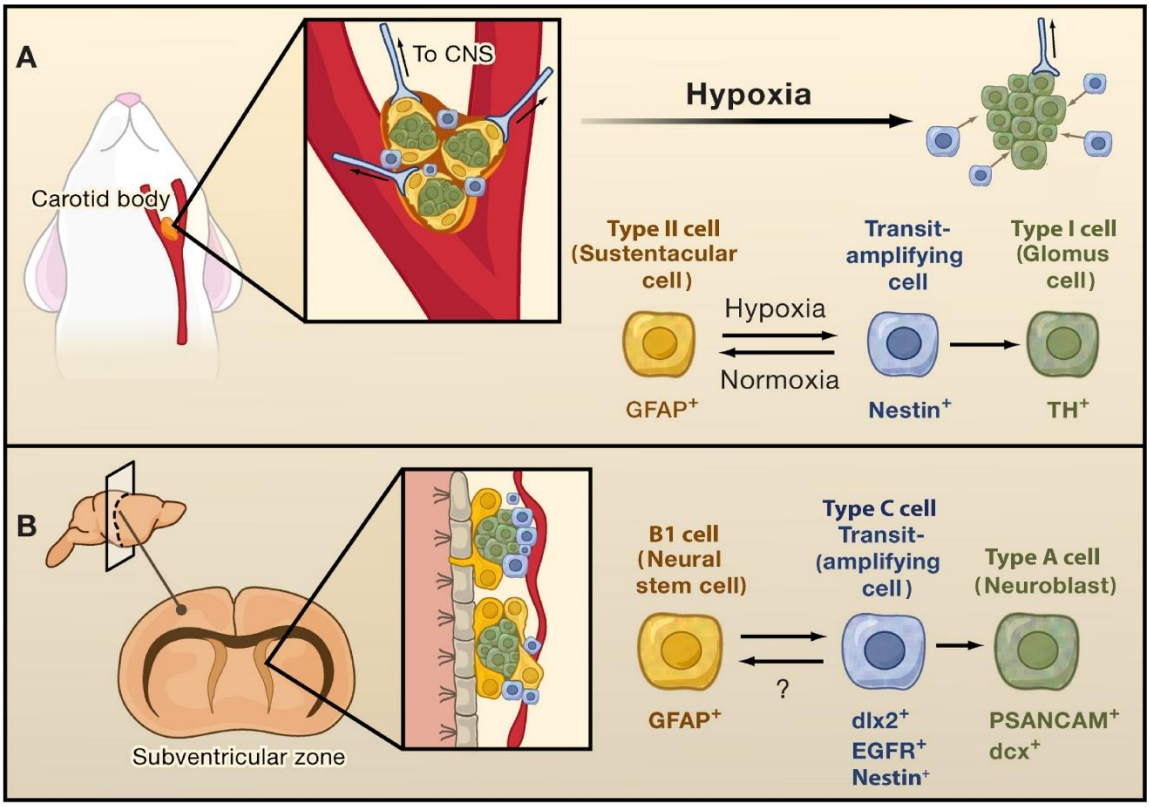


Figure 1.2. Neurogenesis in the carotid body and the subventricular zone.

A) The carotid body of the peripheral nervous system is located at the bifurcation of the carotid artery. Under normoxic conditions, clusters of dopaminergic glomus cells (green) are associated with glia-like sustentacular cells that express glial fibrillary acidic protein ($GFAP^+$) (yellow) and a few $nestin^+$ cells (blue). Afferents to the central nervous system (CNS) are represented in blue and blood vessels in red. Under hypoxic conditions, $GFAP^+$ sustentacular cells proliferate and convert into $GFAP^-$ /$nestin^+$ transit-amplifying cells that give rise to new tyrosine hydroxylase-positive (TH^+) dopaminergic cells. Note that following a return to normoxic conditions, $nestin^+$ transit-amplifying cells convert back to $GFAP^+$ resting sustentacular cells.

B) In the adult subventricular zone (SVZ), $GFAP^+$ stem cells (yellow) give rise to $GFAP^-$ /$nestin^+$ transit-amplifying cells (blue) that ultimately give rise to migratory doublecortin (dcx^+) neuroblasts (green). The transit-amplifying cells express Nestin, dlx2 and high levels of the epidermal growth factor receptor (EGFR).

(figure modified from (Kokovay & Temple, 2007)).

a nestin$^+$ intermediate to mature Type I oxygen sensitive glomus cells (Pardal *et al.*, 2007). If this theory is correct, the presence of proliferating GFAP$^+$ glia-like cells and downstream nestin$^+$ progenitors is strikingly similar to the characteristic proliferative GFAP$^+$ astrocytic lineages of the SVZ and dentate gyrus (Fig. 1.2) (Kokovay & Temple, 2007). It is has been proposed that astrocytic stem cell niches maintain and respond to a unique set of environmental conditions to preserve their stem cell-like behaviour (Alvarez-Buylla & Lim, 2004). It is possible that the proliferative response to hypoxia observed in the carotid body is common to all astrocytic stem cell populations and might be observed in the SVZ and SGZ.

To address whether the hypoxia-induced proliferative response of the carotid body can be observed in some or all CNS neural stem cells, this study aimed to use fluorescent lineage tracing to examine the stem cell populations of the two main neural stem cell niches of the central nervous system: the SVZ and SGZ. The work presented in this chapter will characterize the expression of two lineage tracer lines in two populations of NSCs in each niche, assess the effect of chronic hypoxia in the SVZ and SGZ, and examine the effect of genetic pseudohypoxia *via* PHD2 inactivation in the SVZ.

Results:

Characterisation of two lineage tracer lines in neural stem cell populations in the central nervous system.

The SVZ contains two interconnected neural stem cell (NSC) populations: first, the slowly proliferating quiescent astrocytic GFAP$^+$ B1 cells, which give rise to the second, the nestin$^+$ rapidly proliferating transit-amplifying progenitor C cells (Doetsch *et al.*, 1999; Rietze *et al.*, 2001; Doetsch, 2003; Garcia *et al.*, 2004) (Fig. 1.1). To study the response to

hypoxia in these two populations, two mouse lines were established in which a fluorescent linage tracer was expressed under the control of a tamoxifen-inducible CreER linked promoter specific to each cell type: NestinCreER (Type C precursors) and GFAPCreER (B1 astrocytes). Prior work has shown that the NestinCreER promoter labels the nestin$^+$ and BrdU$^+$ transit-amplifying progenitor NSC populations in the SVZ and the subgranular zone of the dentate gyrus (Lagace *et al.*, 2007). The GFAPCreER line selected for this study has been shown *via* lacZ reporter colocalisation with GFAP immunostaining to label the GFAP positive astrocytes of the SVZ and dentate gyrus (Hirrlinger *et al.*, 2006). Subsequent work with this line has shown that it specifically labels the quiescent NSC population of the SVZ, co-labelling for SOX2, a pluripotency marker (Mich *et al.*, 2014). This line has also been shown to label astrocytic NSCs in the dentate gyrus (Park *et al.*, 2018). This means that, if hypoxia induces proliferation of either lineage line in the SVZ, the increase will be detectable *via* an increase in the number of these cells co-labelling with proliferative markers such as BrdU.

For this study, the fluorescent reporter tdTomato Ai14 was selected as the reporter gene because of its strong fluorescent signal (Madisen *et al.*, 2010). This fluorophore was recombined into a ubiquitously expressed modified Rosa26-CAG locus, with a floxed STOP sequence between promoter and fluorophore to restrict its expression (Fig. 1.3A). Elsewhere in the genome, the tamoxifen-inducible Cre recombinase, CreER(T2) (hereafter referred to as CreER) was expressed under control of a cell type specific promoter: nestin or GFAP. After tamoxifen dosing, Cre is expressed in these nestin$^+$ or GFAP$^+$ cell populations, excising the floxed STOP sequence and resulting in cell type specific expression of the Ai14 tdtomato fluorescent reporter (Fig. 1.3A). Because the expression of the fluorophore is irreversible once induced, this allows the labelling of the targeted cell

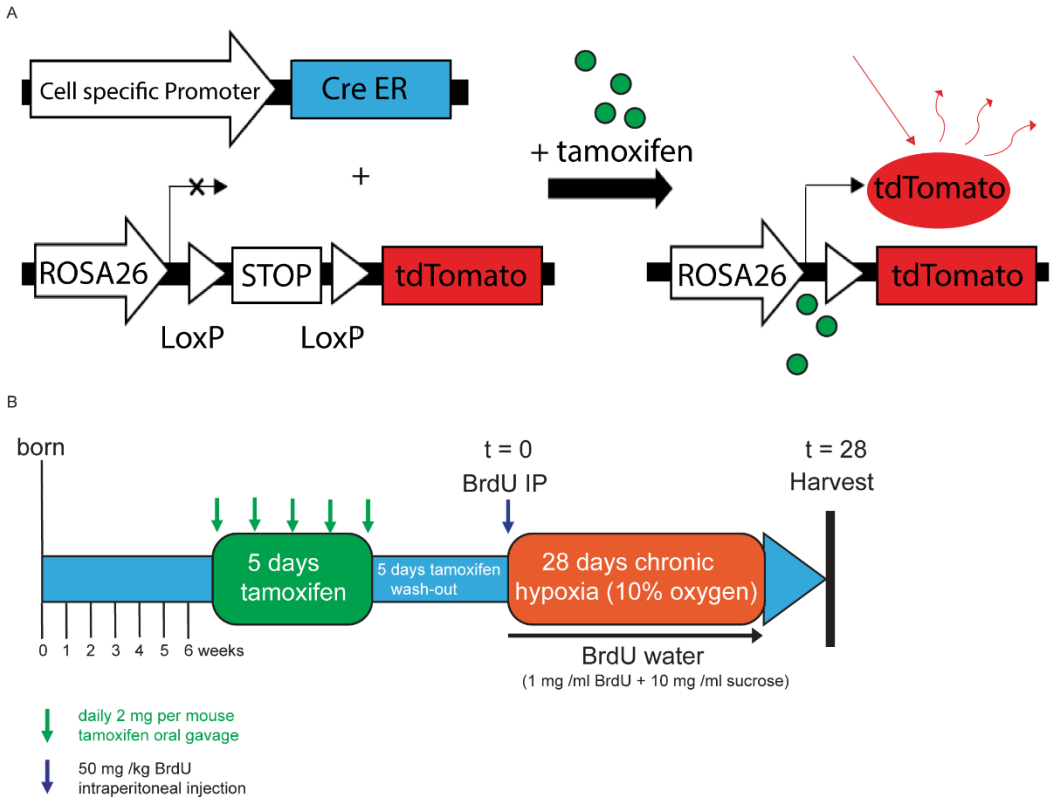


Figure 1.4. Experimental design of a CreER-mediated site-specific recombination fluorescent lineage tracing system.

A) Schematic representation of the genetic elements of the tdTomato-promoter-CreER system. Cre recombinase is fused to a tamoxifen-inducible mutated estrogen receptor ($CreER^{T2}$, hereafter referred to as CreER) and expressed under control of a cell line specific promoter. CreER is expressed in conjunction with a ubiquitous Rosa26-CAG driven fluorescent reporter (tdTomato Ai14) combined with a STOP sequence flanked by *LoxP* sites. In untreated mice, CreER is bound to chaperone heat shock proteins (Hsp90) in the cytoplasm. Upon treatment with tamoxifen, tamoxifen is metabolised to 4-hydroyxy tamoxifen (4-OHT) which binds to the chaperone heat shock proteins and releases the CreER, which translocates to the nucleus. There, it recombines at *LoxP* sites and excises the STOP cassette, resulting in the production of fluorescent tdTomato protein in cells expressing the chosen CreER promoter (in this study: GFAP or nestin). These cells, and any progeny they may have, will continue to express tdTomato throughout their lifespan, allowing the study of the chosen lineage (Kretzschmar & Watt, 2012).

B) Experimental design: 6-week-old mice *tdTomato*$^{f/+}$*;NestinCreER* or *tdTomato*$^{f/+}$*; GFAPCreER* lineage reporter mice are dosed with 2 mg kg^{-1} tamoxifen *via* oral gavage once daily for 5 days. This results in site specific recombination and expression of the

fluorescent tdTomato reporter in the target cell population. These mice are then left to dwell for 5 days in a 'tamoxifen wash-out' period of 5 days to minimize the risk that tamoxifen mediates further recombination during the experimental period. Immediately prior to the experimental period, mice were dosed with 50 mg kg^{-1} BrdU *via* IP injection and then given BrdU water (1 mg ml^{-1} BrdU and 1% sucrose) for the duration of the experiment to label proliferating cells. Mice are then retained in normoxia or placed in a normobaric altitude chamber exposing them to 10% oxygen for the experimental period. Mice dwelled in these experimental conditions for 28 days before being culled in their experimental condition and tissues removed for histology.

population at a set time point (tamoxifen treatment). The label will also be passed on to any progeny of the labelled cells, enabling the expansion or migration of the targeted population after a stimulus (in this case hypoxia) to be tracked (Feil *et al.*, 2009). The resulting *tdTomato$^{f/+}$;GFAPCreER* construct has been shown to have strong recombination and fluorescent signal in the dentate gyrus and SVZ (Mich *et al.*, 2014; Park *et al.*, 2018). This provided security that any increase in labelled cells during hypoxia was attributable to expansion of the previously labelled population and not additional recombination events.

To activate the fluorescent reporter, mice expressing either *tdTomato$^{f/+}$;NestinCreER* or *tdTomato$^{f/+}$;GFAPCreER*, were treated with tamoxifen *via* oral gavage for 5 days followed by 5 days without tamoxifen treatment (a 'wash-out' period prior to treatment with hypoxia /normoxia) (see Fig. 1.3B). This 'wash-out' was included to allow the drug to clear from the system of each experimental mouse, minimizing the amount of active tamoxifen occurring at the start of exposure to chronic hypoxia in order to prevent newly differentiated cells from potentially acquiring the label. This provided security that any increase in labelled cells during hypoxia was attributable to expansion of the previously labelled population, as opposed to additional recombination events.

To check that the chosen fluorescent reporter was indeed expressed in the correct cells prior to exposure to hypoxic stimulus, the expression of tdTomato was assessed immediately after tamoxifen wash-out, a time equivalent to the beginning of hypoxic /normoxic exposure in subsequent experiments (t = 0, Fig. 1.3B). In *tdTomato$^{f/+}$;NestinCreER* mice, tdTomato was widely and strongly expressed in regions reported to contain nestin^{+} NSCs and their progeny in the literature*:* tdTomato expressing cells were observed in the olfactory bulb, the SVZ and the dentate gyrus (Fig. 1.4A, C & E) (Gilyarov, 2008). Some ectopic expression of tdTomato was observed, with tdTomato expression observed in medium spiny neurons in the striatum of *tdTomato$^{f/+}$;NestinCreER* mice, despite these cells not being reported to immunostain for endogenous nestin in the literature (Gilyarov, 2008). This may potentially be explained by the reportedly greater expression of nestin transgenes relative to the expression of endogenous nestin in the brain (Mich *et al.*, 2014). In *tdTomato$^{f/+}$;GFAPCreER* mice, tdTomato^{+} cells with were observed within the SVZ, dentate gyrus and olfactory bulb, and these cells possessed a typically astrocytic appearance when examined at high magnification (Figs. 1.4B, D & F). TdTomato^{+} astrocytes were also observed in the parenchyma immediately adjacent to the SVZ and dentate gyrus, as well as throughout the hindbrain in regions consistent with the reported expression of the GFAPCreER promoter in the literature (Doetsch, 2003; Hirrlinger *et al.*, 2006; Kriegstein & Alvarez-Buylla, 2009).

Some inducible CreER alleles have also been reported to undergo low levels of recombination in the absence of tamoxifen (Feil *et al.*, 2009). To confirm that expression of tdTomato was tightly restricted by tamoxifen treatment and that no aberrant recombination occurred prior to this study's dosing and hypoxic interventions, the

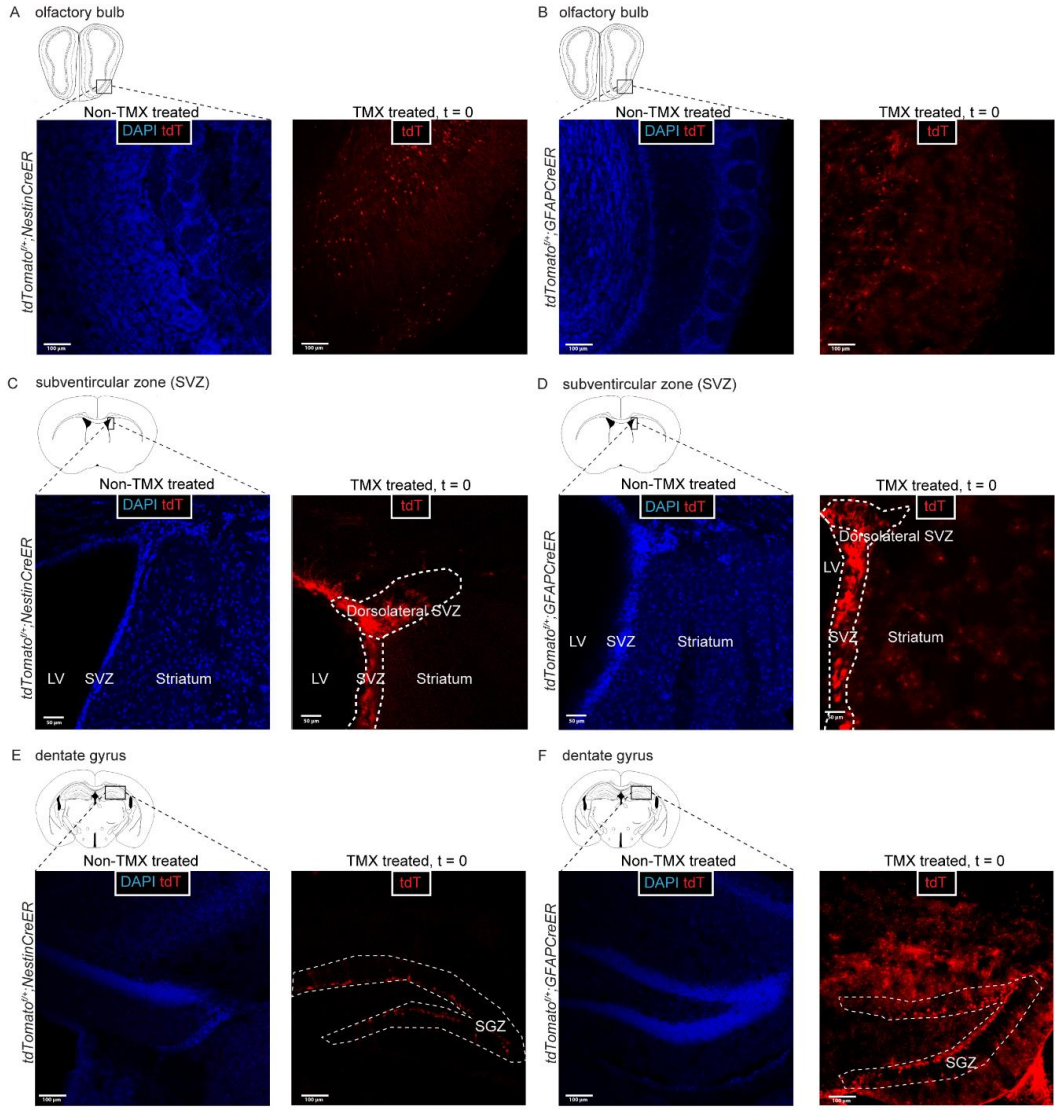


Figure 1.4. Characterization of lineage tracers in the brain of adult mice.

Representative images are shown from non-tamoxifen (TMX) treated mice, left panels, and in mice immediately after tamoxifen 'wash-out' (t = 0), right.

A-B) Characterization of tdTomato (red) expression in the olfactory bulb of A) n = 2 *tdTomato*$^{f/+}$*;NestinCreER* and B) n = 2 *tdTomato*$^{f/+}$*;GFAPCreER* mice. Scale bars = 100 µm.

C-D) Characterization of tdTomato expression in the subventricular zone (SVZ edges outlined in white) and striatum of C) n = 2 *tdTomato*$^{f/+}$*;NestinCreER* and D) n = 2 *tdTomato*$^{f/+}$*;GFAPCreER* mice. TdTomato positive cells are visible in the SVZ and the striatum. LV = lateral ventricles. SVZ = subventricular zone. Scale bars = 50 µm.

E-F) Characterization of tdTomato expression in the dentate gyrus of E) n = 2 *tdTomato*$^{f/+}$*;NestinCreER* and F) n = 2 *tdTomato*$^{f/+}$*;GFAPCreER* mice. SGZ = subgranular zone. Scale bars = 100 µm.

forebrains of 6-week-old non-tamoxifen treated *tdTomato$^{f/+}$;NestinCreER* and *tdTomato$^{f/+}$;GFAPCreER* mice were examined (at a time equivalent to t = 0 in the tamoxifen treated cohort). In contrast to tamoxifen treated mice, no tdTomato fluorescence was observed in the SVZ, dentate gyrus, olfactory bulbs or rostral migratory stream (RMS) of these mice, suggesting that no aberrant recombination occurred (Fig. 1.4).

The effect of chronic hypoxia on lineage labelled populations in the subventricular zone.

Having established that each lineage tracer line is expressed in a tamoxifen-inducible manner in the target populations of the SVZ and dentate gyrus at t = 0, animals were then were exposed to either normoxia or 10% oxygen using a normobaric altitude chamber for 28 days. Thus, the expansion, proliferation or migration of the labelled populations and their progeny could be analysed and compared with control animals maintained in normoxia. This 28-day time point was selected because ischemic /hypoxic treatment has shown maximal effect in a time period of between two and four weeks in the CNS and because it has been shown to capture the majority of proliferation in the parallel carotid body niche (Zhu *et al.*, 2005; Yamashita *et al.*, 2006; Kumar & Prabhakar, 2012). Confocal microscopy was then used to assess whether hypoxia had induced an expansion or migration of either labelled SVZ cell population, assessed *via* quantification of tdTomato$^+$ cell number in the SVZ and the adjacent striatum (into which labelled cells may migrate). Analysis was conducted at fixed stereological co-ordinates (Bregma values) corresponding to the location of the anterior and intermediate SVZ (between Bregma 2.28 mm and 0.12 mm) as proliferative cells are observed in greater numbers towards the anterior of the SVZ (Falcao *et al.*, 2012). TdTomato$^+$ cell number was assessed as the number of tdtomato$^+$ cells per unit length (mm) of the SVZ along the lateral ventricle (Fig. 1.5). Large numbers of tdTomato$^+$ cells were observed in the SVZ of *tdTomato$^{f/+}$;NestinCreER* mice, but no significant difference was observed in tdTomato$^+$

cell density (cells per mm length) between mice exposed to normoxia or hypoxia (10% oxygen) for 28 days (Fig. 1.5A). To assess whether hypoxia induced this population to migrate into the adjacent parenchyma, tdTomato$^+$ cell density was assessed in the adjacent SVZ-striatum. A few tdTomato$^+$ cells were observed in the striatum immediately adjacent to the SVZ (white arrows, Fig. 1.5A), although no significant increase in the density of these cells was observed in mice exposed to hypoxia.

Next, tdTomato expression was examined in the SVZ and striatum of *tdTomato$^{f/+}$;GFAPCreER* mice. Numerous tdTomato$^+$ cells were observed in the SVZ of *tdTomato$^{f/+}$;NestinCreER* mice, although fewer cells were labelled than under the *NestinCreER* promoter. Unlike the *NestinCreER* line, large numbers of tdTomato$^+$ cells were observed in the adjacent parenchyma, consistent with the reported expression of GFAP in striatal astrocytes (Fig. 1.5B) (Doetsch *et al.*, 1999). No significant increase in tdTomato$^+$ cell number or density was observed in the SVZ or SVZ-striatum of *tdTomato$^{f/+}$;GFAPCreER* mice exposed to 28 days of chronic hypoxia relative to normoxic controls (Fig. 1.5B). The downstream destinations of migrating SVZ neurons: the rostral migratory stream and olfactory bulb, were also assessed and no significant increase in labelled cell number was observed after hypoxia treatment (data not shown).

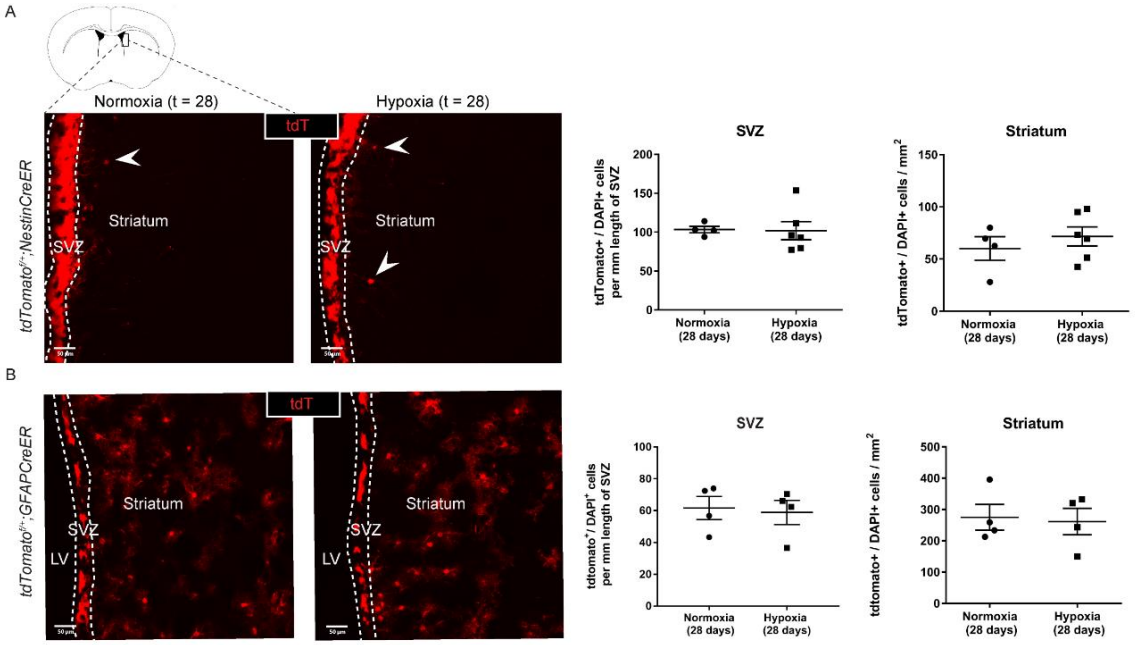


Figure 1.5. The effects of hypoxia on tdTomato$^{f/+}$ lineage labelled populations in the SVZ and striatum.

Representative images and morphometric analyses of tdTomato lineage labelled mice. Characterization and quantification of tdTomato fluorescence (red) in the SVZ (outlined with white dashes) and adjacent striatum (labelled) of hypoxic mice (28 days at 10% oxygen) *versus* normoxic controls (28 days normoxia) in A) n = 5 *tdTomato$^{f/+}$;NestinCreER* mice and B) n = 4 *tdTomato$^{f/+}$;GFAPCreER* mice. Migratory cells originating from the SVZ in the striatum of *tdTomato$^{f/+}$;NestinCreER* are labelled with white arrows.

Values shown are the mean ± SEM. LV = lateral ventricle. SVZ = subventricular zone. Scale bars = 50 µm.

The effect of chronic hypoxia on proliferation in lineage labelled populations in the subventricular zone.

To assess whether hypoxia resulted in any overall increase in proliferation within the niche, regardless of cell type, mice were treated with the thymidine analogue BrdU for the duration of the experimental period (Fig. 1.3B) and BrdU incorporation was examined in the SVZ and SVZ-striatum of normoxic *versus* 28-day chronic hypoxic mice. Consistent with the SVZ's role as a germinal niche, a high level of BrdU incorporation was observed within the SVZ in both normoxia and chronic hypoxia (Fig 1.6). $BrdU^+$ cell number per mm length was not found to significantly increase in the SVZ after chronic hypoxic exposure. However, a significant increase in BrdU incorporation after hypoxia was observed in the adjacent SVZ-striatum (Fig. 1.6). To assess whether this proliferative response originated from the labelled NSC populations of the SVZ, the colocalisation of BrdU with tdtomato was examined in both the *tdTomato$^{f/+}$;GFAPCreER* and *tdTomato$^{f/+}$;NestinCreER* lines. Although many $BrdU^+$ /$tdTomato^+$ cells were observed within the SVZ itself, only ~3% of striatal $BrdU^+$ cells co-labelled for tdtomato in hypoxic *tdTomato$^{f/+}$;GFAPCreER* mice, and no striatal $BrdU^+$ cells were observed to express tdTomato in *tdTomato$^{f/+}$;NestinCreER* (Fig. 1.5 A&B). This lack of co-labelling suggests that the hypoxia-induced proliferation observed in the striatal region adjacent to the SVZ does not originate from either labelled cell population in the SVZ, instead likely representing a separate population in which hypoxia did promote proliferation. Studies have shown that parenchymal structures (including the striatum) contain dormant neuronal precursors which proliferate in response to brain-derived neurotrophic factor (BDNF) and basic fibroblast growth factor (FGF-2) (Palmer *et al.*, 1995; Pencea *et al.*, 2001). This population of dormant precursors is a likely origin of the proliferative response.

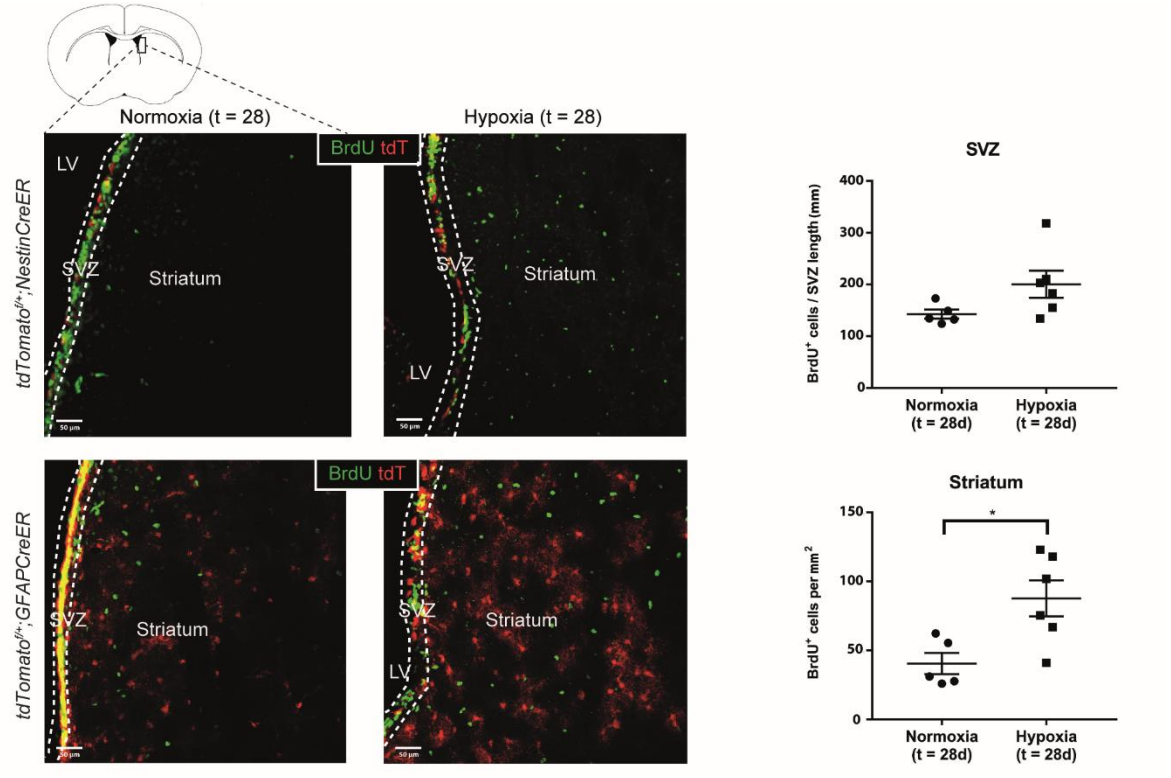


Figure 1.6. Assessment of BrdU proliferation in the SVZ and striatum of tdTomato$^{f/+}$ *NestinCreER* and *GFAPCreER* lineage labelled mice.

Characterization of tdTomato fluorescence (red) with BrdU (green) immunostaining in the SVZ (white edges) and adjacent striatum (labelled) of hypoxic mice (28 days at 10% oxygen) *versus* normoxic controls (28 days normoxia) in A) n = 6 *tdTomato$^{f/+}$;NestinCreER* mice and B) n = 6 *tdTomato$^{f/+}$;GFAPCreER* mice. C) Quantification of BrdU^{+} cells in the striatum and SVZ of normoxic *versus* hypoxic mice. Values shown are the mean ± SEM. LV = lateral ventricle. SVZ = subventricular zone. Scale bars = 50 µm. $* P < 0.01$.

The effect of PHD2 inactivation on lineage labelled populations in the subventricular zone.

It is possible that, although the hypoxic stimulus used in this study is insufficient to induce proliferation in SVZ NSCs, these cells may respond to 'pseudohypoxia', a state in which cells express hypoxia-induced genes and proteins, regardless of actual oxygen availability. Pseudohypoxia can be induced through stabilisation of the HIF family by genetic inactivation of PHD2, the dominant isoform of the regulatory PHD family, which has been shown to drive a pseudohypoxic response in tumour and stem cell populations (Bratslavsky *et al.*, 2007). PHD inhibitors have been developed for clinical use, and some studies have indicated that they have a protective effect on the response of the brain to stroke or ischemic damage (Harten *et al.*, 2010; Ogle *et al.*, 2012). It is possible that this improved response may be due to a pseudohypoxic stimulation of the SVZ stem cell niche.

To examine whether pseudohypoxia is capable of stimulating expansion of the SVZ stem cell population directly, our study also assessed the effect of inducible PHD2 inactivation upon the SVZ stem cell population in lineage labelled *Phd2$^{f/f}$;tdTomato$^{f/+}$;NestinCreER* and *Phd2$^{f/f}$;tdTomato$^{f/+}$;GFAPCreER* mice. Mice were treated with tamoxifen to induce PHD2 inactivation in the target cell types and were assessed 8 weeks after tamoxifen treatment. No significant expansion of the tdtomato^{+} population was observed in either the SVZ or the striatum of *Phd2$^{f/f}$;tdTomato$^{f/+}$;NestinCreER* or *Phd2$^{f/f}$;tdTomato$^{f/+}$;GFAPCreER* mice relative to littermate controls (Fig. 1.7).

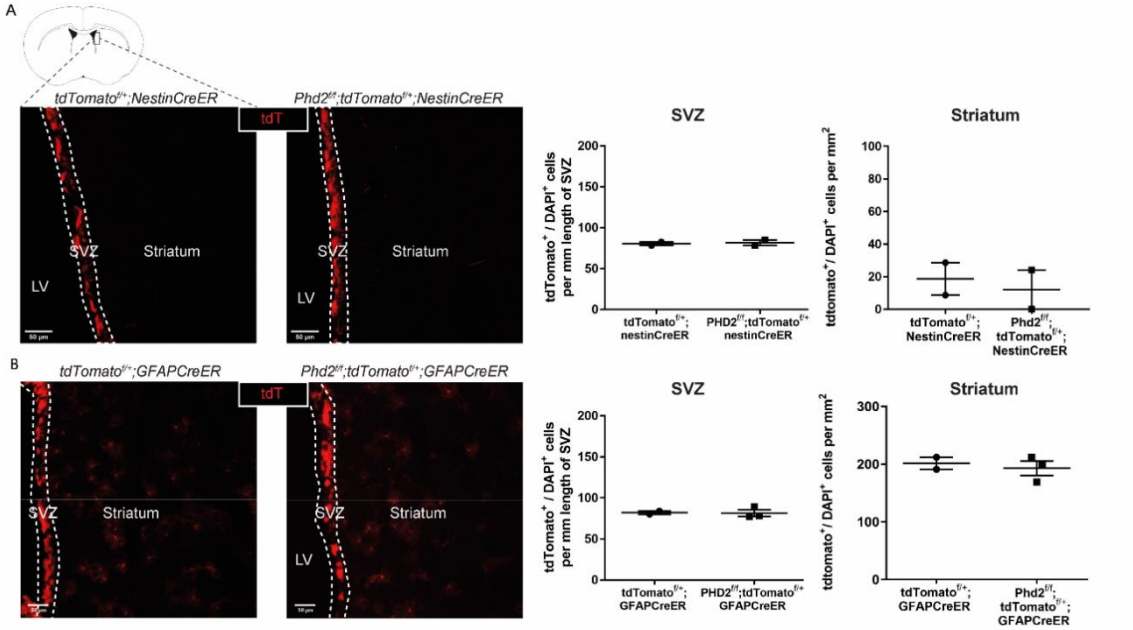


Figure 1.7. The effects of PHD2 inactivation upon the *NestinCreER* and *GFAPCreER* labelled populations in the SVZ.

Representative images and morphometric analyses of lineage labelled populations in the SVZ and striatum of tamoxifen treated A) *n = 2 Phd2$^{f/f}$;tdTomato$^{f/+}$;NestinCreER* and littermate *tdTomato$^{f/+}$;NestinCreER* controls and B) *n = 3 Phd2$^{f/f}$;tdTomato$^{f/+}$;GFAPCreER* and littermate *tdTomato$^{f/+}$;GFAPCreER* controls harvested at 3 months old, 8 weeks after tamoxifen treatment.
Values shown are the mean ± SEM. LV = lateral ventricle. SVZ = subventricular zone.

The effect of chronic hypoxia on lineage labelled populations in the dentate gyrus.

The dentate gyrus (DG) of the hippocampus is the other primary germinal region of the adult brain. The radial glia-like and nonradial stem cells of the dentate gyrus are reported to be marked by GFAP and nestin (Doetsch, 2003; Lagace *et al.*, 2007; Benarroch, 2013). DGs from *tdTomato$^{f/+}$;NestinCreER* and *tdTomato$^{f/+}$;GFAPCreER* mice were assessed for tdtomato$^+$ expression and BrdU$^+$ incorporation following exposure to 28 days of chronic hypoxia (Fig. 1.8). TdTomato$^+$ cells were observed in the subgranular zone of the dentate gyrus in *tdTomato$^{f/+}$;GFAPCreER* and *tdTomato$^{f/+}$;NestinCreER* mice (Fig. 1.8A). No significant increase in labelled tdTomato cell numbers per unit area (mm^2) was observed

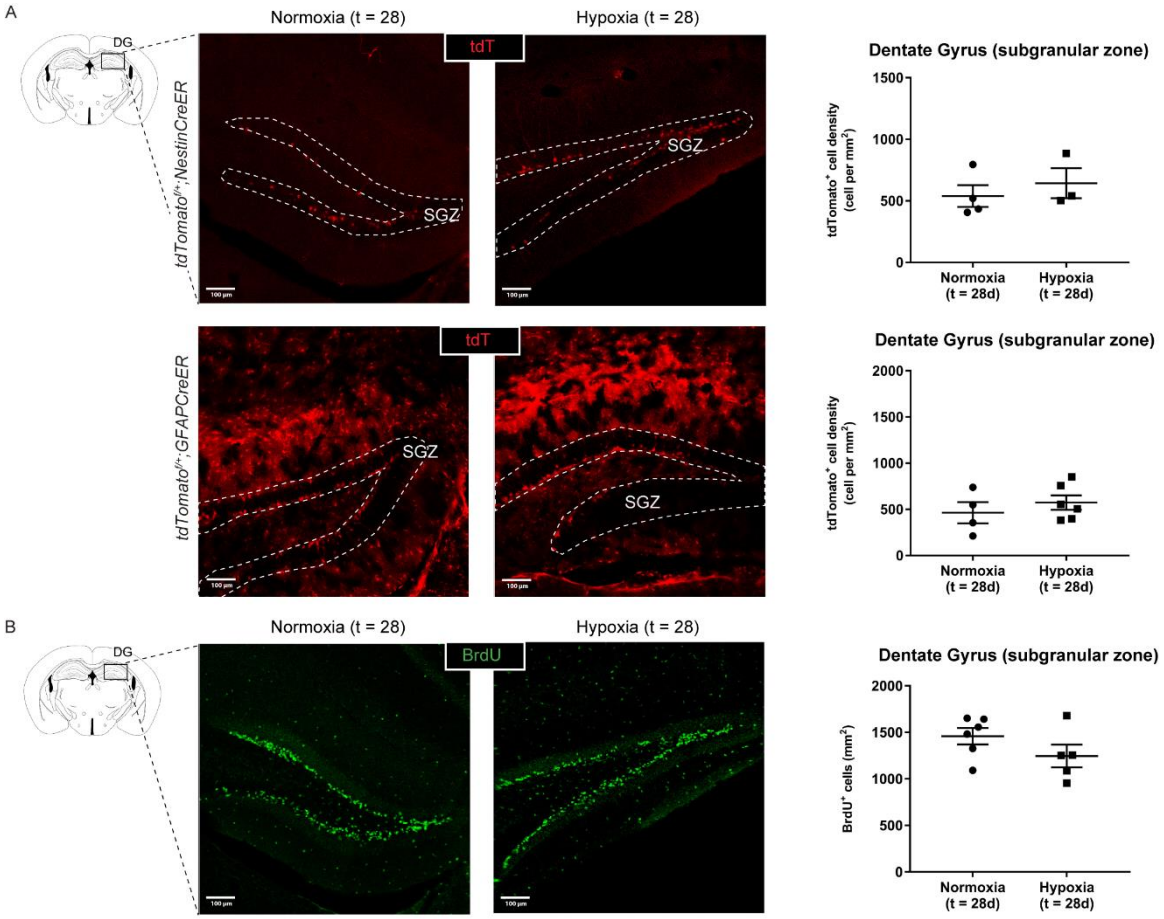


Figure 1.8. The effects of hypoxia on of *tdTomato$^{f/+}$;NestinCreER* and *GFAPCreER* lineage labelled populations in the Dentate Gyrus.

Representative images and morphometric analyses of tdTomato lineage labelled cell populations in the subgranular zone (SGZ, edges marked in white) of the dentate gyrus (DG) from chronic hypoxic mice (28 days at 10% oxygen) *versus* normoxic controls (28 days normoxia). tdTomato positive (Red) cells are also visible in the adjacent parenchyma, likely representing non-proliferative GFAP positive parenchymal astrocytes.

A) n = 4 *tdTomato$^{f/+}$;NestinCreER* mice, top, and n =6 *tdTomato$^{f/+}$;GFAPCreER* mice, middle.

B) quantification of BrdU (green) immunostaining in the subgranular zone of the dentate gyrus, showing BrdU$^+$ cells per mm^2 of dentate gyrus.

Values shown are the mean ± SEM.

between mice exposed to 28-day chronic hypoxia exposure (10% oxygen) *versus* normoxia in either lineage (Fig. 1.8A). Similarly, high levels of BrdU incorporation was observed in the subgranular zone of the dentate gyrus. However, no significant increase in $BrdU^+$ incorporation was observed between hypoxia and normoxia treated mice (Fig. 1.8B).

Discussion:

Whilst the effects of combined focal ischemia and hypoxia upon adult neural stem cell niches have been widely studied, the effect of chronic hypoxia alone is relatively uncharacterised *in vivo*. This chapter investigated whether 28 days of chronic hypoxia exposure was sufficient to induce expansion, proliferation or migration of the two primary neural stem cell populations ($GFAP^+$ and $nestin^+$ cells) in two CNS stem cell niches, the SVZ and SGZ, using two fluorescent reporter lineage tracer lines. Strong expression of tdTomato was observed under both the *NestinCreER* and *GFAPCreER* promoters in both SVZ and dentate gyrus and both these lineages co-labelled with proliferating ($BrdU^+$) cells within the SVZ and SGZ. However, no significant increase in proliferation or migration was observed in either labelled lineage in response to chronic hypoxia in either the SVZ or the SGZ. A statistically significant increase in proliferating ($BrdU^+$) cells in the adjacent striatum was observed, but these cells did not originate with either of the labelled lineages studied. This suggests that the proliferating cell population observed represents a proliferative population which is independent of the SVZ lineage, rather than a migratory population moving into the striatum from the SVZ.

The results of this chapter suggest that chronic hypoxia exposure does not promote proliferation or expansion of the SVZ or dentate gyrus stem cell populations. Although this contrasts with the pro-proliferative effects of hypoxia upon stem cells *in vitro*, this is

consistent with studies showing that the SVZ stem cell niche is resistant to some aspects of hypoxic exposure (Ross *et al.*, 2012; d'Anglemont de Tassigny *et al.*, 2015). Moreover, more severe hypoxia has been shown to have a degenerative, instead of mitogenic, effect on the SVZ: d'Anglemont de Tassingy *et al*. showed that long-term (23 day) exposure to 8% O_2 led to a marked degeneration and disarrangement of the SVZ niche, with the displacement of neurons, thinning of the capillary walls and a particular effect upon the ependymal cell layer, which was not labelled in this current study (d'Anglemont de Tassigny *et al.*, 2015). These authors also reported that this *in vivo* treatment reduced the viability of SVZ NSCs in subsequent *in vitro* culture, a result that contrasts with the findings of Ross *et al.* that a milder, alternating hypoxia treatment enhances the viability of the same stem cell population in producing successful cultures (Ross *et al.*, 2012; d'Anglemont de Tassigny *et al.*, 2015).

Despite the lack of hypoxia-induced proliferation observed in this study, it is possible that the stem cells of the SVZ and dentate gyrus are sensitive to the HIF pathway, which is thought to be the common mediator of hypoxic responses across multiple stem cell populations (Mohyeldin *et al.*, 2010). Indeed, recent studies have implicated a role for HIF-1α in regulating NSC proliferation in normal physiology and stroke (Cunningham *et al.*, 2012). NSCs in both the SVZ and SGZ constitutively express HIF-1α, which has been shown to modulate the proliferation of these cells *via* Notch and Wnt signalling (Li *et al.*, 2009; Mazumdar *et al.*, 2010; Roitbak *et al.*, 2011). Inducible inactivation of HIF-1α in *Hif-1α$^{f/f}$;YFP;NestinCreER* mice resulted in a reduction in the accompanying SVZ vasculature and YFP^+ cells in the SVZ 45 days post TMX treatment, suggesting an impairment of SVZ niche function (Li *et al.*, 2014). The growth of *Hif-1α$^{f/f}$;YFP;NestinCreER* cells in culture was unimpaired, leading the authors to suggest that

the reduction in NSC function was a result of the reduction in SVZ vasculature, presumably *via* paracrine effects from the separate nestin^{+} population. Conversely, stabilisation of the HIF family by inactivation of the regulatory PHDs using PHD inhibitors has been shown to improve blood perfusion and cognitive ability after ischemic brain injury, which may originate from improved stem cell function in the NSC niches, in a HIF-1α dependent manner (Harten *et al.*, 2010; Cunningham *et al.*, 2012; Ogle *et al.*, 2012; Li *et al.*, 2014). These studies suggest that the HIF-1α-PHD couple does play an important role in function of the SVZ and SGZ.

In order to investigate this, this study attempted to stabilise the HIF family *via* PHD2 inactivation (inducing a state known as 'pseudohypoxia') in conjunction with the lineage tracer lines under the GFAPCreER and NestinCreER promoters. However, no major expansion or change in the labelled populations was observed in either cell type after PHD2 inactivation in these mice. It is possible that pseudohypoxia *per se* is insufficient to induce a HIF-mediated response from the SVZ without other growth stimuli. Moreover, although our study used pseudohypoxia and hypoxia to stimulate the SVZ, we did not directly demonstrate an effect on HIF activation. Thus, future work could use immunohistochemical or in situ hybridisation approaches to directly assess HIF-1α and HIF-2α levels in the niche. Further research could also examine the vasculature of the SVZ niche to determine whether vascular remodelling /stability is the major hypoxia sensitive component of the niche, as suggested by the results of Li *et al. (Li et al., 2014).* A second caveat to these results was the choice of lineage markers involved, since the astrocytic marker GFAP labels both NSCs and differentiated glia, making it hard to distinguish between progeny of the SVZ and pre-existing mature neurons. For the moment, no cell type marker exists that can distinguish between differentiated glia and the immature stem

cells of the SVZ and SCG (Zurkirchen & Sommer, 2017).

Although this study observed no statistically significant expansion of either labelled lineage in response to chronic hypoxia in either the SVZ or the dentate gyrus, it did note an increase in BrdU incorporation within the parenchyma adjacent to the SVZ. These cells did not co-label with the labelled SVZ NSC cell lines, suggesting that this proliferative response to hypoxia in the striatum was a separate phenomenon, unrelated to the SVZ stem cell niche. This study did not positively identify these SVZ-striatal $BrdU^+$ cells, which would be of interest due to the apparent hypoxia-sensitivity of their proliferative response. These cells may represent striatal cell types indicated in the ischemic response to injury, such as medium spiny neurons (Liu *et al.*, 2009) or endothelial cells expanding in hypoxia induced angiogenesis, a population which has been suggested to be involved in the HIF-sensitivity of the adjacent niche (Li *et al.*, 2014). Further work could aim to positively identify these cells through other lineage tracer lines or co-localisation with cell type markers (anti-endomucin or CD31 for endothelial cells, anti-FoxP1 for medium spiny neurons) (Lertkiatmongkol *et al.*, 2016; Precious *et al.*, 2016). Despite this adjacent proliferative response, the results of this chapter suggest that the NSC populations of the SVZ and DG niches themselves did not proliferate in response to chronic hypoxia. This is a distinct difference from the hypoxia-induced proliferation observed in the carotid body, calling into question the extent to which it can be considered a parallel neural stem cell niche. To investigate this disparity, subsequent work in this thesis will seek to identify and then examine the responses of the carotid body NSCs to chronic hypoxia and pseudohypoxia

Results Chapter 2: Hypoxia induced proliferation in the carotid body: Type I and Type II cells

Introduction:

The carotid body is the primary peripheral oxygen sensor of the adult mammalian nervous system, responding to acute fluctuations in arterial PO_2 by stimulating a homeostatic hyperventilatory response (Euler *et al.*, 1940; Kay & Laidler, 1977; Kumar & Prabhakar, 2012). Unusually for a mature neuroendocrine tissue, the carotid body responds to chronic hypoxia by proliferating and expanding to several times its original size (Edwards *et al.*, 1971; Edwards *et al.*, 1972; Arias-Stella & Valcarcel, 1973). This expansion is associated with an increase in the size and sensitivity of the ventilatory response to acute hypoxia, known as ventilatory acclimatisation to hypoxia (VAH). Individuals living at altitude also suffer from an increased incidence (10-fold) of a neuroendocrine tumour, carotid paraganglioma (PGL), which otherwise occurs infrequently at sea level (1:1000,000), suggesting PGL may arise from un- or dis- regulated proliferation of the carotid body (Saldana *et al.*, 1973; Dua *et al.*, 2014). Although understanding the origin and mechanisms behind carotid body proliferation is thus of potential therapeutic benefit, it is still unknown which cell, or cells, are responsible for this proliferative response. The carotid body is a composite organ composed of multiple cell types including endothelial cells, fibroblasts, and two primary cell types: oxygen sensitive TH^+ Type I glomus cells and the $GFAP^+$ Type II astrocytes (see Introduction Figure 2). Although previous studies have interpreted the incorporation of nucleotide analogues into Type I cells as evidence that these cells are a proliferating population (Paciga *et al.*, 1999; Wang & Bisgard, 2002; Wang *et al.*, 2008), in recent years it has been proposed that these cells in fact originate from a subpopulation of the $GFAP^+$ astrocytes that are capable of acting as stem cells and

proliferating in response to chronic hypoxia (Kokovay & Temple, 2007; Pardal *et al.*, 2007).

This Stem Cell theory of the carotid body is based on the observation that lineage labelled $GFAP^+$ astrocytes give rise to tyrosine hydroxylase positive ($TH^{+)}$ cells and $nestin^+$ intermediates in *in vitro* neurosphere assays (Pardal *et al.*, 2007). This study also demonstrated that CB $GFAP^+$ cell numbers decrease in response to chronic hypoxia as $nestin^+$ cell numbers increase, followed by TH^+ cells also increasing in number across 16 days (Pardal *et al.*, 2007). Follow up studies also observed differentiation to endothelial and mesenchymal cell types, potentially contributing to the expansion of CB vasculature that is observed in chronic hypoxia (Annese *et al.*, 2017). These results were interpreted as evidence for a Stem Cell function of a subpopulation of $GFAP^+$ astrocytes which proliferate in response to signals from the oxygen sensitive Type I cells and give rise to rapidly amplifying $nestin^+$ intermediaries, which in turn differentiate to give rise to an expanded population of mature TH^+ Type I cells (Pardal *et al.*, 2007). However, the results supporting the Stem Cell theory may not be representative of the function of the niche in normal physiology: due to technical constraints (poor recombination of the LacZ-GFAPCreER promoter) the evidence for a primary role of the Type II cell largely stems from *in vitro* neurosphere assays or animals pre-exposed to hypoxia prior to examination to increase GFAP expression (Pardal *et al.*, 2007; Annese *et al.*, 2017). Moreover, the results of the previous chapter did not support the prediction that the stem cells of the CNS would respond to hypoxia in a similar manner to the proposed GFAP stem cells of the carotid body, further calling the Stem Cell theory of the carotid body into question.

As such, the question remains *in vivo* as to which cell populations of the carotid body are

involved in hypoxia induced proliferation, and to what extent each of these populations contribute to the overall response. To address this, the work presented in this chapter will use the fluorescent lineage labelled constructs employed in Chapter 1 to investigate the $GFAP^+$ Type II population and introduce a labelled THCreER line to investigate the TH^+ Type I cell population. Due to very low recombination in the *tdTomato$^{f/+;}$nestinCreER* mouse and the transient nature of the $nestin^+$ population in the carotid body, this approach was not suitable for investigating this population. This chapter will characterize these Type I and Type II specific lineage tracers in the carotid body (and other tissues), then use them to identify the proliferative response of these cell populations to a chronic hypoxic exposure. Finally, this chapter will use additional techniques such as EM microscopy and in situ hybridisation to further characterize the carotid body's response to chronic hypoxia.

Results:

Characterisation of Type I and Type II cell specific lineage tracers in the carotid body.

To address which population(s) of cells expands in response to chronic hypoxia, this study employed a fluorescent reporter gene, tdTomato Ai14, to label the two primary cell populations of the carotid body: TH^+ Type I and $GFAP^+$ Type II cells. The tdTomato Ai14 was selected for this study due to its strong fluorescence relative to other fluorescent reporters such as EYFP or ZSGreen (Madisen *et al.*, 2010). This fluorescent reporter was recombined into a ubiquitously expressed modified Rosa26-CAG vector and then activated by the excision of the STOP cassette from a LoxP-STOP-LoxP sequence by expression of tamoxifen-inducible Cre recombinase under the control of a TH or GFAP promoter as described in the previous chapter (Fig. 1.3). The THCreER construct chosen for this study

has been shown using a LacZ reporter system to be restricted in its expression to the Type I cell population within the CB (Macias *et al.*, 2014). GFAP is widely expressed in astrocytes (Hirrlinger *et al.*, 2006), and has confirmed expression in the Type II cells of the carotid body, leading to the choice of the GFAPCreER promoter (Nurse & Fearon, 2002; Kameda, 2005; Pardal *et al.*, 2007). Previous studies have demonstrated strong recombination of the *tdTomato$^{f/+}$;GFAPCreER* line in astrocytes within the CNS (Mich *et al.*, 2014; Park *et al.*, 2018).

To ensure recombination and expression of the lineage reporter, each reporter gene was activated by administration of tamoxifen for 5 days followed by a 'washout' period of 5 days (ending at 't = 0') to allow clearance of the drug, following the same experimental design used in Chapter 1 (Fig. 1.3). This clearance minimized recombination during the exposure to chronic hypoxia, ensuring that any labelled cells represented the original Type I and Type II populations. To ensure the integrity of this experimental design, a number of control experiments were conducted. First, the expression of the lineage markers was confirmed to be correctly restricted to tamoxifen treated animals. Carotid bodies from non-tamoxifen treated *tdTomato$^{f/+}$;THCreER* and *tdTomato$^{f/+}$;GFAPCreER* animals were assessed for tdtomato expression and no signal was observed. Because the TH gene is reportedly induced by chronic hypoxia (Hanbauer, 1977; Czyzyk-Krzeska *et al.*, 1992a; Nurse & Fearon, 2002; Schnell *et al.*, 2003), this study also sought to confirm that hypoxia was not sufficient to induce expression of the lineage tracer. To confirm this, non-tamoxifen treated *tdTomato$^{f/+}$;THCreER* and *tdTomato$^{f/+}$;GFAPCreER* were exposed to 28 days of chronic hypoxia. No fluorescent cells were observed in these mice (Fig 2.1A &B).

Next, this study sought to confirm the lineage specificity of each lineage line prior to the

experimental hypoxia exposure. To do this, animals were examined after exposure to 5 days of tamoxifen followed by 5 days of 'wash-out', at a time equivalent to the beginning of hypoxic /normoxic exposure in subsequent experiments (t = 0). At this time point, carotid bodies from *tdTomato$^{f/+}$;THCreER* mice contained large numbers of tdTomato^{+} cells that could be defined as Type I cells through both morphology (large round cells with large rounded nuclei, glomerular architecture) and double labelling with immunohistochemistry for the Type I cell marker Tyrosine hydroxylase (TH^{+}) (Fig. 2.1C). To estimate recombination efficiency, the ratio of tdTomato^{+}-TH^{+} double positive cells to TH^{+} cells was assessed. TH is a cytoplasmic protein, and thus TH^{+} cells appear with green cytoplasm and an empty "ghosted" nucleus. Co-labelling of the fluorescent tdTomato reporter with TH was assessed through both the presence of colocalisation of the tdTomato and TH antibody fluorescent signals (seen as a yellow perinuclear halo in the cytoplasm around the nucleus) and through the use of planar Z-stack analyses to confirm specific cellular identities. Twenty images from each of three pairs of CBs were analysed, and it was observed that ~80% of TH^{+} cells were tdTomato^{+} (Fig. 2.1C*)* indicating a high efficiency of recombination. TdTomato fluorescence was confined (>99%) to these TH^{+} Type I cells (Fig. 2.1C).

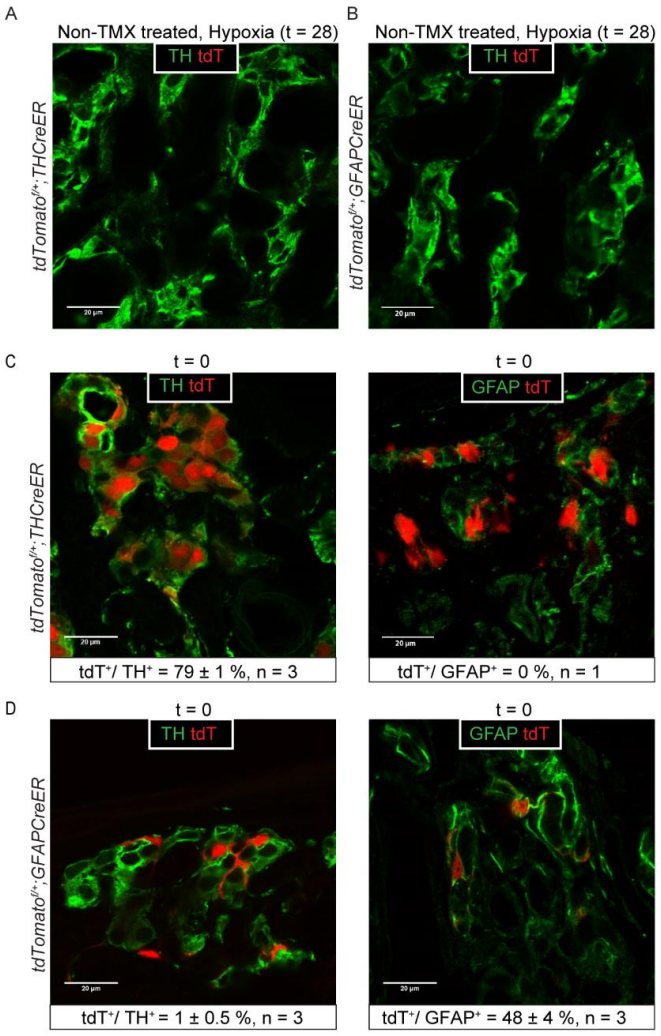


Figure 2.1. Characterization of Type I and Type II cell-specific lineage tracers in the carotid body.

A-B) The fluorescent lineage reporters for Type I and Type II cells are temporally controlled by tamoxifen treatment, and no fluorescence is observed in non-tamoxifen treated control animals. No colocalisation is seen of tdTomato expression (tdT, red) and TH immunostaining (TH, green) in A) n = 3 non-tamoxifen treated *tdTomato$^{f/+}$;THCreER* mice and B) n = 2 *tdTomato$^{f/+}$;GFAPCreER* mice exposed to hypoxia (28 days at 10% oxygen)

C-D) Each lineage line is then shown to be specific to the target cell type: immunostaining for a Type I cell marker (TH) or a Type II marker (GFAP) co-localises with the tdTomato (tdt, red) reporter after tamoxifen treatment. Representative images of C) n = 3 *tdTomato$^{f/+}$;THCreER* mice or D) n = 3 *tdTomato$^{f/+}$;GFAPCreER* mice immediately after tamoxifen 'wash-out' (t = 0). Estimates of recombination efficiency are presented below the relevant panels. Values shown are the mean ± SEM. Scale bars = 20 µm.

The GFAPCreER line was also shown to be specifically expressed in $GFAP^+$ astrocytes, with ~99% of tdtomato expression colocalising with $GFAP^+$, although only 48 ± 2% of the total $GFAP^+$ cell population expressed $tdTomato^+$ (Fig. 2.1D). Overall, fewer $tdtomato^+$ cells were observed than in *tdTomato$^{f/+}$;THCreER* mice, consistent with the fact that there are between 3 and 8 Type I cells per Type II cell in the carotid body, depending on species (De Kock, 1951, 1954; Kumar & Prabhakar, 2012). Both *tdTomato$^{f/+}$;THCreER* and *tdTomato$^{f/+}$;GFAPCreER* showed minimal differentiation to different cell types in normoxia: no $tdTomato^+$ /$GFAP^+$ cells were observed in *tdTomato$^{f/+}$;THCreER* CBs, whilst a small (<1%) number of $tdTomato^+$ /TH^+ cells were observed in *tdTomato$^{f/+}$;GFAPCreER* CBs. (Fig. 2.1C - D).

The effect of chronic hypoxia on lineage labelled carotid body Type I and Type II cells.

Having established the efficiency and specificity of the lineage tracers, the response of each labelled population to hypoxia was assessed by exposing each cohort of mice to 28 days of chronic hypoxia (10% oxygen) or normoxia. Similar time points have been shown to result in a maximal expansion of the carotid body in the literature (Laidler & Kay, 1975; Dhillon *et al.*, 1984; McGregor *et al.*, 1984). These results were replicated in this study: carotid bodies from chronic hypoxic mice were significantly expanded (~3.5 fold) in volume relative to normoxic CBs, as estimated using TH^+ Type I cells to mark the boundary of the carotid body (CB marked in white, 0.00690 ± 0.00056 mm^3 *versus* 0.00191 ± 0.00039 mm^3 in hypoxic *versus* control animals, $P < 0.0001$). (Fig. 2.2A). To assess the behaviour of the Type I cell population, tdTomato expression was assessed in *tdTomato$^{f/+}$;THCreER* exposed to this experimental protocol and was observed to be

significantly increased in hypoxic CBs (2260 ± 214 *versus* 745 ± 50 cells per CB, $P < 0.0001$) (Fig. 2.2B). The expansion in carotid body volume (~3.5 fold) was relatively proportional to that of Type I cell number (~3 fold), resulting in no significant change to the density of Type I cells in these animals (Fig. 2.2B, right panel). To define the response of the Type II cell population, tdTomato expression was also assessed in carotid bodies from tamoxifen treated *tdTomato*$^{f/+}$*;GFAPCreER* mice exposed to 28 days of hypoxia /normoxia. This population was also observed to expand in response to chronic hypoxia *versus* normoxia (258 ± 33 *versus* 145 ± 10 tdTomato^{+} cells per CB, $P < 0.01$) (Fig. 2.3C). This expansion was considerably smaller than the Type I cell expansion (~2 fold *versus* ~3.5 fold) and, due to the increase in volume of the carotid body itself, resulted in a significant decrease in density of labelled tdTomato cells (274 ± 22 *versus* 475 ± 39 tdTomato^{+} cells mm^{-2}, $P = 0.0005$) (Fig. 2.2C, right panel).

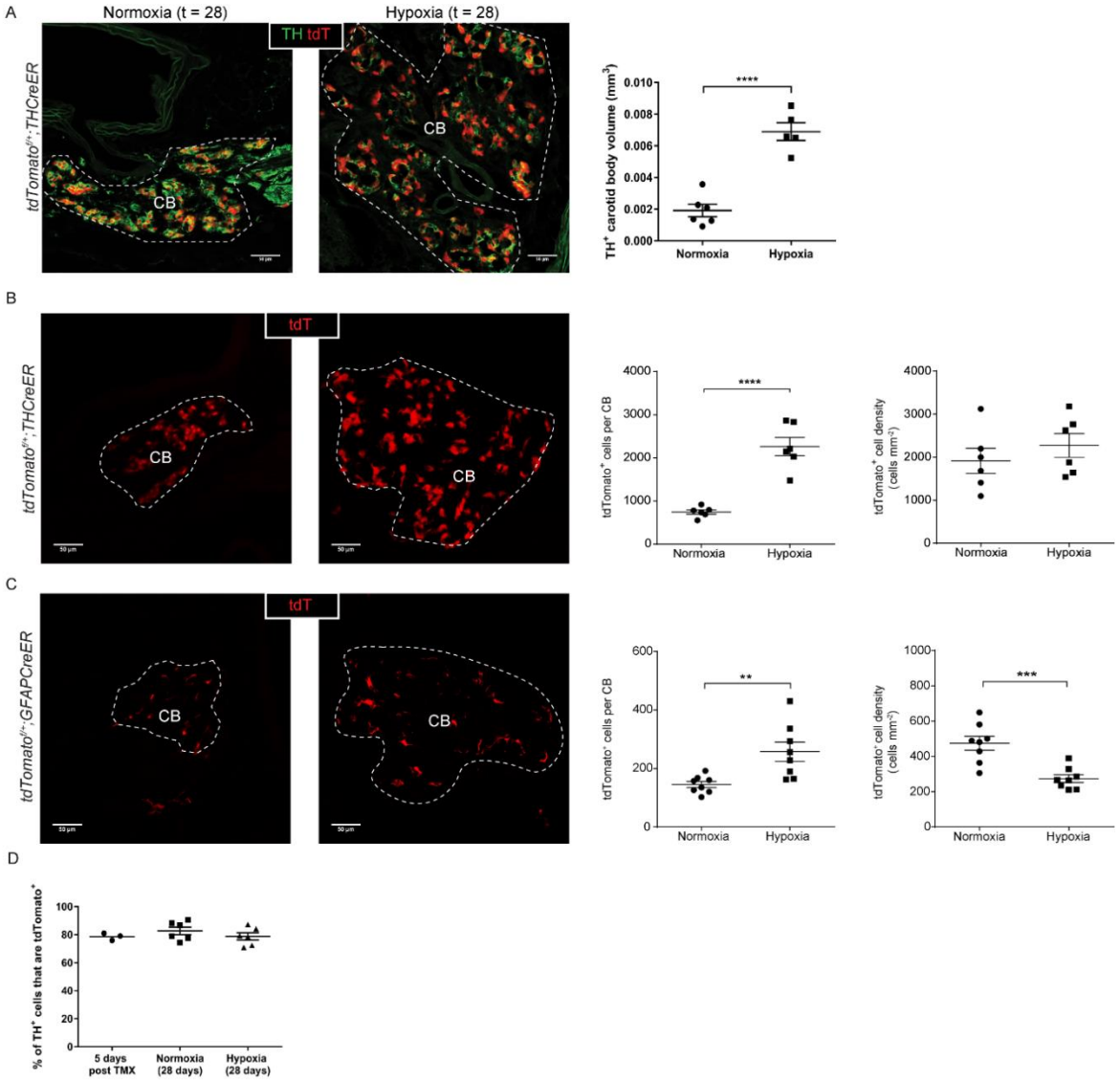


Figure 2.2. The effect of chronic hypoxia on lineage labelled Type I and Type II cells in the CB.

Representative images and quantification of CBs (CB edge outlined in white) of *tdTomato*$^{f/+}$*;THCreER* and *tdTomato*$^{f/+}$*;GFAPCreER* mice.

A) Quantification of carotid body volume, as indicated by TH^+ immunostaining (TH, green) in n = 6 *tdTomato*$^{f/+}$*;THCreER* hypoxic (28 days at 10% oxygen) *versus* normoxic controls (28 days normoxia). The carotid body (outlined in white) expands significantly in volume.

B - C) Representative images and quantification of tdTomato fluorescence (tdT, red) in hypoxia (28 days at 10% oxygen) *versus* normoxic controls in B) n = 6 *tdTomato*$^{f/+}$*;THCreER* mice and C) n = 8 *tdTomato*$^{f/+}$*;GFAPCreER* mice.

D) Quantification of the % of recombined cells under the *tdTomato$^{f/+}$;THCreER* promoter immediately after tamoxifen treatment (t = 0) and after 28 days of normoxic or hypoxic exposure. Recombination is assessed as % of TH$^+$ cells that are also tdTomato$^+$. The % of recombined cells was consistent between conditions, suggesting no additional populations contributed to this proliferative hyperplasia.
Values shown are the mean ± SEM. Scale bars = 50 µm. ** $P < 0.01$, *** $P < 0.001$, **** $P < 0.0001$.

Morphological and immunohistochemical analysis with an anti-tyrosine hydroxylase antibody found that >99% of the expanded tdTomato$^+$ cell population in *tdTomato$^{f/+}$;THCreER* mice remained TH$^+$, suggesting that there was little differentiation of this population (Fig. 2.2B). The proportion of TH$^+$ cells that expressed tdTomato remained constant (~80%) in animals exposed to 28 days of chronic hypoxia relative to normoxic controls and animals at t = 0, indicating that recombination efficiency and labelling was not significantly affected by chronic hypoxia exposure (Fig. 2.2D). In hypoxic *tdTomato$^{f/+}$;GFAPCreER* mice, a few instances of tdTomato$^+$ /TH$^+$ cells were observed, however these cells were rare (<0.5% of assessed cells). This suggests that substantial transdifferentiation of the Type II labelled population into Type I cells (and other cell types) is not a significant factor in the carotid body hyperplastic response to chronic hypoxia under these experimental conditions.

The effect of chronic hypoxia on proliferation in lineage labelled carotid body cells.

To confirm whether this observed expansion was proliferative, mice were treated with BrdU throughout their exposure to 28 days of hypoxia or normoxia. In normoxia, a low level of BrdU incorporation was observed, consistent with the carotid body's function as a quiescent stem cell niche (Fig 2.3). No BrdU$^+$ /TH$^+$ double positive cells were observed in

normoxia and the majority of $BrdU^+$ cells appeared morphologically to be astrocytes or endothelial cells (Fig. 2.3). In response to hypoxia, BrdU incorporation increased in the carotid body. Consistent with the observed expansion of the Type I cell population, many TH^+ /$BrdU^+$ cells were observed in *tdTomato$^{f/+}$;THCreER*. In particular, many TH^+ /$tdTomato^+$ /$BrdU^+$ cells were observed, suggesting Type I cells are capable of proliferation (Fig. 2.3). $TdTomato^+$ /$BrdU^+$ cells were observed in *tdTomato$^{f/+}$;GFAPCreER* mice, representing proliferating Type II cells, but were infrequent. Whilst one third of $BrdU^+$ cells co-labelled with TH^+, a large proportion (40%) of the remaining proliferation in the carotid body co-localised with the endothelial cell marker endomucin (Fig 2.4, white arrows), consistent with reports of hypoxia induced angiogenesis in the carotid body (Laidler & Kay, 1975, 1978). Co-localised cells were defined as cells with cytoplasmic endomucin staining and nuclear BrdU staining.

This study observed a large increase in both overall $endomucin^+$ area and the % proportion of $endomucin^+$ vasculature in the carotid body (Fig 2.4, lower panels). Studies on the purported Type II stem cell population have indicated that these stem cells are capable of giving rise to endothelial cells in the carotid body (Annese *et al.*, 2017). However, no lineage labelled cells from either *tdTomato$^{f/+}$;GFAPCreER* or *tdTomato$^{f/+}$;THCreER* animals were observed to co-label with endomucin in this study, suggesting the observed endothelial proliferation and vascular expansion does not originate from either population (Fig 2.4). This staining was repeated using two other vascular makers, CD31 and isolectin, and replicated these results (data not shown).

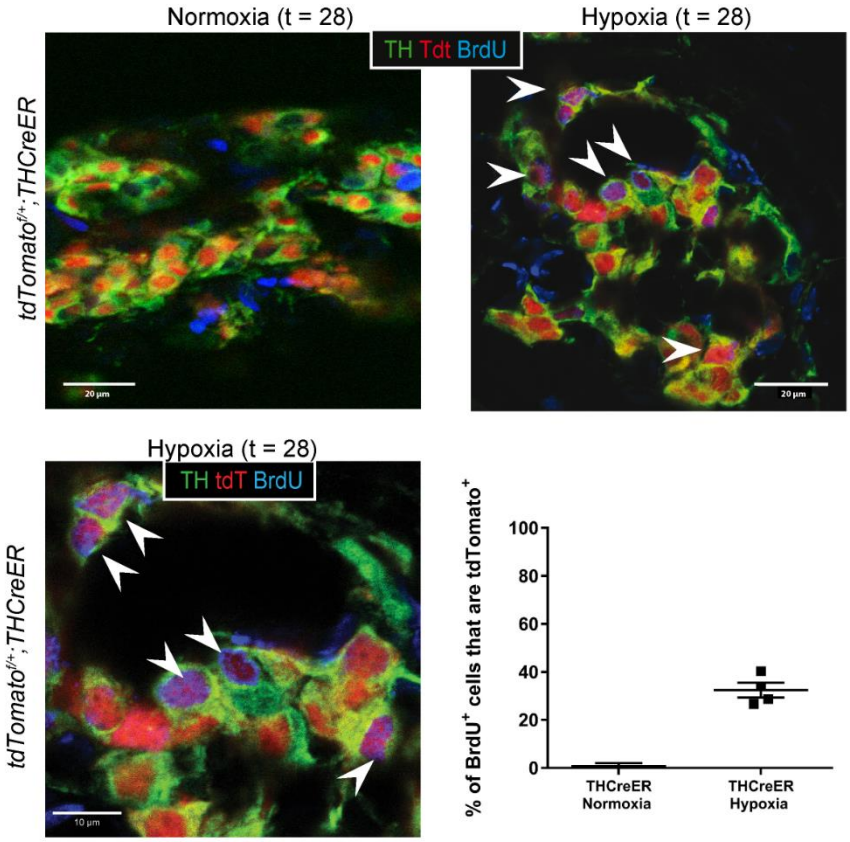


Figure 2.3. Hypoxia-induced proliferation within the carotid body.

Proliferation in Type I cells. Representative images of $BrdU^+$ (blue), TH^+ (green) immunostaining and tdTomato (red) fluorescence in hypoxia (28 days at 10% oxygen) *versus* normoxic controls. Colocalization of tdtomato and BrdU is seen in purple cells, marked with white arrow heads. High magnification is shown in the left-hand bottom panel. Proliferative Type I cells are only observed after chronic hypoxic exposure. Quantification of the proportion of BrdU cells that originate from the fluorescently labelled tdTomato lineage is shown in the right-hand bottom panel.

Values shown are the mean ± SEM. Scale bars = 20 µm (low mag), 10 µm (moderate mag) and 5 µm (high mag). ** $P < 0.01$, *** $P < 0.001$, **** $P < 0.0001$.

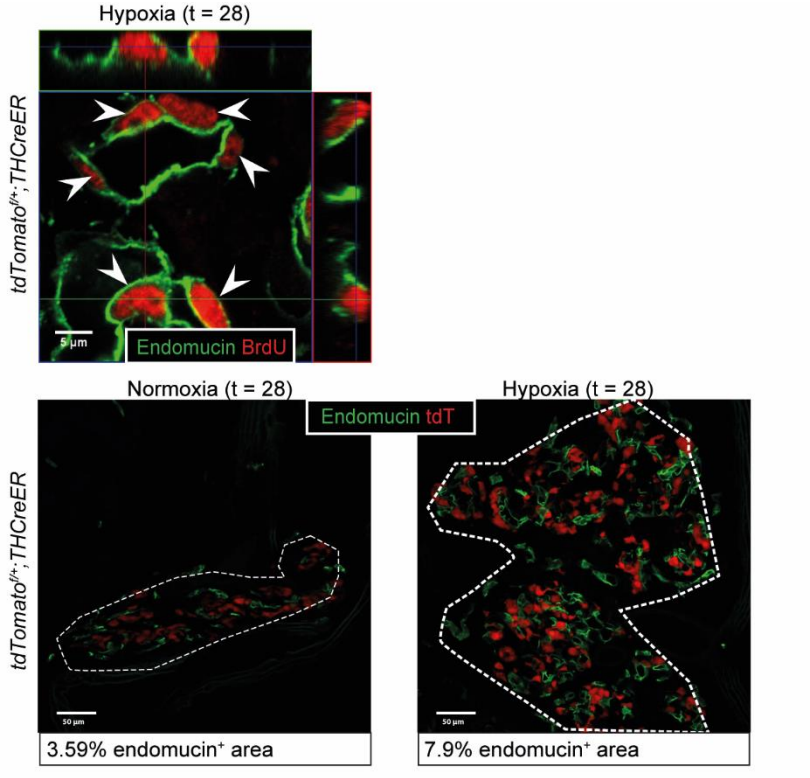


Figure 2.4. Hypoxia-induced neo-vascularization in the carotid body.
Angiogenesis and proliferation in endothelial cells. Top panel, endomucin (green) and BrdU (red) immunostaining in mice exposed to chronic hypoxia (28 days at 10% oxygen), indicating the presence of neo-vascularisation. Bottom panels, endomucin immunostaining (green) and tdTomato (red) expression in *tdTomato$^{f/+}$;THCreER* mice exposed to normoxia or chronic hypoxia. No overlap is observable between the lineage labelled THCreER Type I cells and endomucin^{+} cells.
Values shown are the mean ± SEM.

The effect of chronic hypoxia on carotid body ultrastructure.

In addition to their proliferation, Type I cells are reported to undergo hypertrophy in response to prolonged hypoxia (Wang & Bisgard, 2002). To confirm this, carotid bodies from chronic hypoxic mice were examined using electron microscopy, with Type I cells identified ultrastructurally *via* the presence of characteristic dense core vesicles (Kumar & Prabhakar, 2012). Measurement of Type I cell size found that hypoxia induced a

statistically significant increase in average cell size (48.88 ± 1.05 *versus* 63.38 ± 1.70 μm^2, $P = 0.0003$) (Fig. 2.5A). This analysis was repeated using confocal microscopy on previous samples, in order to examine whether this hypertrophy was affected by the proliferation and division of the Type I cell population. Cell size was compared between $BrdU^+/TH^+$ and $BrdU^-/TH^+$ cells, but no significant difference in size was observed.

Type I cells contain secretory dense core vesicles (DCVs), which contain neuropeptides released in response to hypoxic signals (Fig. 2.5; see inserts). This study observed marked changes in these DCVs after hypoxic exposure: hypoxic mice showed a marked reduction in DVC density *versus* normoxic controls (1.37 ± 0.14 *versus* 7.20 ± 0.25 DCVs μm^{-2}, $P < 0.0001$). The remaining DCV population was characterized by the appearance of enlarged DCVs with a lucent 'halo' around the electron dense core, hereafter referred to as 'eccentric' DCVs (Fig. 2.5A; right panel). It is possible that this 'eccentric' appearance represents a fixation artefact resulting from the reaction of the fixative with the DCV contents. Therefore, the occurrence of these eccentric DCVs may reflect a hypoxia-induced change in the neuropeptides packaged within. The electron microscope analysis also observed Type I cells (identified by their characteristic dense core vesicles) undergoing mitosis (Fig. 2.5B). This is consistent with the observation of proliferating Type I cells reported elsewhere in this chapter.

To further characterize the effect of hypoxia on Type I cell DCV density, this study tested the effect of a shorter (1 hour) hypoxic time course. In response to 1 hour of hypoxia (10% oxygen), DCVs migrated to the cell membrane, but no major differences in overall density were observed (Figure 2.6C).

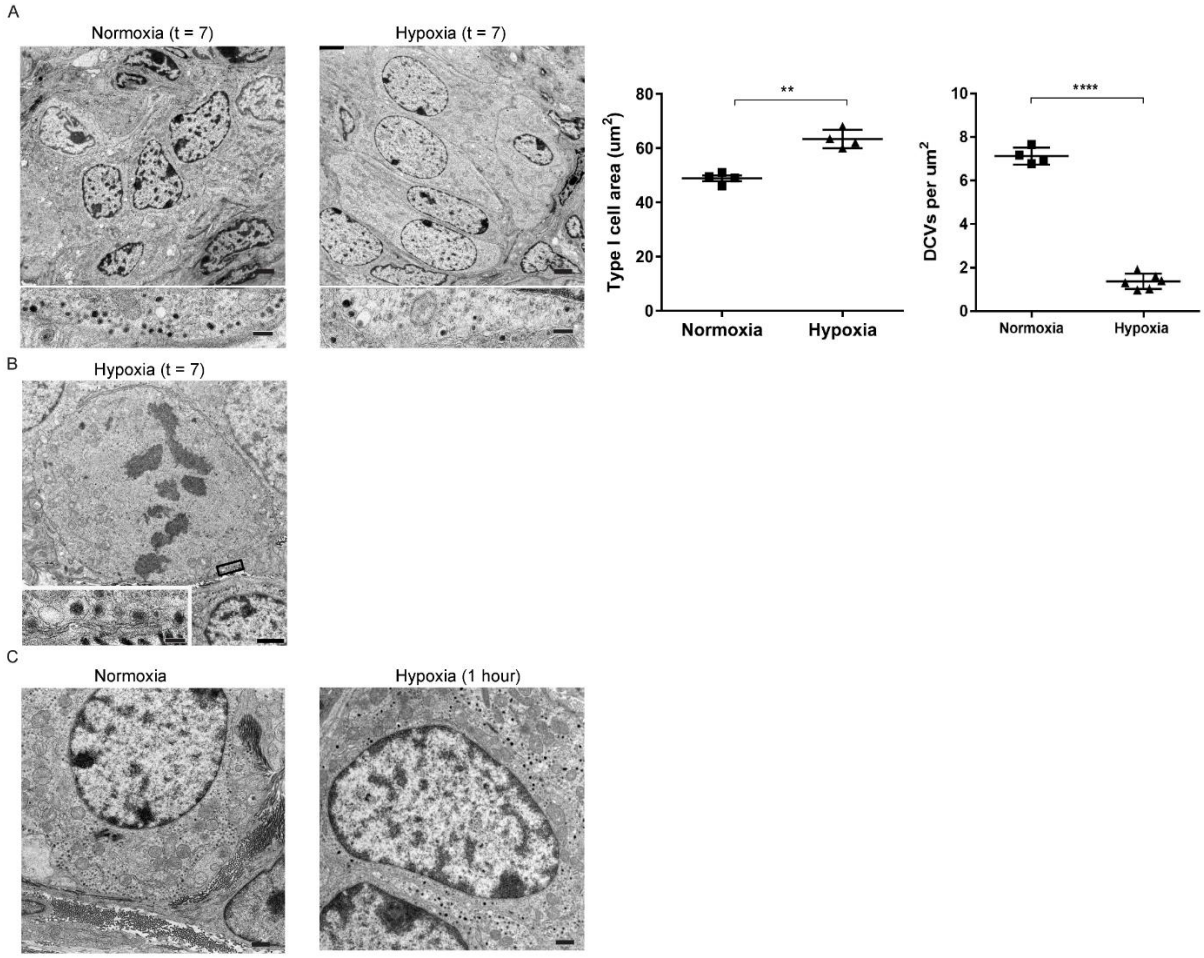


Figure 2.5. The effect of hypoxia on carotid body ultrastructure.

Electron microscopy imaging of carotid body ultrastructure.

A) Type I cell hypertrophy in response to chronic hypoxia. Type I cell identity was confirmed through the presence of dense core vesicles (DCVs; see insert). Morphometric analysis of carotid body Type I cell size and dense core vesicle density in n = 4 mice exposed to 7 days of chronic hypoxia (10% oxygen) versus normoxia. Scale bars = 2 µm (low power) and 200 nm (high power).

B) Electron microscopy image of a Type I cell (confirmed *via* the presence of DCVs; see insert) undergoing mitosis from a mouse exposed to 7 days of hypoxia. Scale bars = 1 µm (low power) and 100 nm (high power).

C) The effect of short term (1 hour) hypoxic exposure on Type I cells, showing a movement of DCVs to the cell membrane but no overall change in DCV appearance or density. Scale bars = 1 µm

The effect of chronic hypoxia on carotid body gene expression.

Several genes have been implicated in the CB's proliferative response to hypoxia and in paraganglioma formation, including endothelin-1, Cyclin D1 and Vegfa (Jyung *et al.*, 2000; Chen *et al.*, 2002; Prabhakar & Jacono, 2005; Pawar *et al.*, 2009; Kumar & Prabhakar, 2012; Hussain *et al.*, 2014). To confirm these reports and extend them to the level of mRNA expression in an intact system, this study performed *in situ* hybridisation for several key genes on tissues from mice exposed to 7 days of chronic hypoxia (10% oxygen). *In situ* hybridisation for mRNA expression was used because VEGFA and endothelin-1 are secreted proteins, making differences in expression hard to infer from standard immunohistochemistry. Although undetectable in normoxia, endothelin-1 is reportedly induced in hypoxic carotid body Type I cells and a potential promoter of proliferation in both Type I and Type II cells (Chen *et al.*, 2002; Platero-Luengo *et al.*, 2014). *In situ* hybridisation for *Edn1* found it was weakly expressed in most carotid body cells in hypoxic animals, although it was abundant in a few select cells (Fig. 2.6A). In contrast to previous reports of endothelin-1 expression in Type I cells (Paciga *et al.*, 1999), these *Edn1*$^{+}$ cells did not co-express TH (Fig. 2.6A) or GFAP (Fig. 2.6B), suggesting they belong to the endothelial population of the carotid body.

A key regulator of the cell cycle S1-G1 transition, Cyclin D1 (*Ccnd1*), was observed to be upregulated by hypoxic exposure, although overall expression was weak (Figure 2.6C). To confirm this result, quantitative RT-PCR was performed on pooled carotid bodies from 5 chronic hypoxic or normoxic mice, and a large increase in relative Cyclin D1 expression was observed (Fig. 2.6D).

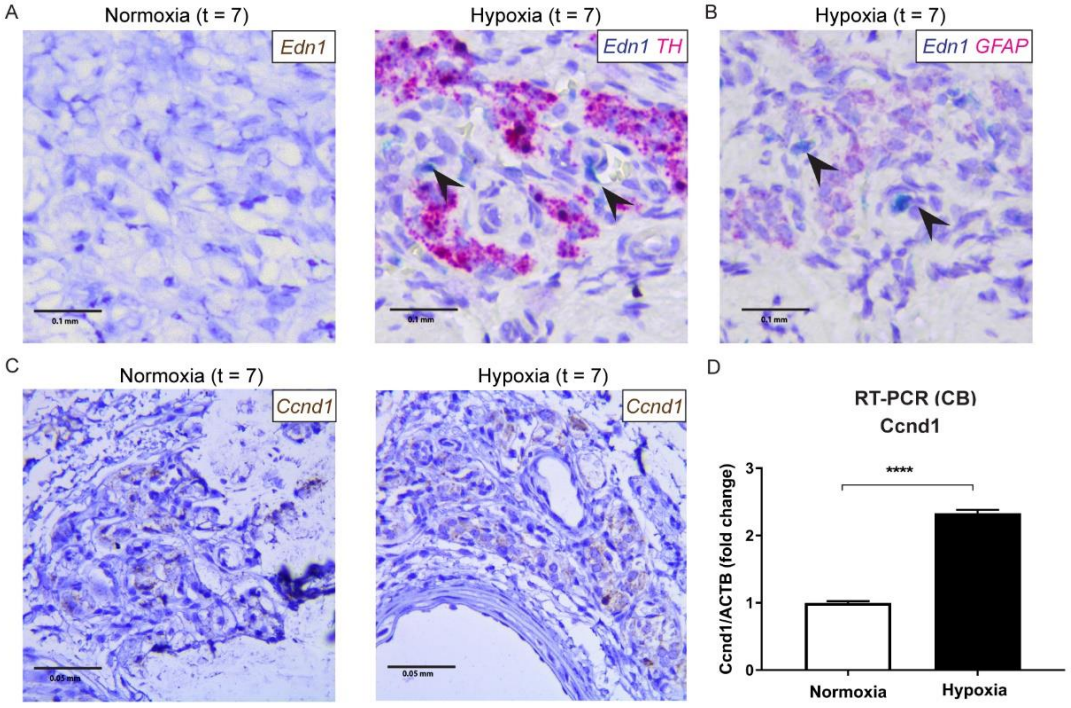


Figure 2.6. The effect of chronic hypoxia on mitogenic gene expression in the carotid body.

A-B) Representative images of *in situ* hybridisation of Endothelin1 (*Edn1*, blue) and A) *TH* (pink) or B) *GFAP* (pink) mRNA in carotid bodies from chronic hypoxic mice (7 days at 10% oxygen).

C) Comparative *in situ* hybridisation for Cyclin D1 (*Ccnd1*, brown) mRNA in carotid bodies from normoxic and hypoxic (7 days at 10% oxygen) wild-type mice, showing a hypoxia-induced increase in *Ccnd1* expression.

D) quantitative RT-PCR for cyclin D1 in homogenised carotid bodies from normoxic and hypoxic (7 days at 10% oxygen) wild-type mice.

**** $P < 0.0001$.

As discussed previously in this thesis, a major component of hypoxia-induced CB hyperplasia is an extensive neo-vascularisation of the carotid body. Neo-vascularisation and angiogenesis is driven by the expression and secretion of vascular endothelial growth factor A (*Vegfa). In situ* hybridisation for *Vegfa* mRNA showed a strong upregulation of *Vegfa* mRNA expression after hypoxic exposure (Fig. 2.7A). Quantitative RT-PCR on pooled carotid bodies replicated this result (Fig. 2.7B). *Vegfa* expression appeared to be localised to cells that were morphologically identifiable as Type I cells. To confirm this, dual *in situ* hybridisation and immunohistochemistry for TH was performed (Fig. 2.7C). These results support the idea that release of VEGFA by Type I cells may drive the observed vascular endothelial cell proliferation characterized in Figure 2.4. The carotid body is reported to contain two receptors for VEGFA: Flt-1, which is reported to mediate hypoxia-induced angiogenesis in the endothelial population, and FLK-1, which is thought to stimulate Type I cell hyperplasia (Jyung *et al.*, 2000; Chen *et al.*, 2003). mRNA for both of these genes was observed in normoxic carotid bodies (Figs. 2.8D-E). mRNA expression for the receptor Flk-1 appeared to be strongly induced in Type I cells by chronic hypoxia exposure (Fig. 2.7D), whilst Flt-1 expression was unaffected (Fig. 2.7D).

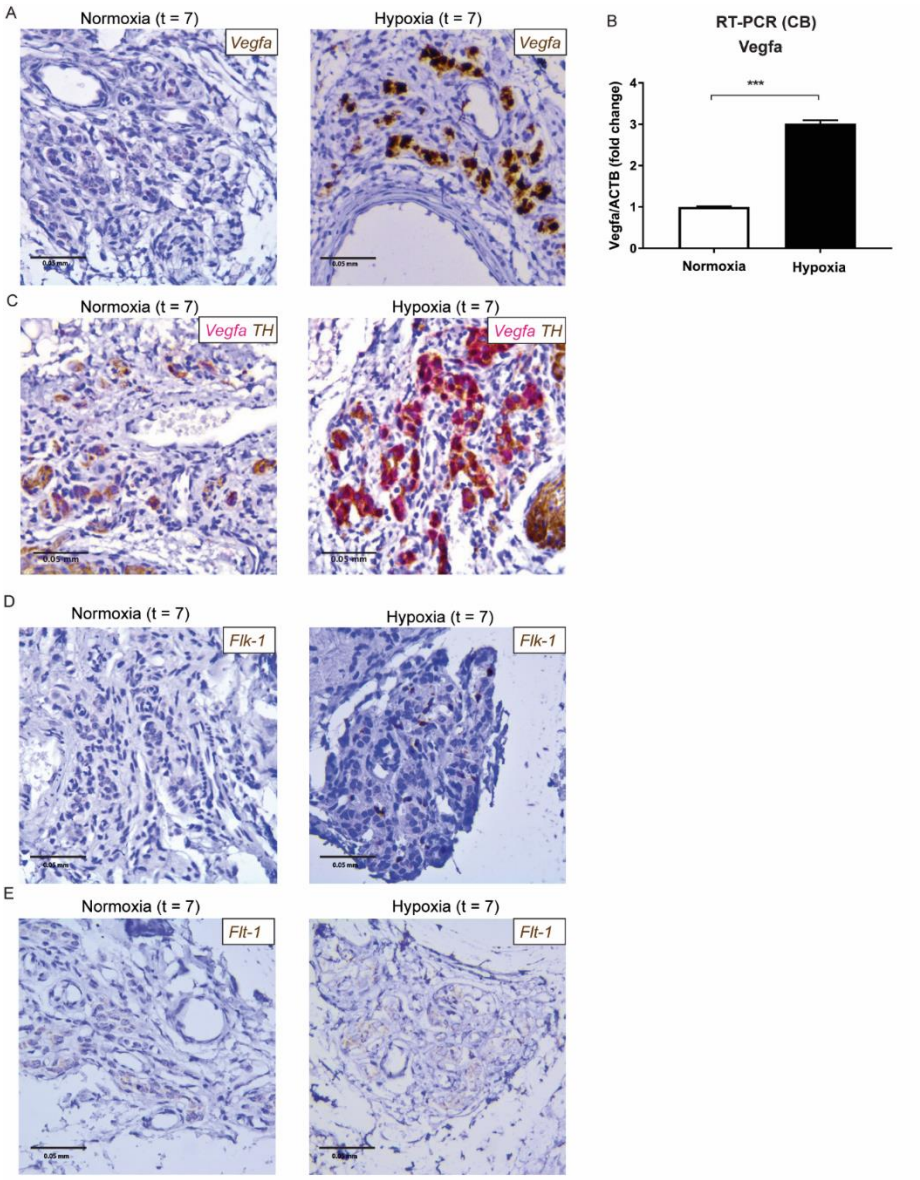


Figure 2.7. The effect of chronic hypoxia on angiogenic gene expression in the carotid body.

A) Comparative *in situ* hybridisation for *Vegf*a (brown) mRNA in carotid bodies from normoxic and hypoxic (7 days at 10% oxygen) wild-type mice. *Vegf*a is strongly induced by chronic hypoxic exposure.

B) quantitative RT-PCR for *Vegf*a in homogenised carotid bodies from normoxic and hypoxic (7 days at 10% oxygen) wild-type mice.

C) Dual *in situ* hybridisation for *Vegf*a (pink) and immunohistochemistry for TH (brown) in carotid bodies from normoxic and hypoxic (7 days at 10% oxygen) wild-type mice. *Vegf*a expression is highly colocalised with the TH^+ Type I cells.

D-E) Comparative *in situ* hybridisation for D) *Flk-1* (brown) or E) *Flt-1* (brown).

Values shown are the mean ± SEM. *** $P < 0.001$.

Characterisation of the THCreER lineage tracer line in other tissues.

Having established robust and specific recombination of the *tdTomato$^{f/+}$;THCreER* line in the carotid body, this study also sought to characterise its expression in the wider animal, particularly tissues noted in the literature to express TH such as the chromaffin cells of the adrenal medulla and mature neuroblasts in the olfactory bulb and substantia nigra (Fig. 2.8). The TH$^+$ neuroendocrine chromaffin cells of the adrenal medulla strongly expressed tdTomato, with 92% of TH$^+$ cells recombining, suggesting that the *tdTomato$^{f/+}$;THCreER* construct might be a useful tool for future examinations of this population (Fig. 2.8A). TdTomato expression was also observed in the olfactory bulb, likely labelling the TH$^+$ migratory neuroblasts originating from the SVZ (Fig. 2.8B). However, despite strong expression of TH in this tissue, no recombination was observed in the substantia nigra (Fig. 2.8C). Due to the role of the brainstem in ventilatory control and their expression of TH, the catecholaminergic cells of the rostral ventrolateral medulla were also assessed. This region was found to weakly express TH but contained minimal recombined tdTomato$^+$ cells, suggestive of poor recombination in this region of the brainstem. No significant changes in tdTomato cell numbers were observed in any of these regions in mice exposed to 28-day chronic hypoxia relative to the normoxic controls.

Together, these results indicate that proliferation in the carotid body occurs across multiple cell populations with minimal trans differentiation between populations, with the Type I cell representing one of the primary proliferative populations in the carotid body.

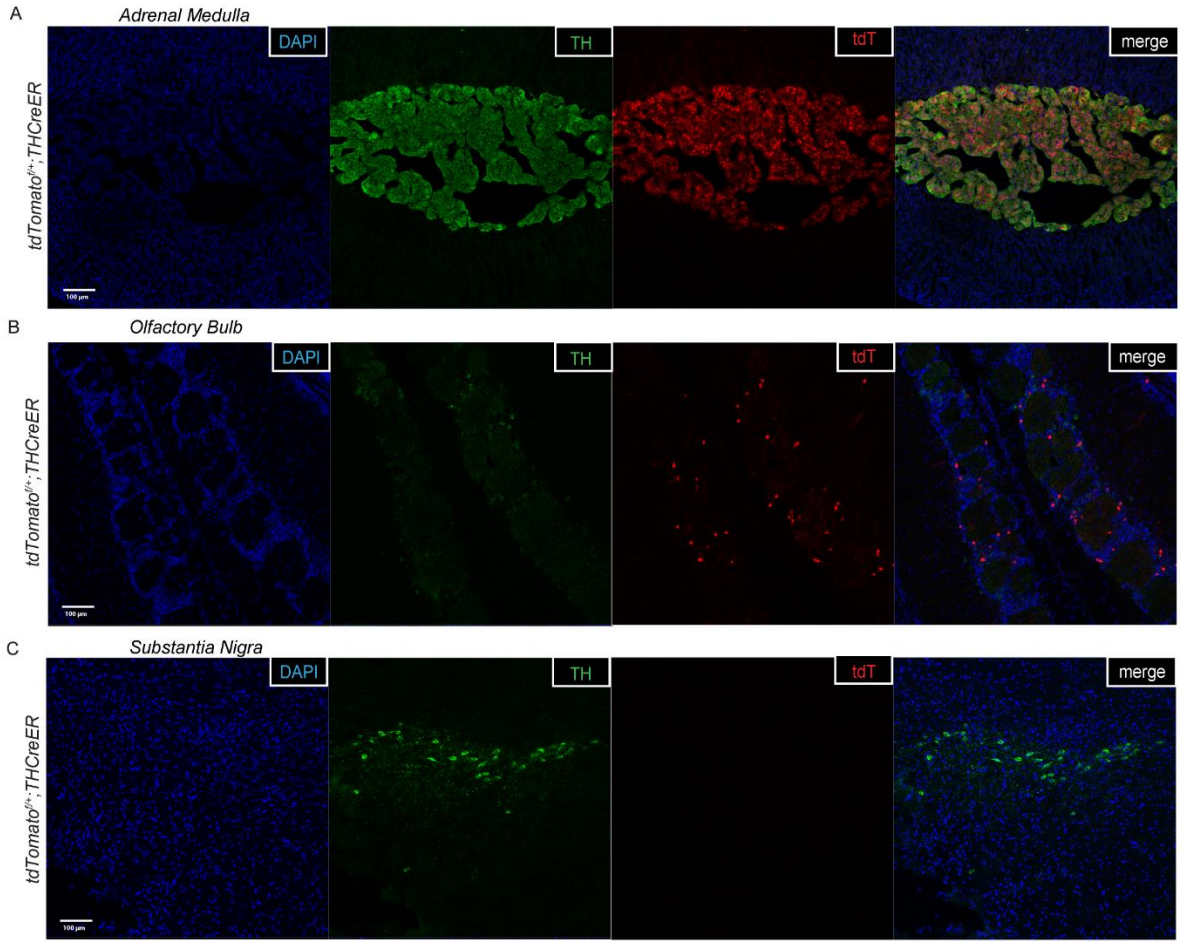


Figure 2.8. Characterization of lineage tracers in the CNS and neuroendocrine tissues of adult mice.

Characterization of DAPI (blue), tyrosine hydroxylase (TH, green) immunostaining and tdTomato fluorescence (tdT, red) in normoxia *tdTomato$^{f/+}$;THCreER* mice in A) the chromaffin cells of the adrenal medulla, B) the olfactory bulb and C) the substantia nigra.

Discussion:

The work presented in this chapter has used lineage labelling to characterize the response of specific carotid body cell types to 28 days of chronic hypoxia, including the two major carotid body cell types: Type I and Type II cells. It has been previously proposed that a subpopulation of the $GFAP^+$ Type II cells function as the stem cells of the carotid body, proliferating and giving rise to different cell types, including Type I cells and endothelial cells, in response to chronic hypoxia (Pardal *et al.*, 2007; Annese *et al.*, 2017). Contrary to the predictions of this Stem Cell theory, this chapter observed that hypoxia induces only a modest expansion of the Type II population and no significant differentiation to give rise to other cell types. This chapter also demonstrates that the labelled Type I population significantly expands and that this expansion originates from proliferation within the Type I population itself, suggesting that this population represents the major proliferative cell type of the niche. A potential explanation for the contrasts with the Stem Cell theory is that this hypothesis was largely based on *in vitro* experimental data, whilst the *in vivo* work presented in this chapter more accurately depicts the behaviour of the niche.

The primary finding of this chapter is that the oxygen sensitive Type I cell population is capable of substantial autonomous proliferation *in vivo*. This is notably unusual for a mature neuronal population with dedicated secretory cellular machinery. A caveat to this result is that Type I cells have been noted to have a limited mitogenic potential *in vivo*, failing to respond to stimuli such as nerve growth factor or FGF (Jackson & Nurse, 1995; Nurse & Vollmer, 1997). A possible insight into the proliferative behaviour of the intact carotid body is a recent report demonstrating that the carotid body contains an immature Type I, TH-positive cell population that is capable of rapid division in response to hypoxia (Sobrino *et al.*, 2018). These cells were distinguished by expression of the human natural

killer-1 (HNK-1) membrane epitope. Although these cells contained secretory vesicles, were electrically excitable and expressed TH, they contained reduced numbers of vesicles and were electrophysiologically insensitive to hypoxia, supporting a view that these Type I cells are immature and may be specifically specialised to proliferate and give rise to the expanded Type I cell population we observed in this study (Sobrino *et al.*, 2018). Targeting this specific population for stem cell culture and investigating its relationship with the Type II population may resolve some of the discrepancies between the results of this study and the Stem Cell theory of the carotid body.

In addition to the expansion of the lineage labelled Type I and Type II cell populations, this study noted a significant proliferation and expansion of the endothelial population, consistent with previous observations that chronic hypoxia induces neovascularisation in the carotid body (Arias-Stella & Valcarcel, 1973; Kumar & Prabhakar, 2012). Although this expanded vasculature was not labelled by either population, previous studies have suggested that Type I cells may drive proliferation in Type II cells and other populations *via* the release of mitogens such as endothelin-1 and VEGFA (Jyung *et al.*, 2000; Chen *et al.*, 2003; Pawar *et al.*, 2009; Kumar & Prabhakar, 2012; Platero-Luengo *et al.*, 2014). Contrary to these reports of endothelin-1 expression and release from hypoxic Type I cells in the literature, this study did not observe the expression of detectable levels of endothelin-1 in Type I cells. This study demonstrated a significant increase in the expression of the endothelial growth factor VEGFA in response to chronic hypoxia, and found that this was restricted to carotid body Type I cells, suggesting that the release of VEGFA from these oxygen sensitive cells may be driving this endothelial proliferation. Thus, the Type I cells of the carotid body may not only drive their own proliferation in an oxygen sensitive manner, but may serve to coordinate a proliferative response across the

niche. A caveat to these results is that the lineage tracing work of this study focused on the 28-day time point of hypoxia exposure, whilst the *in situ* hybridisation and RT-PCR gene expression work was conducted on samples exposed to a shorter 7 day time course. Future work could benefit from characterizing changes in carotid body proliferation, gene expression and ultrastructure at different time points, including the short-term response to 1-24 hours of chronic hypoxia.

Beyond the issues discussed above, a major caveat of the work presented in this chapter is its reliance on – and choice of – promoters for its lineage reporter lines. Neither *tdTomato$^{f/+}$;GFAPCreER* or *tdTomato$^{f/+}$;THCreER* lines were observed to achieve complete recombination, with ~50% of GFAP$^+$ and ~20% of TH$^+$ cells remaining tdTomato negative. Consequently, it is possible that these unlabelled cells may have differentiated or otherwise contradicted the reported results of the other labelled cells, particularly if recombination of a specific sub population was weaker due to low expression of the promoter (for example the HNK-1$^+$ /TH$^+$ proliferative population reported by Sobrino *et al.* (Sobrino *et al.*, 2018)). Conversely, TH is reported to be a hypoxia target gene and thus changes in TH expression may have affected results, although this was partially controlled for with negative controls (Czyzyk-Krzeska *et al.*, 1992a; Czyzyk-Krzeska *et al.*, 1994; Nurse & Fearon, 2002; Schnell *et al.*, 2003). In particular, although the observed rate of recombination (~50%) of the *tdTomato$^{f/+}$;GFAPCreER* is comparable with similar GFAPCre reporter systems employed in other work on the carotid body (Platero-Luengo *et al.*, 2014; Annese *et al.*, 2017), further work would greatly benefit from improvements in the lineage tracers employed. Additional lineage tracer work could also examine specific subpopulations of the carotid body such as recently identified TH$^+$ /HNK-1$^+$ proliferative population (Sobrino *et al.*,

2018).

The findings of this chapter have highlighted a number of avenues for further research. In particular, this study has suggested that the Type I cells of the carotid body are a primary proliferative cell type that proliferates independently of other cells types and are potentially capable of driving proliferation in the Type II and /or endothelial cells of the niche. To investigate this, the next chapter will focus on inactivating elements of the oxygen sensitive HIF pathway specifically within the Type I population.

Results Chapter 3: Genetic manipulation of HIF-2α in carotid body Type I cells

Introduction:

In response to chronic hypoxic exposure at altitude or in disease, mammalian carotid bodies undergo hyperplasia and neovascularisation, expanding 2-3-fold in size (Arias-Stella & Valcarcel, 1973, 1976; Wang & Bisgard, 2002; Kumar & Prabhakar, 2012). The previous chapter used a lineage tracing approach to demonstrate that this hyperplastic response was mediated by proliferation from distinct populations of carotid body Type I and Type II cells, with minimal transdifferentiation between these populations. Work described in this chapter demonstrated that, in response to chronic hypoxia, the oxygen sensitive Type I cells expanded greatly in number, were highly proliferative relative to Type II cells, and induced mitogenic signalling genes such as VEGFA, which may drive the observed proliferation of endothelial cells by paracrine signalling, suggesting that the Type I cells are the primary proliferative cell type involved in carotid body hyperplasia. These results were contrary to previous suggestions that a subpopulation of Type II cells act as stem cells which proliferate and differentiate to Type I cells in response to chronic hypoxia (Pardal *et al.*, 2007).

In mammals, many of the chronic responses to hypoxia are mediated by the hypoxia-inducible factor (HIF) family, which regulates the expression of several hundred genes such as VEGFA, Cyclin D1 and EPO (Kaelin & Ratcliffe, 2008; Kumar & Prabhakar, 2012; Cho *et al.*, 2016). HIF is a α/β heterodimer consisting of a stable HIF-1β subunit and an unstable HIFα subunit. In hypoxia, HIFα stabilizes and dimerises with HIF-1β and then translocates to the nucleus where it binds to hypoxic response elements (HREs) at target gene loci (Kaelin & Ratcliffe, 2008). The HIFα family contains two major isoforms, HIF-

1α and HIF-2α, which regulate an overlapping, but distinct, subset of genes (Hu *et al.*, 2003; Rankin *et al.*, 2007; Arsenault *et al.*, 2013). HIF-1α appears to be the dominant isoform in regulating the response to hypoxia, as it expressed in all cells of mammalian species whilst HIF-2α is restricted in its expression to specific tissues and cells. HIF-2α mRNA is strongly expressed in the Type I cells of the carotid body (Zhou *et al.*, 2016). In line with this high HIF-2α mRNA expression in the carotid body, inducible inactivation of HIF-2α, but not HIF-1α, in mice significantly reduces carotid body proliferation and ventilatory acclimatisation to hypoxia (Hodson *et al.*, 2016).

Whilst Hodson *et al.* demonstrate the importance of HIF-2α integrity to carotid body proliferation and ventilatory acclimatisation, this study used a ubiquitous RosaCreER promoter to inactivate HIF-2α across the organism (Hodson *et al.*, 2016). Thus, the cell(s) in which HIF-2α mediates these effect remains unknown. Moreover, due to the tissue wide nature of hypoxia as a stimulus, it is unknown whether this proliferative response is cell autonomous or whether it relies on hypoxia and mitogen sensing across multiple interrelated carotid body cell types. In order to assess this, the work shown in this chapter will inactivate HIF-2α in specific carotid body cell populations to further characterize the role of HIF-2α in mediating the carotid body's response to hypoxia. The previous chapter demonstrated a major proliferative role for the Type I cells of the carotid body, as well as strong HIF-2α expression in this population. Conversely, the Type II cell population was observed to have a low level of HIF-2α and a minor contribution to the overall proliferative response. However, this population has been previously implicated in carotid body proliferation by the Stem Cell theory of the carotid body (Kokovay & Temple, 2007; Pardal *et al.*, 2007; Platero-Luengo *et al.*, 2014). Therefore, this chapter will employ both the *THCreER* (Type I) and the *GFAPCreER* (Type II) specific promoters characterized in

the previous chapter to assess the effect of HIF-2α inactivation on proliferation, ventilation, neo-vascularisation, ultrastructure and gene expression.

Results:

Expression and inactivation of *Hif-2α* mRNA in carotid body Type I and Type II cells.

Transcriptional profiling has shown that *Hif-2α* mRNA is highly expressed in the whole carotid body (Gao *et al.*, 2017), and in Type I cells specifically, with *Hif-2α* mRNA being the second most highly expressed transcript relative to control tissue in these cells (Zhou *et al.*, 2016). To enable comparisons with these reports, and to characterise the expression of *Hif-2α* mRNA relative to *Hif-1α* in the intact carotid body, *in situ* hybridisation was performed on the carotid body alongside surrounding tissues in samples from wild-type normoxic mice. In the carotid body, *Hif-2α* mRNA was abundant (Fig. 3.1A). By contrast, in nearby neighbouring tissues such as the superior cervical ganglion (SCG), *Hif-2α* mRNA expression was very low, with only a few endothelial cells in the SCG expressing higher levels (Fig. 3.1A). Weak *Hif-2α* signal could be seen in most cells of the carotid body, and strong signal could be seen in groups of cells that appeared morphologically to be Type I cells (Fig. 3.1A). To confirm this, *in situ* hybridisation was performed on adjacent sections from normoxic wild-type mice in combination with immunostaining for tyrosine hydroxylase (TH), a Type I cell marker. *Hif-2α* mRNA largely colocalised with TH (Fig. 3.1B), indicating strong and specific HIF-2α expression in the CB Type I cells>r , and confirming the transcriptomic results of Zhou et al. (Zhou *et al.*, 2016). By contrast, hybridisation for a probe for *Hif-1α* showed a relatively lower signal for *Hif-1α* mRNA that was uniformly expressed across the CB and adjacent tissue (Fig. 3.1C).

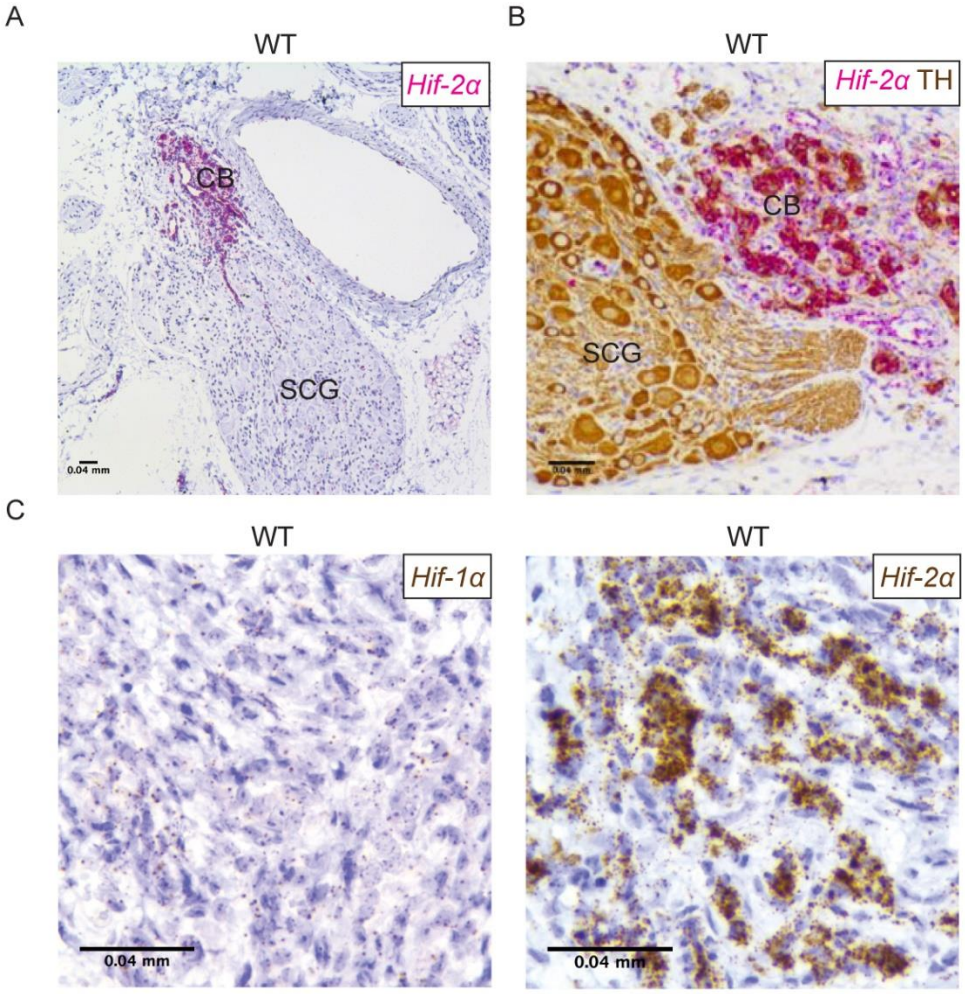


Figure 3.1. HIF mRNA expression in the carotid body.

A) *In situ* hybridisation for *Hif-2α* (pink). Representative image showing *Hif-2α* expression around the carotid bifurcation including the carotid body (CB) and superior cervical ganglion (SCG) (left panel) in carotid bodies from normoxic wild-type (WT) mice.

B) Dual *in situ* hybridisation and immunostaining for *Hif-2α* mRNA (pink) and TH (brown) in the carotid body of normoxic wild-type (WT) mice. *Hif-2α* strongly colocalised with TH signal, which is partly obscured by the intensity of *Hif-2α* expression.

C) Representative images of CB tissue showing *in situ* hybridisation for *Hif-1α* (left panel) (brown) and *Hif-2α* (right panel) expression (brown).

The effects of HIF-2α inactivation in carotid body Type I and Type II cells on carotid body morphology.

To study the specific functions of HIF-2α in Type I *versus* Type II cells, mice bearing a *Hif-2α$^{f/f}$* allele were intercrossed with the inducible *THCreER* (Type I cell) or *GFAPCreER* (Type II cells) promoters characterised in the previous chapter, hereafter referred to as *Hif-2α$^{f/f}$;THCreER* or *Hif-2α$^{f/f}$;GFAPCreER* mice respectively. To test the effect of this reduction in HIF-2α in specific cell types on the proliferative response to hypoxia, *Hif-2α$^{f/f}$;THCreER, Hif-2α$^{f/f}$;GFAPCreER* and *Hif-2α$^{f/f}$* mice were administered tamoxifen *via* oral gavage for 5 days. Animals were then treated with BrdU and then placed into a normobaric altitude chamber (10% oxygen) for 7 days, 5 days following the end of tamoxifen treatment to allow time for recombination to take place. Proliferation in the carotid body was assessed using BrdU incorporation. As with wild-type mice, control *Hif-2α$^{f/f}$* mice (which lack a CreER promoter, and thus do not recombine and excise the floxed HIF-2α allele after tamoxifen treatment) contained high levels of BrdU proliferation across the organ after 7 days of chronic hypoxia (2993 ± 153 $BrdU^+$ cells mm^{-2}, Fig. 3.2A). *Hif-2α$^{f/f}$;GFAPCreER* mice showed no significant reduction in carotid body proliferation *versus Hif-2α$^{f/f}$* controls (3059 ± 226 *versus* 2993 ± 153 $BrdU^+$ cells mm^{-2}, Fig. 3.2A, right hand panel). On the other hand, *Hif-2α$^{f/f}$;THCreER* mice showed a marked reduction in BrdU incorporation relative to these control mice, although proliferating cells were still present in moderate numbers (1743 ± 162 *versus* 2993 ± 153 $BrdU^+$ cells mm^{-2} in *Hif-2α$^{f/f}$;THCreER versus Hif-2α$^{f/f}$*, $P = 0.0006$, Fig. 3.2A, middle panel).

Inactivation of *Hif-2α$^{f/f}$* under the *THCreER* did not completely ablate proliferation in the carotid body in Type I or non-Type I cells. This contrasts with the almost total ablation of BrdU incorporation observed in previous work using *Hif-2α$^{f/f}$* inactivation under the

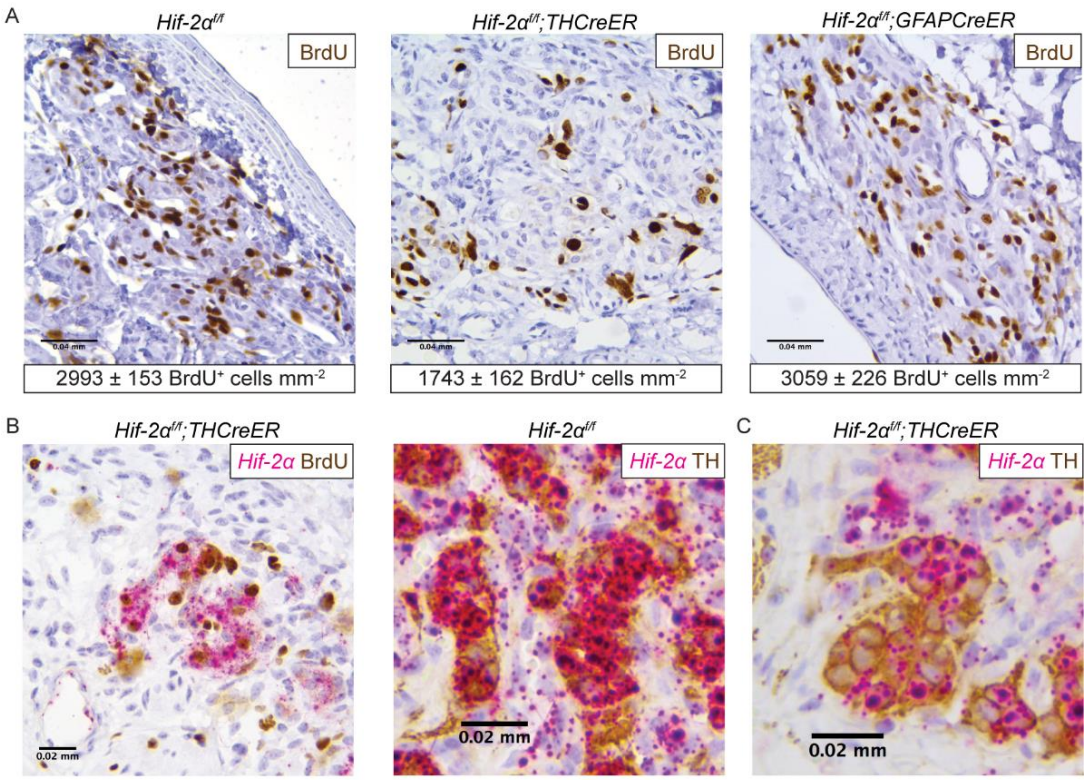


Figure 3.2. The effect of conditional HIF-2α inactivation in carotid body Type I and Type II cells upon proliferation and gene expression.

Representative images of immunostaining and *in situ* hybridisation in carotid bodies of mice exposed to 10% oxygen for 7 days.

A) BrdU (brown) immunostaining in *Hif-2α*$^{f/f}$*;THCreER*, *Hif-2α*$^{f/f}$*;GFAPCreER* and *Hif-2α*$^{f/f}$ littermate control mice after exposure to 10% oxygen for 7 days. Morphometric analyses showing pairwise comparison with the control values are presented in the right hand panel. n = 4-11. BrdU incorporation was significantly reduced in *Hif-2α*$^{f/f}$*;THCreER* relative to controls.

B) Dual *in situ* hybridisation and immunostaining for *Hif-2α* mRNA (pink) and TH (brown) in the carotid bodies of *Hif-2α*$^{f/f}$*;THCreER* and *Hif-2α*$^{f/f}$ littermate control mice. *Hif-2α* mRNA strongly colocalises with TH, suggesting its expression is restricted to Type I cells. *Hif-2α* is reduced in *Hif-2α*$^{f/f}$*;THCreER* mice, but clusters of cells remain with high *Hif-2α* mRNA expression, suggesting these cells have not recombined.

C) Dual *in situ* hybridisation and immunostaining for *Hif-2α* mRNA (pink) and BrdU (brown) in carotid bodies from *Hif-2α*$^{f/f}$*;THCreER* mice. BrdU incorporating cells overlapped with, or were located immediately adjacent to, remaining clusters of *Hif-2α* mRNA containing cells. ** $P < 0.01$.

ubiquitous, tissue wide *RosaCreER* promoter (Hodson *et al.*, 2016). A possible explanation for this is that the incomplete recombination of the THCreER promoter permits specific unrecombined Type I cells to proliferate and/or to drive proliferation in adjacent cell types through paracrine signalling. Chapter 2 of this thesis observed that recombination of a monoallelic tdTomato construct occurred in ~79% of TH cells (Fig. 2.3C), whereas successful inactivation of HIF-2α in *Hif-2α$^{f/f}$;THCreER* requires complete (biallelic) inactivation, likely leading to an even lower rate of recombination. To assess this hypothesis, the loss of *Hif-2α* mRNA after tamoxifen treatment was examined in hypoxia treated *Hif-2α$^{f/f}$;THCreER* mice *versus Hif-2α$^{f/f}$* controls. Although tamoxifen treatment resulted in a large reduction in overall HIF-2α signal in Type I cells of *Hif-2α$^{f/f}$;THCreER* mice, a small proportion of TH^{+} cells retained *Hif-2α* mRNA signal, likely indicating cells that failed to recombine (Figure 3.2B). Dual staining for BrdU incorporation and *in situ* hybridisation for *Hif-2α* demonstrated that the remaining BrdU^{+} signal in hypoxic *Hif-2α$^{f/f}$;THCreER* mice strongly colocalised with, or was directly adjacent to, this remaining *Hif-2α* mRNA signal (Fig. 3.2C), suggesting that these unrecombined cells are capable of driving proliferation. These remaining BrdU cells included both cells which morphologically resembled Type I cells and non-Type I cells (Type II /endothelial cells), suggesting that the remaining unrecombined cells may be driving proliferation of both Type I cells and non-Type I cells *via* paracrine effects.

The effects of HIF-2α inactivation in carotid body Type I cells on carotid body vascularization and gene expression.

To test whether proliferation of non-Type I cells might also be affected by loss of HIF-2α in Type I cells *via* paracrine effects, the effect of HIF-2α inactivation under the THCreER promoter on non-Type I cells was investigated. In the previous chapter, carotid body

endomucin$^+$ endothelial cells were shown to proliferate in response to chronic hypoxia independently of the labelled Type I or Type II lineages in adult mice. These BrdU$^+$ /endomucin$^+$ cells were tightly clustered around the carotid body vasculature and represented ~40% of the overall BrdU$^+$ CB cells after 28 days of chronic hypoxic exposure (Fig. 2.5). To assess whether the proliferative response of this endothelial cell population is affected by the loss of HIF-2α in the Type I cell lineage, this study examined whether there was a loss in proliferating endothelial cells after HIF-2α inactivation by scoring the number of cells which stain positively for both BrdU and endomucin in CBs from 7 day hypoxic *Hif-2α$^{f/f}$;THCreER* mice and *Hif-2α$^{f/f}$* controls (Fig. 3.3A). BrdU$^+$ /endomucin$^+$ cell density was significantly reduced in *Hif-2α$^{f/f}$;THCreER* mice *versus Hif-2α$^{f/f}$* controls (762 ± 114 *versus* 1256 ± 101 BrdU$^+$ /endomucin$^+$ cells mm^{-2}, $P < 0.05$, Fig. 3.3A). This reduction suggests that hypoxia-induced proliferation of the endothelial cell population is dependent on the presence of HIF-2α in Type I cells, further supporting the existence of a paracrine signal from this population.

A candidate for such a paracrine signal from Type I to endothelial cells is the secreted protein VEGFA, which promotes endothelial cell proliferation when binding to VEGFR receptors (Chen *et al.*, 2003). The previous chapter demonstrated that hypoxia induces VEGFA mRNA expression in Type I cells. *In situ* hybridisation for *Vegfa* mRNA found that HIF-2α inactivation under the *RosaCreER* promoter significantly ablated *Vegfa* expression across the whole tissue (Fig. 3.3B, middle panel) whilst inactivation under the THCreER promoter resulted in a weaker reduction in *Vegfa* signal (Fig 3.3B, right hand panel), with the remaining clusters of *Vegfa*$^+$ cells in the later likely representing unrecombined cells.

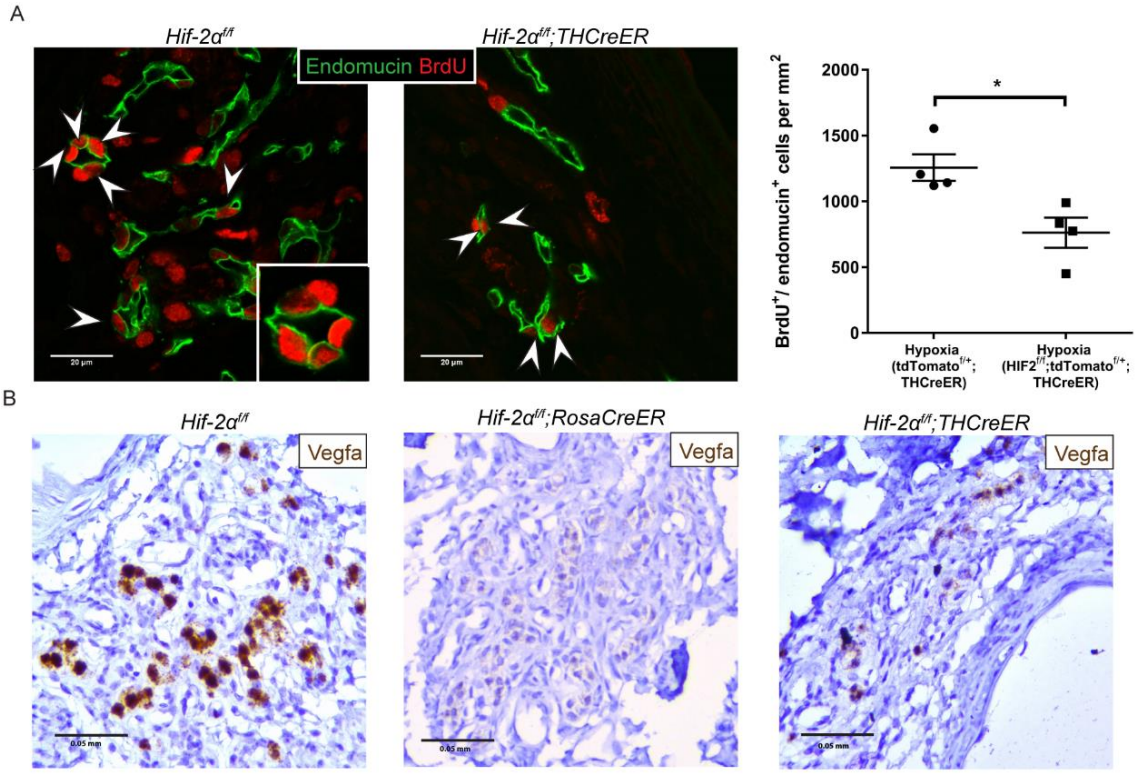


Figure 3.3. The effect of conditional HIF-2α inactivation upon carotid body neo-vascularisation.

A) Proliferation in the carotid body vasculature. Endomucin (green) and BrdU (red) immunostaining (cells with colocalisation are marked with white arrowheads) in *Hif-2α$^{f/f}$;THCreER* and *Hif-2α$^{f/f}$* littermate control mice exposed to 7 day chronic hypoxia. Proliferation in the CB vasculature was reduced by the inactivation of HIF-2α in the separate Type I cell population.

B) *In situ* hybridization for *Vegf*a (brown) in carotid bodies from *Hif-2α$^{f/f}$*, *Hif-2α$^{f/f}$;RosaCreER* and *Hif-2α$^{f/f}$;THCreER* mice after exposure to 10% oxygen for 7 days. Values shown are mean ± SEM. * $P < 0.05$.

These results suggest that inactivating HIF-2α in Type I cells leads to a general reduction in carotid body proliferation – both Type I and non-Type I cells (such as endothelial cells), the latter *via* paracrine effects. To test whether this reduction in proliferation translates to the prevention of overall hypoxia-induced hyperplasia, this study then sought to assess

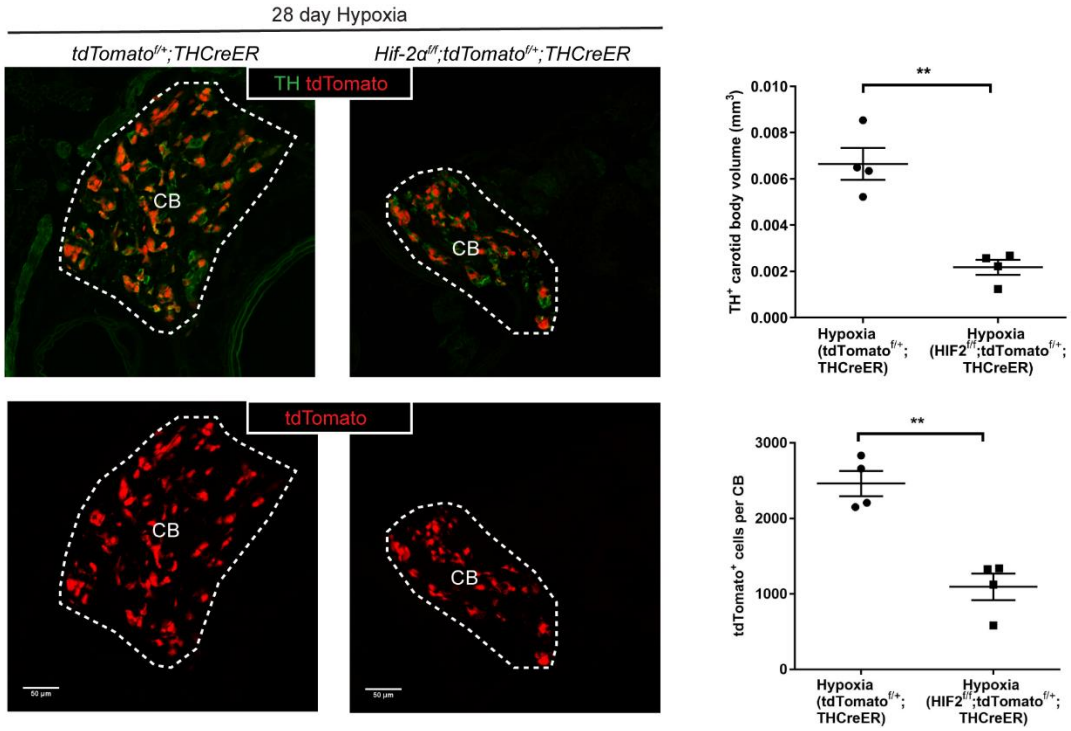


Figure 3.4. The effect of conditional HIF-2α inactivation in Type I cells upon carotid body hyperplasia.

Representative images and quantification of TH^+ CB volume and $tdTomato^+$ (red) cell numbers from n = 4 *Hif-2α$^{f/f}$;tdtomato$^{f/+}$;THCreER* and *tdtomato$^{f/+}$;THCreER* littermate control mice exposed to chronic hypoxia (28 days at 10% oxygen). *tdtomato$^{f/+}$;THCreER* controls show a hypoxia-induced increase in CB volume and cell number (hyperplasia), but this response was largely ablated by the inactivation of HIF-2α in the Type I cell population.

Values shown are mean ± SEM. ** $P < 0.01$.

carotid body size at a later 28-day time point. To assess this, TH^+ CB volume and $tdTomato^+$ cell number was assessed from carotid bodies of *Hif-2α$^{f/f}$;tdtomato$^{f/+}$; THCreER* and *tdtomato$^{f/+;}$THCreER* mice exposed to 28 days of hypoxia (10% oxygen) (Fig 3.4). This longer time point was chosen to parallel the time point at which long-term hyperplasia was observed in Chapter 2 (Fig. 2.3B). A large reduction in lineage labelled Type I cell number was observed in *Hif-2α$^{f/f}$;tdtomato$^{f/+;}$THCreER* mice relative to controls. A large reduction in overall TH^+ CB volume was also was observed in *Hif-*

2α$^{f/f}$;tdtomato$^{f/+;}$THCreER mice relative to controls (0.002185 ± 0.000329 mm^3 *versus* 0.006654 ± 0.000658 mm^3) (Fig. 3.4). This reduction is consistent with the effects of HIF-2α inactivation in Type I cells reducing overall carotid body proliferation, both in the Type I cells and *via* reducing the expression of mitogenic genes such as VEGFA, suggesting that HIF-2α in Type I cells is sufficient to ablate most of the carotid body's hyperplastic response to hypoxia.

The effects of HIF-2α inactivation in carotid body Type I and Type II cells upon hypoxia-induced erythropoiesis.

Chronic hypoxia induces polycythaemia, leading to a measurable increase in haematocrit over a period of several days (Haase, 2010), which our group has previously shown to be ablated by global inducible HIF-2a inactivation under the ubiquitous RosaCreER promoter (Hodson et al., 2016). This response appeared to be significantly enhanced in *Hif-2α$^{f/f}$;THCreER* mice *versus Hif-2α$^{f/f}$* controls (65.8 ± 0.4 versus 61.2 ± 1.1% haematocrit, $P = 0.002$, Fig. 3.5A). This exaggerated erythropoietic response could result from the presumed increased systemic hypoxia experienced by in *Hif-2α$^{f/f}$;THCreER* mice due to the ablation of the carotid body mediated ventilatory acclimatisation to hypoxia. This increased systemic hypoxia could result in greater EPO production in the kidneys and thus erythropoiesis. Consistent with the lack of effect on ventilation, hypoxic *Hif-2α$^{f/f}$;GFAPCreER* mice also showed no differences in haematocrit relative to Hif-2αf/f control animals (58.2 ± 0.7 *versus* 58.4 ± 0.4% haematocrit, ns, Fig. 3.5B).

The effects of HIF-2α inactivation in carotid body Type I and Type II cells upon ventilatory acclimatisation in response to chronic hypoxia.

The oxygen sensitive Type I cells are the primary transducer of the carotid body, releasing

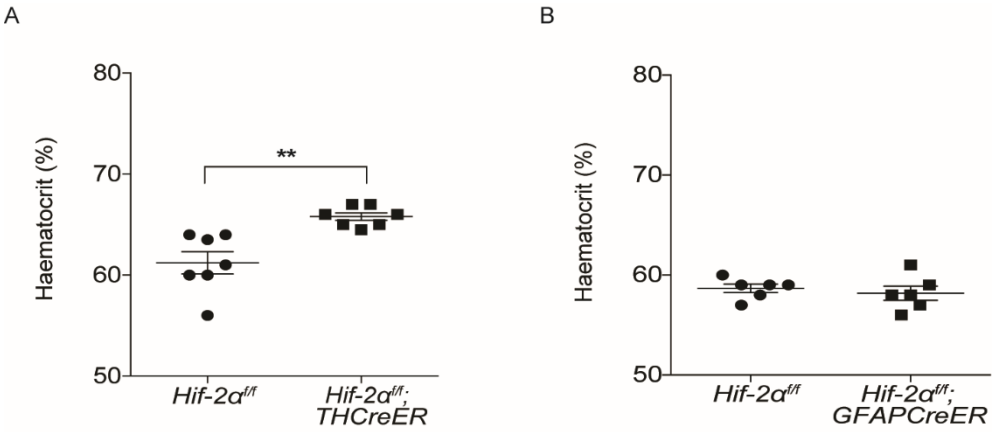


Figure 3.5. The effect of conditional HIF-2α inactivation carotid body Type I and Type II cells upon haematocrit in mice acclimatizing to chronic hypoxia.
A-B) Haematocrit measures of blood samples taken from A) n = 7 *Hif-2α$^{f/f}$;THCreER* and *Hif-2α$^{f/f}$* littermate controls and B) n = 6 *Hif-2α$^{f/f}$;GFAPCreER* and *Hif-2α$^{f/f}$* littermate controls acclimatized to 10% oxygen for 7 days
Values shown are mean ± SEM; ** $P < 0.01$.

neurotransmitters in response to acute hypoxia, which in turn act on the carotid sinus nerve to stimulate a hypoxic ventilatory response (HVR). In wild-type mice, prolonged chronic hypoxia results in an increased HVR in response to acute hypoxic exposure, known as ventilatory acclimatisation to hypoxia (VAH). Previously, this group has shown that ubiquitous inactivation of HIF-2α under the *RosaCreER* promoter is sufficient to ablate this VAH and reduce HVRs in unacclimated mice (Hodson *et al.*, 2016). This study therefore sought to test whether acute HIF-2α inactivation specifically in the Type I (or Type II) cell population affects hypoxic ventilatory responses, in addition to its effects on CB proliferation noted above.

To assess this, *Hif-2α$^{f/f}$;THCreER, Hif-2α$^{f/f}$;GFAPCreER* and *Hif-2α$^{f/f}$* mice were assessed

for ventilatory function prior to, during and immediately after their hypoxic acclimatisation (0 h, 48 h and 7 days of chronic hypoxia, Table 3.1 and Fig 3.6). Mice were removed from their experimental condition and their response to a short (5 minute) hypoxic challenge (10% oxygen /3% carbon dioxide, balance nitrogen or 10% oxygen, balance nitrogen) was assessed using plethysmography. The hyperventilatory response to 10% oxygen alone may result in the rapid clearing of CO_2 inducing ventilatory alkalosis which in turn depresses ventilation. This may be offset by supplementation of the ventilatory stimulus with 3% carbon dioxide, which has been shown to prevent any significant rise in arterial pH or fall in $PaCO_2$ with 7% oxygen exposure (Ishiguro *et al.*, 2006) and has been used in recent studies with 10% oxygen to assess ventilation (Bishop *et al.*, 2013; Slingo *et al.*, 2014; Hodson *et al.*, 2016). Thus, the primary measurements reported in this chapter are conducted with a 10% oxygen /3% carbon dioxide balance nitrogen stimulus, although 10% oxygen balance nitrogen exposure was also conducted. Plethysmography measures both the respiratory rate (breaths per minute) and the tidal volume of the mice (ml per gram), which is then used to calculate their minute ventilation (ml min^{-1} g^{-1}), a measure of the volume of gas inhaled or exhaled per minute. For the purposes of this study, the hypoxic ventilatory response (HVR) was calculated as the difference in minute ventilation between the first one minute of acute hypoxic exposure and the prior one minute of normoxia.

No significant effect of *Hif-2α$^{f/f}$;THCreER* was seen on baseline ventilation in normoxia (0 h timepoint), although a non-significant trend towards reduced HVR in response to acute hypoxic exposure was observed (0 h, Table 3.1). This is reminiscent of the reduction in

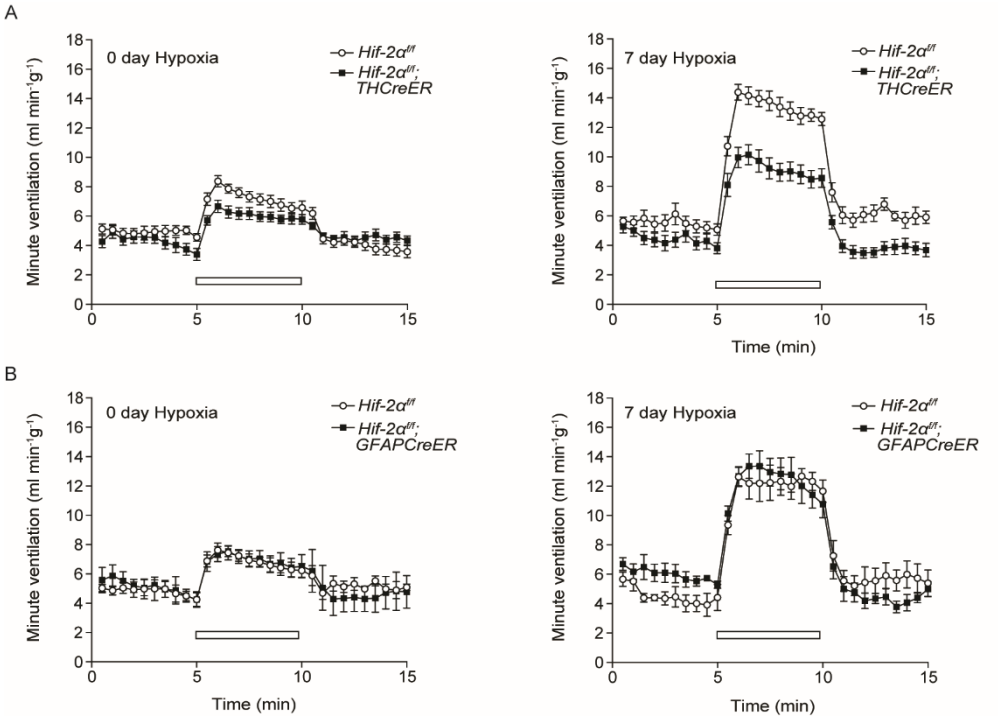


Figure 3.6 The effect of conditional HIF-2α inactivation carotid body Type I and Type II cells upon ventilatory responses in mice acclimatizing to chronic hypoxia.
A) Minute ventilation before, during and after an acute hypoxic stimulus (10% oxygen with 3% carbon dioxide - white bars) taken from *Hif-2α$^{f/f}$;THCreER* and *Hif-2α$^{f/f}$* littermate controls. Measurements made before (0 day hypoxia) and after (7 day hypoxia) acclimatisation to 10% oxygen for 7 days. Minute ventilation was calculated from respiratory rate and tidal volume measurements made *via* plethysmography.
B) Similar measurements from *Hif-2α$^{f/f}$;GFAPCreER* mice and littermate controls.
Values shown are mean ± SEM; n = 5-12.
Plethysmography was conducted by Dr Emma Hodson.

non-acclimatised HVR in *Hif-2α$^{f/f}$;RosaCreER* mice reported in Hodson *et al.*, and a similar non-significant trend towards a reduction in non-acclimatised HVR *Hif-2α$^{+/-}$* mice (Hodson *et al.*, 2016). It is therefore possible that HIF-2α in Type I cells may play a role in mounting an acute HVR in even non-acclimatised mice. As expected, control *Hif-2α$^{f/f}$* mice acclimatised following 48 hour and 7 days of hypoxia, and displayed ventilatory acclimatisation to hypoxia (VAH, an enhanced HVR to acute hypoxic exposure) (Table

3.1, Fig. 3.4). However, inactivation of HIF-2α in Type I cells resulted in a reduced VAH relative to *Hif-2α*$^{f/f}$ control mice after 48 hours of chronic hypoxic exposure (4.58 ± 0.46 *versus* 6.43 ± 0.56 ml min^{-1} g^{-1} HVR, $P = 0.023$, Table 3.1). This effect was also seen after 7 days of chronic hypoxia (5.99 ± 0.42 *versus* 9.13 ± 0.78 ml min^{-1} g^{-1} HVR, $P = 0.003$, Fig. 3.4A, Table 3.1) chronic hypoxia.

In contrast, *Hif-2α*$^{f/f}$;*GFAPCreER* animals showed no difference in hypoxic ventilatory responses in normoxia or after chronic hypoxic acclimatisation relative to *Hif-2α*$^{f/f}$ mice. *Hif-2α*$^{f/f}$;*GFAPCreER* mice mounted an acclimatised HVR mice in response to acute hypoxia at both 48 hours and 7 days of acclimatisation (Fig 3.6B, Table 3.1). These results are consistent with the low HIF-2α expression in Type II cells and may also be attributable to the lower levels of recombination observed under the GFAPCreER promoter in Chapter 2 (Fig. 2.2C).

As discussed above, both 10% oxygen /3% carbon dioxide and 10% oxygen were employed as the acute hypoxic stimulus for this study. 10% oxygen alone was tested for all genotypes and recapitulated the results of 10% oxygen /3% carbon dioxide mix (Table 3.1) However, as anticipated, respiratory depression from ventilatory alkalosis resulted in lower HVR values and a lower level of significance (Table 3.1).

A

Acute hypoxic stimulus	**Chronic hypoxia duration**	**Hypoxic ventilatory response (ml min^{-1} g^{-1})**			**ANOVA *P* value**
		Hif-2α$^{f/f}$	***Hif-2α$^{f/f}$; THCreER***	***t*-test *P* value**	
10% O_2	0 hours	-0.05 ± 0.30	0.03 ±0.34	0.858	**<0.0001**
	48 hours	2.86 ± 0.33	1.70 ± 0.34	**0.028**	
	7 days	4.24 ± 0.21	2.84 ± 0.45	**0.013**	
ANOVA *P* value		**0.0069**			**0.069**
10% O_2/ 3% CO_2	0 h	3.32 ± 0.28	2.89 ± 0.30	0.314	**<0.0001**
	48 h	6.43 ± 0.56	4.58 ± 0.46	**0.023**	
	7 days	9.13 ± 0.78	5.99 ± 0.42	**0.003**	
ANOVA *P* value		**<0.0001**			**0.012**

B

Acute hypoxic stimulus	**Chronic hypoxia duration**	**Hypoxic ventilatory response (ml min^{-1} g^{-1})**			**ANOVA *P* value**
		Hif-2α$^{f/f}$	***Hif-2α$^{f/f}$; GFAPCreER***	***t*-test *P* value**	
10% O_2	0 hours	-0.24 ± 0.40	0.82 ± 0.57	0.167	**0.0004**
	48 hours	1.30 ± 1.12	1.79 ± 0.85	0.804	
	7 days	3.70 ± 0.87	3.06 ± 0.42	0.530	
ANOVA *P* value		0.631			0.405
10% O_2/ 3% CO_2	0 hours	3.15 ± 0.36	3.06 ± 0.31	0.844	**<0.0001**
	48 hours	6.66 ± 1.17	6.64 ± 0.49	0.987	
	7 days	8.25 ± 1.02	7.51 ± 0.73	0.571	
ANOVA *P* value		0.647			0.873

Table 3.1. Acute hypoxic ventilatory responses of mice after conditional inactivation of HIF-2α in Type I or Type II cells before and after chronic hypoxia exposure.
Hypoxic ventilatory responses of A) *Hif-2α$^{f/f}$;THCreER* and B) *Hif-2α$^{f/f}$;GFAPCreER* mice *versus Hif-2α$^{f/f}$* littermate controls. Measurements were taken after tamoxifen-induced

recombination and before (0 hours) and after (48 hours, 7 days) exposure to 10% oxygen. Values shown are mean changes in minute ventilation (± SEM) in response to the indicated acute hypoxic stimulus; n = 5-12 littermate pairs for each genotypic comparison. Significance of data was tested using two-way ANOVAs (right hand column *P* value = chronic hypoxia factor; bottom row *P* value = genotype factor; right column, bottom row *P* value = chronic hypoxia /genotype interaction factor), followed by *t*-tests (with Holm-Sidak correction) for analysis of individual time points; $P < 0.05$ comparisons are highlighted in bold.
Plethysmography was conducted by Dr Emma Hodson.

The effects of HIF-2α inactivation on carotid body Type I cell ultrastructure.

This study has demonstrated that HIF-2α in Type I cells is important for the proliferative and functional effects of the carotid body in response to hypoxia. In addition to the effects on HVRs and CB proliferation, hypoxia alters dense core vesicle characteristics in CB Type I cells, as demonstrated in the previous chapter. This study therefore sought to test whether HIF-2α in Type I cells is important for the Type I cell intrinsic changes characterized in the previous chapter. These changes include the enlargement of Type I cells in hypoxic mice and a reduction in the density of DCVs relative to cells from normoxic controls (Fig. 2.5). Remaining DCVs were characterized by an increased frequency of enlarged DCVs with a lucent 'halo' around the electron dense core, hereafter referred to as 'eccentric' DCVs (Fig. 2.5A). For this analysis, *Hif-2α*$^{f/f}$ and *Hif-2α*$^{f/f}$;*THCreER* animals were examined after 7 days of normoxia or chronic hypoxia (10% oxygen) (Fig. 3.7). In wild-type carotid bodies, chronic hypoxic exposure resulted in a reduction in DCV density (Fig. 2.5). Chronic hypoxia also resulted in an increased incidence of 'eccentric' DCVs, which possessed an enlarged lucent membrane and an eccentrically displaced dense core, potentially reflecting a fixation artefact caused by a change in DCV content.

Electron microscopy analysis found that the hypoxia-induced reduction in dense core vesicle density was blocked by HIF-2*α* inactivation in the Type I cells (4.45 ± 0.94 *versus* 1.37 ± 0.14 DCVs μm^{-2} in hypoxic *Hif-2α$^{f/f}$;THCreER versus Hif-2α$^{f/f}$* mice, $P < 0.05$) (Fig. 3.7, right hand columns). A large proportion of Type I cells from hypoxic *Hif-2α$^{f/f}$;THCreER* mice contained a high density of DCVs, broadly rescuing the normoxic wild-type cell ultrastructural appearance. The remaining proportion of Type I cells in these mice resembled those from hypoxic control mice, with a low density of DCVs. This may be consistent with the incomplete recombination under the *THCreER* promoter previously shown in Fig. 3.2B, indicating that these cells are unrecombined, and thus have an intact HIF-2α mediated response to hypoxia which results in a reduced DCV density. A high incidence of 'eccentric' DCVs remained in Type I cells from these *Hif-2α$^{f/f}$;THCreER*, suggesting this may be a distinct phenomenon (Fig. 3.7, lower panel centre right insert).

In addition to these effects on secretory vesicles, this study has previously noted that hypoxia has a hypertrophic effect on Type I cell size (Fig. 2.5A). This increase in cell size was reversed in *Hif-2α$^{f/f}$;THCreER* mice (63.38 ± 1.7 *versus* 43.73 ± 4.495 μm^2 Type I cell area in hypoxic *Hif-2α$^{f/f}$ versus Hif-2α$^{f/f}$;THCreER*, $P < 0.01$). Together, these results suggest that HIF-2α integrity is a crucial component of the cell intrinsic DCV function in Type I cells, in addition to its importance to the proliferative and ventilatory phenotypes reported previously. Indeed, these effects on DCV function may mediate some of the ablation of the proliferative and ventilatory responses to hypoxia also reported in this chapter.

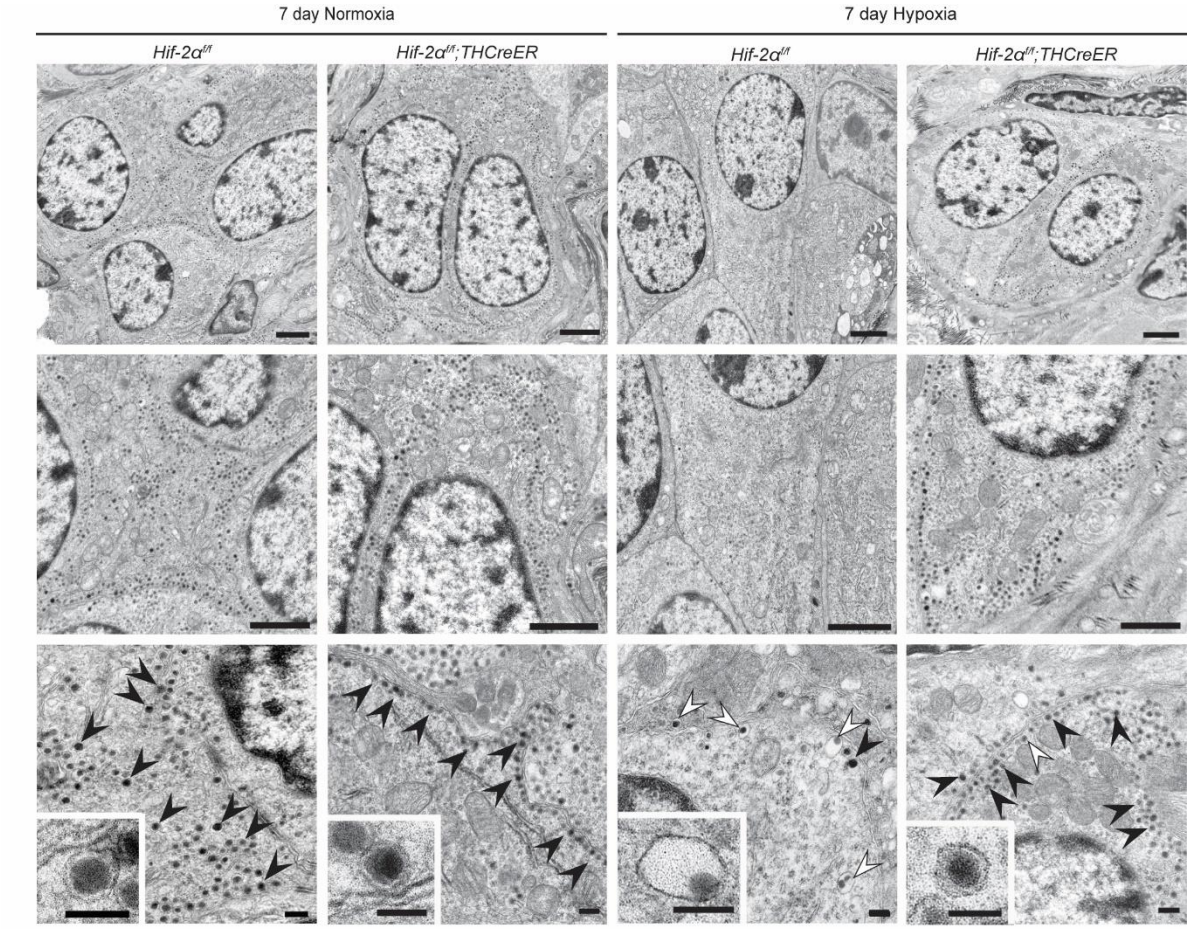


Figure 3.7. The effect of chronic hypoxia and HIF-2α inactivation upon Type I cell ultrastructure.

Electron microscopy imaging of Type I cells from carotid bodies of *Hif-2α*$^{f/f}$;*THCreER* mice and *Hif-2α*$^{f/f}$ littermate controls exposed to 7 days of 10% oxygen (n = 7) or normoxia (n = 3). Hypoxia induces a reduction in dense core vesicle (DCV) density in carotid body Type I cells, but this was ablated by the inactivation of HIF-2α in these cells. Upper panels: low power electron microscope images showing the general appearance of Type I cells. Middle panels: intermediate magnification showing the presence of large numbers of DCVs in the Type I cells of both normoxia samples (left panels) and in the hypoxic *Hif-2α*$^{f/f}$;*THCreER* mice (far right panel) in contrast to the few DCVs present in the hypoxic *Hif-2α*$^{f/f}$ littermate control (middle right panel). Lower panels: high magnification showing typical DCVs (back arrowheads) and eccentric DCVs (marked with white arrowheads). Shown is the increased proportion of eccentric to normal DCVs in the hypoxic *Hif-2α*$^{f/f}$ (middle right panel) but not hypoxic *Hif-2α*$^{f/f}$;*THCreER* mice (far right panel). Representative and eccentric DCVs shown in inserts. Scale bars = 1 μm (upper and middle panels) and 100 nm (lower panel and inserts).

Discussion:

The results presented in this chapter show a major role for HIF-2α in carotid body Type I cell in mediating proliferation, ventilatory acclimatisation, and Type I cell intrinsic responses to chronic hypoxia. Having demonstrated in the previous chapter that carotid body proliferation occurs across multiple, independent lineages (including both Type I and Type II cells), this chapter refined these observations by demonstrating that the inactivation of HIF-2α in Type I, but not Type II, cells results in a reduction in hypoxia-induced proliferation in both the Type I cell population themselves and in other nearby population. This inactivation also led to a reduction in CB hyperplasia, Type I cell hypertrophy, polycythaemia and ventilatory acclimatisation, as well as resulting in cell intrinsic changes in the Type I cells themselves. This suggest an important role for stable HIF-2α in Type I cells in mediating the major hypoxia-inducible functions of the carotid body, and is in keeping with the high expression of Hif-2α mRNA in Type I cells also observed in this chapter.

It has been previously shown that the carotid body proliferative and ventilatory responses to hypoxia can be almost completely inhibited by global inducible knockdown of HIF-2*α* in tamoxifen treated *Hif-2α*$^{f/f}$;*RosaCreER* mice (Hodson *et al.*, 2016) and this chapter extends these results to show that the majority of these effects are caused by the ablation of HIF-2*α* in the Type I cell. HIF-2α has also been shown to play an important role in Type I cells during development, with studies showing that HIF-2*α* is necessary for CB development, as well as its function in the adult CB. Constitutive inactivation of HIF-2α in Type I cells prevents developmental formation of the CBs (Macias *et al.*, 2018) whilst constitutive, stable HIF-2α overexpression in TH^{+} cells (including Type I cells) results in enlargement of the carotid body (Macias *et al.*, 2014) . The results shown in this chapter

have extended these results from developmental models into adult mice. These inducible THCreER results demonstrate that HIF-2α in Type I cells is critical for the acute /chronic ventilatory and proliferative functions of the carotid body. This in turn suggests that manipulation of HIF-2α may help characterize the underlying HIF-2α mechanisms that mediate these processes, and suggests that HIF-2α may be an important target for therapeutically controlling carotid body function. The presence of a low number of unrecombined cells expressing HIF-2α and staining for the proliferative maker BrdU suggests that unrecombined Type I cells are capable of driving their own proliferation in a cell intrinsic manner, likely through HIFα stabilization and the upregulation of cell cycle pathway genes including the HIF-2α target gene Ccnd1, which was shown to be strongly induced by hypoxia in Chapter 2 of this thesis. These results could be refined by assessing samples for proliferation and gene expression at earlier time points. Suitable timepoints for this could be 4 hours after hypoxic exposure, at which point many of the acute responses to hypoxia have occurred or finished, and the 48 hour time point, when elements of ventilatory acclimatisation and some proliferating cells are observable (Powell *et al.*, 1998; Pardal *et al.*, 2007).

This chapter has noted that inactivation of HIF-2α in Type I cells also reduces proliferation and neo-vascularisation in other non-Type I cell populations. A possible mechanism through which HIF-2α might be acting to control is by mediating a paracrine signalling response from the Type I cells. Support for this can be found in the literature: previous studies have suggested that the Type I population drives carotid body proliferation *via* paracrine and /or synaptic signalling to the Type II and other cell populations (Platero-Luengo *et al.*, 2014; Sobrino *et al.*, 2019). Although the previous chapter did not support a major role for Type II cells in carotid body hyperplasia as also suggested by these papers,

the results of this chapter do support a potential paracrine signalling function for Type I cells. Potential candidates for this proliferative signal include VEGF and Endothelin-1, which are both reportedly strongly expressed in Type I cells and released from these cells in response to hypoxia (Jyung *et al.*, 2000; Chen *et al.*, 2002; Chen *et al.*, 2003). Treatment of rats with the endothelin receptor blocker bosentan has been show to largely reduce carotid body hyperplasia (Chen *et al.*, 2007). Notably, endothelin receptor ET-RA is abundant only in the Type I cells themselves, suggesting some level of cross talk between Type I cells may occur during CB hyperplasia (Paciga *et al.*, 1999; Chen *et al.*, 2007). However, it should be noted that the previous chapter did not observe endothelin mRNA expression in Type I cells, disputing the role of endothelin-1 in this process. More promisingly, VEGFA expression has been shown by the previous chapter to be strongly induced in Type I cells by chronic hypoxia in a HIF-2α dependent manner, and two VEGFA receptors, Flt-1 and Flk-1, have been shown to be expressed in the carotid body by this study and others (Jyung *et al.*, 2000). Flk-1 has been reported to mediate neovascularization in other niches, and may thus mediate the proliferation of the endothelial cell population reported in the previous chapter of this thesis (Chen *et al.*, 2003). Flt-1 is reportedly expressed on the Type I cells themselves and its activation has been linked to increases in cell size (Jyung *et al.*, 2000), suggesting that the ablation of Type I cell hypoxia-induced hyperplasia by HIF-2α inactivation may be due to a reduction in VEGF signalling. Pharmacological VEGFA receptor antagonists are available, and could be used to confirm these hypotheses.

A potential mechanism through which HIF-2α may regulate these paracrine-driven proliferative responses is suggested by this study's observation of significant cell intrinsic, HIF-2α dependent effects of hypoxia upon Type I cell ultrastructure. DCVs are reported to

contain a wide variety of chemicals, including ATP, acetylcholine, dopamine, endothelin-1, serotonin, noradrenaline, VEGFA and neuropeptides including enkephalin and neuropeptide Y (Chiocchio *et al.*, 1966; Oomori *et al.*, 1994; Kameda, 2005). In particular, endothelin-1 and VEGFA are potential mitogens acting on the Type I, Type II and endothelial populations of the carotid body. It is possible, therefore, that in hypoxia HIF-2α modifies the contents or release rate of these vesicles, permitting paracrine signalling. Supporting this, blockade of calcium-induced exocytosis with cadmium has been demonstrated to impair carotid body proliferation, suggesting a direct link between Type I cell electrophysiology and morphological changes (Platero-Luengo *et al.*, 2014). Future work could examine vesicular release in intact *Hif-2α*$^{f/f}$;*THCreER* carotid bodies *via* HPLC or other methods to determine whether these ultrastructural changes are reflected in quantitative changes in neuropeptide release in response to acute or chronic hypoxic exposure. This work could focus on assessing the contents of the DCVs and correlating changes in known DCV-packaged compounds (such as ATP, acetylcholine, dopamine, endothelin-1, serotonin, noradrenaline, VEGFA, enkephalin and neuropeptide Y (Chiocchio *et al.*, 1966; Oomori *et al.*, 1994; Kameda, 2005)) with changes in gene expression to determine whether the phenotypes reported in this chapter are mediated by direct transcriptional activity of HIF-2α or *via* indirect effects on DCV secretion or *via* non-canonical HIF-2α ligand binding (as suggested by (Scheuermann *et al.*, 2013). However, the small size and number of carotid body Type I cells may make it difficult to isolate them in experimentally relevant numbers using currently available techniques such as sucrose gradient fractionation.

This chapter has also suggested that the integrity of stable HIF-2α in Type I cells is a key regulator of carotid body proliferation and ventilatory acclimatisation. However, the exact

link between HIF-2*α* in Type I cells and the proliferative and ventilatory responses of the carotid body remains unknown. Although HIF-2α dependent proliferation will result in higher numbers of Type I cells (and thus higher neurotransmitter release and ventilatory drive), ventilatory acclimatisation to hypoxia occurs in a matter of hours to days, depending on species, before a significant increase in mature Type I cells has occurred (Powell *et al.*, 1998; Kline *et al.*, 2002; Pardal *et al.*, 2007; Kumar & Prabhakar, 2012). Moreover, the ventilatory response to hypoxia is not solely mediated by the carotid body peripheral chemoreceptors and also includes input from the CNS (Powell *et al.*, 1998; Powell *et al.*, 2000b). Brainstem neurons, including TH^+ rostral ventrolateral medullary neurons, regulate aspects of ventilation and are reportedly affected by chronic hypoxic exposure (Burke *et al.*, 2014; Wenker *et al.*, 2017). In the previous chapter, the expression of the THCreER promoter was characterised and noted to be expressed in several regions of the brain, adrenal medulla and brainstem, although recombination was notably poor in the brainstem (such that tdTomato was only detectable in a handful of cells in the rostral ventrolateral medulla). Thus some elements of the observed *HIF-2α$^{f/f}$;THCreER* phenotype reported in this chapter may not be solely attributable to changes in Type I cell function, although HIF-2α expression is generally low in the CNS and brainstem.

Similar to the proliferative response, a possible mechanism for HIF-2α's regulation of these ventilatory responses in the carotid body is suggested by our observations of HIF-2α-dependent hypoxia mediated effects on the Type I cell ultrastructure. The reported changes in DCV appearance and density indicate that HIF-2α is integral to some aspect of hypoxia-inducible vesicle release or synthesis. Some vesicle release must be maintained as *Hif-2α$^{f/f}$;THCreER* mice mount an HVR response to acute hypoxia (0 h, Table 3.1), but an impairment of vesicle release or a change in content might explain the non-significant

trend in decreased HVR observable in these mice (also observed as a statistically significant decrease in HVR in *Hif-2α$^{f/f}$;ROSACreER* in (Hodson *et al.*, 2016)). Ventilatory acclimatization to hypoxia has been linked to changes in the synthesis of the compound contained in the DCVs, with VAH in cats reportedly accomplished by a decrease in dopaminergic inhibition of D2 receptors at the carotid sinus (Powell *et al.*, 1998; Tatsumi, 1999). This suggests that the reduced ventilatory acclimatisation observed in *Hif-2α$^{f/f}$;THCreER* mice may be explained by the ablation of VAH-linked changes to DCVs by HIF-2α inactivation.

Finally, the data shown in this chapter have potential implications for our understanding of chronic mountain sickness (CMS), also known as Monge's disease. CMS is characterized by polycythaemia, pulmonary hypertension and a decrease in the oxyhaemoglobin saturation of the blood. CMS is most common in chronically adapted populations living at high altitude, such as Tibetan and Ethiopian highlanders. The CMS phenotype is commonly attributed to an overstimulation of the polycythaemic response to hypoxia. Genetic studies have implicated HIF dependent genes such as SENP1, SGK3, and COPS5 in the development of CMS (Stobdan *et al.*, 2017), and studies of Tibetan highlanders have found selection for SNPs located near HIF-2α that correlated strongly with a blunted erythropoietic phenotype and protection from CMS (Beall *et al.*, 2010; Yi *et al.*, 2010). These studies suggest that hypomorphic mutations in HIF-2α may be protective against CMS by blunting HIF-2α dependent polycythaemia. Bigham and Lee have proposed that genetic adaptation to altitude may be achieved through several possible modifications to the HIF-2α-PHD2 pathway (Bigham & Lee, 2014): PHD2 alleles which are either GOF (gain-of-function, enhanced hydroxylase) or LOF (loss-of-function, diminished hydroxylase) and HIF-2α alleles which are either GOF (enhanced activity) or LOF

(diminished activity), paired such that the ultimate consequence is a loss of HIF-2α activity. Thus, Bigham and Lee dismiss the possibility of a PHD2 (LOF): HIF-2α (GOF) combination resulting in adaptation (Bigham & Lee, 2014). However, this chapter reports that specific knockdown of HIF-2α in the carotid body can result in increased polycythaemia by impairing respiratory drive, which in turn impairs oxyhaemoglobin saturation and induces polycythaemia. This provides an alternate route to the CMS phenotype that emphasises respiratory drive, not polycythaemia, as the main causal factor. This suggests that some hypermorphic, enhanced activity mutations in HIF-2α could be beneficial in populations adapted to chronic hypoxia and protective against CMS: by boosting respiratory drive from the carotid body, oxygen saturation may be improved and thus erythropoietic drive decreased. Alongside the significant role of HIF-2α in the carotid body shown by this chapter, these studies suggest that pharmacological inhibition of HIF-2α could have considerable experimental and therapeutic utility. The effect of these inhibitors on the carotid body will be explored in the next chapter.

Results Chapter 4: Pharmacological manipulation of HIF-2a in the carotid body

Introduction:

Although HIF-1α has been viewed as the dominant HIF isoform, transcriptional analysis has shown that HIF-2α, but not HIF-1α, is strongly expressed in the Type I cells of the carotid body (Zhou *et al.*, 2016), and the previous chapter replicated this result using an *in situ* hybridization approach. Previous work by our group has shown that ubiquitous inactivation of HIF-2α, but not HIF-1α, is sufficient to ablate ventilatory acclimatisation to hypoxia and hypoxia-induced proliferation in the carotid body (Hodson *et al.*, 2016). In line with the strong expression of HIF-2α in Type I cells, work described in the previous chapter demonstrated that Type I cell specific inactivation of HIF-2α was sufficient to replicate these phenotypes and to ablate hypoxia-induced changes in angiogenesis, gene expression and Type I cell ultrastructure. These results suggest that HIF-2α, and not HIF-1α, is the major HIF isoform mediating the response of the carotid body to hypoxia.

Both HIF-1α and HIF-2α contain Per-ARNT-Sim (PAS) binding domains, which promote the formation of the HIF /ARNT heterodimer necessary for their function as transcription factors (Erbel *et al.*, 2003). Recent biophysical studies have found that, despite their high sequence similarity, the structure of HIF-2α differs from HIF-1α in the presence of a 290Å hydrophobic pocket within the PAS B domain of HIF-2α (Scheuermann *et al.*, 2009; Rogers *et al.*, 2013). This binding pocket has allowed a pharmaceutical company, Peloton Therapeutics, to use an iterative structure-based design approach to develop a new class of small molecule inhibitors specific to HIF-2α, but not HIF-1α (Scheuermann *et al.*, 2013; Wallace *et al.*, 2016). These inhibitors include the compounds PT2399, PT2977 and the commercially available PT2385 (Wallace *et al.*, 2016; Toledo, 2017). These compounds

bind to the pocket within the PAS B domain of HIF-2α and allosterically disrupt protein-protein interaction between HIF-2α and HIF-1β (ARNT), leading to a marked reduction in the formation of the HIF-2α /ARNT heterodimer and any subsequent gene regulation. The absence of the 290Å hydrophobic pocket from the PAS B domain of the HIF-1α isoform leads to a high selectivity for HIF-2α: the inhibitor PT2385 has been shown to have no effect on the formation or stability of the HIF-1α /ARNT heterodimer (Wallace *et al.*, 2016).

Although initial studies of these compounds have indicated they may have therapeutic benefits upon HIF-2α associated conditions such as ccRCC (Chen *et al.*, 2016; Courtney *et al.*, 2016; Wallace *et al.*, 2016; Courtney *et al.*, 2018), these studies have yet to assess their effects upon the carotid body and HIF-2α associated conditions such as carotid paraganglioma. Given the importance of HIF-2α in carotid body function, it was hypothesized that treatment of mice with a small molecule HIF-2α inhibitor will replicate the effects of genetic HIF-2α inactivation observed in previous chapter. In support of this, a Phase I clinical trial of PT2385 on patients with pre-treated and refractory ccRCC reported hypoxia as a unexpected side effect occurring in 20% of patients (Courtney *et al.*, 2018). Courtney *et al.* suggest that these incidences of hypoxia may be due to the effect of PT2385 upon carotid body mediated ventilation (Courtney *et al.*, 2018). To investigate the effects of these inhibitors, this chapter will characterize the effects of the commercially available PT2385 (purchased from Medchem Xpress) upon the carotid body and its previously identified responses to hypoxia: increased proliferation, hyperplasia, neovascularization, ventilatory acclimatization, and changes in gene expression and ultrastructure.

Results:

Experimental design: Chronic hypoxia exposure with PT2385 treatment.

To characterise for the first time the effect of a new class of small molecule antagonists for HIF-2α upon the carotid body, this study chose to examine the effect of PT2385 on wild-type mice. The commercially available PT2385 was selected from the current range of PAS B domain inhibitors, which includes PT2385, PT2399 and PT2977. PT2385 has been demonstrated to downregulate several genes that are implicated in carotid body proliferation, including Cyclin D1 and VEGFA (Chen *et al.*, 2016; Cho *et al.*, 2016; Wallace *et al.*, 2016) and its pattern of metabolic breakdown has been published in mice (Xie *et al.*, 2018).

To characterise the effect of PT2385 upon carotid body responses to hypoxia, wild-type mice were orally dosed with 3 or 10 mg kg^{-1} PT2385 in a suspension of 0.5% methylcellulose, 0.5% Tween 80 in water (W/V) twice daily. These two concentrations of PT2385 were chosen to match the 3 mg kg^{-1} and 10 mg kg^{-1} doses used in Wallace *et al*., which were shown to result in high levels of PT2385 in blood plasma and reductions in mouse xenograft tumour size (Wallace *et al.*, 2016). Wallace *et al*. showed that the 10 mg kg^{-1} dose achieved a greater reductions in tumour size than the lower 3 mg kg^{-1} dose (Wallace *et al.*, 2016). As such the majority of this chapter will focus on the 10 mg kg^{-1} dose, although the effect of the lower 3 mg kg^{-1} dose will also be assessed for comparison.

In the work described in previous chapters, 7 days of chronic hypoxia (10% oxygen) was shown to result in changes in ventilation, haematocrit and carotid body morphology. Therefore, a similar time course and protocol was adopted for the experiment used in this chapter to test the effect of PT2385. Mice were dosed with PT2385 24 hours prior to

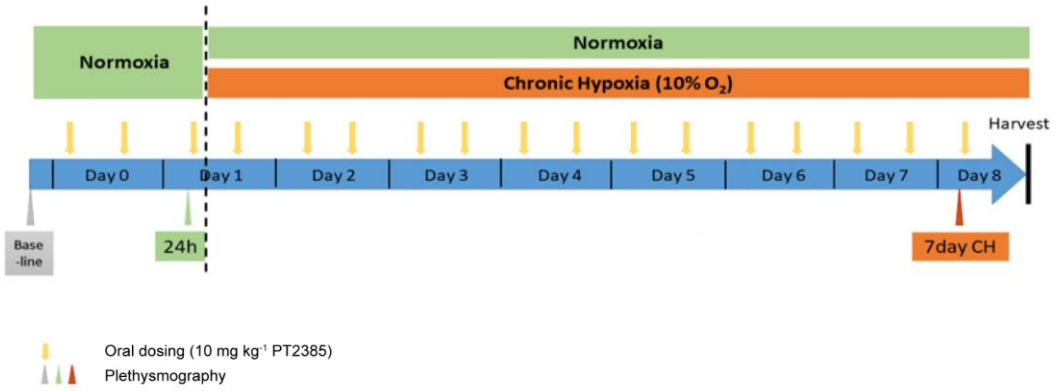


Figure 4.1. Experimental design and dosing regimen for PT2385 treated mice exposed to chronic hypoxia.

Schematic representation of the experimental procedures used in this chapter. Prior to dosing, the baseline response of the mice to 5 minutes of acute hypoxic challenge was assessed *via* plethysmography. 6-week-old wild-type mice were then given a twice daily dose of either a solvent control or 10 mg kg PT23385 in solvent solution. After the first oral dose, mice were assed *via* plethysmography at 24 hours (post-first dose). After one day of dosing, mice were split into normoxic and chronic hypoxic cohorts and dosed with 50 mg kg^{-1} BrdU *via* IP injection. Mice were then maintained on BrdU water (1 mg ml^{-1} BrdU and 1% sucrose). Normoxic mice were maintained at baseline conditions for 7 more days until harvest. Chronic hypoxic mice were placed in a normobaric altitude chamber exposing them to 10% oxygen for the experimental period. During this experimental period, plethysmography was performed at the 7-day (post chronic hypoxic exposure) time point.

chronic hypoxia exposure, in order to ensure that PT2385 was metabolized and to ensure that the effect of PT2385 on the acute response to hypoxia could be assessed. After 24 hours, these mice were then exposed to 7 days of chronic hypoxia (10% oxygen) or normoxia in an experimental design based on that used in the previous chapters (Fig. 4.1). Solvent control animals were dosed with the suspension only. PT2385 has a half-life of 4 hours (Wallace *et al.*, 2016) and has been shown in mice to be metabolized to 12 separate compounds within 24 hours of dosing (Xie *et al.*, 2018). As such, dosing was conducted

twice daily for the duration of the experimental period, beginning one day prior to exposure to hypoxia or normoxia to ensure that HIF-2α inhibition had occurred prior to hypoxic exposure. Twice daily dosing was chosen with this half-life in mind to ensure physiological levels of PT2385 whilst minimizing the disruption of oral dosing and removal from the altitude chamber. Carotid bodies from these mice were harvested at the end of the experimental period and assessed using immunohistochemistry and *in situ* hybridisation.

The effect of a pharmacological HIF-2α inhibitor upon carotid body gene expression.

Work presented in previous chapters of this thesis has shown that 7 days of chronic hypoxia exposure upregulates the expression of several HIF-2α dependent genes, such as Cyclin D1 and VEGFA. This upregulation was blocked by genetic HIF-2α inactivation. To test whether pharmacological inhibition of HIF-2α using PT2385 also affected the expression of these HIF-2α dependent genes, fixed tissue samples were examined for these candidate genes using *in situ* hybridisation with target probes. Samples were also examined for the expression of the Hif-2α mRNA transcript itself, which should not be affected by PT2385 treatment. In line with this, the expression of Hif-2α mRNA itself is unaffected by PT2385 treatment (Fig. 4.2A). The expression of VEGFA, which was shown in Chapter 2 to be dependent on HIF-2a in the carotid body (Fig. 3.3B), was reduced by PT2385 treatment (Fig. 4.2B), although some expression still remained. No significant effect was observed upon the low levels of Cyclin D1 mRNA present in the carotid body (Fig. 4.2C).

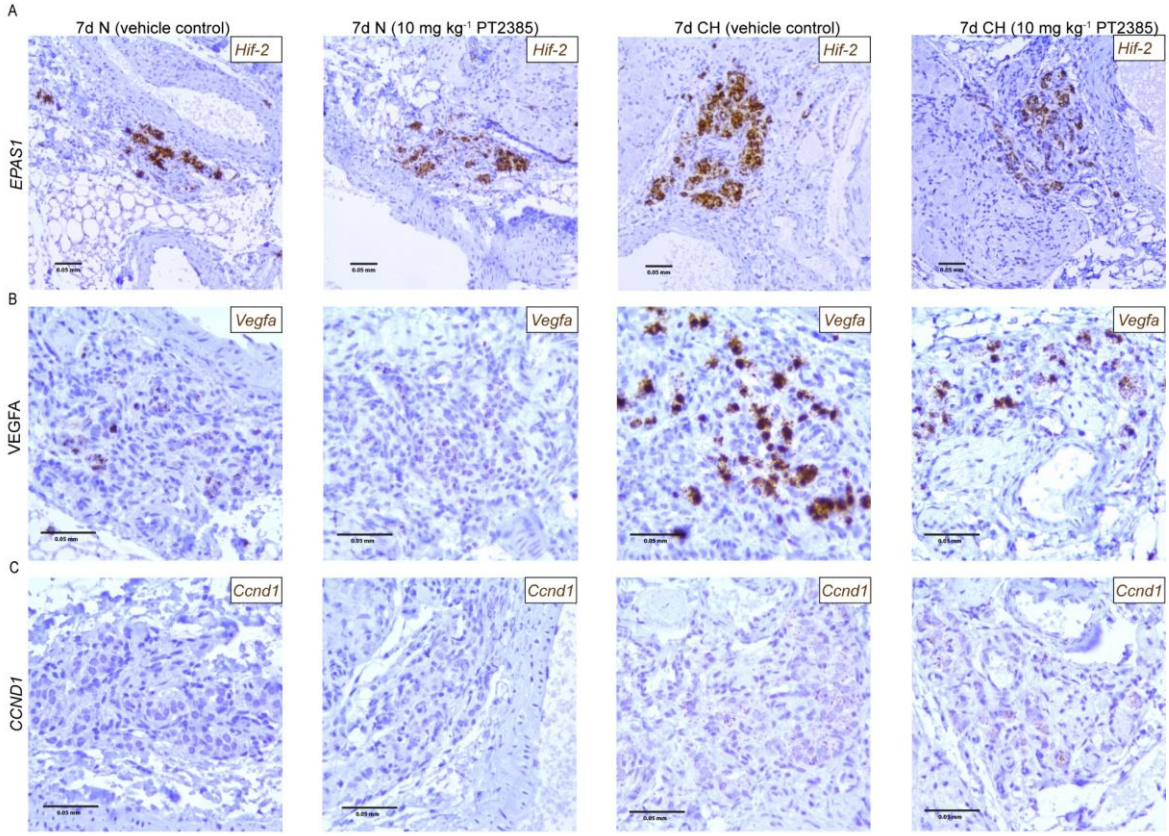


Figure 4.2. The effect of the HIF-2α antagonist PT2385 upon carotid body gene expression in mice exposed to chronic hypoxia.

In situ hybridisation on wild-type mice treated with 8 days of 10 mg kg^{-1} PT2385 compound or a solvent control. Mice are either exposed to normoxia (left hand columns) or chronic hypoxia (10% oxygen for 7 days) (right hand columns). *In situ* hybridisation using probes for mRNA is shown for A) *Hif-2α* mRNA (brown); B) *Vegfa* mRNA (brown) and C) *Cylcin D1 (ccnd1)* mRNA (brown). PT2385 treatment ablates the hypoxia-induced upregulation of *Vegfa* and *Cylcin D1* mRNA.

The effect of varying dosage of pharmacological HIF-2α inhibitors upon carotid body morphology and gene expression.

To assess the effect of PT2385 on carotid body hyperplasia and proliferation, carotid bodies from these mice were examined using immunohistochemistry for the proliferative marker BrdU. Consistent with previous results, solvent treated mice demonstrated a marked carotid body proliferative response to hypoxia, with high levels of BrdU

incorporation (Fig 4.3A & B). Mice treated with 8 days of 10 mg kg^{-1} PT2385 demonstrated a severe ablation of this proliferative response (2729 ± 253 *versus* 321 ± 139 $BrdU^+$ cells mm^{-2}, P <0.0001, Fig 4.2A & B, left panel). The number of cells labelling positively for BrdU in these chronic hypoxic PT2385 treated mice were not significantly different from those of mice maintained in normoxic conditions and given either a control solvent (407 ± 113 $BrdU^+$ cells mm^{-2}) or PT2385 (156 ± 47 $BrdU^+$ cells mm^{-2}) (Fig. 4.3B). This suggests that 10 mg kg^{-1} PT2385 treatment is sufficient to almost totally ablate the proliferative response to chronic hypoxia (Fig. 4.3B). The previous chapters of this thesis have shown that this proliferative response results in an expansion of carotid body volume over a period of days to weeks. Given the observed reduction in the proliferative response to chronic hypoxia, it was hypothesized that PT2385 treatment would also ablate this carotid body hyperplasia. To test whether PT2385 treatment ablates this response, total carotid body volume was assessed in these mice. Carotid body volume was significantly reduced in size in PT2385 treated chronic hypoxic mice relative to solvent treated hypoxia treated controls (0.003106 ± 0.000363 mm^3 *versus* 0.004498 ± 0.000385 mm^3, P < 0.05) and was of comparable size to CBs in normoxic mice in both drug and solvent treated conditions (Fig 4.3B, right panel).

This chapter has shown that PT2385 treatment reduces, but does not totally block, the induction of VEGFA mRNA by chronic hypoxic exposure. VEGFA expression and secretion drives the proliferation of vascular endothelial cells in angiogenesis, a major component of the overall hyperplastic response of the carotid body (Kay & Laidler, 1977). To investigate whether this reduction in VEGFA mRNA expression affects the hypoxia-induced neovascularisation response of the carotid body, the carotid body vasculature was assessed using the endothelial cell marker endomucin. This staining replicated the result

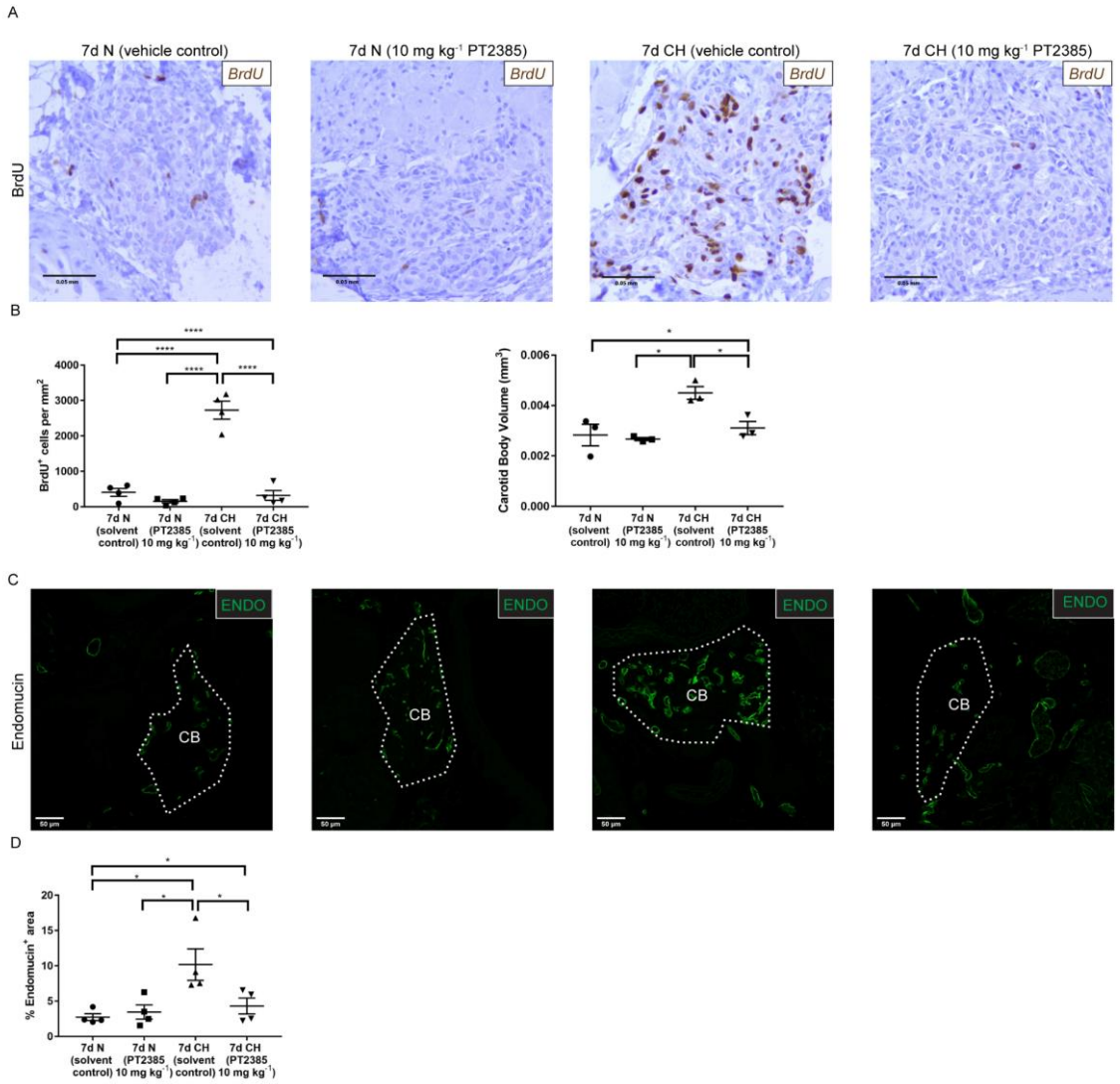


Figure 4.3. The effect of the HIF-2*α* antagonist PT2385 upon carotid body hyperplasia in mice exposed to chronic hypoxia.

Carotid body morphology in n = 4 wild-type mice treated with 8 days of 10 mg kg^{-1} PT2385 compound or a solvent control immediately prior to, and during, exposure to normoxia or chronic hypoxia (10% oxygen for 7 days).

A) Representative images of immunohistochemical staining for BrdU incorporation (brown)

B) Quantification of $BrdU^+$ cell density ($P < 0.0001$) and carotid body volume ($P = 0.0185$)

C) Endomucin (green) immunostaining (CB edges in white) showing hypoxia-induced neovascularisation and its ablation by PT2385 treatment.

D) Quantification of vascular $endomucin^+$ area. $P < 0.001$.

Values shown are mean ± SEM; * $P < 0.05$, **** $P < 0.0001$.

displayed in previous chapters that 7 days of chronic hypoxia leads to an increase in endomucin^{+} cells and the overall % area of the carotid body staining for endomucin. In line with the observed reduction of VEGFA mRNA, this study then found that treatment with 10 mg kg^{-1} PT2385 reversed the hypoxia-induced increase in overall endomucin^{+} area in hypoxic carotid bodies (Fig. 4.3C and Fig 4.3D).

The effect of varying dosage of pharmacological HIF-2α inhibitors upon carotid body morphology and gene expression.

The 10 mg kg^{-1} dosage of PT2385 used in this study was selected based on prior work by Wallace *et al.*, who tested the efficacy and metabolomics of 3 mg kg^{-1}, 10 mg kg^{-1} and 20 mg kg^{-1} dosing of the compound in mice (Wallace *et al.*, 2016). Wallace *et al*. observed that the dosing of 3 mg kg^{-1} PT2385 achieved a similar, if slightly reduced, effect on tumour volume to the 10 mg kg^{-1} dose. To determine whether a lower dose of PT2385 retains the same physiologically relevant effects on carotid body, this study examined the effects of the 3 mg kg^{-1} dosage, using the same experimental design as previously (Fig. 4.1). Chronic hypoxic mice treated with 3 mg kg^{-1} PT2385 demonstrated a similar phenotype to those treated with 10 mg kg^{-1} PT2385. These mice had a reduced carotid body proliferative response to hypoxia and reduced expression of VEGFA mRNA (Fig. 4.4A). The reduction of BrdU incorporation was not significantly different than that observed in mice treated with 10 mg kg^{-1} PT2385 (Fig. 4.4C) although there was a trend towards a reduced effect of both BrdU reduction and VEGFA reduction.

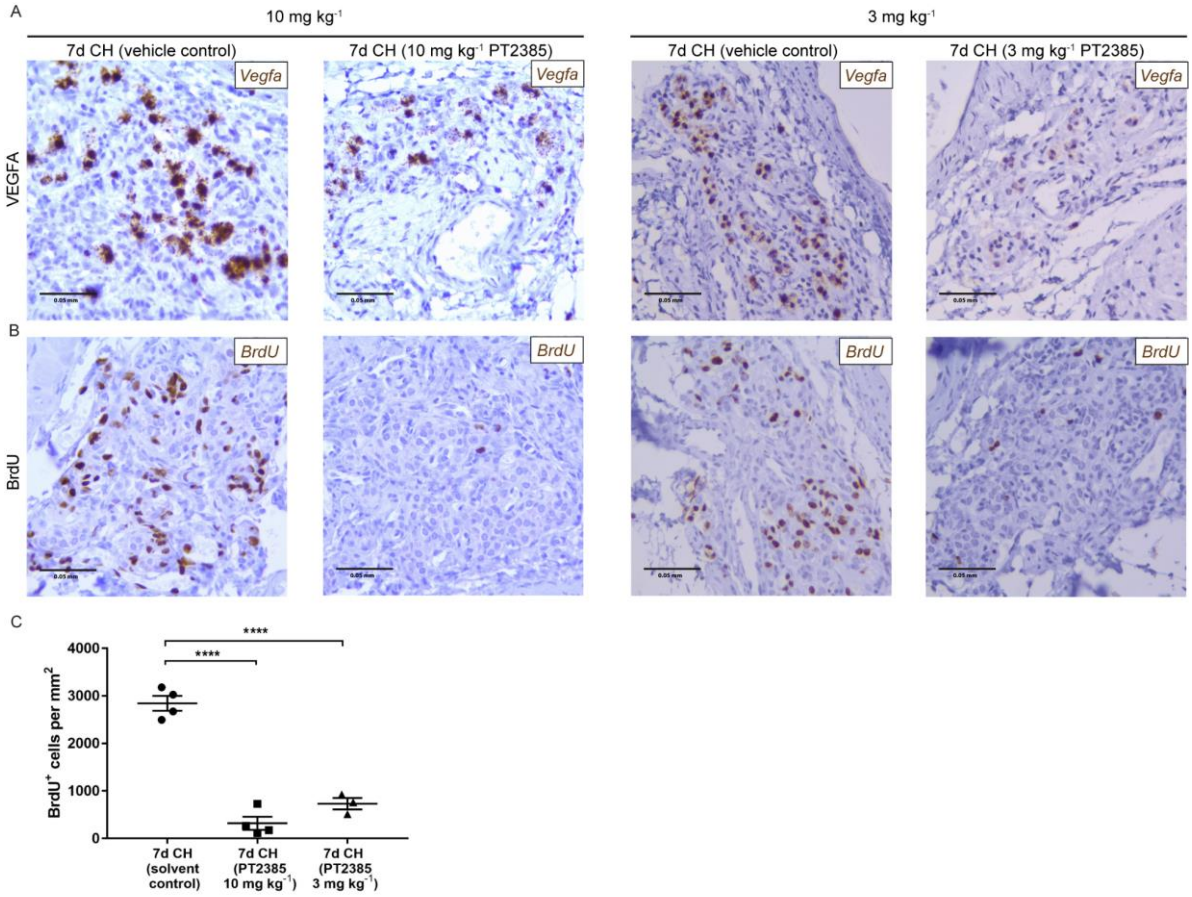


Figure 4.4. Characterization of different doses of PT2385 upon carotid body morphology.

Comparison of mice treated with 8 days of either 10 mg kg^{-1} PT2385, 3 mg kg^{-1} PT2385 or a solvent control immediately prior to, and during, acclimatisation to 7 days of chronic hypoxia (10% oxygen).

A-B) Representative images of carotid body tissue from mice treated with either 10 mg kg^{-1} PT2385 (left) or 3 mg kg^{-1} PT2385 (right). A) *In situ* hybridisation for *Vegfa* mRNA (brown); B) BrdU incorporation (brown).

C) Quantification of $BrdU^+$ (brown) cell density.

Values shown are mean ± SEM; **** $P < 0.0001$.

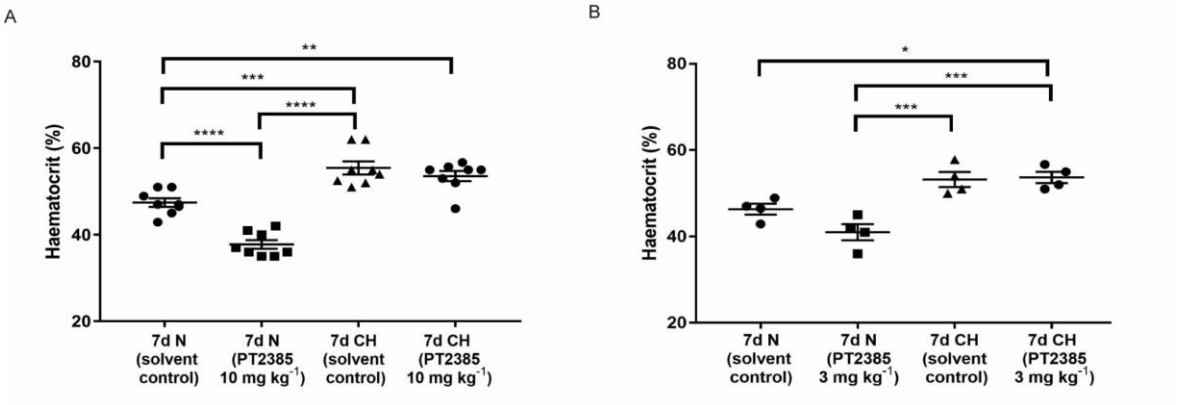


Figure 4.5. The effect of the HIF-2α antagonist PT2385 upon haematocrit in mice acclimatizing to chronic hypoxia.

A) Haematocrit measured from blood taken from the inferior vena cava of n = 8 wild-type mice treated with 8 days of 10 mg kg^{-1} PT2385 compound or a solvent control immediately prior to, and during, exposure to normoxia or chronic hypoxia (10% oxygen for 7 days). $P < 0.0001$.

B) Haematocrit measured from n = 4 wild-type mice treated with 8 days of 3 mg kg^{-1} PT2385 compound or a solvent control immediately prior to, and during, exposure to normoxia or chronic hypoxia (10% oxygen for 7 days). $P < 0001$.

Values shown are mean ± SEM; * $P < 0.05$, ** $P < 0.01$, *** $P < 0.001$, **** $P < 0.0001$.

The effect of a pharmacological HIF-2α inhibitor upon hypoxia-induced polycythaemia.

In addition to proliferative and ventilatory responses to chronic hypoxia, the homeostatic response to hypoxia in mammals also includes erythrocytosis. In normoxic mice, treatment with 10 mg kg^{-1} PT2385 resulted in a reduction in haematocrit relative to solvent treated normoxic controls (Fig. 4.5A). In contrast, 10 mg kg^{-1} PT2385 treatment was not found to significantly reduce haematocrit in chronic hypoxic mice after 7 days of treatment (Fig. 4.5A). This contrasts with its depressive effect in normoxic mice and the effects of ubiquitous HIF-2α inactivation, which ablates hypoxia-induced polycythaemia (Hodson *et al.*, 2016). This study also assessed the effects of treatment with 3 mg kg^{-1} PT2385 upon

haematocrit. This lower dosage broadly reproduced the same effects, but did not show a significant difference between haematocrit between PT2385 and solvent control treated normoxic mice (Fig. 4.5B), suggesting this may be a dose-dependent phenomenon.

The effect of a pharmacological HIF-2α inhibitor upon ventilatory acclimatisation to hypoxia.

To assess whether the regulation of the ventilatory response to hypoxia by the carotid body was disrupted by PT2385 treatment, plethysmography was used to assess the response of mice to a short (5 minute) hypoxic challenge (10% oxygen, a 5-minute pause, and then a 10% oxygen /3% carbon dioxide mix). Mice were tested with plethysmography at several time points throughout the experimental period (Fig. 4.1, Table 4.1, 4.2 and 4.3) and, as in previous chapters, plethysmography measurements of respiratory rate and tidal volume were used to calculate minute ventilation. To examine whether there were any effects of PT2385 treatment on ventilation alone, a baseline plethysmograph was taken immediately prior to the first dose of PT2385 (0 h), then both PT2385 and control treated groups were measured 24 hours post-dose after dwelling in normoxic conditions for that time (Figure 4.6A & B, Table 4.1). At baseline, no statistically significant difference was observable between the groups before PT2385 treatment (Fig. 4.6A, Table 4.1). However, 24 hours after initial dosing a trend was observable of a decreased ventilatory response to acute hypoxic exposure, although this did not reach statistical significance (Fig. 4.6B, Table 4.1). These results were consistent when the animals were exposed to both 10% oxygen /3% carbon dioxide (Fig. 4.6, Table 4.1) and 10% oxygen (Table 4.1) as the acute hypoxic stimulus.

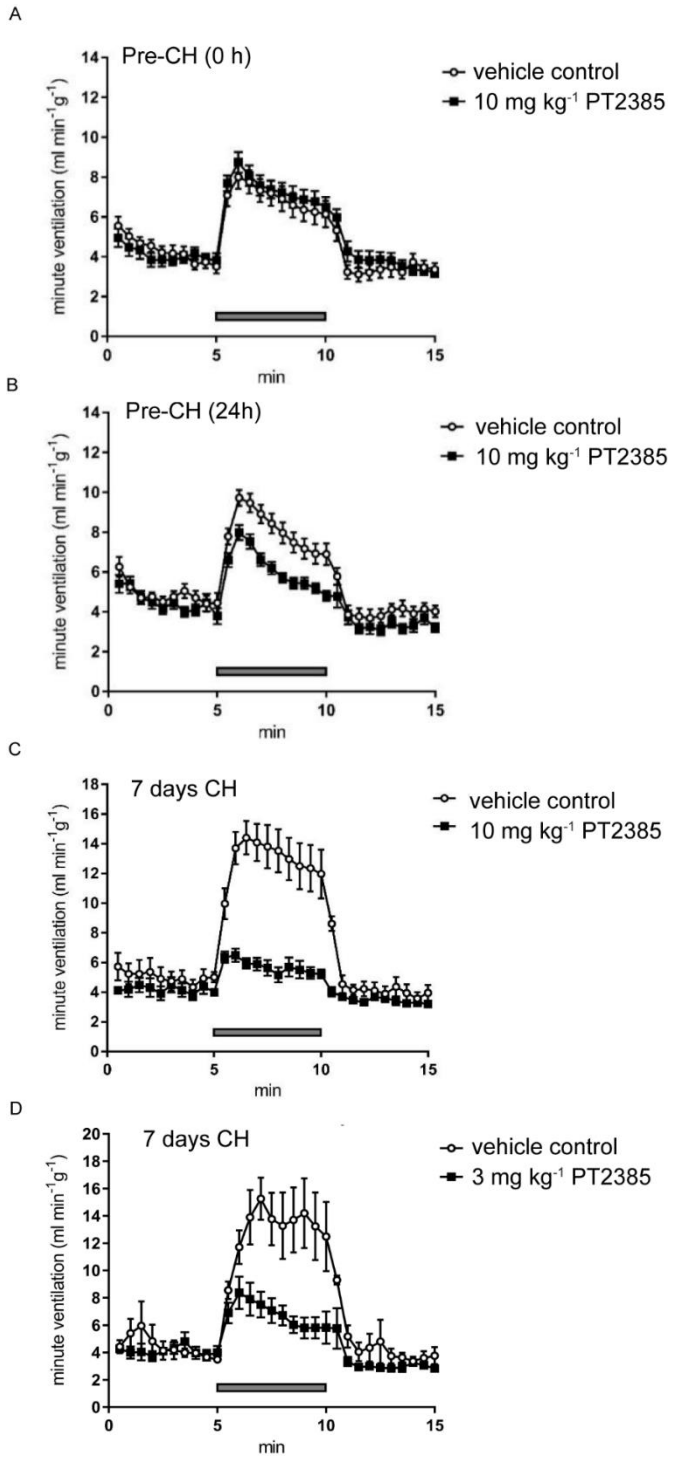


Figure 4.6. The effect of the HIF-2α antagonist PT2385 upon ventilatory responses in mice acclimatizing to chronic hypoxia.

Ventilatory response from n = 8-9 wild-type mice treated with 8 days of PT2385 compound or a solvent control. Measurements were made before, during and after an acute hypoxic stimulus (10% oxygen with 3% carbon dioxide - white bars). Minute ventilation was calculated from respiratory rate and tidal volume measurements made *via*

plethysmography.
A-B) Minute ventilation in mice A) immediately (0 h) and B) 24 hours (24 h) after treatment with 10 mg kg^{-1} PT2385 compound or a solvent control.
C) Minute ventilation in mice after 8 days of treatment with 10 mg kg^{-1} PT2385 or a solvent control and 7 days of acclimatisation to normoxia or chronic hypoxia (10% oxygen for 7 days).
D) Minute ventilation in mice after 8 days of treatment with 3 mg kg^{-1} PT2385 or a solvent control and 7 days of acclimatisation to normoxia or chronic hypoxia (10% oxygen for 7 days).
Plethysmography was conducted by Dr Xiaotong Cheng and Maria Prange-Barczynska.

After acclimatisation to chronic hypoxia, plethysmography was performed 7 days after first exposure to hypoxia (and thus 8 days after PT2385 treatment began). Wild-type mice acclimatised to chronic hypoxia develop an exaggerated ventilatory response to acute hypoxia in a process known as ventilatory acclimatisation to hypoxia (VAH). This VAH to chronic hypoxia was prevented by PT2385 treatment, with PT2385 treated animals showing a significantly reduced HVR when exposed to 10% oxygen /3% carbon dioxide relative to solvent treated controls after one week of chronic hypoxic exposure (Fig. 4.6C, Table 4.2). This result was reproduced when animals were exposed to 10% oxygen as the acute hypoxic stimulus (Table 4.2).

This study also assessed the effects of treatment of a reduced 3 mg kg^{-1} dose of PT2385 upon ventilation. After 7 days of exposure to chronic hypoxia, this lower dosage reproduced the same effects, ablating the ventilatory acclimatisation to hypoxia seen in the solvent treated controls (Fig. 4.6D, Table 4.3). This result was observed when animals were exposed to both 10% oxygen and 10% oxygen /3% carbon dioxide as the acute hypoxic stimulus (Table 4.3).

Acute hypoxic stimulus	Chronic hypoxia duration	Hypoxic ventilatory response (ml min^{-1} g^{-1})			ANOVA *P* value
		Vehicle control	10 mg kg^{-1} PT2385	*t*-test *P* value	
10% O_2	0 hours	0.4297 ± 0.3547	0.1114 ± 0.3147	0.7538	0.525
	24 hours	0.4644 ± 0.2587	0.4419 ± 0.3948	0.9986	
ANOVA *P* value		0.4572			0.344
10% O_2/ 3% CO_2	0 hours	4.248 ± 0.4847	4.544 ± 0.4441	0.8927	0.9984
	24 hours	5.161 ± 0.5556	3.633 ± 0.4783	0.0637	
ANOVA *P* value		0.2161			0.0692

Table 4.1. Acute hypoxic ventilatory responses in mice dosed with 10 mg kg^{-1} PT2385. Hypoxic ventilatory responses of wild-type mice dosed twice daily with 10 mg kg^{-1} PT2385 before (0 hour) the first dose and at 24 hours after the first dose. Values shown are mean changes in minute ventilation (± SEM) in response to the acute hypoxic stimulus. Significance of data was tested using two-way ANOVAs (right hand column *P* value = time factor; bottom row *P* value = drug factor; right column, bottom row right hand *P* value = time /drug interaction factor), followed by *t*-tests (with Holm-Sidak correction) for analysis of individual time points; n = 15. $P < 0.05$ comparisons are highlighted in bold. Plethysmography was conducted by Dr Xiaotong Cheng and Maria Prange-Barczynska.

Acute hypoxic stimulus	**Chronic hypoxia duration**	**Hypoxic ventilatory response (ml min^{-1} g^{-1})**			**ANOVA *P* value**
		Vehicle control	**10 mg kg^{-1} PT2385**	***t*-test *P* value**	
10% O_2	0 hours	0.7701 ± 0.5511	-0.1216 ± 0.6319	0.2799	**0.0208**
	7 days	3.317 ± 0.6567	0.1807 ± 0.3938	**0.0018**	
ANOVA *P* value		**<0.0020**			0.0620
10% O_2/ 3% CO_2	0 hours	4.842 ± 0.8668	4.305 ± 0.7263	0.6469	0.2473
	7 days	9.078 ± 0.9987	2.015 ± 0.6249	**0.0001**	
ANOVA *P* value		**<0.0002**			**0.0007**

Table 4.2. Acute hypoxic ventilatory responses of mice dosed with 10 mg kg-1 PT2385 during acclimatisation to chronic hypoxia.

Hypoxic ventilatory responses of wild-type mice dosed twice daily with 10 mg kg^{-1} PT2385 and exposed to 10% oxygen in a normobaric altitude chamber. Results were recorded before the first dose and immediately prior to hypoxic exposure (0 hour) and at 7 days after placement in chronic hypoxia. Values shown are mean changes in minute ventilation (± SEM) in response to the acute hypoxic stimulus. Significance of data was tested using two-way ANOVAs (right hand column *P* value = time factor; bottom row *P* value = drug factor; right column, bottom row *P* value = time /drug interaction factor), followed by *t*-tests (with Holm-Sidak correction) for analysis of individual time points; n = 6. $P < 0.05$ comparisons are highlighted in bold.

Plethysmography was conducted by Dr Xiaotong Cheng and Maria Prange-Barczynska.

Acute hypoxic stimulus	**Chronic hypoxia duration**	**Hypoxic ventilatory response (ml min^{-1} g^{-1})**			**ANOVA**
		Vehicle control	**3 mg kg^{-1} PT2385**	***t*-test *P* value**	***P* value**
10% O_2	0 hours	0.1409 ± 0.6077	-0.2395 ± 0.9713	0.3804	**0.0075**
	7 days	3.068 ± 0.4574	1.022 ± 0.4288	0.0915	
ANOVA *P* value		0.0879			0.2263
10% O_2/ 3% CO_2	0 hours	4.348 ± 0.9085	4.178 ± 0.4339	0.9920	**0.0360**
	7 days	9.224 ± 1.6	4.24 ± 0.8961	**0.0111**	
ANOVA *P* value		**0.0298**			**0.0401**

Table 4.3. Acute hypoxic ventilatory responses of chronically acclimatized wild-type mice exposed to 3 mg kg-1 PT2385.

Hypoxic ventilatory responses of wild-type mice dosed twice daily with 3 mg kg^{-1} PT2385 for 7 days and exposed to 10% oxygen. Ventilatory responses to acute hypoxia are shown for recordings taken at 7 days after exposure to chronic hypoxia. Values shown are mean changes in minute ventilation (± SEM) in response to the indicated acute hypoxic stimulus. Significance of data was tested using two-way ANOVAs (right hand column *P* value = time factor; bottom row *P* value = drug factor; right column, bottom row *P* value = time /drug interaction factor), followed by *t*-tests (with Holm-Sidak correction) for analysis of individual time points; n = 4. $P < 0.05$ comparisons are highlighted in bold. Plethysmography was conducted by Dr Xiaotong Cheng and Maria Prange-Barczynska.

The effect of a pharmacological HIF-2α inhibitor upon carotid body Type I cell ultrastructure.

This study has previously observed that hypoxia induces clear ultrastructural changes in Type I cell size and a decrease in the number of dense core vesicles present in these cells (Fig. 2.5A and Fig 3.4) These changes were reversed by inducible genetic inactivation of HIF-2α in Type I cells in *HIF-2α$^{f/f}$;THCreER* mice (Fig 3.7). These cell intrinsic changes may represent changes to Type I cell secretion and neurotransmitter release. Given the effects of PT2385 treatment upon both these processes, this study sought to characterise the effects of 10 mg kg^{-1} PT2385 upon carotid body Type I cell ultrastructure. Type I cells from chronic hypoxic PT2385 treated mice were examined under electron microscopy and were found to have a significantly increased density of DCVs relative to solvent treated controls (Fig.4.7). No change in DCV density was observed in PT2385 *versus* solvent treated normoxic mice. These results suggest that pharmacological inhibition of HIF-2α, like the genetic inactivation reported in the previous chapter, ablates the hypoxia induced decrease in DCV density reported in Chapter 2, but has no significant effects on the normoxic carotid body. Eccentric DCVs were seen at a high frequency in both PT2385- and solvent-treated Type I cells from hypoxia treated mice, and their occurrence did not appear to be affected by PT2385 treatment. No other major abnormalities were observed in the carotid body in this analysis of CB ultrastructure.

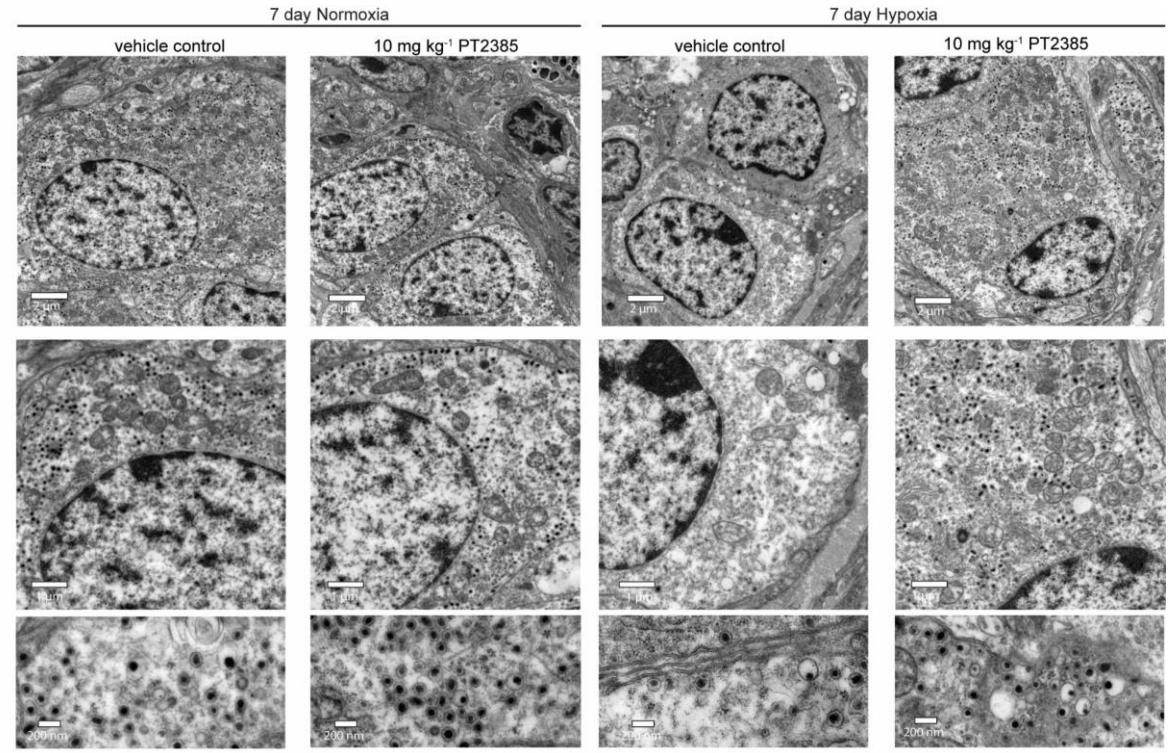


Figure 4.7. The effect of the HIF-2α antagonist PT2385 upon carotid body ultrastructure in mice exposed to chronic hypoxia.

Electron microscopy imaging of Type I cells from carotid bodies of n = 2 wild-type mice treated with 8 days of 10 mg kg^{-1} PT2385 compound or a solvent control immediately prior to, and during, exposure to normoxia or chronic hypoxia (10% oxygen for 7 days). PT2385 ablates hypoxia-induced changes in dense core vesicle (DCV) density.

Upper panels: low power electron microscope images showing the general appearance of Type I cells. Scale bars = 2 µm.

Middle and lower panels: high power electron microscope images showing the appearance and density of dense core vesicles (see lower panel inserts) in Type I cells. Scale bars = 1 µm or 200 nm.

Discussion:

The results shown in this chapter have demonstrated that treatment with a small molecule HIF-2α antagonist, PT2385, ablates hypoxia-induced ventilatory acclimatisation, carotid body proliferation, hyperplasia and the accompanying changes in Type I cell ultrastructure reported in previous chapters. A reduced dose of PT2385 reproduced these effects. These results suggest that the two doses employed in this study fall within a pharmacologically relevant range for the treatment of hypoxic mice in a non-malignant setting, and recapitulated effects on gene expression and proliferation similar to those observed in the treatment of malignant HIF-2α dependent xenografts (Wallace *et al.*, 2016). Most of these phenotypes recapitulate the effects of ubiquitous genetic inactivation of HIF-2α as reported by Hodson *et al* (Hodson *et al.*, 2016). An exception to this was observed in the effect of PT2385 on erythropoiesis: instead of ablating hypoxia-induced polycythaemia as in Hodson *et al*., PT2385 treatment had a depressive effect on haematocrit in normoxic mice, but no effect on chronic hypoxic mice at the 7-day timepoint (Hodson *et al.*, 2016).

This work corroborates evidence for the effects of genetic HIF-2α upon the carotid body which were reported in the previous chapter. Together, these results indicate that pharmacological or inducible genetic HIF-2α inhibition prevents carotid body proliferation and ventilatory changes, suggesting that HIF-2α mediates these effects. In turn, this suggests that stabilisation of HIF-2α *via* pseudohypoxia may be capable of driving proliferation and ventilatory acclimatisation, as well as highlighting the potential of HIF-2α for therapeutic or experimental manipulation of the niche.

The development of small molecule inhibitors of HIF-2α provides several opportunities for future research and clinical therapies. The results of this chapter have shown that PT2385

is capable of attenuating many of the physiological adaptations to chronic hypoxia, including ventilatory acclimatisation to hypoxia. This suggests that PT2385 may be useful for clinical treatments of conditions in which HIF-2α has been implicated, such as sleep apnoea, pulmonary hypertension and chronic mountain sickness (CMS) (Beall *et al.*, 2010; Semenza, 2014). HIF-2$\alpha^{+/-}$ mice have previously been shown to be protected against pulmonary hypertension (Brusselmans *et al.*, 2003). Genetic studies of high-altitude acclimatised populations have found that hypomorphic mutations in HIF-2α, which result in a blunted erythropoietic response to hypoxia, are in turn associated with protection against CMS. These results suggest that a pharmacological inhibitor of HIF-2α may provide similar protective effects to patients with these conditions. To assess its use for treating patients suffering from altitude-related diseases, it would be beneficial to examine the effect of PT2385 upon already acclimatised mice. Hyperplastic carotid bodies have been shown to return to a normal size over 4-8 weeks when returned to normoxic conditions (Kusakabe *et al.*, 2004; Pardal *et al.*, 2007), whilst VAH is slowly reversed over a similar time scale upon return to normoxia in a process known as ventilatory de-acclimatization from hypoxia (VDH) (Bisgard, 1995; Powell *et al.*, 1998). Long-term PT2385 treatment could accelerate this regression in normoxic animals, or replicate it in chronic hypoxic animals and /or patients.

Beyond their potential in pulmonary hypertension and altitude sickness, the most exciting application for small molecule HIF-2α inhibitors is their potential for clinical therapies in pseudohypoxic cancers. Stable HIF-2α expression occurs in hypoxic tumour regions and is a noted feature of a range of pseudohypoxic cancers including ccRCC, pheochromocytoma and carotid paraganglioma (Kaelin, 2002; Acker *et al.*, 2005; Toledo *et al.*, 2013; Toledo, 2017). In support of this link, HIF-2α knockout has been shown to inhibit tumour growth

(Kondo *et al.*, 2003; Zimmer *et al.*, 2004). In these tumours, HIF-2α is thought to promote oncogenesis by upregulating VEGFA expression, which in turn mediates neo-angiogenesis and increased access to nutrients and oxygen for the tumour (Kaelin, 2008). This understanding has already led to the use of tyrosine kinase inhibitors that block VEGFR receptors, such as sunitinib, sorafenib and cabozantinib, as effective therapeutic treatments for ccRCC. However, treatment with these anti-angiogenetic drugs is often limited by the development of resistance in many patients (Shojaei, 2012). The development of small molecule HIF-2α inhibitors thus presents a novel route to intervene in the progression of pseudohypoxic cancers and both PT2385 and PT2399 have entered clinical trials. The first of these trials have indicated that PT2385 has a safe clinically effective dosing range and showed positive effects on patients with pre-treated refractory VHL-deficient ccRCC (Courtney *et al.*, 2018). Recent work on these compounds has shown that they are capable of reducing oncogenesis *in vitro* and *in vivo* (Chen *et al.*, 2016; Cho *et al.*, 2016). These compounds have been shown to be effective in combination with other methods of immunotherapy, including PD-1 immune checkpoint inhibitors and VEGFR2 inhibitors (Chen *et al.*, 2016). However, sustained treatment with HIF inhibitors on VHL-mutated ccRCC xenograft models resulted in the development of resistance partially mediated by mutations in the PAS B domain of HIF-2α (Chen *et al.*, 2016). The possibility for alterations to the PAS B domain to render cancers refractory to PT2385 and other related compounds is a potential therapeutic concern that should be factored into future research and could be examined using the HIF-2α$^{S305M/S305M}$ mutant developed by Feng *et al*. (Feng *et al.*, 2018).

A caveat to this study's conclusions is that PT2385 may have off-target effects beyond the action of HIF-2α in the carotid body. Because PT2385 was administered systemically, this

study cannot be certain that its reported effects are wholly mediated by the inhibition of HIF-2α in the carotid body. As previously noted in Chapter 3, ventilation is partially regulated by brainstem neurons which are reportedly affected by chronic hypoxic exposure (Burke *et al.*, 2014; Wenker *et al.*, 2017). In addition to ventilation, the erythropoietic phenotype reported in this chapter may represent the action of PT2385 outside the carotid body. Erythropoiesis is primarily mediated by HIF-2α dependent expression of EPO in the kidneys, which is inhibited by small molecule HIF-2α inhibitors such as PT2399 and PT2385 (Wallace *et al.*, 2016; Feng *et al.*, 2018). Thus, the observed depression of normoxic haematocrit may be due to the inhibition of EPO in the kidney by PT2385. The restoration of elevated haematocrit levels at the 7-day time point may be caused by the ablation of ventilatory acclimatisation resulting in greater levels of physiological hypoxia, which in turn causes increased erythropoietic signalling *via* HIF-2α independent mechanisms, such as HIF-1α stabilization. The difference between the effect of PT2385 and genetic inactivation may thus simply reflect a difference in the efficacy of PT2385 on EPO and respiratory control.

However, this does not fully explain the contrast with the effect of ubiquitous genetic knockdown of HIF-2α in *HIF-2α$^{f/f}$;RosaCreER* mice, which have normal normoxic haematocrits and an ablated hypoxia-induced polycythaemia (Hodson *et al.*, 2016). This difference between genetic and pharmacological inhibition of HIF-2α suggests that PT2385 may have other off-target effects, for example by acting on non-HIF-2α targets. To address this, future work could examine the effect of PT2385 upon mice with HIF-2α or ARNT inactivation, where any additional effects of PT2385 upon the HIF-2α or ARNT phenotype could indicate off-target effects not mediated by the activity of the HIF-2α /ARNT heterodimer. However, genetic knockdown of these genes rarely achieves

complete recombination, and thus an observed effect could represent the inhibition of some remaining unrecombined cells. As an alternative approach, the effect of PT2385 could be tested on the newly developed HIF-2α PAS B mutant (HIF-2α$^{S305M/S305M}$) mouse line, which has been shown to be resistant to PT2399 treatment (Feng *et al.*, 2018). The S305M mutation inhibits the binding of inhibitors to the PAS B domain, and thus this line may be useful for identifying any off-target effects of PT2385 not mediated *via* allosteric inhibition of the PAS B /ARNT complex.

The above work on the therapeutic potential of PT2385 in pseudohypoxic cancers, combined with this chapter's work showing an effect of PT2385 treatment on the carotid body, indicates that these compounds may have a positive clinical benefit on paraganglioma patients. These tumours of the head and neck (including the carotid body) are often highly vascular, presenting severe difficulties during surgical resection, making the development of pharmacological treatments particularly appealing. Chapter 5 of this study will investigate the use of pseudohypoxic stimulation of the carotid body Type I cells to create a potential mouse model of carotid paraganglioma, which may in turn be useful to test the potential efficacy of PT2385 upon this condition

Results Chapter 5: The Effect of PHD2 inactivation in the carotid body Type I cells

Introduction:

The previous chapters have shown that carotid body proliferation is dependent on the expression of HIF-2α in the Type I cells of the carotid body. The HIF family is negatively regulated by a family of oxygen-dependent HIF prolyl hydroxylases: PHD1, PHD2 and PHD3 (Epstein *et al.*, 2001; Berra *et al.*, 2003; Appelhoff *et al.*, 2004). Of these, PHD2 is universally expressed in mammalian tissue whilst PHD1 and PHD3 have more tissue specific expression patterns. Inactivation of a PHD isoform leads to a reduction in PHD mediated HIF degradation and a resultant accumulation of stable HIF-α protein, leading to translocation to the nucleus and subsequent gene regulation, a condition known as 'pseudohypoxia' (Bratslavsky *et al.*, 2007). Pseudohypoxia has been implicated in the formation of carotid paragangliomas, and is a feature of VHL syndrome, in which pseudohypoxia drives neo-angiogenesis and the formation of tumours including renal cell carcinoma (RCC) and pheochromocytoma (Kaelin, 2002; Toledo, 2017). Previous work has shown that hemizygous PHD2 inactivation results in enlarged carotid bodies and an exaggerated ventilatory response to hypoxia in *Phd2*$^{+/-}$ mice (Bishop *et al.*, 2013). Our group has shown that global inducible inactivation of PHD2 using the RosaCreER promoter results in increased ventilatory sensitivity (Hodson *et al.*, 2016). Concomitant inactivation of HIF-2α, but not HIF-1α, ablated these changes, suggesting a specific role for the HIF-2α /PHD2 couple (Hodson *et al.*, 2016).

Chapter 3 of this study found that this requirement for HIF-2α is specific to the Type I cells of the carotid body, which have been suggested to be capable of driving proliferation in the rest of the niche *via* the release of mitogens such as VEGFA (Platero-Luengo *et al.*,

2014). Given the importance of HIF-2α to Type I cell function and proliferation in hypoxia, would the pseudohypoxic activation of HIF in these cells replicate some of the effects of hypoxia characterized in the previous chapters? If so, can this be used to demonstrate that stable HIF-2α is not only necessary but sufficient to drive Type I cell hypoxic responses and the responses of the rest of the niche? To answer these questions, this chapter will inactivate the dominant PHD2 isoform in the Type I cells using the inducible *THCreER* promoter characterized in previous chapters and a constitutive *THCre* promoter, which will be characterized here. Inactivation of PHD2 will lead to the stabilization of both HIF isoforms in the Type I cells and this study will examine these mice for changes in ventilatory function, carotid body morphology, gene expression and ultrastructure. The relative roles of HIF-1α and HIF-2α will then be assessed by concomitant inactivation of these isoforms alongside this pseudohypoxic inactivation of PHD2. If this chapter observes that major changes are driven by inducible or constitutive PHD2 inactivation, these mice may provide a useful model for the study of pseudohypoxic cancers and other conditions.

Results:

The effect of constitutive 'pseudohypoxic' PHD2 inactivation in Type I cells.

Of the PHD isoforms, PHD2 is the most universally expressed and has been shown to be strong expressed in the carotid body. Previous work by our group has shown that that hemizygous PHD2 inactivation in *Phd2*$^{+/-}$ mice results in carotid body hyperplasia (Bishop *et al.*, 2013). Given the importance of HIF-2α demonstrated in previous chapters, it is likely, though unconfirmed, that this effect is mediated by 'pseudohypoxic' stabilisation of HIF-2α in the carotid body Type I cells driving proliferation in the Type I cells themselves

and by paracrine signalling to other populations. In order to test this hypothesis, this study examined constitutive inactivation of PHD2 under the THCre promoter. This *Phd2$^{f/f}$;THCre* construct results in the inactivation of PHD2 in TH expressing cells when TH is expressed at embryonic stage E13.5 (Son *et al.*, 1996). The effects of the inactivation will thus affect both the development of the carotid body and its function in adulthood. To test the efficacy of the THCre promoter, this study first examined the expression of the fluorescent reporter tdTomato Ai14 under control of this promoter. Strong red fluorescent signal was observed in 99% of TH$^+$ Type I cells in a *tdTomato$^{f/+}$;THCre* mouse, indicating strong recombination (Fig. 5.1A). No fluorescent signal was observed in TH- cells, indicating specificity to the TH line and a lack of differentiation of this population to other populations during development (Fig. 5.1A). The effect of PHD2 inactivation under the THCre promoter was then assessed in *Phd2$^{f/f}$;THCre* animals and *Phd2$^{f/f}$* controls at 3 months of age. This time point was chosen to allow time for potential adult phenotypes to develop. Because previous chapters have shown that ventilatory acclimatisation is dependent on HIF-2α, and previous work by our group has shown that inducible global inactivation of PHD2 is sufficient to increase ventilatory sensitivity to hypoxia in *Phd2$^{f/f}$;RosaCreER* animals, this study examined the ventilatory response to acute (5 minute) hypoxic exposure to 10% oxygen alone, and to 10% oxygen and 3% carbon dioxide. This chapter found that these *Phd2$^{f/f}$;THCre* mice did not show a statistically significant increase in baseline ventilation and acute hypoxic ventilatory responses compared to *Phd2$^{f/f}$* controls in either condition (Fig. 5.1B, Table 5.1). However, a slight trend to an increased baseline and acute hypoxic ventilatory response was observed.

To assess any morphological changes to the carotid bodies from *Phd2$^{f/f}$;THCre* animals,

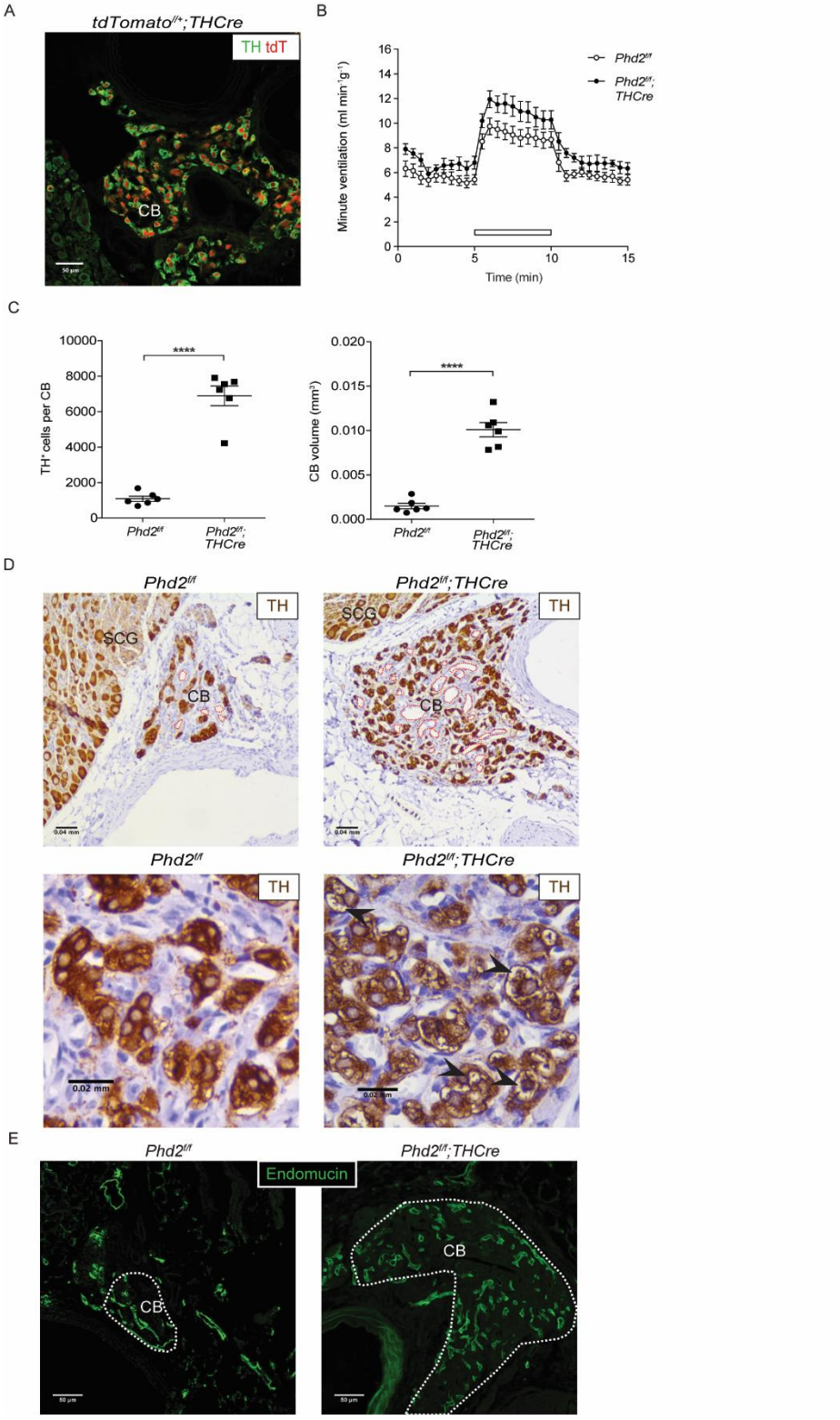


Figure 5.1. The effect of constitutive Type I cell-specific PHD2 inactivation upon CB morphology and function.

Constitutive inactivation of PHD2 in Type I cells results in pseudohypoxic stimulation and the formation of hyperplastic carotid bodies.

A) TH immunostaining (green) and tdTomato fluorescence (red) showing high rate of recombination under the constitutive THCre driver in *tdTomato$^{f/f}$;THCre* mice
B-E) Carotid body morphology and ventilation in n = 6 *Phd2$^{f/f}$;THCre* and *Phd2$^{f/f}$* littermate control mice:
B) Minute ventilation before, during and after an acute hypoxic stimulus (10% oxygen with 3% carbon dioxide - white bars). Minute ventilation was calculated from respiratory rate and tidal volume measurements made *via* plethysmography.
Plethysmography was conducted by Dr Emma Hodson.
C) Quantification of TH^+ cell number and carotid body volume.
D) Representative images of TH (brown) immunostaining with vascularisation marked in red. Low magnification images (upper panels) show both the carotid body (CB) and the superior cervical ganglion (SCG). High magnification images (lower panels) showing the presence or absence of clearing in Type I cells (marked with black arrowheads).
E) Endomucin immunostaining (green, CB edges outlined in white).

carotid bodies from these mice were stained for the Type I cell marker tyrosine hydroxylase (TH). TH positive cell numbers were counted, and the outline of the carotid body across multiple slides was measured and used to assess the overall volume of each carotid body. This study found that the number of TH^+ cells was significantly increased in *Phd2$^{f/f}$;THCre* mice relative to *Phd2$^{f/f}$* controls (6892 ± 558 *versus* 1089 ± 145 TH^+ cells, $P < 0.0001$, Fig. 5.1C). In line with this increase in TH^+ cell number, the volume of the *Phd2$^{f/f}$;THCre* carotid bodies were significantly enlarged relative to control carotid bodies, with a ~7 fold increase in TH^+ volume observed (Fig. 5.1C). These carotids resembled but exceeded the size of hyperplastic carotid bodies from chronically acclimatised mice characterized in Chapter 2. These hyperplastic carotid bodies were highly vascular (vasculature marked in red, Fig 5.1D, upper panels). In addition to this increase in Type I cell numbers, TH- cell numbers were also markedly increased. Staining for the Type II cell marker GFAP indicated that a proportion of these TH^- cells represented Type II astrocytes, suggesting that a proliferative expansion had occurred across multiple cell types.

As suggested by the disconnect between carotid body expansion and a lack of ventilatory changes, this multi-lineage CB hyperplasia may not be fully functional. Indeed, several abnormalities were noted under light microscopy, most notably the appearance of large clear spaces inside numerous Type I cells. This 'clear cell' phenotype was observed in approximately half of the hyperplastic carotid bodies (Fig. 5.1D, lower panels). This phenotype appears similar to the vacuolated cytoplasm reported in enlarged carotid bodies in high altitude dwellers (Edwards *et al.*, 1971; Edwards *et al.*, 1972; Arias-Stella & Valcarcel, 1976) and in carotid paragangliomas (Ashley & Evans, 1966; Robertson & Cooney, 1980; Wieneke & Smith, 2009). Diagnostic staining with Oil Red O and periodic acid–Schiff (PAS) stains indicated these cleared regions contained neither lipid nor glycogen, commonly suggested contents for cellular cleared regions.

In addition to the Type I cell hypertrophy observed in the *Phd2$^{f/f}$;THCre* carotid bodies, an expanded vasculature was observed. To confirm this neovascularisation of the carotid body, immunostaining for an endothelial cell marker, endomucin^{+}, was conducted. This staining demonstrated a significant expansion of carotid body endothelial^{+} cells (Fig. 5.1E). This staining was repeated using two other vascular makers, CD31 and isolectin, and replicated these results (data not shown).

The effect of constitutive 'pseudohypoxic' PHD2 inactivation in Type I cells upon carotid body gene expression.

Previous chapters have discussed the role of HIF-mediated gene regulation in driving proliferation in the carotid body, both within the Type I cell population and in the wider CB parenchyma. These chapters have demonstrated expression of the cell cycle regulator

Ccnd1 and the angiogenesis signalling protein VEGF is induced by hypoxia, and that this effect is HIF-2α dependent. Given the expansion of the Type I cell population and the adjacent endothelial cell population (in which no genetic inactivation occurred), we hypothesised that PHD2 'pseudohypoxic' inactivation may be driving the overexpression of these genes.

Consistent with this hypothesis, *in situ* hybridisation for vascular endothelial growth factor (*Vegfa*) mRNA showed *Vegfa* was strongly expressed in hyperplastic *Phd2$^{f/f}$;THCre* carotid bodies relative to controls (Fig. 5.2A). Double staining with TH immunohistochemistry showed that this *Vegfa* expression was strictly confined to the Type I cell population within the carotid body (Fig. 5.2B), in contrast to its minimal expression in other cell types in the carotid body and other nearby TH^{+} tissues such as the SCG. Notably, *Vegfa* expression was not upregulated in the endothelial cell population, despite the expansion of this population. This suggests that inducing pseudohypoxia in the Type I cell population is sufficient to drive the expansion of other cell types, likely through paracrine release of VEGFA and other compounds. This increase in *Vegfa* expression was reproduced with quantitative RT-PCR analysis on homogenized carotid bodies from *Phd2$^{f/f}$;THCre* mice and *Phd2$^{f/f}$* mice and found to be statistically significant (Fig. 5.2C).

In addition to the changes in *Vegfa*, *in situ* hybridisation indicated that Cyclin D1 (*Ccnd1*) mRNA expression was increased in *Phd2$^{f/f}$;THCre* carotids relative to controls (Fig. 5.2D). Quantitative RT-PRC on homogenised carotid bodies replicated these results, demonstrating a significant increase in *Ccnd1* expression in *Phd2$^{f/f}$;THCre* mice relative to controls *Phd2$^{f/f}$* (Fig. 5.2E). The change in *Ccnd1* expression with pseudohypoxic PHD2 inactivation was equivalent to that observed in CBs acclimatised to chronic hypoxia.

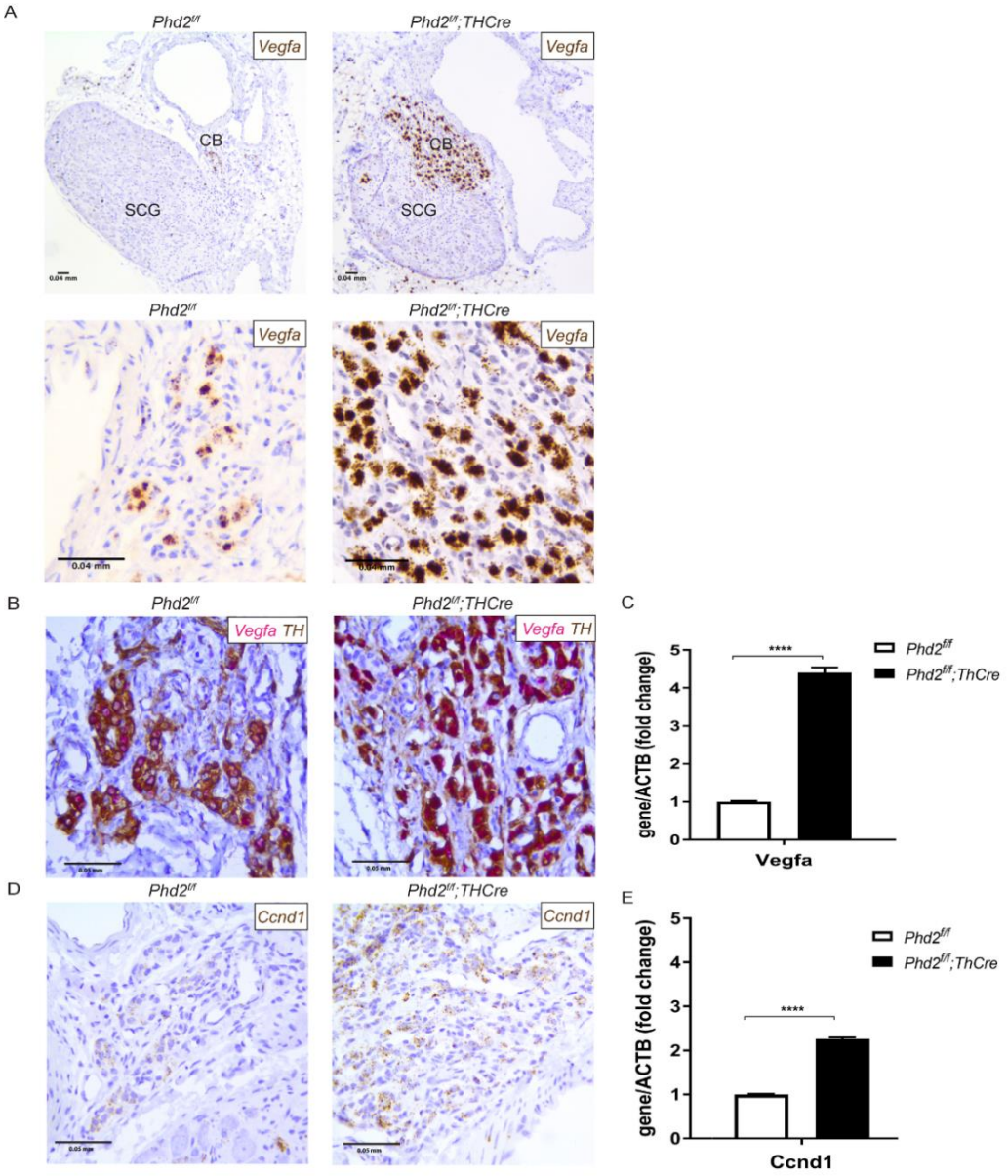


Figure 5.2. The effect of Type I cell-specific PHD2 inactivation upon carotid body gene expression.

Representative images of CB tissues from *Phd2$^{f/f}$;THCre* and *Phd2$^{f/f}$* littermate controls.

A) *In situ* hybridisation for *Vegfa* mRNA (brown) in the carotid body (CB) and the superior cervical ganglion (SCG).

B) Dual *in situ* hybridisation for *Vegfa* mRNA (pink) and TH immunostaining (brown).

C) quantitative RT-PCR for *Vegfa* in homogenised carotid bodies from *Phd2$^{f/f}$;THCre* and *Phd2$^{f/f}$* littermate control mice.

D) *In situ* hybridisation for cyclin D1 *Ccnd1* mRNA (brown).

E) quantitative RT-PCR for *Ccnd1* in homogenised carotid bodies from *Phd2$^{f/f}$;THCre* and *Phd2$^{f/f}$* littermate control mice.

The role of HIF-1α and HIF-2α in 'pseudohypoxia'-driven carotid body hyperplasia.

These results suggest that PHD2 inactivation is sufficient to drive hypoxic gene expression and hypoxic signalling in Type I cells, which is in turn sufficient to drive a multilineage hyperplasia through autonomous, autocrine and /or paracrine effects. The effects of PHD2 inactivation are likely mediated through the stabilization of the HIF transcription factors, which are negatively regulated by PHD2 in normal physiology. Experimental data presented by this thesis in previous chapters has suggested that of the HIF isoforms, HIF-2α is the primary mediator of hypoxia induced hyperplasia in the carotid body. These results have also demonstrated no major effects of HIF-1α inactivation. Therefore, we hypothesized that the *Phd2$^{f/f}$;THCre* phenotype presented in this chapter is primarily mediated through the stabilisation and transcriptional activity of HIF-2α in the carotid body Type I cell.

To confirm this, this study examined the effect of concomitant inactivation of the *Hif-1α* or *Hif-2α* inactivation with *Phd2* inactivation. *Phd2$^{f/f}$;Hif-1α$^{f/f}$;THCre* and *Phd2$^{f/f}$;Hif-2α$^{f/f}$;THCre* animals were bred and examined at the 3 month time point. These mice were examined with plethysmography to determine any functional effects on ventilation on the acute response to hypoxia. *Phd2$^{f/f}$;Hif-1α$^{f/f}$;THCre* animals showed a similar acute hypoxia-induced ventilatory response as *Phd2$^{f/f}$;THCre* mice (4.07 ± 0.50 *versus* 5.17 ± 0.51 ml min^{-1} g^{-1}, Fig. 5.3A, Table 5.1). However, *Phd2$^{f/f}$;Hif-2α$^{f/f}$;THCre* mice were unable to mount a hypoxic ventilatory response to 10% oxygen /3% carbon dioxide (Fig. 5.3A, Table 5.1). Moreover, these mice were intolerant of 10% oxygen exposure alone, collapsing and requiring removal from the experimental conditions. These *Phd2$^{f/f}$;Hif-2α$^{f/f}$;THCre* mice also showed no increase in baseline ventilation relative to controls (0.30 ± 0.62 *versus* 5.17 ± 0.51 ml min^{-1} g^{-1}, $P < 0.01$, Fig. 5.3A, Table 5.1).

Morphologically, *Phd2$^{f/f}$;Hif-1α$^{f/f}$;THCre* mice broadly replicated the phenotypes observed in *Phd2$^{f/f}$;THCre* mice. Carotid bodies from *Phd2$^{f/f}$;Hif-1α$^{f/f}$;THCre* were significantly larger in volume than *Phd2$^{f/f}$* controls, and were comparable in size to those observed in *Phd2$^{f/f}$;THCre* mice (Fig. 5.3B, right panel). However, these carotid bodies did have a reduced TH^{+} cell number relative to *Phd2$^{f/f}$;THCre* carotid bodies, suggesting a decrease in TH^{+} cell density. These carotid bodies contained a higher frequency of the "clear cell" Type I cell phenotype observed in the *Phd2$^{f/f}$;THCre* Type I cells. In contrast, *Phd2$^{f/f}$;Hif-2α$^{f/f}$;THCre* mice contained small or atrophic carotid bodies in which few or no TH^{+} cells were visible (Fig. 5.3C). The absence of these oxygen sensitive Type I cells may explain the failure of these mice to tolerate acute hypoxia. Whilst the Type I cell population was reduced or entirely absent, the number of Type II cells was relatively unchanged relative to *Phd2$^{f/f}$* controls (Fig 5.3C). *Phd2$^{f/f}$;Hif-1α$^{f/f}$;THCre* carotids appeared highly vascular under light microscopy, and this was confirmed by endomucin staining (Fig. 5.3D). Conversely, *Phd2$^{f/f}$;Hif-2α$^{f/f}$;THCre* carotids contained minimal vasculature and endomucin staining.

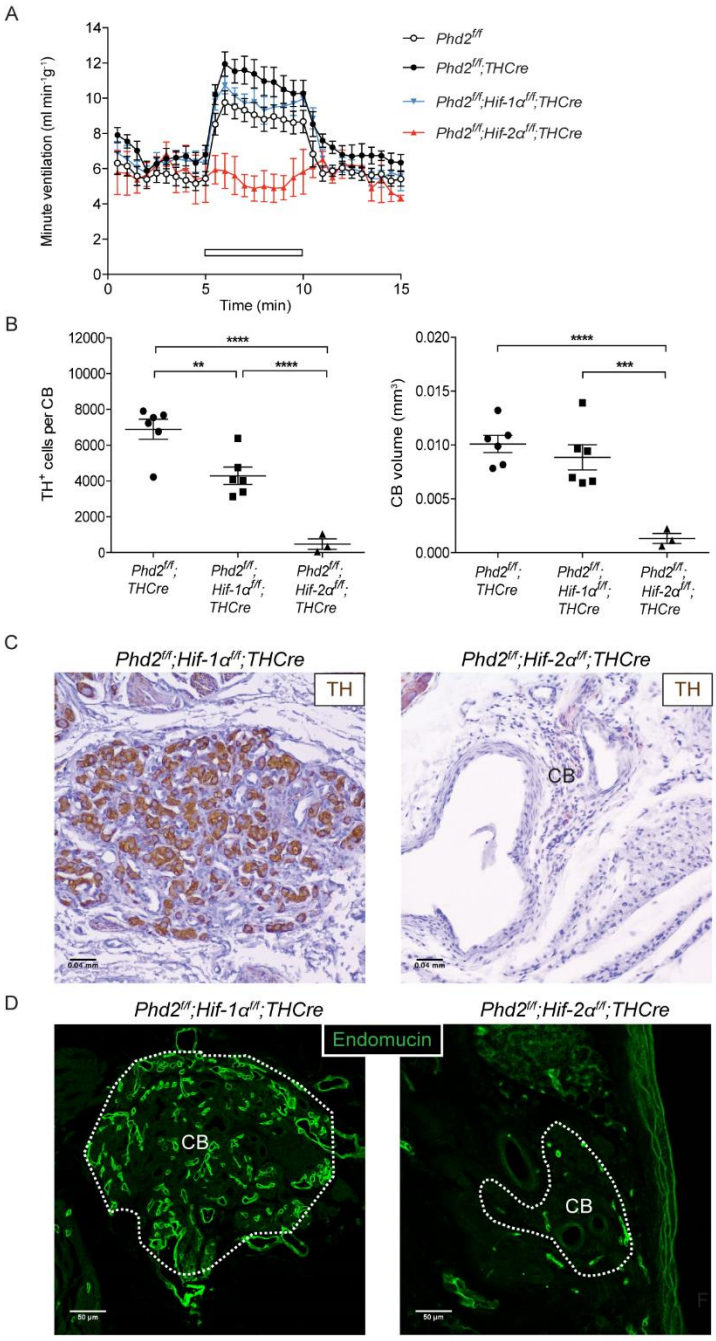


Figure 5.3. The effect of PHD2 inactivation in Type I cells combined with HIF-1α or HIF-2α inactivation upon CB morphology and function.

A) Minute ventilation before, during and after an acute hypoxic stimulus (10% oxygen with 3% carbon dioxide - white bars) in n = 3-11 *Phd2*$^{f/f;}$*THCre*, *Phd2*$^{f/f}$*Hif-1α*$^{f/f}$*;THCre*, *Phd2*$^{f/f}$*;Hif-2α*$^{f/f}$*;THCre* mice and *Phd2*$^{f/f}$ littermate controls. Minute ventilation was calculated from respiratory rate and tidal volume measurements made *via* plethysmography. Plethysmography was conducted by Dr Emma Hodson.

B) Quantification of TH^+ cell number and CB volume and from *Phd2$^{f/f;}$THCre* (n = 6), *Phd2$^{f/f}$;Hif-1α$^{f/f}$;THCre* (n = 6) and *Phd2$^{f/f}$;Hif-2α$^{f/f}$;THCre* mice (n = 3).
C-D) Representative images of CBs from *Phd2$^{f/f}$;Hif-1α$^{f/f}$;THCre* and *Phd2$^{f/f}$;Hif-2α$^{f/f}$;THCre* mice. C) immunostaining for TH (brown); D) Endomucin (green) immunostaining (CB edges in white);
Data from Fig. 5.1A-B are reproduced in Fig. 5.3A-B for comparative purposes.

In line with these results, carotid bodies from these *Phd2$^{f/f}$;Hif-1α$^{f/f}$;THCre* showed strong *Vegfa* and *Ccnd1* mRNA expression (Fig. 5.4A-B). Consistent with the lack of Type I cells, which previous chapters have indicated are the primary site of *Vegfa* and *Ccnd1* expression, minimal *Vegfa* or *Ccnd1* mRNA expression was observed within *Phd2$^{f/f}$;Hif-2α$^{f/f}$;THCre* vestigial carotid bodies (Fig. 5.4A-B). These results suggest that HIF-1α inactivation does not significantly block the pseudohypoxic phenotypes induced by PHD2 inactivation, and demonstrate that these effects are blocked by HIF-2α. Moreover, HIF-2α inactivation results in the formation of vestigial carotid bodies which lack the primary oxygen sensitive Type I cells. Taken together, these results suggest that many of the hyperplastic and ventilatory features of acclimatisation to chronic hypoxia are mediated by the HIF-2α /PHD2 couple.

Genotype	**Hypoxic ventilatory response (ml min^{-1} g^{-1})**	
	10% O_2	10% O_2 /3% CO_2
Phd2$^{f/f}$	-0.31 ± 0.42	4.33 ± 0.62
Phd2$^{f/f}$;THCre	-0.41 ±0.43	5.17 ± 0.51
Phd2$^{f/f}$;Hif-1α$^{f/f}$;THCre	0.07 ±0.68	4.07 ± 0.50
Phd2$^{f/f}$;Hif-2α$^{f/f}$;THCre	-2.91 ± 0.50 ** §§	0.30 ± 0.62 ** §§
ANOVA *P* value	**0.0017**	**0.0023**

Table 5.1 Acute hypoxic ventilatory responses in mice with inactivation of PHD2 in Type I cells combined with HIF-1α or HIF-2α inactivation.

Mean hypoxic ventilatory response values (± SEM) in age matched male mice measured at 3 months of age. Values shown are mean changes in minute ventilation (± SEM) in response to the indicated acute hypoxic stimulus; n = 3 - 11 mice per genotype. Data were analysed by one-way ANOVA followed by Tukey's multiple comparison test. ** $P < 0.01$, significantly different from tamoxifen treated *Phd2$^{f/f}$* controls; §§ $P < 0.01$, significantly different from *Phd2$^{f/f}$;THCre* mice. $P < 0.05$ comparisons are highlighted in bold. Plethysmography was conducted by Dr Emma Hodson.

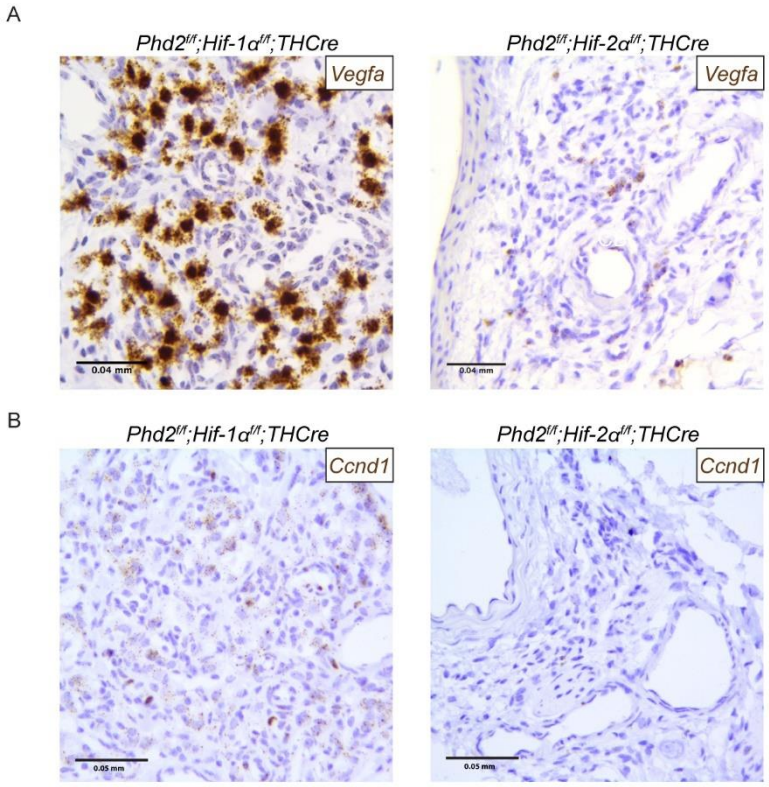


Figure 5.4. The effect of PHD2 inactivation in Type I cells combined with HIF-1α or Hif-2α inactivation upon carotid body gene expression.

Representative images of *in situ* hybridisation for mRNA from CB tissues from *Phd2$^{f/f}$Hif-1α$^{f/f}$;THCre* and *Phd2$^{f/f}$;Hif-2α$^{f/f}$;THCre* mice. A) *In situ* hybridisation for *Vegfa* mRNA (brown); B) *In situ* hybridisation for *Ccnd1* mRNA (brown).

The effect of 'pseudohypoxic' PHD2 inactivation in Type I cells upon Type I cell ultrastructure.

To investigate this phenotype further, carotid bodies from *Phd2$^{f/f}$;THCre* mice were examined using electron microscopy. This analysis observed that, similar to Type I cells from animals exposed to chronic hypoxia (Fig. 3.7), Type I cells from *Phd2$^{f/f}$;THCre* CB's contained a lower density of dense core vesicles (0.79 ± 0.09 *versus* 8.82 ± 1.09 DCVs μm^{-2} in *Phd2$^{f/f}$;THCre versus Phd2$^{f/f}$* , $P = 0.0018$). However, these remaining DCVs were very frequently 'eccentric' in appearance, with an enlarged lucent membrane (200-500 nm diameter *versus* 90 nm diameter control DCVs) and large expanded electron dense cores relative to the DCVs observable in control Type I cells (150 nm *versus* 90 nm, Fig 5.5A). A significant proportion of Type I cells possessed larger membranous spaces (>500 nm), possibly representing multiple fused DCVs, although the absence of an electron dense core made these impossible to categorise. These Type I cells were also hypertrophic, and were significantly larger in total cellular area than Type I cells from *Phd2$^{f/f}$* controls (Fig. 5.5B). These changes resembled, but exceeded in magnitude and severity, the changes associated with chronic hypoxia reported in the previous chapters.

Electron microscopy analysis on Type I cells from *Phd2$^{f/f}$;Hif-1α$^{f/f}$;THCre* observed similar phenotypes, with an even greater frequency of large membranous spaces, often occupying the majority of the cytoplasmic space (Fig. 5.5C). Due to the vestigial nature of carotid bodies from *Phd2$^{f/f}$;Hif-2α$^{f/f}$;THCre* mice, which contained either few or no Type I cells, it was not possible to fix, identify or image Type I cells under electron microscopy from this genotype.

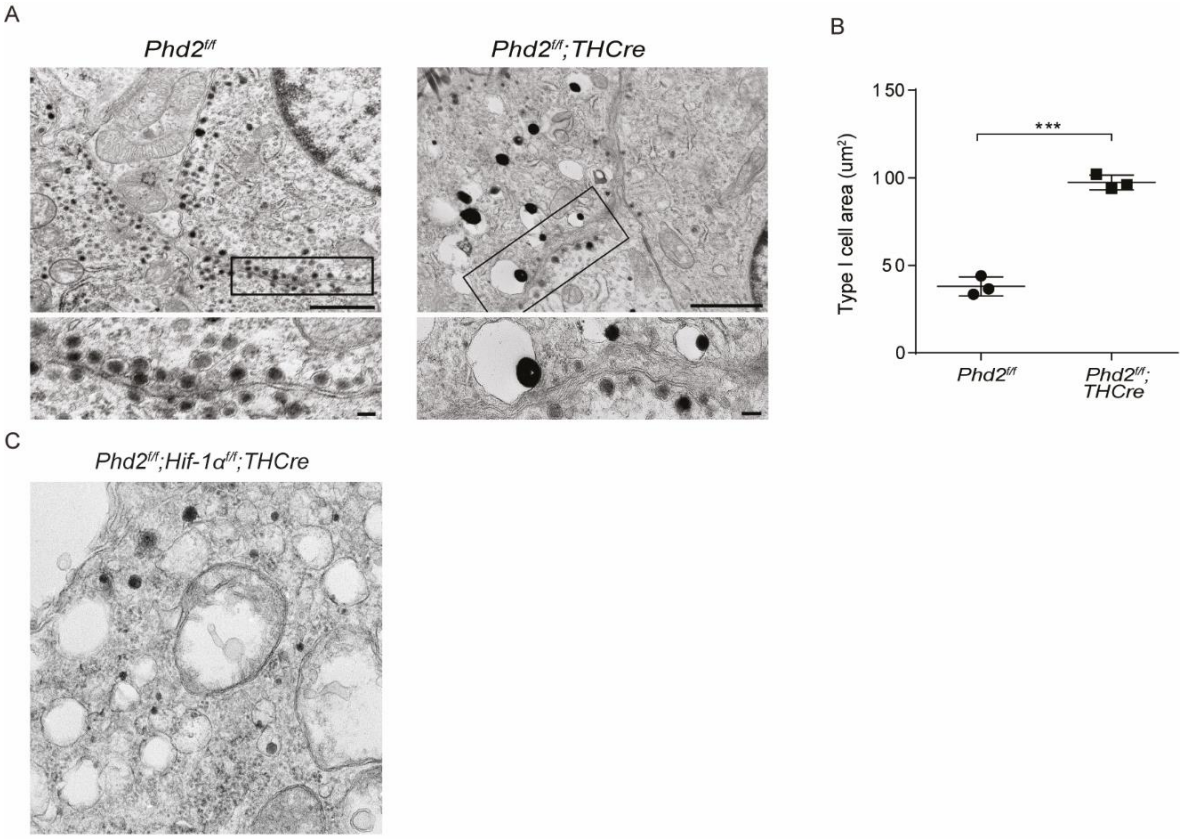


Figure 5.5. The effect of constitutive Type I cell-specific PHD2 inactivation upon carotid body ultrastructure.

Electron microscopy imaging of cellular ultrastructure and eccentric DCVs in Type I cells. Representative DCVs and eccentric DCVs show in inserts. Scales bars = 1 µm (low power) and 100 nm (high power).

A) Type I cell ultrastructure, eccentric vesicles and enlarged vacuoles from *Phd2$^{f/f}$;THCre* and *Phd2$^{f/f}$* littermate control mice.

B) Quantification of Type I cell area from *Phd2$^{f/f}$;THCre* and *Phd2$^{f/f}$* littermate control mice.

C) Type I cell ultrastructure, eccentric vesicles and enlarged vacuoles from *Phd2$^{f/f}$Hif-1α$^{f/f}$;THCre* mice. No EM data was obtainable on Type I cells from *Phd2$^{f/f}$;Hif-2α$^{f/f}$;THCre* due to the vestigial nature of CBs from these mice.

The effect of inducible 'pseudohypoxic' PHD2 inactivation in Type I cells

The phenotypes reported above employed a constitutive THCre promoter to achieve high levels of recombination during development and into adulthood. However, this means that the reported phenotypes may represent developmental phenotypes, and may not be representative of the effects of pseudohypoxia in the adult. To address this, this study also sought to test the effect of inducible inactivation of PHD2 in the Type I cell population in adult mice. This study intercrossed animals bearing a homofloxed *Phd2*$^{f/f}$ allele with the inducibly active *THCreER* construct characterised in previous chapters (Fig 2.2, Fig. 3.2). These *Phd2*$^{f/f}$*;THCreER* mice and *Phd2*$^{f/f}$ controls were treated with tamoxifen and examined for ventilatory responses, haematocrit and carotid body morphology three months after tamoxifen treatment. This time point was chosen to assess the effect of inactivation in the adult, rather than during development.

In contrast to previous results with the more ubiquitously expressed RosaCreER promoter (Hodson *et al.*, 2016), *Phd2*$^{f/f}$*;THCreER* animals did not have significantly elevated hypoxic ventilatory responses compared to control animals, although there was a trend towards statistical significance and an elevated baseline (Fig. 5.6A). Whilst prolonged global PHD2 inactivation has been shown to result in dramatic polycythaemia (Takeda *et al.*, 2008; Hodson *et al.*, 2016), haematocrits from *Phd2*$^{f/f}$*;THCreER* mice were not significantly different from littermate controls, as might be expected given low expression of TH in EPO producing regions such as the kidney (Fig. 5.6B). In contrast to the phenotypes observed in constitutive *Phd2*$^{f/f}$*;THCre* carotid bodies, no significant increase in carotid body volume or a proliferative marker (Ki67 positive cell number) was observed in carotid bodies from *Phd2*$^{f/f}$*;THCreER* mice (Fig. 5.6B). *In situ* hybridisation for HIF-2α

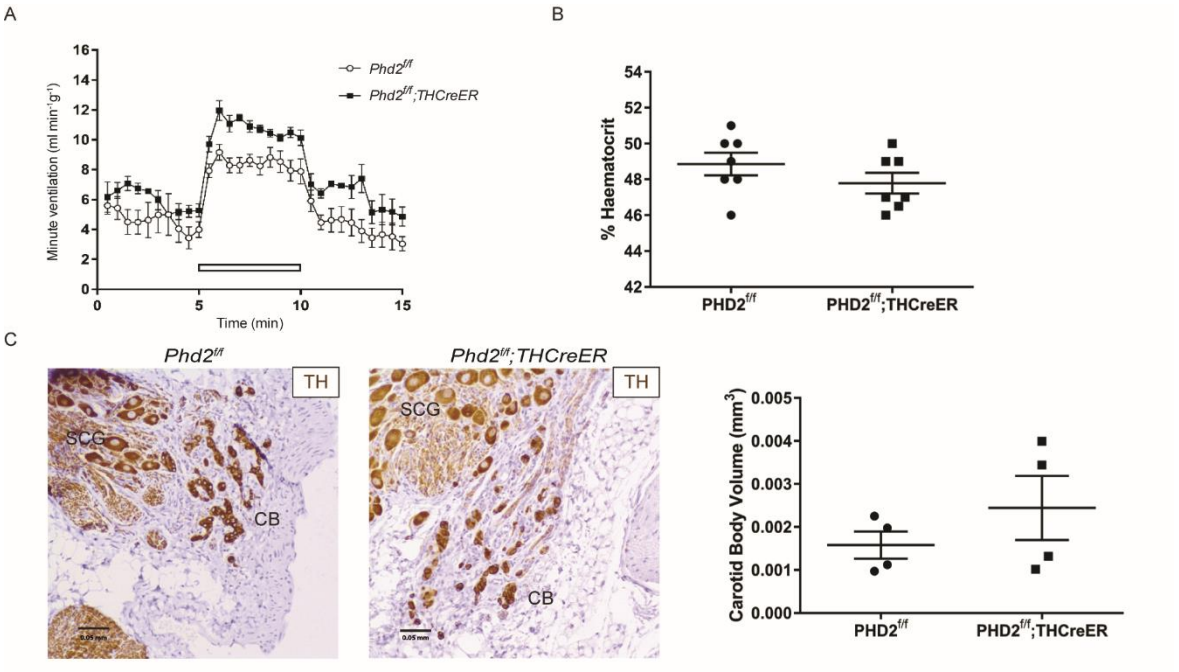


Figure 5.6. The effect of conditional Type I cell-specific PHD2 inactivation upon CB morphology and function.

Carotid body morphology and ventilation in n = 4-7 *Phd2$^{f/f}$;THCreER* mice and *Phd2$^{f/f}$* littermate controls.

A) Minute ventilation before, during and after an acute hypoxic stimulus (10% oxygen with 3% carbon dioxide - white bars). Plethysmography was conducted by Dr Emma Hodson.

B) Haematocrit measures taken from blood from the inferior vena cava.

C) Representative images of TH (brown) immunostaining and comparative quantification of carotid body volume.

Values shown are mean ± SEM.

confirmed that HIF-2α mRNA was still strongly expressed in both control and *Phd2$^{f/f}$;THCreER* carotid bodies (Fig. 5.7A). *In situ* hybridisation for *Vegfa* found that *Vegfa* levels were increased in *Phd2$^{f/f}$;THCreER* mice, suggesting that some pseudohypoxic increases in target gene expression were occurring (Fig. 5.7A) However, the lack of any major morphological changes in these includible *Phd2$^{f/f}$;THCreER* mice suggests that a substantial proportion of the observed phenotypes in the constitutive *Phd2$^{f/f}$;THCre* mouse model represent the effects of pseudohypoxia in development, rather than adulthood. Alternatively, lower recombination under the THCreER promoter may also be moderating the effects of this inactivation.

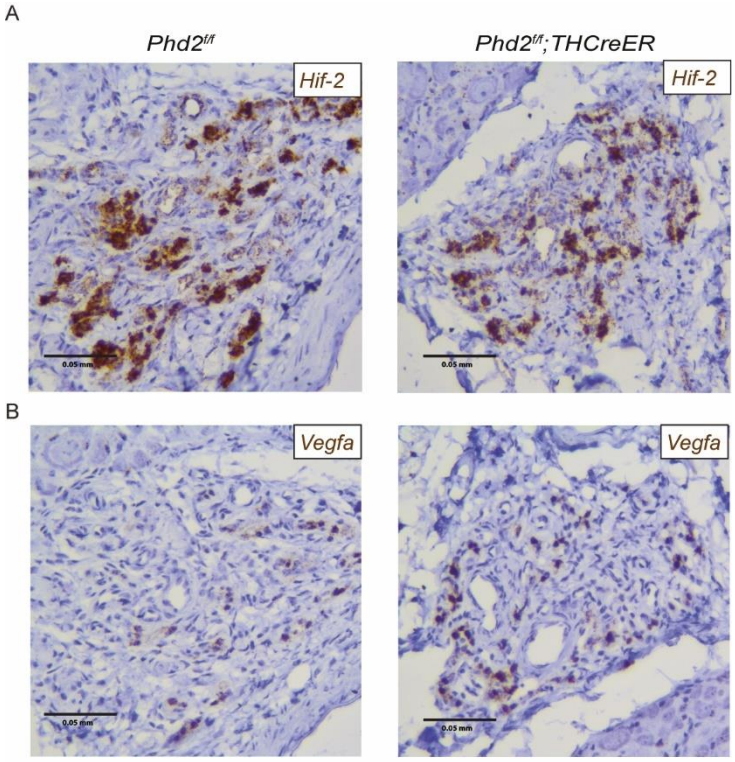


Figure 5.7. The effect of conditional Type I cell-specific PHD2 inactivation upon carotid body gene expression.

Representative images of *in situ* hybridisation for mRNA from CB tissues from *Phd2$^{f/f}$;THCreER* mice and *Phd2$^{f/f}$* littermate controls. A) *In situ* hybridisation for *Hif-2α* mRNA (brown); B) *In situ* hybridisation for *Vegfa* mRNA (brown). Pseudohypoxic inducible inactivation of PHD2 leads to increase expression of *Vegfa* mRNA.

Discussion:

The carotid body undergoes a marked hyperproliferative response to chronic hypoxia, and recent results have suggested that this is in part mediated by the stabilisation and expression of HIF-2α in Type I cells (Hodson *et al.*, 2016; Macias *et al.*, 2018). This chapter has demonstrated that constitutive inactivation of PHD2 to create a state of 'pseudohypoxia' through HIF stabilisation in Type I cells of the carotid body is sufficient to drive carotid body hyperplasia across multiple cell lines. This hyperplasia resulted in carotid bodies that resembled, but were significantly larger than, those observed in animals acclimatised to chronic hypoxia (~7 fold *versus* 3~ to 4~ fold). However, despite this hyperplasia, no significant increase in the ventilatory response to hypoxia was observed, suggesting these hyperplastic Type I cells may not be functional. This was supported by electron microscopy observations of these Type I cells, which noted multiple ultrastructural abnormalities. This carotid body hyperplasia was demonstrated to be dependent on HIF-2α, but not HIF-1α, emphasising the role of the HIF-2α – PHD2 couple in regulating carotid body acclimatisation to hypoxia. This expansion was associated with an increased expression of HIF target genes associated with mediating proliferative responses, including VEGFA and Cyclin D1, potentially providing a mechanistic link between HIF-2α and the resultant multi-lineage hyperplasia. However, this study failed to replicate the phenotype using an inducible mouse model of PHD2 inactivation, suggesting that a large proportion of the effects reported may be developmentally mediated.

These results support the theory advanced in previous chapters that Type I cells can mediate and drive proliferation in the wider carotid body parenchyma: PHD2 inactivation specifically in the Type I cell population was demonstrated to drive an expansion of the entire carotid body, including $GFAP^+$ Type II cells and $endomucin^+$ endothelial cells. A

possible mechanism for this expansion is suggested by the abundance of *Vegfa* mRNA within Type I cells of *Phd2$^{f/f}$;THCre* mice, suggesting that Type I cells may be synthesising and releasing this and other mitogens. Conversely, *Phd2$^{f/f}$;Hif-2α$^{f/f}$;THCre* mice contained vestigial carotid bodies which contained few or absent Type I cells but a normal (relative to wild-type carotids) number of Type II cells. This suggests that this Type II population is not reliant on the Type I cell population for survival and is consistent with reports of a separate developmental origin of Type II cells (Kumar & Prabhakar, 2012) and the effects of *Hif-2α$^{f/f}$;THCre* inactivation alone (Macias *et al.*, 2018). The relatively minor effect of concurrent HIF-1α inactivation upon the carotid body contrasts with the reversal observed in *Phd2$^{f/f}$;Hif-2α$^{f/f}$;THCre*. This supports the observations of previous chapters that HIF-2α is the major transcriptional regulator of the hypoxic responses of the carotid body. The fact that somatic gain of function mutations in HIF-2α, but not HIF-1α, are associated with human paraganglioma suggests that this observation is true in both mouse and human tissues (Zhuang *et al.*, 2012; Pacak *et al.*, 2013; Toledo *et al.*, 2013).

Despite the observed carotid body hyperplasia and the corresponding increase in oxygen sensitive Type I cells, this study did not observe any statistically significant changes in HVR after hypoxic exposure. These results suggest a separation between carotid body hypertrophy and enhanced carotid body sensitivity during ventilatory acclimatization to hypoxia. This contrasts with previous studies that have reported significantly enhanced hypoxic ventilatory sensitivity following hypoxic acclimatisation or induced PHD2 inactivation (Bishop *et al.*, 2013; Hodson *et al.*, 2016). This may reflect long-term effects of HIF-2α inactivation which may be a component of ventilatory desensitisation to hypoxia in some high altitude residents (Severinghaus *et al.*, 1966; Lahiri *et al.*, 1976).

Alternatively, these results could stem from a level of dysplasia and loss of function in carotid body Type I cells in *Phd2$^{f/f}$;THCre* mice. In this context, the ultrastructural abnormalities observed under electron microscopy are consistent with a potential loss of Type I cell function: many Type I cells contained large vacuolated areas of cytoplasm and enlarged cellular bodies. Despite these signs of poor cellular condition, minimal levels of apoptosis were visible in these tissues through either Apoptag staining or morphological examination under electron microscopy.

Most notably, several aspects of the *Phd2$^{f/f}$;THCre* phenotype resemble the histological appearance of carotid body paragangliomas *(PGL).* Paragangliomas are tumours of the autonomic paraganglia, including the carotid body, and are closely related to phaeochromocytomas (PCC), a tumour of the TH^+ chromaffin cells of the adrenal gland. PGLs are highly heritable, with ~40% being associated with a germline mutation, and a high proportion of hypoxia signalling pathway genes (such as VHL, SDH, EPAS1, EGLN1) have been implicated in confirming susceptibility to PGL /PCC (Amorim-Pires *et al.*, 2016; Lussey Lepoutre *et al.*, 2018). Carotid paragangliomas are high vascular multi-lineage tumours containing both Type I and Type II cells, as observed in the hyperplastic carotid bodies reported in this study. The vascularity of PGL is attributed to overexpression of VEGFA (Jyung *et al.*, 2000), which this thesis has observed was strongly expressed in the hyperplastic *Phd2$^{f/f}$;THCre* carotid bodies. Regions of Type I cells from *Phd2$^{f/f}$;THCre* and *Phd2$^{f/f}$;Hif-1α$^{f/f}$;THCre* CBs examined under light miscopy frequently showed a ‘clear cell’ phenotype, containing large clear regions which resemble the vacuolated histology of Type I cells in human paraganglioma (Ashley & Evans, 1966; Robertson & Cooney, 1980; Kliewer & Cochran, 1989; Wieneke & Smith, 2009). Under electron microscopy, these cells were shown to contain large vacuoles and enlarge

'eccentric' dense core vesicles: it would be of considerable benefit to assess whether these cells resemble the ultrastructural appearance of human paragangliomas.

A major caveat to the results discussed above is the use of a constitutive PHD2 inactivation to create the reported phenotypes. Notably, inducible inactivation of PHD2 in Type I cells (*Phd2$^{f/f}$;THCreER*) resulted in a significantly more minimal expansion of the carotid body than that achieved by constitutive inactivation. The carotid body is sensitive to oxygen levels during development, and has been shown to be reduced in size or ablated by perinatal hyperoxic exposure (Bavis *et al.*, 2013; Logan *et al.*, 2016) and impaired in function by prenatal hypoxia (Roux *et al.*, 2001). It is thus possible that some degree of the marked hyperplasia of *Phd2$^{f/f}$;THCre* may result from aberrant embryonic development of the carotid body in pseudohypoxic conditions. Similarly, the reversal of the phenotype may be due to the ablation of the nascent Type I cell population which display an absolute requirement for HIF-2α in development (as reported by (Macias *et al.*, 2018)), rather than the HIF-2α dependence of a later oxygen sensitive response in the mature adult (although the demonstration of HIF-2α dependent proliferation in previous chapter supports this theory). However, the marked upregulation and expression of mitogens such as Cyclin D1 and VEGFA suggests these proliferative signals are still present and driving expansion in these adult carotid bodies, and increased *Vegfa* mRNA expression was also found in the inducible *Phd2$^{f/f}$;THCreER* mice, suggesting that this pseudohypoxic inactivation is sufficient to drive some aspects of the carotid body proliferative signalling pathway.

However, the dramatic hyperplasia and changes in gene expression observed in the *Phd2$^{f/f}$;THCre* mice may still represent the first mouse model of carotid body paraganglioma. If so, these mice may provide a useful model system for testing the effect

of HIF-pathway inhibitors upon these tumours. One of these inhibitors, the commercially available P2385, was characterized in Chapter 4 of this study, and observed to ablate hypoxia-induced proliferation in the carotid body. PT2385 has already proved efficacious at reducing VEGFA and inducing a regression in mouse xenograft tumours and clear cell renal cell carcinoma (ccRCC), a cancer with a strong association with HIF-2α stabilisation (Wallace *et al.*, 2016; Courtney *et al.*, 2018). Future work could test the effect of PT2385 upon these enlarged *Phd2$^{f/f}$;THCre* carotid bodies to examine whether this inhibitor is sufficient to induce a regression of the hyperplastic phenotype and /or to reduce the observed expression of angiogenic and mitogenic genes such as VEGFA and Cyclin D1 reported in this chapter.

Chapter 6: Thesis Discussion

The work presented in this thesis has demonstrated that the Type I oxygen sensitive cells of the carotid body respond to hypoxia both through their canonical function, in which they drive a ventilatory response *via* exocytotic signalling, but also by expanding in number in an autonomous proliferative response. Lineage analysis has shown that this expanded Type I cell population originates from the Type I cells themselves, rather than differentiating from a stem cell-like population of CB Type II cells as suggested by the Stem Cell theory of CB proliferation. Ultrastructural analysis also demonstrated that hypoxia induces cell-intrinsic changes in the structure and density of Type I cell dense core vesicles, which mediate many of the signalling functions of the Type I cells. Further, gene expression and immunohistochemical analysis demonstrated that the Type I cells are capable of driving proliferation in other carotid body cell types, likely *via* a paracrine signalling method. Thus, this thesis demonstrates that the Type I cells of the carotid body can be considered both the primary oxygen sensor of the niche and its primary proliferative population.

Previous work by our group has shown that the proliferative and ventilatory responses of the carotid body to hypoxia are reliant on the integrity of HIF-2α, but the cell type(s) in which HIF-2α is necessary for this response were unknown. This thesis has used cell specific genetic inactivation to demonstrate that the proliferative, ventilatory and cell-intrinsic (dense core vesicle) responses of the CB are reliant on the integrity of HIF-2α in the Type I cells, and not the Type II cells. Type I cell specific HIF-2α inactivation was shown to impair proliferation in other carotid body cell types. Pharmaceutical inhibition of HIF-2α recapitulated these results on a systemic level. Since little to no transdifferentiation

between cell types was observed, it was considered likely that the observed effects on cells other than Type I cells represented the effects of paracrine signals from Type I cells. underscoring the paracrine function of Type I cells. Supporting this, “pseudohypoxic” activation of the HIFs *via* inactivation of the regulatory PHD2 in Type I cells induced a multi-lineage hyperplasia and neovascularization of the carotid body. This was accompanied by changes in gene expression and cell-intrinsic abnormalities in dense core vesicles that were reminiscent of carotid body paragangliomas. Like the response to hypoxia, this response was shown to be dependent on the integrity of HIF-2α, but not HIF-1α, in the carotid body Type I cells. Together, these results demonstrate that the function of the HIF-2α-PHD2 couple in carotid body Type I cells is vital for the oxygen sensitive functions of the organ.

This discussion section will highlight several of these topics for further analysis. In particular, this discussion will assess our current understanding of carotid body Type I and Type II cell proliferation in light of these results and other recent studies published during the preparation of this thesis. It will also assess the implications of these results for other tissues, and for the therapeutic and experimental use of pharmacological HIF-2α inhibitors.

What is the nature of carotid body proliferation?

The carotid body undergoes a proliferative hyperplasia in response to sustained hypoxia, a response which includes a multilineage expansion of multiple carotid cell types including the Type I, Type II and endothelial cells of the carotid body. This thesis has demonstrated that the Type I cells of the carotid body are the primary proliferative population of the carotid body, calling into question the validity of the widely accepted Stem Cell theory of the carotid body. A widely accepted conclusion of this theory is that the carotid body

represents the first and only neural stem cell niche of the peripheral nervous system (Kokovay & Temple, 2007; Lopez-Barneo *et al.*, 2016; Sobrino *et al.*, 2019). If the carotid body can act as a stem cell niche, its relatively accessible position makes it an ideal source of neural stem cells and induced pluripotent stem cells (Kokovay & Temple, 2007). In particular, a transplantable source of stem cells capable of giving rise to mature Type I cells could have utility as a potential treatment for Parkinson's disease due to the highly dopaminergic nature of these cells (Espejo *et al.*, 1998; Arjona *et al.*, 2003; Villadiego *et al.*, 2005). In light of the results of this thesis, are the conclusions of the Stem Cell theory still valid? Even if not, can the carotid body still be understood and used as a neural stem cell niche?

A reassessment of the Stem Cell theory of the carotid body

The Stem Cell theory of the carotid body has proposed that a subpopulation of astrocytic Type II cells are capable of proliferating and differentiating to give rise to the carotid body's multilineage expansion both in cell culture and in the *in vivo* response to chronic hypoxia (Kokovay & Temple, 2007; Pardal *et al.*, 2007; Sobrino *et al.*, 2019). A compelling aspect of this theory is that astrocytic neural stem cells are also a feature of the other two neural stem cell niches, the SVZ and SGZ, positioning the carotid body as a parallel niche to these two compartments. However, the findings of this thesis run contrary to the predictions of the Stem Cell theory. This thesis used lineage tracing to demonstrate that there is minimal transdifferentiation between the Type I, Type II and endothelial populations during the *in vivo* proliferative response to hypoxia. This contrasts with the results of Pardal *et al.* and others, who employed a LacZ reporter under control of a different human GFAP promoter to the one used in this study to demonstrate that the Type II population can give rise to TH^+ Type I cells in the intact CB after chronic hypoxic

exposure (Pardal *et al.*, 2007; Annese *et al.*, 2017). However, these authors did not measure this quantitively, giving no indication of how significant a contribution this Type II to Type I transition makes to the overall carotid body hyperplasia. Moreover, recombination under this human GFAP promoter was reportedly poor, and a pre-exposure and subsequent de-acclimatisation was employed to improve GFAP expression and thus recombination (Pardal *et al.*, 2007; Annese *et al.*, 2017). This pre-exposure to hypoxia and subsequent re-normoxia may have modified the function of the carotid body, for example by modifying the nature of the Type II cells or simply *via* the demonstrated increase in the number of $GFAP^+$ Type II cells during re-normoxia (Pardal *et al.*, 2007). By contrast, the current study examined the behaviour of populations which were lineage labelled at a high level of recombination under baseline conditions. Thus, the results of this study are likely to give a more accurate reflection of the relative contributions of each population to the normal physiological response to hypoxia as might be experienced during altitude acclimatisation.

It is possible that the evidence that supports the Stem Cell theory may still provide insights into the capabilities of the carotid body cell types. In contrast to its *in vivo* work, the Type II Stem Cell theory is well supported by *in vitro* neurosphere assays, which convincingly demonstrate that cultured astrocytes generate neurospheres in culture and can give rise to Type I (Pardal *et al.*, 2007) and endothelial cells (Annese *et al.*, 2017). By contrast, Type I cells do not form neurospheres (Pardal *et al.*, 2007), have a limited ability to proliferate in culture, and do not respond to classical mitogenic stimuli (Jackson & Nurse, 1995; Nurse & Vollmer, 1997). In this thesis, lineage labelling of the Type II cell population observed a handful of labelled Type II cells acquiring other cell type markers (typically the Type I cell marker tyrosine hydroxylase, TH). This suggests that the Type II cells of the carotid body

may be capable of acting as stem cells and supporting multi-lineage neurogenesis in specific conditions, for example in cell culture conditions and as a minor component of the hyperplastic response to hypoxia, which may be enhanced after hypoxia /re-normoxic exposure as used in Pardal *et al.* (Pardal *et al.*, 2007). In many other niches, stem cell-like activity of astrocytic precursors has an adaptive function in maintaining the function of the niche in the face of depletion of individual cell populations (Alvarez-Buylla & Garcia-Verdugo, 2002; Alvarez-Buylla & Lim, 2004). It is possible, therefore, that this function may have an adaptive role in the carotid body by maintaining the ratio of Type I and Type II cells in the face of carotid body hyperplasia and regression in normoxia, as might be experienced upon accent and decent from altitude. However, this process has not been extensively studied, and no experimental evidence currently strongly supports this theory. Thus, despite this potential role in altitude physiology, the results of this thesis have shown that it is the Type I cells that are the primary proliferative cell of the niche, and this has more pronounced implications for our understanding of carotid body in physiology and pathophysiology.

Carotid body Type I cell proliferation: an autonomous HIF-2α dependent stem cell?

Since its initial discovery, it has been understood that the hypoxia-induced hypertrophy of the carotid body primarily results from an increase in the number and size of the Type I cells (Arias-Stella & Valcarcel, 1976). This thesis has shown that the Type I cells themselves are the major proliferating population that gives rise to this increase in cell number. This proliferation was shown to be dependent on the integrity of HIF-2α in the Type I cells themselves, and to be independent of differentiation from the Type II cells.

This Type I cell proliferation is highly unusual for a mature, differentiated glomus cell

population, making understanding this proliferative capacity particularly significant. It is possible, therefore, that the proliferation of this population requires a reversion to a more immature, pluripotent and stem cell-like population. However, the electron microscope work of this thesis noted a perhaps surprising observation: multiple Type I cells undergoing mitosis. These Type I cells contained a complement of dense core vesicles, suggesting they represented differentiated, relatively mature and electrically excitable secretory Type I cells, rather than an intermediate progenitor. In line with this, whilst this thesis was under preparation, a study was published that demonstrated a stem cell-like proliferative capacity in a subset of the Type I cell population (Sobrino *et al.*, 2018). Sobrino *et al.* identified an immature, electrically excitable dopaminergic subpopulation of Type I cells which were identifiable by their expression of human natural killer-1 (HNK-1) membrane epitope (Sobrino *et al.*, 2018). In the context of the results of this thesis, it is possible that this subpopulation accounts for some, or all, of the Type I cell proliferation underlying carotid body hyperplasia.

However, neither this study nor that of Sobrino *et al*. has presented evidence that these cells represent *pluripotent* stem cells. This thesis did not observe any contribution of the lineage labelled TH population to other carotid body cellular populations *in vivo*, and work by other groups has shown that Type I cells do not proliferate in response to classic mitogenic stimuli such as nerve growth factor or FGF *in vitro* (Jackson & Nurse, 1995; Nurse & Vollmer, 1997). However, this topic has not been conclusively studied, and further work with the lineage tracer lines presented in this thesis could be used to identify whether the Type I cells are capable of giving rise to other populations of cells over long time courses *in vivo* and in specific cell culture conditions *in vitro*. This work would be particularly worthwhile for our understanding of whether Type I cells can give rise to

multilineage tumours such as carotid paraganglioma, and also because a transplantable proliferative cell type that highly expresses dopamine and glial-derived neurotrophic factor (GDNF) may be of considerable therapeutic potential for Parkinson's disease (Villadiego *et al.*, 2005). An initial experimental approach could be to identify the overall contribution of HNK-1^{+} cells to carotid body hyperplasia using the lineage tracers employed in this study, combined with *in situ* hybridisation and immunohistochemistry to further characterize this subpopulation. Developing an HNK-1 cell specific inducible lineage tracer (such as a tdTomato$^{f/+}$;HNK1CreERT2 line) would be worthwhile to further characterize this subtype. In particular, it would be interesting to determine if the HNK-1 subtype is the only proliferative Type I cell population, or whether the more mature Type I cells also retain a proliferative capacity, as suggested by the electron microscope work presented by this thesis. This could be dissected using HNK-1 immunohistochemistry and lineage tracing.

Moreover, this thesis has demonstrated the necessity for HIF-2α in mediating the proliferative response of the carotid body Type I cell, and it would be of note to identify whether this requirement is mediated at the level of the HNK-1 subpopulation. Interestingly, these HNK-1 cells have been shown to be electrically excitable but, unlike the classical Type I cell population, were not excitable by acute hypoxia (Sobrino *et al.*, 2018). Therefore, it is possible that the proliferation of the HNK-1 subpopulation is instead mediated by other, mature Type I cells *via* HIF-2α-dependent paracrine signalling.

The paracrine nature of carotid body Type I cell-dependent proliferation

Ever since its initial characterization, the hyperplastic growth of the carotid body in response to sustained hypoxia has been understood to be a multicellular phenomenon,

including both an increase in the Type I cell population and an associated neovascular expansion of the endothelial population (Edwards *et al.*, 1971; Arias-Stella & Valcarcel, 1973). Since then, a number of studies, including this thesis, have also reported that the Type II cell population of the carotid body also proliferates, although to a lesser degree (Pardal *et al.*, 2007). Thus, to understand carotid body hyperplasia, it is important to understand how the proliferation of each carotid body cell population is mediated, and to establish whether the proliferation of each cell type is driven by a single integrated mechanism.

Indeed, this thesis has demonstrated multiple pieces of evidence that suggest that hypoxia-induced proliferation in the carotid body is driven by a shared, HIF-PHD pathway dependent mechanism centred around paracrine signalling from the oxygen sensitive Type I cells of the niche. Firstly, this thesis has demonstrated that inactivation of HIF-2α in the specific Type I cell population results in a reduction of proliferative cell numbers in not only the Type I cells themselves, but also the endothelial and Type II cell populations. Secondly, pseudohypoxic stimulation of these Type I cells was sufficient to induce a multilineage hyperplasia in the entire carotid body. Thirdly, key angiogenic growth factor genes such as Vegfa were found to be strongly expressed in the Type I cells, and not in the adjacent CB vasculature. Other studies have noted that the endothelial population of this CB vasculature expresses receptors such as Flt-1 (Jyung *et al.*, 2000) and this thesis replicated these results. Together, these results suggest that the Type I cells of the carotid body are capable of driving the proliferation of other cell types in the niche, likely *via* paracrine signalling methods.

Further evidence for the nature of this proliferative signalling from the Type I cells can be

inferred from the literature. The Type I cells of the carotid body are a neuroendocrine, exocytotic cell type characterized by their high content of dense core vesicles (DCVs) and the importance of Type I cell exocytosis to CB hyperplasia is highlighted by the fact that inhibition of calcium-induced exocytosis with cadmium impairs carotid body proliferation (Platero-Luengo *et al.*, 2014). Ultrastructural analysis of the glomeruli have identified a close, almost synapse-like association between Type I cell and Type II & endothelial cell processes (Platero-Luengo *et al.*, 2014), providing structural evidence that close range paracrine signalling between these cell types may help co-ordinate the function of the niche. Moreover, the contents of the Type I cell DCVs, which are released in response to chronic hypoxia (Nielsen *et al.*, 1988; Montoro *et al.*, 1996; Weir *et al.*, 2005), include multiple growth factors and signalling peptides associated with tissue growth. These include including endothelin-1 and VEGFA, which have both been identified as HIF-2α target genes and implicated in driving the growth of carotid paragangliomas (Jyung *et al.*, 2000; Chen *et al.*, 2002; Kameda, 2005). In particular, an endothelin-1 receptor antagonist, Bosentan, has been shown to reduce hypoxia-induced hyperplasia in the carotid body (Jyung *et al.*, 2000). This suggests that paracrine signalling from the Type I cells is the principle driving force of carotid body multi-lineage hyperplasia, including the enlarged carotids that were observed in pseudohypoxic *Phd2$^{f/f}$;THCre* mice. Mechanistically, these results suggest that paracrine signalling from Type I cells is driven by the exocytotic release of DCV-held substances in response to hypoxia. Given that the exocytotic release of DCV-held neurotransmitters has been shown to drive the acute oxygen sensitive properties of the carotid body (Hornbein *et al.*, 1961; Gonzalez *et al.*, 1994; Fitzgerald, 2000; Pardal *et al.*, 2000; Nurse, 2005), this directly links the acute and chronic responses of the carotid body.

An interesting facet of this paracrine signalling from Type I cells using DCV-contained proteins is that this current study and others have reported that several receptors of these proteins, such as the VEGFA receptor, Flk-1 (Jyung *et al.*, 2000; Chen *et al.*, 2003), and the endothelin-1 receptor ET-RA (Paciga *et al.*, 1999; Chen *et al.*, 2007), are only expressed in the Type I cells themselves. This suggests that some level of autocrine self-signalling may be occurring within the Type I cell population, and experimental work has attributed Type I cell hypertrophy to the activity of the Flk-1 receptor (Chen *et al.*, 2003). Notably, the HNK-1 proliferative Type I cell subpopulation characterized by Sobrino *et al.*, has been shown to be insensitive to acute hypoxia (Sobrino *et al.*, 2018). Thus, this proliferative Type I cell subpopulation, which mediates some or all of the Type I cell hyperplastic response, may itself rely on paracrine signals such as VEGFA or endothelin-1 from other, oxygen sensitive Type I cells.

Several unanswered questions remain, including to how HIF-2α mediates this signalling, to what extent non-hypoxic stimuli can induce this mitogenic paracrine signalling, whether Type I cell proliferation is cell autonomous, and whether other methods of inducing proliferation are relevant in the carotid body. Although the evidence discussed above suggests that Type I cell paracrine cell signalling drives the majority of hypoxia-induced proliferation in the carotid body, it is important to understand that it is not the only driver of proliferation in the organ. Type II cell proliferation can occur independently of the Type I population: Isolated Type II cells have been shown to proliferate in cell culture (Pardal *et al.*, 2007) whilst multiple studies, including this thesis, have also demonstrated that the inactivation of key HIF pathway genes results in the formation of vestigial carotid bodies which lacked Type I cells but contained a population of Type II cells which proliferated (Kameda, 2005; Macias *et al.*, 2018). This thesis and others have noted that non-Type I

cell proliferation occurs at a low level in the quiescent normoxic carotid body, likely involved in the maintenance of the niche. Studies have reported normoxic carotid bodies with tissue PO_2 of 52.5 and 72 mmHg (Whalen & Nair, 1976; Lahiri *et al.*, 1993) whilst Type I cell depolarisation and exocytosis initiates at a PO_2 of between 20 – 40 mmHg (Biscoe & Duchen, 1990b). Moreover, this low level low level proliferative turnover is present in carotid bodies which lack a Type I cell population entirely due to genetic knockout of key genes (Macias *et al.*, 2018). Therefore, it can be concluded that, although important for the hypoxia-induced response, Type I cell paracrine signalling is a negligible component of the low level of non-Type I cell proliferation present in the normoxic carotid body.

The question remains as to how HIF-2α mechanistically mediates this paracrine response, for example *via* long term upregulation of genes such as VEGFA, endothelin-1 and their receptors, or perhaps through a novel interaction with dense core vesicle release. To further characterize the nature of this proliferative signalling in the carotid body, future work could employ advanced *in situ* hybridisation techniques such as proximity ligation *in situ* hybridization (PLISH). PLISH analysis allows the imaging of the expression of dozens of genes from a single fixed tissue slide (Roussis *et al.*, 2017). PLISH could be used in combination with lineage tracers and immunohistochemistry to create a "map" of carotid body cell types, proliferative markers, mitogenic gene expression and receptor expression across multiple time points, shedding light on proliferation of Type I cells and the nature of their proliferative signalling to other proliferative subpopulations of in the carotid body. Target population cell makers could include HNK-1, TH, GFAP, nestin and endomucin. Target proliferative cell intrinsic and paracrine signals could include VEGFA, endothelin-1 and Cyclin D1, and the receptors for these signals such as Flt-1, Flk-1

(VEGFA receptors) and ET-RA & ET-RB (endothelin-1 receptors). PLISH could be used on hypoxic mice and mice with cell specific HIF-2α and PHD2 inactivation, further characterizing the nature of proliferation in the niche. As an alternative to this "candidate" based approach, RNA sequencing could be used as a non-biased transcriptomic approach, aiming to identify HIF-2α target genes in the carotid body.

Carotid body Type I cell proliferation: developmental vs adult effects of HIF pathway manipulation

This thesis has demonstrated that constitutive inactivation of PHD2 in carotid body Type I cells is sufficient to drive the formation of grossly hyperplastic, paraganglioma-like carotid bodies. No mouse model of paraganglioma (PGL) is currently available, making this result particularly significant for enabling future research into the treatment of the condition (for example with the pharmacological HIF-2α antagonists characterized in this study). However, this thesis failed to replicate this phenotype using an inducible model of pseudohypoxia (*Phd2$^{f/f}$;THCreER*), suggesting that this phenotype may be partly or primarily driven by the effect of pseudohypoxia on carotid body development. This result fits with a broader pattern in genetic studies of the HIF-PHD pathway: manipulation of the HIF-PHD pathway typically has major consequences in development, but results in much milder phenotypes in adulthood. For example, *phd2$^{-/-}$* mice are embryonic lethal, *Hif-1α$^{-/-}$* mice die at E10.5, and *Hif-2α$^{-/-}$* have high rates of embryonic lethality, with serious cardiopulmonary defects in surviving animals (Iyer *et al.*, 1998; Tian *et al.*, 1998; Takeda *et al.*, 2006). By contrast, inducible ubiquitous inactivation of these genes had much milder effects, with *Phd2$^{f/f}$;RosaCreER* mice displaying mild polycythaemia and HIF-2α inactivation resulting in severe anaemia (Bishop *et al.*, 2013). This suggests that a large proportion of the phenotype we report is due to developmental effects.

This does provide some insights into the development of the carotid body, particularly in light of the possible stem cell-like activity of Type I and Type II cells. This thesis demonstrated that simultaneous HIF-2α inactivation prevented the hyperplastic PHD2 phenotype and frequently resulted in the formation of a vestigial carotid body which lacked Type I cells and contained only Type II cells. Both vestigial and non-vestigial $Phd2^{f/f}$;*Hif-2α*$^{f/f}$;*THCre* carotids did not display the hyperplastic paraganglioma-like phenotype, and this was interpreted as evidence that the hyperplastic response was controlled by the HIF-2α-PHD2 couple. However, the vestigial phenotype likely also represents a fundamental requirement for HIF-2α for the development or survival of Type I cells during development. In support of this, a study published whilst this thesis was under preparation reported a similar vestigial phenotype resulting from inactivation of HIF-2α alone under control of the THCre driver (Macias *et al.*, 2018). Similarly, *Mash1*$^{-/-}$ mice have been shown to form vestigial carotid bodies that contain Type II, but not Type I cells, suggesting a fundamental requirement for Mash1 in their development (Kameda, 2005). The ablation of Type I cells without affecting the Type II population suggests differences in the development of Type I and Type II cells, contrasting with the proposal that all carotid body cell types share a Type II-like mesenchymal origin. Alternatively, this Type II-mesenchymal origin may be correct, and these results could be accounted for by a requirement for HIF-2α and Mash1for the differentiation, survival and /or maintenance of Type I cells deriving from these mesenchymal precursors. However, this thesis also demonstrated that Type I cells with inducible inactivation of HIF-2α in adult life resulted in no major morphological abnormalities, which might be anticipated if HIF-2α was required for these processes.

Other developmental interventions on the HIF pathway have shown contrasting results. Overexpression of HIF-2α under the constitutive, Type I specific THCre driver has been shown to drive hyperplastic expansion of the carotid body (Macias *et al.*, 2018), and a mouse model of the Chuvash VHL mutation has been shown to cause enlarged carotid bodies and ventilatory acclimatization (Slingo *et al.*, 2014). However, in direct contrast to this, inactivation of the VHL allele itself has been shown to result in impaired adaptation to chronic hypoxia and sympathoadrenal cell death, including the carotid body (Macias *et al.*, 2014). VHL and PHD2 inactivation are both predicted to result in the pseudohypoxic stabilization of HIFs, making the direct contrasts between the results of these inactivations intriguing. A potential explanation is these genetic inactivations result in differing levels of HIF-2α (& HIF-1α) activation, and that the maintenance and /or expansion of the carotid body requires a specific, quantitative level of HIF-2α activation during development (and adulthood). Thus, different interventions on individual components of the HIF pathway may result in differing levels of stable HIF and thus different phenotypes. To investigate this further, future experiments could make mouse models with inducible or constitutive inactivation of VHL or other PGL associated genes such as SDH to examine whether these models better mimic the PGL phenotype.

The importance of a quantitative level of HIF-2α during development (and perhaps adulthood) for the development of hyperplastic carotid bodies may explain the unusually high heritability of paragangliomas. ~40% of paragangliomas result from germline mutations (~40%), relative to a common ~10% in many other cancers, making them amongst the most heritable of tumours (Amorim-Pires *et al.*, 2016; Lussey Lepoutre *et al.*, 2018), and it has been found that somatic PGL is frequently associated with mosaicism and pre-disposing mutations (Favier *et al.*, 2015). Therefore, although this study has failed to

replicate the hyperplastic PGL-like phenotype with an inducible model, the *Phd2$^{f/f}$;THCre* mice presented in this thesis may have clinical utility as a model of germline paraganglioma.

These varying effects of HIF-PHD pathway manipulation during development, adulthood and tumorigenesis will be important to consider when assessing the therapeutic benefits of manipulating the pathway, for example through treatment with the small molecule inhibitors of HIF-2α characterized in this thesis.

What is the role of HIF-2α in acute oxygen sensing?

The primary function of the carotid body is to mediate the acute reflex ventilatory response to hypoxia. This thesis has shown that the inhibition of HIF-2α not only affects carotid body morphology but also affects the ventilatory function of the organ, ablating ventilatory acclimatisation to hypoxia. Does HIF-2α also affect the acute ventilatory function of the tissue? In particular, this study has observed that pharmacological inhibition of HIF-2α with PT2385 had a depressant effect on the hypoxic ventilatory response (HVR) of treated mice within 1 hour of treatment. If this effect is on target, it suggests that HIF-2α has an exceptionally rapid transcriptional effect on ventilatory control, or is acting *via* a non-transcriptional mechanism. If so, we would expect to see HIF-2α interacting with the acute transduction machinery of the carotid body Type I cells. Is there evidence that this occurs?

An acute effect of HIF-2α is suggested by its extreme abundance in the carotid body Type I cells. HIF-2α mRNA is the second highest expressed transcript relative to control tissues in the carotid body (Zhou *et al.*, 2016). The normoxic carotid body has been estimated to have a normal to high tissue oxygen tension (PO_2 of ~52.5 ± 3.6 mmHg (Lahiri *et al.*,

1993) or ~72 ± 4 mmHg (Whalen & Nair, 1976)), and under these conditions the majority of the HIF being synthesised in the carotid body will be immediately degraded by the proteasome, representing an enormous energetic burden on carotid body Type I cells. This high level of HIF turnover is presumably adaptive, and a simple adaptive explanation is that this high turnover enables the carotid body to achieve the fastest possible accumulation of HIF-2α (and thus hypoxia-induced transcriptional activity) upon exposure to hypoxic conditions. If HIF-2α expression is functionally specialised to enable its rapid accumulation, it is possible that this enables HIF-mediated effects to play a role in early-to-medium term chemosensory functions of the carotid body, whether *via* transcriptional activity or through non-canonical activity.

Carotid body Type I cell chemotransduction is a complex process which links oxygen sensor(s) to the calcium dependent exocytosis of a wide range of excitatory and inhibitory neurotransmitters. HIF-2α could interact with multiple stages of this process. In response to hypoxia or other stimuli, Type I cells depolarise and release neurotransmitters and other substances contained in dense core vesicles (DCVs), which in turn stimulate (or modulate) afferent nerves to control the central respiratory response. Type I cells contain a wide range of neurosecreted substances which include but are not limited to: acetylcholine, dopamine, norepinephrine, 5-HT, ATP, enkephalin, substance P, NO, neuropeptide Y, endothelin-1 and VEGFA (Chiocchio *et al.*, 1966; Wang *et al.*, 1992; Gonzalez *et al.*, 1994; Hohler *et al.*, 1994; Oomori *et al.*, 1994; Vicario *et al.*, 2000; Kameda, 2005). This study has observed that hypoxia induces HIF-2α-dependent effects on the density and structural appearance of these DCVs, including the formation of ‘eccentric’ DCVs. This ‘eccentric’ appearance likely represents an artefact caused by a change in DCV contents. Although species and experimental differences are a major caveat to understanding carotid

body chemosensitivity, several studies have indicated that a significant proportion of the ventilatory acclimatisation to hypoxia is achieved by changes in the synthesis and release of specific substances such as dopamine, noradrenalin and substance P from the carotid body Type I cells (Tatsumi *et al.*, 1991; Bisgard, 2000). Many of the substances synthesised and released by Type I cells are known HIF-1α and /or HIF-2α targets including endothelin-1 and VEGFA (Hu *et al.*, 1998; Takeda *et al.*, 2004; Dengler *et al.*, 2014), or are regulated by HIF target genes such as TH or nitric oxide synthase (Czyzyk-Krzeska *et al.*, 1994; Prabhakar *et al.*, 1996; Lim *et al.*, 2015). Thus, HIF-2α may directly affect the acute ventilatory response by transcriptionally modifying the expression of key Type I cell neurosecretory substances and thereby modifying the content of the DCVs. This hypothesis could be examined by future work using ELISA or immunogold assay techniques to examine changes in DCV content and neurosecretion in mice treated with the pharmacological HIF-2α inhibitors used in this study. However, the speed of this process will be rate limited by transcription and protein synthesis, and therefore may not be sufficient to explain the relatively rapid effects of HIF-2α inhibition observed at the 1-hour time point by this study.

Although canonically understood to be a transcription factor, it has been recently proposed that HIF-2α may also function as a receptor for an as-yet-unknown ligand, the binding of which may modulate its activity or participate in other processes. Crystallography has demonstrated that HIF-2α contains a large internal 290Å hydrophobic cavity which is capable of binding small-molecule ligands which modulate the protein's activity in *in vitro* screens (Scheuermann *et al.*, 2009). The binding of artificial ligands to this cavity results in a reduction in the affinity of HIF-2α for the ARNT heterodimer (serving as the basis for the pharmacological HIF-2α specific inhibitors used in this thesis), and although no

endogenous HIF-2α ligand has been identified, the presence of this binding pocket suggests that one may exist. Indeed, PAS B domains are present in a wide range of proteins, including ARNT, PYP, AHR and LOV2 (Genick *et al.*, 1997; Pandini *et al.*, 2007; Yao *et al.*, 2008; Evans *et al.*, 2009; Möglich *et al.*, 2009), and the binding of small molecules to these cavities are understood to be major regulators of the activity of these proteins and can confer signalling activity (Genick *et al.*, 1997; Crosson & Moffat, 2002; Rajagopal *et al.*, 2005). Given this, endogenous ligand binding may serve as a non-canonical mechanism of inducing rapid changes in HIF-2α affinity which may in turn play a role in mediating acute HIF-dependent processes in the carotid body. Moreover, screens of non-natural HIF-2α ligands found that they did not bind to the HIF-1α isoform, which contains a smaller, less accessible PAS domain (Scheuermann *et al.*, 2009). Thus, an endogenous ligand may be important for understanding the functional differences between the HIF isoforms. Identifying this ligand (if it exists) could be the next major milestone in the field of oxygen sensing.

In addition to its putative effect on DCV content, HIF-2α may also modulate other components of Type I cell chemotransduction, including the oxygen sensor(s) itself. Type I cell oxygen sensitivity is thought to originate from the inhibition of an oxygen sensitive TASK channel K^+ current (Buckler *et al.*, 2000; Weir *et al.*, 2005; Buckler, 2015) and has also been linked to mitochondrial oxygen sensitivity (Biscoe & Duchen, 1990a; Holmes *et al.*, 2018), the accumulation of mitochondria derived reactive oxygen species (ROS) (Fernandez-Aguera *et al.*, 2015), ATP synthesis (Buckler & Turner, 2013), lactate accumulation (Chang *et al.*, 2015) and the activity of AMP-activated protein kinase (Wyatt *et al.*, 2007; Mahmoud *et al.*, 2016). The HIF system has been implicated in the transcriptional regulation of multiple components of each of these processes. In particular,

multiple mitochondrial subunits are HIF-target genes (Fuhrmann & Brüne, 2017) and the HIF system has been implicated in multiple adaptive mitochondrial changes to hypoxia, which include reduction in mitochondrial mass ("mitophagy") and a rapid adaptive replacement of individual proteins (Anand *et al.*, 2013; Fuhrmann *et al.*, 2013). The HIF system is additionally implicated in ROS production, whilst several reactive oxygen species themselves inhibit PHD activity (Dehne & Brune, 2014) providing potential crosstalk in the sensitivity of any ROS-based oxygen sensing mechanism. Multiple studies have also reported that hypoxia upregulates the number and sensitivity of several Ca^{2+} channels (Del Toro *et al.*, 2003; Caceres *et al.*, 2007) which contribute to the extracellular influx of calcium during hypoxia-induced exocytosis. The HIF system thus influences multiple stages of the acute oxygen sensing machinery in the carotid body, suggesting multiple pathways through which HIF-2α could specifically influence the hypoxic ventilatory response. This is of particular significance because the potential effects of the HIF-PHD pathway on the acute functions of the carotid body will be important to consider when assessing the therapeutic benefits of manipulating the pathway, for example *via* the small molecule inhibitors of HIF-2α characterized in this thesis.

What are the implications of small molecule inhibitors of HIF-2α for the carotid body?

This thesis has investigated the effects of PT2385, a novel small molecule inhibitor of HIF-2α developed by Peloton therapeutics. Chapter 4 of this thesis demonstrated that this pharmacological inhibition corroborates many of the effects of ubiquitous genetic inhibition of HIF-2α, in that PT2385 treatment ablated the ventilatory and proliferative responses of the carotid body to hypoxia. This thesis also found no significant distinction

between two doses of PT2385 (10 mg kg^{-1} and 3 mg kg^{-1}) which have been employed in previous studies on its efficacy in treating ccRCC (Wallace *et al.*, 2016).

This compound was administered systemically, and thus these results cannot be used to confirm the Type I specificity of these responses. However, *in situ* hybridisation and immuno-histochemistry work in this thesis demonstrated that PT2385 treatment reduced the expression of several genes which this thesis and other studies have demonstrated are intrinsic to the Type I cells of the carotid body and mediate the hyperplastic response to hypoxia, including VEGFA and cyclin D1. Thus, we hypothesise that many of the effects of PT2385 upon the carotid body are mediated by its inhibitory effects on HIF-2α in Type I cells, which in turn prevents hypoxia-induced changes in gene expression within these cells. Although this thesis does not directly test this hypothesis, Chapter 3 of this thesis demonstrated that HIF-2α mRNA is tightly restricted to the Type I cells of the carotid body whilst Chapter 4 noted that PT2385 induced marked ultrastructural changes in the carotid Type I cells, suggesting its likely mode of action.

Current work using these HIF-2α inhibitors has highlighted their potential use in treating HIF-2α associated tumours such as clear cell renal cell carcinoma (ccRCC), showing positive effects on tumour regression and a favourable clinical safety profile (Chen *et al.*, 2016; Courtney *et al.*, 2018). Given the results of this thesis, it is possible that the peloton compounds may also be capable of inducing tumour regression in carotid paraganglioma.

In support of this, this thesis has shown that PT2385 inhibits the expression of mitogenic factors such as VEGFA in the carotid body, which in turn are thought to drive the vascular components of carotid paraganglioma (Jyung *et al.*, 2000) while treatment with small

molecule HIF-2α inhibitors has been shown to reduce VEGFA expression and growth in ccRCC cell lines and mouse xenografts (Wallace *et al.*, 2016). In this regard, the paraganglioma-like mouse model developed by Chapter 5 might be an ideal model to test the efficacy of PT2385 in inducing tumour regression. These paraganglioma-like carotids from *Phd2$^{f/f;}$THCre* are grossly hyperplastic and strongly express VEGFA, suggesting that they represent an ideal model for testing the effects of small molecule HIF-2α inhibitors on a PGL-like tissue, in which regression could be measured *via* a reduction in size, vascularity, proliferation and /or the expression of mitogenic genes such as VEGFA. Hypoxia-induced hyperplasia has also been shown to reverse upon return to normoxia over a period of days to weeks (Kusakabe *et al.*, 2004), suggesting that a pre-existing physiologically relevant mechanism exists to mediate the regression of hyperplastic carotid bodies. This mechanism is relatively unstudied, but could be tied to the absence of stable HIF upon return to normoxic conditions. This hyperplastic carotid body regression is mediated by an as yet unstudied but potentially HIF-mediated pathway. It would be of considerable interest to examine whether PT2385 treatment on pre-acclimatised mice at altitude is sufficient to replicate the physiological effects of return to normoxia. If so, this physiological regression could be exploited to halt or reverse paraganglioma progression, and this could be tested with the *Phd2$^{f/f;}$THCre* model. However, as discussed above, it is possible that a major component of the *Phd2$^{f/f;}$THCre* phenotype is mediated by developmental effects. If so, treatment of adult *Phd2$^{f/f;}$THCre* may have reduced or no effect on carotid body size.

The results of this thesis suggest that these HIF-2α inhibitors may have clinically relevant effects beyond their currently studied effects on ccRCC, which implies these compounds may have additional clinical applications (for example on carotid body paraganglioma) but

may also complicate their current clinical use. In particular, the work presented in this study is of clinical importance because it provides insights into the side effect profiles reported for PT2385 and other HIF-2α inhibitors. Notably, hypoxia was reported as a side effect in 20% of patients (Courtney *et al.*, 2018) and the work presented in this thesis has demonstrated the importance of HIF-2α for carotid body function. Thus, it is possible that these side effects of PT2385 originate from impairment of carotid body function upon ventilation. Given that this thesis demonstrates that PT2385 ablates ventilatory acclimatisation to hypoxia, these side effects may become more significant at altitude, and this should be accounted for by clinicians when prescribing these drugs to patients. Moreover, HIF-2α inhibitor treatment may not be suitable for patient groups with potential co-morbidity for conditions that induce patho-physiological hypoxia, such as sleep apnoea and COPD. In particular, low levels of HIF-2α mRNA in lung tissue have been shown to be associated with COPD (Yoo *et al.*, 2015) and thus treatment with HIF-2α may increase risk factors for this condition. It is important, therefore, for clinicians and researchers to understand that systemic application of HIF-2α antagonists will have effects on a wide range of tissues, many of which have not yet been the focus of specific research using these compounds. Although the effects of these compounds have not been specifically examined, it is possible to identify a range of tissues in which HIF-PHD pathway manipulation may have specific effects, and this will be explored in the final section of this discussion.

What is the effect of HIF-PHD pathway manipulation on other tissues?

This thesis has demonstrated a central role for the HIF-2α-PHD2 couple in the maintenance and function of the carotid body. However, HIF-2α and PHD2 are not exclusive to the carotid body, and are both strongly expressed across multiple mammalian

tissues (Berra *et al.*, 2003; Willam *et al.*, 2006; Kaelin & Ratcliffe, 2008). Therefore, manipulation of the HIF-2α-PHD2 couple may have substantial effects in multiple tissues and processes. HIF-2α has been shown to be the key isoform mediating erythrocytosis, primarily through effects on the kidney (Gruber *et al.*, 2007; Rankin *et al.*, 2007; Arsenault *et al.*, 2013). HIF-2α has also be linked to cancer progression and poor prognosis in tumours derived from several tissues, including the SVZ (Li *et al.*, 2009). Therefore, manipulation of the HIF pathway may have effects on oxygen-sensitive proliferation in multiple tissues and cell types – particularly those which have oxygen sensing properties and developmental origins which are analogous to the Type I cells of the carotid body. If so, it will be important to identify and characterize these proliferative responses. Potential sites of HIF-PHD pathway mediated proliferation might include other neural-crest derived tissues such as the aortic bodies and the adrenal medulla, as well as proposed oxygen sensitive cells such as the neuroepithelial bodies of the lungs, which have been suggested to originate from the lung epithelium rather than the neural crest. Given the presence of somatostatinomas in the HIF-2α gain-of-function condition Pacak-Zhuang syndrome (Zhuang *et al.*, 2012; Pacak *et al.*, 2013), the delta cells of the pancreas may be of particular interest.

The adrenal medulla

The adrenal glands are a paired neuroendocrine organ, located above the kidneys, which contain a neuroendocrine population of chromaffin cells in the adrenal medulla. The adrenal medulla contains tyrosine hydroxylase expressing chromaffin cells, the chief physiological function of which is to release catecholamines in response to stimuli. This catecholamine secretion mediates increases in heart rate, blood pressure, bronchodilation, intestinal smooth muscle relaxation and peripheral vasoconstriction (Tank & Lee Wong,

2015). The chromaffin cells of the adrenal medulla have several notable parallels to the Type I cells of the carotid body, which are derived from the same sympathoadrenal neural crest lineage during development (Pearse *et al.*, 1973). The chromaffin cells of the adrenal medulla are structurally similar to the Type I cells, with large nuclei and the presence of large numbers of secretory dense core vesicles (DCVs) which they release when depolarised (Gorgas & Böck, 1976). These chromaffin cells have been demonstrated to be oxygen sensitive during development, with fetal rat medullary cells releasing catecholamines in response to acute hypoxia (Thompson *et al.*, 1997). Conversely, carotid body Type I cells also produce noradrenalin (but not adrenalin), and the carotid body has been shown to be sensitive to the levels of catecholamines in the blood, with noradrenalin injections leading to an increase in carotid body discharge rates (Llados & Zapata, 1978b, a). The adrenal medulla is also a source of phaeochromocytomas (PCC), a neuroendocrine tumour type that is considered a parallel tumour to carotid paragangliomas (PGL). A significant proportion (15-20%) of PGL /PCCs are associated with pseudohypoxic mutations (Amorim-Pires *et al.*, 2016; Lussey Lepoutre *et al.*, 2018), and PGLs are a common feature of VHL syndrome, a familial condition in which inactivation of the VHL tumour suppressor leads to the development of pseudohypoxic tumours (Kaelin, 2007, 2017). Notably, non-pseudohypoxic phaeochromocytomas are typically adrenergic, whilst pseudohypoxic PCC have a noradrenergic phenotype (Amorim-Pires *et al.*, 2016).

HIF-2α expression has been implicated in mediating sympatho-adrenal development and differentiation and its inactivation has been shown to reduce the sensitivity of sympatho-adrenal cells to growth factors, whilst pseudohypoxic constitutive PHD inactivation has been demonstrated to result in developmental abnormalities (Bishop *et al.*, 2008; Richter *et al.*, 2013). In conjunction with the oxygen sensitive nature of the adrenal medulla during

development, it is possible that some elements of HIF-PHD mediated oxygen sensitivity may be conserved in adulthood and potentially manipulated *via* pseudohypoxic inactivation of PHD2. Although beyond the scope of this thesis, the THCre and THCreER promoters employed by this study will also result in recombination in the TH^+ chromaffin cells of the adrenal medulla, and thus these medullas could be examined for developmental abnormalities, electrical excitability or changes in catecholamine release. In particular, due to the PGL-like phenotypes observed in the carotid body and the formation of phaeochromocytomas, it would be worthwhile examining medullas from *Phd2$^{f/f;}$THCre* or *Phd2$^{f/f;}$THCreER* for phaeochromocytoma-like phenotypes.

In another parallel to the carotid body, ultrastructural analysis of the adrenal medullary chromaffin cells has found that they contain both normal DCVs and a large number of enlarged DCVs with large lucent vacuoles (Gorgas & Böck, 1976), which represent a quantitively and functionally distinct population (Grabner *et al.*, 2005) and appear remarkably similar to the 'eccentric' DCVs reported by this thesis in the Type I cells of hypoxic and *Phd2$^{f/f;}$THCre* mice. It is theorised elsewhere in this thesis that this 'eccentric' appearance is an artefact caused by a change in the content of the DCVs. Therefore, electron microscope analysis of the chromaffin cells of the adrenal medulla may detect similar shifts in the nature of the secretory DCVs. If effects of hypoxic and pseudohypoxic stimulation are observed within these adrenal medullas, study of the *Phd2$^{f/f}$;Hif-2α$^{f/f}$;THCre* mice may indicate whether, as in the carotid body, these proliferative or secretory phenotypes are HIF-2α dependent. If so, it will be worthwhile to examine whether treatment with the HIF-2α inhibitor PT2385 can reverse any aspects of the phenotype. This will help characterize the efficacy of these small molecule inhibitors of HIF upon PGL and PCC.

The lung

As the primary route of oxygenation in the body, it is unsurprising that the HIF pathway has been implicated in the function of several cell types in the lungs, most notably the pulmonary neuroendocrine cells (PNECs) and their derivatives, the neuroepithelial bodies (NEBs) and the Club cells (also known as Clara cells) of the bronchiole epithelium. Lung tissues express high levels of HIF-2α, PHD1, PHD2 and PHD3 in mice (Wiesener *et al.*, 2003; Willam *et al.*, 2006). In humans, expression of HIF-2α expression is low in tissues from patients with chronic obstructive pulmonary disease (COPD) relative to controls, and genetic analysis has shown that HIF-2α is associated with COPD risk and severity (Yoo *et al.*, 2015), whilst hypoxic acclimatisation and gain of function mutations in HIF-2α are associated with pulmonary hypertension (Brusselmans *et al.*, 2003; Tan *et al.*, 2013).

Pulmonary neuroendocrine cells (PNECs) are a population of lung epithelial cells which mediate endocrine and paracrine secretory mechanisms and have been identified as a potential pluripotent stem cell niche (Linnoila, 2006). One PNEC subtype, the pulmonary neuroepithelial bodies (NEBs), has been proposed as airway hypoxia sensors, and has also been suggested to be similar in this regard to the Type I cells of the carotid body (Lauweryns *et al.*, 1977; Livermore *et al.*, 2015). These cells are innervated, and respond to hypoxia, hypercapnia and acidosis through the release of serotonin (Livermore *et al.*, 2015). NEBs are numerous in fetal and neonatal lungs, but decrease in number into adulthood (Cho *et al.*, 1989), suggesting that they play a role in mediating post-natal adaptation to air breathing. PHD inactivation has been shown to drive hyperplasia and hypertrophy of these NEBs: *Phd1*$^{-/-}$ and *Phd3*$^{-/-}$ inactivation resulted in an increase in synaptophysin expression, a NEB marker, and individual NEB cells displayed a marked

hypertrophy (Pan *et al.*, 2012; Pan *et al.*, 2016). No significant increase in cell number was observed in *Phd2*$^{+/-}$ heterozygous knockout mice, but these NEBs did display a mild hypertrophy (Pan *et al.*, 2016). Further work in this field could investigate the HIF-2α dependence of this response and the potential applications of PT2385 on this population.

Hypoxic exposure has been shown to induce proliferation in the lung bronchiole and alveolar epithelium (Jain & Sznajder, 2005; Torres-Capelli *et al.*, 2016). In the bronchiole epithelium, this hypoxia-induced proliferation primarily occurred in the secretory Club cells. Club cells are an essential component of the bronchiole epithelium, where they primarily play a role in protecting and maintain the epithelium *via* secretion of the anti-inflammatory protein CC10 (Hiemstra & Bourdin, 2014). Intriguingly, ubiquitous inducible inactivation of HIF-2α (*Hif-2α*$^{f/f}$*;UbcCreER*) showed that this proliferative response was dependent on the expression of HIF-2α, acting by mediating the expression of growth factors such as FoxM1, RELMα and RELMβ (Torres-Capelli *et al.*, 2016). Given the role of these cells in protecting and regenerating the epithelium, this proliferation is likely an adaptive HIF-2α mediated response to chronic hypoxia and other conditions such as COPD. PNECs have been shown to differentiate to give rise to Club cells in response to injury (Reynolds *et al.*, 2000a; Reynolds *et al.*, 2000b). It is possible that this may also play a role in the hypoxia-induced proliferative responses of both populations, something which could be tested with further immunohistochemical and fluorescent lineage tracing experiments targeting PNEC and Club cell type markers such as CC10. This pathway could be further characterized through the use of PT2385 and other small molecule inhibitors of HIF-2α.

The importance of this should not be understated, as PNECs, NEBs and Clara cells have

all been suggested as precursors for both small-cell and non-small cell lung cancers (Reynolds *et al.*, 2000a), with PNEC markers considered characteristic of small-cell pulmonary tumours (van Meerbeeck *et al.*, 2011). Therefore, determining the HIF-2α dependence of these populations could pave the way for the use of small molecule inhibitors of HIF-2α for potential clinical therapies of these tumours.

Summary and Conclusions:

The work presented in this thesis has defined the proliferative responses of the carotid body Type I and Type II cell populations, prompting a re-evaluation of the stem cell-like nature of Type II cells and suggesting that the Type I cell acts as the primary proliferative cell of the niche. This thesis has demonstrated the central importance of the HIF-2α-PHD2 couple in the Type I cells of the carotid body for the oxygen sensitive functions of the organ, both in normal physiology and during acute acclimatisation and the development of the tissue. Moreover, this study has demonstrated that genetic and pharmaceutical manipulations of the PHD2- HIF-2α can ablate many of the oxygen sensitive responses of the carotid body, whilst genetic inactivation of PHD2 in Type I cells is sufficient to drive a pseudohypoxic paraganglioma-like phenotype. This PGL-like mouse may represent the first mouse model of carotid paraganglioma.

Thus, whilst this thesis is primarily concerned with mouse models of the carotid body, it provides insights which may be relevant for the study and therapeutic treatment of pseudohypoxic cancers. This work opens the door to novel pharmacological manipulations of the HIF pathway, and suggests that the carotid body Type I cell is an important target for future research

Chapter 7: Methods

Ethical approval

Animal procedures were compliant with the UK Home Office Animals (Scientific Procedures) Act 1986 and local ethical review. All procedures were authorised by project and personal licences. These procedures were approved by the University of Oxford Medical Sciences Division Ethical Review Committee.

Animals

Mice were housed in individually ventilated cages with free access to water and fed *ad libitum* on a standard chow diet as described in (Fielding *et al.*, 2018). Male mice approximately 3 months old were used for all comparisons with littermate matched controls except where stated otherwise. Experiments on wild-type mice were performed on C57BL/6 mice. Each additional mouse line used in this study was backcrossed with C57BL/6 for a minimum of five generations and then was intercrossed to generate littermates of appropriate genotypes. Multiple mouse lines in this study share a temporally regulated, tamoxifen inducible flox-CreER mechanism, summarised in Figure 1.3 and as described in Feil *et al*. (Feil *et al.*, 2009). *Phd2*$^{f/f}$, *Hif-1α*$^{f/f}$ and *Hif-2α*$^{f/f}$ (where f denotes the floxed allele) conditional knockouts have been described previously and were obtained from these sources: (Cramer *et al.*, 2003; Gruber *et al.*, 2007; Mazzone *et al.*, 2009). Mouse lines in which tamoxifen regulated Cre recombinase are expressed from the TH (*TH-IRES-CreER*, hereafter referred to as *THCreER*), GFAP (*GFAPCreERT2*, hereafter referred to as *GFAPCreER*) and nestin (*NestinCreERT2*, hereafter referred to as *NestinCreER*) promoters, have been previously described (Hirrlinger *et al.*, 2006; Lagace *et al.*, 2007; Rotolo *et al.*, 2008). The Ai14 *tdTomato* fluorescent reporter line has been

previously described, and has been shown to give robust fluorescence in a high proportion of the targeted cells following activation by Cre recombinase (Madisen *et al.*, 2010). The THCre line contains a Cre recombinase expressed from the TH promoter *via* an internal ribosomal entry sequence (IRES) (*TH-IRES-Cre*, hereafter referred to as *THCre*) and is described in Lindeberg and Macias *et al.*, demonstrating expression in catecholaminergic neurones (Lindeberg *et al.*, 2004; Macias *et al.*, 2014). In this THCre line, Cre is constitutively expressed and recombination occurs once TH is expressed at embryonic stage E13.5 (Son *et al.*, 1996). In this line some recombination has been described to occur in germ cells, leading to constitutive recombination in offspring (Lindeberg *et al.*, 2004). Therefore, all mice used for mating and experiments were screened for germline recombination using ear biopsy samples, and affected animals were eliminated from the study.

Genotyping

All mice used in this study were genotyped with ear biopsies and PCR analysis. Ear biopsies were taken from mice at 4 weeks of age or at 10 days post tamoxifen treatment for PCR analysis of genotype. Tissue samples were digested in proteinase K digest solution overnight at 55°C. Tail clips were also taken immediately after harvest of mice after the conclusion of the experiment, and this tissue was stored and later used to confirm the assigned genotype. Ear biopsies were taken by Douglas Dos Santos Passos, tail clips were taken by James Fielding, and PCR analysis was conducted by Dr Xiaotong Cheng. Primers used were as follows:

Genotype	Source & Reference	Background	Primers
Rosa CreERT2	Jackson Lab. US (Soriano, 1999; Vooijs *et al.*, 2001; Takeda *et al.*, 2007)	C57BL/6	(1) 5'-CGGTCGATGCAACGAGTGATGAGG (2) 5'-CCAGAGACGGAAATCCATCGCTCG (3) 5'-CTCATACCAGTTCGCACAGGCGGC (4) 5'-CCGCTAGCACTCACGTTGGTAGGC CreERT2 allele: 350 bp Wild type allele: 550 bp (all unique CreER lines were genotyped using the above primers targeting the Cre locus)
GFAP CreERT2	(Hirrlinger *et al.*, 2006)	C57BL/6	As above
Nestin CreERT2	(Lagace *et al.*, 2007)	C57BL/6	As above
TH-IRES-CreER	(Rotolo *et al.*, 2008)	C57BL/6	As above

THCre	(Lindeberg *et al.*, 2004)	C57BL/6	(1) 5'-CGGTCGATGCAACGAGTGATGAG (2) 5'-CCAGAGACGGAAATCCATCGCTC (3) 5'-CTCATACCAGTTCGCACAGGCGG (4) 5'-CCGCTAGCACTCACGTTGGTAGG
tdTomato Ai14	(Madisen *et al.*, 2010)	C57BL/6	(1) 5'-AAGGGAGCTGCAGTGGAGTA (2) 5'-CCGAAAATCTGTGGGAAGTC (3) 5'-GGCATTAAAGCAGCGTATCC (4) 5'-CTGTTCCTGTACGGCATGG Ai14 allele: 196 bp Wild type allele: 297 bp
Phd2 flox/flox	Jackson Lab. US (Takeda *et al.*, 2007)	C57BL/6	(1) 5'-CAAATGGAGATGGAAGATGC (2) 5'-TCAACTCGAGCTGGAAACC 2-loxP (floxed) allele: 840 bp Wild type allele: 389 bp
Hif-1α flox/flox	(Higgins *et al.*, 2004)	C57BL/6	(1) 5'-TTGGGGATGAAAACATCT GC (2) 5'-GCAGTTAAGAGCACTAGT TG (3) 5'-GGAGCTATCTCTCTAGACC 2-loxP allele: 260 bp 1-loxP allele: 270 bp

Hif-2α flox/flox	(Gruber *et al.*, 2007)	C57BL/6	(1) 5'-CAGGCAGTATGCCTGGCTAATTCCAGTT (2) 5'-CTTCTTCCATCATCTGGGATCTGGGACT (3) 5'-GCTAACACTGTACTGTCTGAAAGAGTAGC 2-loxP allele: 444 bp (P1 and P2) 1-loxP allele: 340 bp (P1 and P3) Wild type allele: 410 bp (P1 and P2)

Table M1. Primers for Genotyping

Drug administration

To induce CreER mediated recombination in NestinCreER, GFAPCreER and THCreER mice, tamoxifen (prepared to 20 mg ml^{-1} in corn oil containing 10% ethanol; Sigma Aldrich, USA) was administered by oral gavage to ~ 6-week-old mice at a dose of 2 mg per day for 5 consecutive days as described previously (Arsenault *et al.*, 2013; Hodson *et al.*, 2016; Fielding *et al.*, 2018). After a 5-day tamoxifen 'wash-out' period (t = 0 days), littermate mice were divided into hypoxia and normoxia groups. Mice were administered 50 mg kg^{-1} BrdU *via* intraperitoneal injection immediately prior to exposure to hypoxia or normoxia followed by supplementation of drinking water with BrdU (1 mg ml^{-1} BrdU and 1% sucrose) for the duration of the experiment.

The HIF-2α inhibitor PT2385 was purchased from Medcam Express. Mice to be treated with this HIF-2α specific antagonist were orally dosed with the drug in a suspension of 0.5% methylcellulose, 0.5% Tween 80 in water (W/V) with 10 mg kg^{-1} or 3 mg kg^{-1} PT2385. Solvent control animals were dosed with the suspension only. Dosing was conducted twice daily for the duration of the experimental period, beginning one day prior to exposure to hypoxia or normoxia. Oral dosing was conducted by FGF staff with James Fielding and /or Dr Xiaotong Cheng.

Chronic hypoxic exposure of mice

Hypoxic mice were placed into a normobaric altitude chamber and acclimatised to decreasing oxygen levels over 24 hours, then held at 10% oxygen for 7 or 28 days. The chamber had a constant airflow and temperature, humidity and carbon dioxide levels were monitored and no gross disturbances were detected. Normoxic littermate controls were maintained in normal housing conditions. Normoxic and hypoxic mice were given free access to food and their water was supplemented with BrdU (1 mg ml^{-1} BrdU and 1% sucrose). All mice were weighed at the start of the procedure and monitored daily for general condition and changes in body weight.

Plethysmography

Tidal volume and respiratory rate were measured in awake, unrestrained mice using individual whole body plethysmographs (600 ml volume; Model PLY4211, Buxco, DSI, St. Paul, MI, USA) (as described in (Bishop *et al.*, 2013; Hodson *et al.*, 2016; Fielding *et al.*, 2018)). Ventilatory parameters were derived using FinePointe software (Buxco) and

adjusted to bodyweight as measured immediately prior to plethysmography. Premixed gas was delivered to each chamber as described previously (Bishop *et al.*, 2013; Hodson *et al.*, 2016). The acute hypoxic stimuli consisted of 10% oxygen, balance nitrogen or 10% oxygen, 3% carbon dioxide, balance nitrogen. Minute ventilation was calculated from tidal volume and respiratory rate. The hypoxic ventilatory response (HVR) to each stimulus was defined as the difference between minute ventilation during the one minute prior to the onset of hypoxia and the first one minute of stable hypoxia (Bishop *et al.*, 2013; Hodson *et al.*, 2016; Fielding *et al.*, 2018). Plethysmography was conducted by Dr Emma Hodson, Dr Xiaotong Cheng or Maria Prange-Barczynska.

Blood measurements

After terminal anaesthesia, blood was taken from the inferior vena cava of mice using heparinised capillary tubes. Haematocrits were measured from blood spun using a haematocrit centrifuge (model C-MH30, Unico, Dayton, NJ, USA) as in (Fielding *et al.*, 2018).

Tissue Preparation

Mice were killed by overdose of isoflurane and exsanguination while still in their experimental oxygen condition i.e. hypoxic mice were culled in the normobaric altitude chamber and normoxic controls were culled in normoxia. This was immediately followed by perfusion fixation with 4% paraformaldehyde and dissection of tissues that were then immersed in 4% paraformaldehyde /PBS overnight. Tissues for cyrosectioning were then transferred to 30% sucrose /PBS whilst tissues for paraffin embedding were transferred to 70% ethanol prior to processing and embedding. Paraffin embedded tissues were sectioned

to a 4 µm thickness using a Leica RM2135 microtome (Leica Biosystems) or a Thermo HM3355 Rotary Microtome (Thermo Fisher Scientific, Loughborough, UK). Carotid body tissues for immunofluorescence were embedded in OCT embedding compound (Thermo Fisher Scientific, Loughborough, UK) and cryosectioned to an 8 µm thickness using a Leica CM-3050-S Cryostat (Leica Biosystems, Wetzlar, Germany). Brain sections were cryosectioned to a 30 µm thickness using a Leica Sliding Microtome (Leica Biosystems), then 1 in 8 sections were mounted on a slide for each immunofluorescent staining run. Brain structures (such as the SVZ and dentate gyrus) and bregma values were manually identified by analysis of structural features. SVZ sections were selected for analysis throughout the anterior to intermediate SVZ between bregma 1 and 0 as defined by the literature (Paxinos & Franklin, 2003; Falcao *et al.*, 2012). Paraffin embedded tissues were sectioned to a 4 µm thickness using a Leica RM2135 microtome (Leica Biosystems) or a Thermo HM3355 Rotary Microtome (Thermo Fisher Scientific, Loughborough, UK).

Immunohistochemistry

Immunohistochemistry was performed on both paraffin-embedded sections and OCT - embedded cryosections sections using commercially available antibodies, staining kits and standardized supplier-recommended protocols. Immunohistochemistry on paraffin-embedded sections was combined with a hematoxylin counterstain and then mounted using DPX mounting reagent (#1005790500, Merck Chemicals Ltd, Southampton, UK). Immunofluorescent staining was conducted with Alexa Fluor fluorescent secondary antibodies and a DAPI nuclear counter stain, then samples were mounted with a Fluoromount-G mounting medium (0100-01, Cambridge Bioscience Ltd, Cambridge, UK). Primary antibodies, secondary antibodies, staining kits and other stains are listed below:

Primary Antibody	Use	Dilution	Source
NB300-109. Rabbit polyclonal anti-tyrosine hydroxylase (TH)	Paraffin immunohistochemistry (IHC) and immunofluorescence (IF)	1:5000 (IHC) 1:500 (IF)	Novus Biologicals, Cambridge, UK
ZO33429-2. Rabbit polyclonal anti-glial fibrillary acidic protein (GFAP)	Immunofluorescence	1:500 (IHC)	Dako, Ely, UK
Ab134436. Chicken anti-GFAP	Immunofluorescence	1:500 (IF)	Abcam, Cambridge, UK
sc-65495, rat anti-endomucin	Immunofluorescence	1:50 (IF)	Santa Cruz Biotechnology, Santa Cruz, US
#550274. Purified Rat anti-mouse CD31	Immunofluorescence	1:100 (IF)	Becton Dickinson Biosciences, Oxford, UK
ab1893. Sheep anti-5-bromo-2'-deoxyuridine (BrdU)	Immunofluorescence	1:500 (IF)	Abcam, Cambridge, UK
#551321, biotinylated anti-BrdU	Paraffin immunohistochemistry	1:10 (IHC)	Becton Dickinson Biosciences, Oxford, UK

Table M2. Primary antibodies

Secondary Antibody	Use	Dilution	Source
#R37116. Alexa Fluor 488 goat anti-rabbit	Immunofluorescence	1:500	Thermo Fisher Scientific
A11006. Alexa Fluor 488 goat anti-rat	Immunofluorescence	1:500	Thermo Fisher Scientific
A11039. Alexa Fluor 488 goat anti-chicken	Immunofluorescence	1:500	Thermo Fisher Scientific
S11223. Streptavidin, Alexa Fluor 488 conjugate.	Immunofluorescence	1:500	Thermo Fisher Scientific
S21374. Streptavidin, Alexa Fluor 647 conjugate.	Immunofluorescence	1:500	Thermo Fisher Scientific

Table M3. Secondary antibodies

IHC kits & Other Stains	Use	Source
K4011. EnVision^{+} System /HRP. Rabbit DAB kit	Immunohistochemistry	Dako, Ely, UK
K500711-2. REAL EnVision Detection System, Peroixdase /DAB. Rabbit /Mouse kit	Immunohistochemistry	Dako, Ely, UK
#551321. RUO biotinylated anti-BrdU kit II	Immunohistochemistry	Becton Dickinson Biosciences, Oxford, UK)
Ab104139. 4′,6-diamidino-2-phenylindole, DAPI (1:2000)	IF nuclear counterstain	Abcam, Cambridge, UK
HHS32-1L. Harris' Modified Hematoxylin solution	IHC nuclear counterstain	Sigma Aldritch, St. Louis, USA
Ab150678. Oil Red O	Lipid stain	Abcam, Cambridge, UK
#1.09034.0250. Periodic acid-Schiff's. Schiff's reagent kit	Glycogen stain	VWR international, Lutterworth, UK

Table M4. Immunohistochemistry kits and miscellaneous stains

In situ hybridisation

Hif-1α, Hif-2α, Vegfa, Flt-1, Flk-1, Edn1 and *Ccnd1* transcripts were detected using appropriate probes *via in situ* hybridisation on sections from paraffin embedded tissues. *In situ* hybridisation was conducted using the RNAscope manual assay according to manufacturer's instructions (Advanced Cell Diagnostics, Newark, USA). Loss of *Hif-2α* expression in mice with conditional gene inactivation was demonstrated using the BaseScope™ kit (Advanced Cell Diagnostics) and a customised probe targeted to exon 2 (Advanced Cell Diagnostics), which is flanked in the *Hif-2α* floxed allele by *LoxP* sites and hence absent in any transcripts from cells where Cre mediated recombination has taken place (Gruber *et al.*, 2007). To obtain dual *in situ* hybridisation /immunohistochemically stained images, the RNAscope protocol was performed first followed by immunostaining with anti-TH, anti-GFAP or anti-BrdU antibodies as described above. The following probes were used:

Probe	Catalogue No.	Target Region	Manufacturer
RNAScope Mm-Hif-1α	313821	1182 – 2154	Advanced Cell Diagnostics, Newark, USA
RNAScope Mm-Epas1	314371	3112 - 3511	Advanced Cell Diagnostics
RNAScope Mm-Vegfa-01	436961	1015 - 2656	Advanced Cell Diagnostics
RNAScope Mm-Flt1-01	443931	4913 - 5946	Advanced Cell Diagnostics

RNAScope Mm-kdr	414811	1766 - 2673	Advanced Cell Diagnostics
RNAScope Mm-End1	435221	902 - 2053	Advanced Cell Diagnostics
RNAScope Mm-TH-C2	317621	483 - 1603	Advanced Cell Diagnostics
RNAScope Mm-GFAP	313211	2 - 1761	Advanced Cell Diagnostics
RNAScope Mm-Ccnd1	442671	2 - 1478	Advanced Cell Diagnostics
BaseScope probe BA-Mm-Epas1	Custom ordered	Exon 2. Exact sequence is proprietary.	Advanced Cell Diagnostics

Table M5. RNAScope and BaseScope probes

Microscopy

Immunofluorescent samples were imaged using a Leica 710 confocal microscope (Leica Biosystems). Light microscopy was performed using a Leica DM 1000 LED microscope (Leica Biosystems). Stereological estimation of carotid body cell number, cell density, organ size and volume was performed using ImageJ software on alternate cryosections or on every fourth paraffin section as previously described (Bishop *et al.*, 2008; Bishop *et al.*, 2013; Hodson *et al.*, 2016; Fielding *et al.*, 2018). Analysis of the SVZ brain region was performed on the anterior and intermediate SVZ, excluding the posterior and post-posterior regions. The anterior SVZ is defined by Falcao *et al*. as the region of SVZ

between bregma 2.28 mm and 1.44 mm, and the intermediate SVZ as the region between bregma 1.44 mm and 0.12 mm (Falcao *et al.*, 2012).

Electron microscopy

Electron microscopy (EM) work presented in Chapter 2 was in performed in collaboration with Dr David Ferguson at the Oxford EM facility and used the following protocol. The bifurcation of the carotid artery, containing the carotid body, was removed and immediately placed in 4% glutaraldehyde in 0.1 M phosphate buffer and processed for transmission electron microscopy (TEM). The tissue was post-fixed in osmium tetroxide and treated *en* block with uranyl acetate. The tissue was then dehydrated in ethanol and treated with propylene oxide and embedded in epoxy resin. Blocks were then sectioned to a 1 µm thickness, and these sections were examined under light microscopy to identify the location of the carotid body within the block. Thin sections of selected areas were then stained with uranyl acetate and lead citrate prior to examination with a transmission electron microscope (JEOL 1200EX, JEOL, Tokyo, Japan) as previously described (Fielding *et al.*, 2018).

Due to the closure of the Oxford EM facility during the production of this thesis, EM work in Chapter 4 was performed in collaboration with Dr Lucy Collinson and Alana Burrell at the EM department in the Francis Crick Institute, London. The bifurcation of the carotid artery, containing the carotid body, was removed and immediately placed in 2.5% glutaraldehyde plus 4% formaldehyde in 0.1 M phosphate buffer. After resin embedding and polymerisation, samples were imaged using a Zeiss Xradia 510 Versa 3D x-ray microscope to aid carotid body identification and localisation (4x objective lens, 40 kV and 3 watts). Sections were then cut at 750 nm for light microscopy and then stained using

1% toludine blue plus 1% sodium tetraborate in water. Sections were then cut at 70 nm thickness, collected onto uncoated copper mesh TEM grids and post stained using 2% aqueous uranyl acetate (15 min) followed by Reynold's lead citrate solution (5min). Sections were then examined with a Tecnai^{TM} G^2 Spirit BioTwin transmission electron microscope (FEI Company, Hillsboro, Oregon).

RT-PCR

Tissues were harvested and then snap frozen for RT-PCR, before being ground into a fine powder with a cryogenic tissue pulveriser. Tissues for quantitative RT-PCR were pooled from five animals to provide sufficient tissue for analysis. mRNA was extracted using Direct-zolTM RNA Miniprep Kit (Zymo Research Corp). Expression analysis was performed using Taqman Assay (Applied Biosystems) with *Ccnd1* and *Vegfa* probes on a StepOne thermocycler (Applied Biosystems) using the 2-DeltaDeltaC(T) method (Schmittgen & Livak, 2008). Statistical analysis was performed upon technical repeats. RT-PCR was conducted by Dr Xiatong Cheng on samples harvested and isolated by James Fielding.

Statistical methods

Data are shown as mean ± SEM. The statistical significance of differences between control and experimental groups was calculated using unpaired Student's *t* tests. For repeated measurements, data were analysed by one or two way ANOVA followed by Tukey's multiple comparison test as appropriate and as described previously (Hodson *et al.*, 2016; Fielding *et al.*, 2018). P values < 0.05 were considered significant.

References:

Acker T, Diez-Juan A, Aragones J, Tjwa M, Brusselmans K, Moons L, Fukumura D, Moreno-Murciano MP, Herbert JM, Burger A, Riedel J, Elvert G, Flamme I, Maxwell PH, Collen D, Dewerchin M, Jain RK, Plate KH & Carmeliet P. (2005). Genetic evidence for a tumor suppressor role of HIF-2alpha. *Cancer Cell* **8,** 131-141.

Alcayaga J, Sanhueza Y & Zapata P. (1993). Thermal dependence of chemosensory activity in the carotid body superfused in vitro. *Brain research* **600,** 103-111.

Alvarez-Buylla A & Garcia-Verdugo JM. (2002). Neurogenesis in adult subventricular zone. *Journal of Neurosciences* **22,** 629-634.

Alvarez-Buylla A & Lim DA. (2004). For the long run: maintaining germinal niches in the adult brain. *Neuron* **41,** 683-686.

Amorim-Pires D, Peixoto J & Lima J. (2016). Hypoxia Pathway Mutations in Pheochromocytomas and Paragangliomas. *Cytogenetic and genome research* **150,** 227-241.

Anand R, Langer T & Baker MJ. (2013). Proteolytic control of mitochondrial function and morphogenesis. *Biochim Biophys Acta* **1833,** 195-204.

Annese V, Navarro-Guerrero E, Rodriguez-Prieto I & Pardal R. (2017). Physiological Plasticity of Neural-Crest-Derived Stem Cells in the Adult Mammalian Carotid Body. *Cell reports* **19,** 471-478.

Appelhoff RJ, Tian YM, Raval RR, Turley H, Harris AL, Pugh CW, Ratcliffe PJ & Gleadle JM. (2004). Differential function of the prolyl hydroxylases PHD1, PHD2, and PHD3 in the regulation of hypoxia-inducible factor. *The Journal of biological chemistry* **279,** 38458-38465.

Arias-Stella J & Valcarcel J. (1973). The human carotid body at high altitudes. *Pathologia et microbiologia* **39,** 292-297.

Arias-Stella J & Valcarcel J. (1976). Chief cell hyperplasia in the human carotid body at high altitudes; physiologic and pathologic significance. *Human pathology* **7,** 361-373.

Arjona V, Minguez-Castellanos A, Montoro RJ, Ortega A, Escamilla F, Toledo-Aral JJ, Pardal R, Mendez-Ferrer S, Martin JM, Perez M, Katati MJ, Valencia E, Garcia T & Lopez-Barneo J. (2003). Autotransplantation of human carotid body cell aggregates for treatment of Parkinson's disease. *Neurosurgery* **53,** 321-328; discussion 328-330.

Arsenault PR, Pei F, Lee R, Kerestes H, Percy MJ, Keith B, Simon MC, Lappin TR, Khurana TS & Lee FS. (2013). A knock-in mouse model of human PHD2 gene-

associated erythrocytosis establishes a haploinsufficiency mechanism. *The Journal of biological chemistry* **288,** 33571-33584.

Ashley DJ & Evans CJ. (1966). Intrathoracic carotid-body tumour (chemodectoma). *Thorax* **21,** 184-185.

Astrom K, Cohen JE, Willett-Brozick JE, Aston CE & Baysal BE. (2003). Altitude is a phenotypic modifier in hereditary paraganglioma type 1: evidence for an oxygen-sensing defect. *Human genetics* **113,** 228-237.

Barer GR, Edwards CW & Jolly AI. (1976). Changes in the carotid body and the ventilatory response to hypoxia in chronically hypoxic rats. *Clinical science and molecular medicine* **50,** 311-313.

Bavis RW, Fallon SC & Dmitrieff EF. (2013). Chronic hyperoxia and the development of the carotid body. *Respiratory physiology & neurobiology* **185,** 94-104.

Beall CM, Cavalleri GL, Deng L, Elston RC, Gao Y, Knight J, Li C, Li JC, Liang Y, McCormack M, Montgomery HE, Pan H, Robbins PA, Shianna KV, Tam SC, Tsering N, Veeramah KR, Wang W, Wangdui P, Weale ME, Xu Y, Xu Z, Yang L, Zaman MJ, Zeng C, Zhang L, Zhang X, Zhaxi P & Zheng YT. (2010). Natural selection on EPAS1 (HIF2alpha) associated with low hemoglobin concentration in Tibetan highlanders. *Proceedings of the National Academy of Sciences of the United States of America* **107,** 11459-11464.

Benarroch EE. (2013). Adult neurogenesis in the dentate gyrus. *Neurology* **81,** 1443.

Berra E, Benizri E, Ginouves A, Volmat V, Roux D & Pouyssegur J. (2003). HIF prolyl-hydroxylase 2 is the key oxygen sensor setting low steady-state levels of HIF-1alpha in normoxia. *The EMBO Journal* **22,** 4082-4090.

Bert P. (1874). Recherches experimentales sur l'influence que les modifications dans la pression barometrique exercent sur les phénomènes de la vie. *Annales des sciences naturelles* **5,** 1-167.

Besarab A, Provenzano R, Hertel J, Zabaneh R, Klaus SJ, Lee T, Leong R, Hemmerich S, Yu KH & Neff TB. (2015). Randomized placebo-controlled dose-ranging and pharmacodynamics study of roxadustat (FG-4592) to treat anemia in nondialysis-dependent chronic kidney disease (NDD-CKD) patients. *Nephrology, dialysis, transplantation : official publication of the European Dialysis and Transplant Association - European Renal Association* **30,** 1665-1673.

Bigham AW & Lee FS. (2014). Human high-altitude adaptation: forward genetics meets the HIF pathway. *Genes & development* **28,** 2189-2204.

Biscoe TJ. (1971). Carotid body: structure and function. *Physiological reviews* **51,** 437-495.

Biscoe TJ & Duchen MR. (1990a). Cellular basis of transduction in carotid chemoreceptors. *Am J Physiol* **258,** L271-278.

Biscoe TJ & Duchen MR. (1990b). Responses of type I cells dissociated from the rabbit carotid body to hypoxia. *The Journal of physiology* **428,** 39-59.

Bisgard GE. (1995). Peripheral and central effects of hypoxia. *Regulation of Breathing,* 617-668.

Bisgard GE. (2000). Carotid body mechanisms in acclimatization to hypoxia. *Respiration physiology* **121,** 237-246.

Bishop T, Gallagher D, Pascual A, Lygate CA, de Bono JP, Nicholls LG, Ortega-Saenz P, Oster H, Wijeyekoon B, Sutherland AI, Grosfeld A, Aragones J, Schneider M, van Geyte K, Teixeira D, Diez-Juan A, Lopez-Barneo J, Channon KM, Maxwell PH, Pugh CW, Davies AM, Carmeliet P & Ratcliffe PJ. (2008). Abnormal sympathoadrenal development and systemic hypotension in PHD3-/- mice. *Molecular and cellular biology* **28,** 3386-3400.

Bishop T & Ratcliffe PJ. (2014). Signaling hypoxia by hypoxia-inducible factor protein hydroxylases: a historical overview and future perspectives. *Hypoxia* **2,** 197-213.

Bishop T, Talbot NP, Turner PJ, Nicholls LG, Pascual A, Hodson EJ, Douglas G, Fielding JW, Smith TG, Demetriades M, Schofield CJ, Robbins PA, Pugh CW, Buckler KJ & Ratcliffe PJ. (2013). Carotid body hyperplasia and enhanced ventilatory responses to hypoxia in mice with heterozygous deficiency of PHD2. *The Journal of physiology* **591,** 3565-3577.

Blumcke S, Rode J & Niedorf HR. (1967). The carotid body after oxygen deficiency. *Zeitschrift fur Zellforschung und mikroskopische Anatomie (Vienna, Austria : 1948)* **80,** 52-77.

Bratslavsky G, Sudarshan S, Neckers L & Linehan WM. (2007). Pseudohypoxic pathways in renal cell carcinoma. *Clinical cancer research : an official journal of the American Association for Cancer Research* **13,** 4667-4671.

Braun RD, Lanzen JL, Snyder SA & Dewhirst MW. (2001). Comparison of tumor and normal tissue oxygen tension measurements using OxyLite or microelectrodes in rodents. *American journal of physiology Heart and circulatory physiology* **280,** H2533-2544.

Brezis M & Rosen S. (1995). Hypoxia of the renal medulla--its implications for disease. *The New England journal of medicine* **332,** 647-655.

Brusselmans K, Compernolle V, Tjwa M, Wiesener MS, Maxwell PH, Collen D & Carmeliet P. (2003). Heterozygous deficiency of hypoxia-inducible factor-2alpha protects mice against pulmonary hypertension and right ventricular dysfunction during prolonged hypoxia. *The Journal of clinical investigation* **111,** 1519-1527.

Buckler KJ. (1997). A novel oxygen-sensitive potassium current in rat carotid body type I cells. *The Journal of physiology* **498,** 649-662.

Buckler KJ. (2015). TASK channels in arterial chemoreceptors and their role in oxygen and acid sensing. *Pflugers Archiv : European journal of physiology* **467,** 1013-1025.

Buckler KJ & Turner PJ. (2013). Oxygen sensitivity of mitochondrial function in rat arterial chemoreceptor cells. *The Journal of physiology* **591,** 3549-3563.

Buckler KJ & Vaughan-Jones RD. (1994). Effects of hypercapnia on membrane potential and intracellular calcium in rat carotid body type I cells. *The Journal of physiology* **478 (Pt 1),** 157-171.

Buckler KJ, Williams BA & Honore E. (2000). An oxygen-, acid- and anaesthetic-sensitive TASK-like background potassium channel in rat arterial chemoreceptor cells. *The Journal of physiology* **525,** 135-142.

Buffet A, Smati S, Mansuy L, Menara M, Lebras M, Heymann MF, Simian C, Favier J, Murat A, Cariou B & Gimenez-Roqueplo AP. (2014). Mosaicism in HIF2A-related polycythemia-paraganglioma syndrome. *The Journal of clinical endocrinology and metabolism* **99,** E369-373.

Burke PGR, Abbott SBG, Coates MB, Viar KE, Stornetta RL & Guyenet PG. (2014). Optogenetic stimulation of adrenergic C1 neurons causes sleep state-dependent cardiorespiratory stimulation and arousal with sighs in rats. *American journal of respiratory and critical care medicine* **190,** 1301-1310.

Caceres AI, Obeso A, Gonzalez C & Rocher A. (2007). Molecular identification and functional role of voltage-gated sodium channels in rat carotid body chemoreceptor cells. Regulation of expression by chronic hypoxia in vivo. *Journal of neurochemistry* **102,** 231-245.

Carreau A, El Hafny-Rahbi B, Matejuk A, Grillon C & Kieda C. (2011). Why is the partial oxygen pressure of human tissues a crucial parameter? Small molecules and hypoxia. *Journal of cellular and molecular medicine* **15,** 1239-1253.

Carroll VA & Ashcroft M. (2005). Targeting the molecular basis for tumour hypoxia. *Expert reviews in molecular medicine* **7,** 1-16.

Chang AJ, Kim NS, Hireed H, de Arce AD, Ortega FE, Riegler J, Madison DV & Krasnow MA. (2018). Chang et al. reply. *Nature* **561,** E41-E41.

Chang AJ, Ortega FE, Riegler J, Madison DV & Krasnow MA. (2015). Oxygen regulation of breathing through an olfactory receptor activated by lactate. *Nature* **527,** 240-244.

Chen J, Dinger B, Jyung R, Stensaas L & Fidone S. (2003). Altered expression of vascular endothelial growth factor and FLK-1 receptor in chronically hypoxic rat carotid body. *Advances in experimental medicine and biology* **536,** 583-591.

Chen J, He L, Dinger B, Stensaas L & Fidone S. (2002). Role of endothelin and endothelin A-type receptor in adaptation of the carotid body to chronic hypoxia. *American journal of physiology Lung cellular and molecular physiology* **282,** L1314-1323.

Chen J, He L, Liu X, Dinger B, Stensaas L & Fidone S. (2007). Effect of the endothelin receptor antagonist bosentan on chronic hypoxia-induced morphological and physiological changes in rat carotid body. *American journal of physiology Lung cellular and molecular physiology* **292,** L1257-1262.

Chen W, Hill H, Christie A, Kim MS, Holloman E, Pavia-Jimenez A, Homayoun F, Ma Y, Patel N, Yell P, Hao G, Yousuf Q, Joyce A, Pedrosa I, Geiger H, Zhang H, Chang J, Gardner KH, Bruick RK, Reeves C, Hwang TH, Courtney K, Frenkel E, Sun X, Zojwalla N, Wong T, Rizzi JP, Wallace EM, Josey JA, Xie Y, Xie XJ, Kapur P, McKay RM & Brugarolas J. (2016). Targeting renal cell carcinoma with a HIF-2 antagonist. *Nature* **539,** 112-117.

Chiocchio SR, Biscardi AM & Tramezzani JH. (1966). Catecholamines in the carotid body of the cat. *Nature* **212,** 834-835.

Cho H, Du X, Rizzi JP, Liberzon E, Chakraborty AA, Gao W, Carvo I, Signoretti S, Bruick RK, Josey JA, Wallace EM & Kaelin WG. (2016). On-target efficacy of a HIF-2alpha antagonist in preclinical kidney cancer models. *Nature* **539,** 107-111.

Cho T, Chan W & Cutz E. (1989). Distribution and frequency of neuro-epithelial bodies in post-natal rabbit lung: quantitative study with monoclonal antibody against serotonin. *Cell and tissue research* **255,** 353-362.

Cipolleschi MG, Dello Sbarba P & Olivotto M. (1993). The role of hypoxia in the maintenance of hematopoietic stem cells. *Blood* **82,** 2031-2037.

Courtney KD, Infante JR, Lam ET, Figlin RA, Rini BI, Brugarolas J, Zojwalla NJ, Lowe AM, Wang K, Wallace EM, Josey JA & Choueiri TK. (2018). Phase I Dose-Escalation Trial of PT2385, a First-in-Class Hypoxia-Inducible Factor-2α Antagonist in Patients With Previously Treated Advanced Clear Cell Renal Cell Carcinoma. *Journal of Clinical Oncology* **36,** 867-874.

Courtney KD, Infante JR, Lam ET, Figlin RA, Rini BI, Brugarolas J, Zojwalla NJ, Wang K, Wallace E, Josey JA & Choueiri TK. (2016). A phase I dose escalation trial of PT2385, a first-in-class oral HIF-2a inhibitor, in patients with advanced clear cell renal cell carcinoma. *Journal of Clinical Oncology* **34,** 2506-2506.

Cramer T, Yamanishi Y, Clausen BE, Forster I, Pawlinski R, Mackman N, Haase VH, Jaenisch R, Corr M, Nizet V, Firestein GS, Gerber H-P, Ferrara N & Johnson RS. (2003). HIF-1a is essential for myeloid cell-mediated inflammation. *Cell* **112,** 645-657.

Crosson S & Moffat K. (2002). Photoexcited structure of a plant photoreceptor domain reveals a light-driven molecular switch. *Plant Cell* **14,** 1067-1075.

Cunningham LA, Candelario K & Li L. (2012). Roles for HIF-1α in neural stem cell function and the regenerative response to stroke. *Behavioural brain research* **227,** 410-417.

Czyzyk-Krzeska MF, Bayliss DA, Lawson EE & Millhorn DE. (1992a). Regulation of tyrosine hydroxylase gene expression in the rat carotid body by hypoxia. *Journal of neurochemistry* **58,** 1538-1546.

Czyzyk-Krzeska MF, Furnari BA, Lawson EE & Millhorn DE. (1994). Hypoxia increases rate of transcription and stability of tyrosine hydroxylase mRNA in pheochromocytoma (PC12) cells. *The Journal of biological chemistry* **269,** 760-764.

Czyzyk-Krzeska MF, Lawson EE & Millhorn DE. (1992b). Expression of D2 dopamine receptor mRNA in the arterial chemoreceptor afferent pathway. *Journal of the autonomic nervous system* **41,** 31-39.

d'Anglemont de Tassigny X, Sirerol-Piquer MS, Gomez-Pinedo U, Pardal R, Bonilla S, Capilla-Gonzalez V, Lopez-Lopez I, De la Torre-Laviana FJ, Garcia-Verdugo JM & Lopez-Barneo J. (2015). Resistance of subventricular neural stem cells to chronic hypoxemia despite structural disorganization of the germinal center and impairment of neuronal and oligodendrocyte survival. *Hypoxia* **3,** 15-33.

D'Ippolito G, Diabira S, Howard GA, Roos BA & Schiller PC. (2006). Low oxygen tension inhibits osteogenic differentiation and enhances stemness of human MIAMI cells. *Bone* **39,** 513-522.

De Burgh Daly M, Lambertsen CJ & Schweitzer A. (1954). Observations on the volume of blood flow and oxygen utilization of the carotid body in the cat. *The Journal of physiology* **125,** 67-89.

De Castro F. (1926). F. Sur la structure et l'innervation de la glande intercarotidienne(glomus caroticum) de l'homme et des mammiferes, et sur un nouveau syst&me d'innervation autonome du nerf glossopharyngien. Trav. *Laboratory Investigation* **24,** 365-432.

De Castro F. (2009). Towards the sensory nature of the carotid body: hering, de castro and heymansdagger. *Frontiers in neuroanatomy* **3,** 23.

De Castro F & Rubio M. (1968). Arterial Chemoreceptors. *Proceedings of the Wates Symposium,* 267-278.

De Kock L & Dunn A. (1966). An electron microscope study of the carotid body. *Cells Tissues Organs* **64,** 163-178.

De Kock LL. (1951). Histology of the Carotid Body. *Nature* **167,** 611.

De Kock LL. (1954). The intra-glomerular tissues of the carotid body. *Acta anatomica* **21,** 101-116.

Dehne N & Brune B. (2014). Sensors, transmitters, and targets in mitochondrial oxygen shortage-a hypoxia-inducible factor relay story. *Antioxidants & redox signaling* **20,** 339-352.

Del Toro R, Levitsky KL, Lopez-Barneo J & Chiara MD. (2003). Induction of T-type calcium channel gene expression by chronic hypoxia. *The Journal of biological chemistry* **278,** 22316-22324.

Dengler VL, Galbraith M & Espinosa JM. (2014). Transcriptional regulation by hypoxia inducible factors. *Crit Rev Biochem Mol Biol* **49,** 1-15.

Dhillon DP, Barer GR & Walsh M. (1984). The enlarged carotid body of the chronically hypoxic and chronically hypoxic and hypercapnic rat: a morphometric analysis. *Quarterly journal of experimental physiology (Cambridge, England)* **69,** 301-317.

Dhillon S. (2019). Roxadustat: First Global Approval. *Drugs* **79,** 563-572.

Dings J, Meixensberger J, Jager A & Roosen K. (1998). Clinical experience with 118 brain tissue oxygen partial pressure catheter probes. *Neurosurgery* **43,** 1082-1095.

Dirken MN & Heemstra H. (1948). Alveolar oxygen tension and lung circulation. *Quarterly journal of experimental physiology (Cambridge, England)* **34,** 193-211.

Doetsch F. (2003). The glial identity of neural stem cells. *Nature neuroscience* **6,** 1127-1134.

Doetsch F, Caille I, Lim DA, Garcia-Verdugo JM & Alvarez-Buylla A. (1999). Subventricular zone astrocytes are neural stem cells in the adult mammalian brain. *Cell* **97,** 703-716.

Douglas CG, Haldane JS, Henderson Y & Schneider EC. (1913). VI. Physiological observations made on Pike's Peak, Colorado, with special reference to adaptation to low barometric pressures. *Philosophical Transactions of the Royal Society of London Series B, Containing Papers of a Biological Character* **203,** 185-318.

Dua A, Spees T, Hernandez FC, Igbadumhe AA, Algodi M & Desai S. (2014). Trends in the incidence of carotid body tumors in the United States from 1998 to 2011. *Vascular Disease Management* **11,** 298-302.

Duchen MR, Caddy KW, Kirby GC, Patterson DL, Ponte J & Biscoe TJ. (1988). Biophysical studies of the cellular elements of the rabbit carotid body. *Neuroscience* **26,** 291-311.

Edwards C, Heath D & Harris P. (1972). Ultrastructure of the carotid body in high-altitude guinea-pigs. *J Pathol* **107,** 131-136.

Edwards C, Heath D, Harris P, Castillo Y, Krüger H & Arias-Stella J. (1971). The carotid body in animals at high altitude. *The Journal of Pathology* **104,** 231-238.

Epstein AC, Gleadle JM, McNeill LA, Hewitson KS, O'Rourke J, Mole DR, Mukherji M, Metzen E, Wilson MI, Dhanda A, Tian YM, Masson N, Hamilton DL, Jaakkola P, Barstead R, Hodgkin J, Maxwell PH, Pugh CW, Schofield CJ & Ratcliffe PJ. (2001). C. elegans EGL-9 and mammalian homologs define a family of dioxygenases that regulate HIF by prolyl hydroxylation. *Cell* **107,** 43-54.

Erbel PJ, Card PB, Karakuzu O, Bruick RK & Gardner KH. (2003). Structural basis for PAS domain heterodimerization in the basic helix--loop--helix-PAS transcription factor hypoxia-inducible factor. *Proceedings of the National Academy of Sciences of the United States of America* **100,** 15504-15509.

Erecinska M & Silver IA. (2001). Tissue oxygen tension and brain sensitivity to hypoxia. *Respiration physiology* **128,** 263-276.

Espejo EF, Montoro RJ, Armengol JA & Lopez-Barneo J. (1998). Cellular and functional recovery of Parkinsonian rats after intrastriatal transplantation of carotid body cell aggregates. *Neuron* **20,** 197-206.

Euler US, Liljestrand G & Zotterman Y. (1940). The Excitation Mechanism of the Chemoreceptors of the Carotid Body. *Skandinavisches Archiv Für Physiologie* **83,** 132-152.

Evans MR, Card PB & Gardner KH. (2009). ARNT PAS-B has a fragile native state structure with an alternative beta-sheet register nearby in sequence space. *Proceedings of the National Academy of Sciences of the United States of America* **106,** 2617-2622.

Eyzaguirre C & Koyano H. (1965). Effects of hypoxia, hypercapnia, and pH on the chemoreceptor activity of the carotid body in vitro. *The Journal of physiology* **178,** 385-409.

Falcao AM, Palha JA, Ferreira AC, Marques F, Sousa N & Sousa JC. (2012). Topographical analysis of the subependymal zone neurogenic niche. *PLoS One* **7,** 1-12.

Favier J, Amar L & Gimenez-Roqueplo AP. (2015). Paraganglioma and phaeochromocytoma: from genetics to personalized medicine. *Nature reviews Endocrinology* **11,** 101-111.

Fehrer C, Brunauer R, Laschober G, Unterluggauer H, Reitinger S, Kloss F, Gully C, Gassner R & Lepperdinger G. (2007). Reduced oxygen tension attenuates differentiation capacity of human mesenchymal stem cells and prolongs their lifespan. *Aging cell* **6,** 745-757.

Feil S, Valtcheva N & Feil R. (2009). Inducible Cre mice. *Methods in molecular biology (Clifton, NJ)* **530,** 343-363.

Feng Z, Zou X, Chen Y, Wang H, Duan Y & Bruick RK. (2018). Modulation of HIF-2α PAS-B domain contributes to physiological responses. **115,** 13240-13245.

Fernandez-Aguera MC, Gao L, Gonzalez-Rodriguez P, Pintado CO, Arias-Mayenco I, Garcia-Flores P, Garcia-Perganeda A, Pascual A, Ortega-Saenz P & Lopez-Barneo J. (2015). Oxygen Sensing by Arterial Chemoreceptors Depends on Mitochondrial Complex I Signaling. *Cell metabolism* **22,** 825-837.

Fielding JW, Hodson EJ, Cheng X, Ferguson DJP, Eckardt L, Adam J, Lip P, Maton-Howarth M, Ratnayaka I, Pugh CW, Buckler KJ, Ratcliffe PJ & Bishop T. (2018). PHD2 inactivation in Type I cells drives HIF-2α-dependent multilineage hyperplasia and the formation of paraganglioma-like carotid bodies. *The Journal of physiology* **596,** 4393-4412.

Fitzgerald RS. (2000). Oxygen and carotid body chemotransduction: the cholinergic hypothesis - a brief history and new evaluation. *Respiration physiology* **120,** 89-104.

Formenti F, Beer PA, Croft QP, Dorrington KL, Gale DP, Lappin TR, Lucas GS, Maher ER, Maxwell PH, McMullin MF, O'Connor DF, Percy MJ, Pugh CW, Ratcliffe PJ, Smith TG, Talbot NP & Robbins PA. (2011). Cardiopulmonary function in two human disorders of the hypoxia-inducible factor (HIF) pathway: von Hippel-Lindau disease and HIF-2alpha gain-of-function mutation. *FASEB journal : official publication of the Federation of American Societies for Experimental Biology* **25,** 2001-2011.

Forsythe JA, Jiang BH, Iyer NV, Agani F, Leung SW, Koos RD & Semenza GL. (1996). Activation of vascular endothelial growth factor gene transcription by hypoxia-inducible factor 1. *Molecular and cellular biology* **16,** 4604-4613.

Franke K, Gassmann M & Wielockx B. (2013). Erythrocytosis: the HIF pathway in control. *Blood* **122,** 1122-1128.

Fuhrmann DC & Brüne B. (2017). Mitochondrial composition and function under the control of hypoxia. *Redox Biol* **12,** 208-215.

Fuhrmann DC, Wittig I, Heide H, Dehne N & Brune B. (2013). Chronic hypoxia alters mitochondrial composition in human macrophages. *Biochim Biophys Acta* **1834,** 2750-2760.

Gallego R & Belmonte C. (1979). The effects of blood osmolality changes on cat carotid body chemoreceptors in vivo. *Pflugers Archiv : European journal of physiology* **380,** 53-58.

Gao L, Bonilla-Henao V, García-Flores P, Arias-Mayenco I, Ortega-Sáenz P & López-Barneo J. (2017). Gene expression analyses reveal metabolic specifications in acute O2-sensing chemoreceptor cells. *The Journal of physiology* **595,** 6091-6120.

Garcia-Fernandez M, Mejias R & Lopez-Barneo J. (2007a). Developmental changes of chromaffin cell secretory response to hypoxia studied in thin adrenal slices. *Pflugers Archiv : European journal of physiology* **454,** 93-100.

Garcia-Fernandez M, Ortega-Saenz P, Castellano A & Lopez-Barneo J. (2007b). Mechanisms of low-glucose sensitivity in carotid body glomus cells. *Diabetes* **56,** 2893-2900.

Garcia AD, Doan NB, Imura T, Bush TG & Sofroniew MV. (2004). GFAP-expressing progenitors are the principal source of constitutive neurogenesis in adult mouse forebrain. *Nature neuroscience* **7,** 1233-1241.

Genick UK, Borgstahl GE, Ng K, Ren Z, Pradervand C, Burke PM, Srajer V, Teng TY, Schildkamp W, McRee DE, Moffat K & Getzoff ED. (1997). Structure of a protein photocycle intermediate by millisecond time-resolved crystallography. *Science (New York, NY)* **275,** 1471-1475.

Gerber HP, Condorelli F, Park J & Ferrara N. (1997). Differential transcriptional regulation of the two vascular endothelial growth factor receptor genes. Flt-1, but not Flk-1/KDR, is up-regulated by hypoxia. *The Journal of biological chemistry* **272,** 23659-23667.

Gilyarov AV. (2008). Nestin in central nervous system cells. *Neuroscience and behavioral physiology* **38,** 165-169.

Gonzalez C, Almaraz L, Obeso A & Rigual R. (1994). Carotid body chemoreceptors: from natural stimuli to sensory discharges. *Physiological reviews* **74,** 829-898.

Gorgas K & Böck P. (1976). Morphology and histochemistry of the adrenal medulla. *Histochemistry* **50,** 17-31.

Grabner CP, Price SD, Lysakowski A & Fox AP. (2005). Mouse Chromaffin Cells Have Two Populations of Dense Core Vesicles. *Journal of Neurophysiology* **94,** 2093-2104.

Grocott MP, Martin DS, Levett DZ, McMorrow R, Windsor J & Montgomery HE. (2009). Arterial blood gases and oxygen content in climbers on Mount Everest. *The New England journal of medicine* **360,** 140-149.

Gruber M, Hu CJ, Johnson RS, Brown EJ, Keith B & Simon MC. (2007). Acute postnatal ablation of Hif-2alpha results in anemia. *Proceedings of the National Academy of Sciences of the United States of America* **104,** 2301-2306.

Gustafsson MV, Zheng X, Pereira T, Gradin K, Jin S, Lundkvist J, Ruas JL, Poellinger L, Lendahl U & Bondesson M. (2005). Hypoxia requires notch signaling to maintain the undifferentiated cell state. *Developmental cell* **9,** 617-628.

Haase VH. (2010). Hypoxic regulation of erythropoiesis and iron metabolism. *American journal of physiology Renal physiology* **299,** F1-F13.

Hackett PH & Roach RC. (2001). High-altitude illness. *The New England journal of medicine* **345,** 107-114.

Haldane JS, Kellas AM & Kennaway EL. (1919). Experiments on acclimatisation to reduced atmospheric pressure. *The Journal of physiology* **53,** 181-206.

Hanbauer I. (1977). Regulation of tyrosine hydroxylase in carotid body. *Advances in biochemical psychopharmacology* **16,** 275-280.

Harrison JS, Rameshwar P, Chang V & Bandari P. (2002). Oxygen saturation in the bone marrow of healthy volunteers. *Blood* **99,** 394.

Harten SK, Ashcroft M & Maxwell PH. (2010). Prolyl hydroxylase domain inhibitors: a route to HIF activation and neuroprotection. *Antioxidants & redox signaling* **12,** 459-480.

Heeringa J, Berkenbosch A, de Goede J & Olievier CN. (1979). Relative contribution of central and peripheral chemoreceptors to the ventilatory response to CO2 during hyperoxia. *Respiratory Physiology* **37,** 365-379.

Heymans J & Heymans C. (1927). Sur les modifications directes et sur la régulation réflexe de l'activité du centre respiratoire de la tête isolée du chien. *Arch Int Pharmacodyn Ther* **33,** 273-372.

Hiemstra PS & Bourdin A. (2014). Club cells, CC10 and self-control at the epithelial surface. *The European respiratory journal* **44,** 831-832.

Higgins DF, Biju MP, Akai Y, Wutz A, Johnson RS & Haase VH. (2004). Hypoxic induction of Ctgf is directly mediated by Hif-1. *American journal of physiology Renal physiology* **287,** F1223-1232.

Hirrlinger PG, Scheller A, Braun C, Hirrlinger J & Kirchhoff F. (2006). Temporal control of gene recombination in astrocytes by transgenic expression of the tamoxifen-inducible DNA recombinase variant CreERT2. *Glia* **54,** 11-20.

Hodson EJ, Nicholls LG, Turner PJ, Llyr R, Fielding JW, Douglas G, Ratnayaka I, Robbins PA, Pugh CW, Buckler KJ, Ratcliffe PJ & Bishop T. (2016). Regulation of ventilatory sensitivity and carotid body proliferation in hypoxia by the PHD2/HIF-2 pathway. *The Journal of physiology* **594,** 1179-1195.

Hohler B, Mayer B & Kummer W. (1994). Nitric oxide synthase in the rat carotid body and carotid sinus. *Cell and tissue research* **276,** 559-564.

Holmes AP, Ray CJ, Coney AM & Kumar P. (2018). Is Carotid Body Physiological O(2) Sensitivity Determined by a Unique Mitochondrial Phenotype? *Front Physiol* **9,** 562-562.

Holmes AP, Turner PJ, Buckler KJ & Kumar P. (2016). Moderate inhibition of mitochondrial function augments carotid body hypoxic sensitivity. *Pflugers Archiv : European journal of physiology* **468,** 143-155.

Hornbein TF, Griffo ZJ & Roos A. (1961). Quantitation of chemoreceptor activity: interrelation of hypoxia and hypercapnia. *J Neurophysiol* **24,** 561-568.

Hu CJ, Iyer S, Sataur A, Covello KL, Chodosh LA & Simon MC. (2006). Differential regulation of the transcriptional activities of hypoxia-inducible factor 1 alpha (HIF-1alpha) and HIF-2alpha in stem cells. *Molecular and cellular biology* **26,** 3514-3526.

Hu CJ, Wang LY, Chodosh LA, Keith B & Simon MC. (2003). Differential roles of hypoxia-inducible factor 1alpha (HIF-1alpha) and HIF-2alpha in hypoxic gene regulation. *Mol Cell Biol* **23,** 9361-9374.

Hu J, Discher DJ, Bishopric NH & Webster KA. (1998). Hypoxia regulates expression of the endothelin-1 gene through a proximal hypoxia-inducible factor-1 binding site on the antisense strand. *Biochemical and biophysical research communications* **245,** 894-899.

Hultgren HN & Grover RF. (1968). Circulatory adaptation to high altitude. *Annual review of medicine* **19,** 119-152.

Hussain I, Husain Q, Baredes S, Eloy JA, Jyung RW & Liu JK. (2014). Molecular genetics of paragangliomas of the skull base and head and neck region: implications for medical and surgical management. *Journal of neurosurgery* **120,** 321-330.

Ihrie RA & Alvarez-Buylla A. (2011). Lake-front property: a unique germinal niche by the lateral ventricles of the adult brain. *Neuron* **70,** 674-686.

Ishiguro T, Iwase M, Kanamaru M, Izumizaki M, Ohshima Y & Homma I. (2006). Impaired ventilation and metabolism response to hypoxia in histamine H1 receptor-knockout mice. *Respiratory physiology & neurobiology* **154,** 331-341.

Iyer NV, Kotch LE, Agani F, Leung SW, Laughner E, Wenger RH, Gassmann M, Gearhart JD, Lawler AM, Yu AY & Semenza GL. (1998). Cellular and developmental control of O2 homeostasis by hypoxia-inducible factor 1 alpha. *Genes & development* **12,** 149-162.

Izal-Azcarate A, Belzunegui S, San Sebastian W, Garrido-Gil P, Vazquez-Claverie M, Lopez B, Marcilla I & Luquin MA. (2008). Immunohistochemical characterization of the rat carotid body. *Respiratory physiology & neurobiology* **161,** 95-99.

Jackson A & Nurse C. (1995). Plasticity in cultured carotid body chemoreceptors: environmental modulation of GAP-43 and neurofilament. *Journal of neurobiology* **26,** 485-496.

Jain M & Sznajder JI. (2005). Effects of hypoxia on the alveolar epithelium. *Proceedings of the American Thoracic Society* **2,** 202-205.

Jiang RG & Eyzaguirre C. (2004). Effects of hypoxia and putative transmitters on [Ca2+]i of rat glomus cells. *Brain research* **995,** 285-296.

Joharapurkar AA, Pandya VB, Patel VJ, Desai RC & Jain MR. (2018). Prolyl Hydroxylase Inhibitors: A Breakthrough in the Therapy of Anemia Associated with Chronic Diseases. *Journal of medicinal chemistry* **61,** 6964-6982.

Johnson RP, O'Kelly IM & Fearon IM. (2004). System-specific O2 sensitivity of the tandem pore domain K+ channel TASK-1. *American journal of physiology Cell physiology* **286,** C391-397.

Jyung RW, LeClair EE, Bernat RA, Kang TS, Ung F, McKenna MJ & Tuan RS. (2000). Expression of angiogenic growth factors in paragangliomas. *The Laryngoscope* **110,** 161-167.

Kaelin WG, Jr. (2002). Molecular basis of the VHL hereditary cancer syndrome. *Nature reviews Cancer* **2,** 673-682.

Kaelin WG, Jr. (2007). Von Hippel-Lindau disease. *Annual review of pathology* **2,** 145-173.

Kaelin WG, Jr. (2008). The von Hippel-Lindau tumour suppressor protein: O2 sensing and cancer. *Nature reviews Cancer* **8,** 865-873.

Kaelin WG, Jr. (2017). The VHL Tumor Suppressor Gene: Insights into Oxygen Sensing and Cancer. *Transactions of the American Clinical and Climatological Association* **128,** 298-307.

Kaelin WG, Jr. & Ratcliffe PJ. (2008). Oxygen sensing by metazoans: the central role of the HIF hydroxylase pathway. *Molecular cell* **30,** 393-402.

Kameda Y. (1996). Immunoelectron microscopic localization of vimentin in sustentacular cells of the carotid body and the adrenal medulla of guinea pigs. *The journal of histochemistry and cytochemistry : official journal of the Histochemistry Society* **44,** 1439-1449.

Kameda Y. (2005). Mash1 is required for glomus cell formation in the mouse carotid body. *Developmental biology* **283,** 128-139.

Kay JM & Laidler P. (1977). Hypoxia and the carotid body. *Journal of Clinical Pathology Supplement* **11,** 30-44.

Kliewer KE & Cochran AJ. (1989). A review of the histology, ultrastructure, immunohistology, and molecular biology of extra-adrenal paragangliomas. *Archives of pathology & laboratory medicine* **113,** 1209-1218.

Kline DD, Peng YJ, Manalo DJ, Semenza GL & Prabhakar NR. (2002). Defective carotid body function and impaired ventilatory responses to chronic hypoxia in mice partially deficient for hypoxia-inducible factor 1 alpha. *Proceedings of the National Academy of Sciences of the United States of America* **99,** 821-826.

Kokaia Z, Thored P, Arvidsson A & Lindvall O. (2006). Regulation of Stroke-Induced Neurogenesis in Adult Brain—Recent Scientific Progress. *Cerebral cortex* **16,** 162-167.

Kokovay E & Temple S. (2007). Taking neural crest stem cells to new heights. *Cell* **131,** 234-236.

Kondo H, Iwanaga T & Nakajima T. (1982). Immunocytochemical study on the localization of neuron-specific enolase and S-100 protein in the carotid body of rats. *Cell and tissue research* **227,** 291-295.

Kondo K, Kim WY, Lechpammer M & Kaelin WG, Jr. (2003). Inhibition of HIF2alpha is sufficient to suppress pVHL-defective tumor growth. *PLoS biology* **1,** E83.

Kretzschmar K & Watt FM. (2012). Lineage tracing. *Cell* **148,** 33-45.

Kriegstein A & Alvarez-Buylla A. (2009). The glial nature of embryonic and adult neural stem cells. *Annual review of neuroscience* **32,** 149-184.

Krylov S & Anichkov S. (1968). The effect of metabolic inhibitors on carotid chemoreceptors. *Arterial Chemoreceptors***,** 103-109.

Kumar P & Bin-Jaliah I. (2007). Adequate stimuli of the carotid body: more than an oxygen sensor? *Respiratory physiology & neurobiology* **157,** 12-21.

Kumar P & Prabhakar NR. (2012). Peripheral chemoreceptors: function and plasticity of the carotid body. *Comprehensive Physiology* **2,** 141-219.

Kusakabe T, Hirakawa H, Oikawa S, Matsuda H, Kawakami T, Takenaka T & Hayashida Y. (2004). Morphological changes in the rat carotid body 1, 2, 4, and 8 weeks after the termination of chronically hypocapnic hypoxia. *Histology and histopathology* **19,** 1133-1140.

Lagace DC, Whitman MC, Noonan MA, Ables JL, DeCarolis NA, Arguello AA, Donovan MH, Fischer SJ, Farnbauch LA, Beech RD, DiLeone RJ, Greer CA, Mandyam CD & Eisch AJ. (2007). Dynamic contribution of nestin-expressing stem cells to adult neurogenesis. *The Journal of neuroscience : the official journal of the Society for Neuroscience* **27,** 12623-12629.

Lahiri S, DeLaney RG, Brody JS, Simpser M, Velasquez T, Motoyama EK & Polgar C. (1976). Relative role of environmental and genetic factors in respiratory adaptation to high altitude. *Nature* **261,** 133-135.

Lahiri S, Rumsey WL, Wilson DF & Iturriaga R. (1993). Contribution of in vivo microvascular PO2 in the cat carotid body chemotransduction. *Journal of Applied Physiology* **75,** 1035-1043.

Laidler P & Kay JM. (1975). A quantitative morphological study of the carotid bodies of rats living at a simulated altitude of 4300 metres. *The Journal of pathology* **117,** 183-191.

Laidler P & Kay JM. (1978). Ultrastructure of carotid body in rats living at a simulated altitude of 4300 metres. *The Journal of pathology* **124,** 27-33.

Lauweryns JM, Cokelaere M, Deleersnyder M & Liebens M. (1977). Intrapulmonary neuro-epithelial bodies in newborn rabbits. *Cell and tissue research* **182,** 425-440.

Leary TS, Klinck JR, Hayman G, Friend P, Jamieson NV & Gupta AK. (2002). Measurement of liver tissue oxygenation after orthotopic liver transplantation using a multiparameter sensor. A pilot study. *Anaesthesia* **57,** 1128-1133.

Lertkiatmongkol P, Liao D, Mei H, Hu Y & Newman PJ. (2016). Endothelial functions of platelet/endothelial cell adhesion molecule-1 (CD31). *Current opinion in hematology* **23,** 253-259.

Li L, Candelario, Ventura P, Lagace D, Eisch A & Cunningham L. (2010). Focal Cerebral Ischemia Induces a Multi lineage Cytogenic Response from Adult Subventricular Zone that is Predominantly Gliogenic. *Glia* **58,** 1610-1619.

Li L, Candelario KM, Thomas K, Wang R, Wright K, Messier A & Cunningham LA. (2014). Hypoxia inducible factor-1alpha (HIF-1alpha) is required for neural stem cell maintenance and vascular stability in the adult mouse SVZ. *The Journal of neuroscience : the official journal of the Society for Neuroscience* **34,** 16713-16719.

Li Z, Bao S, Wu Q, Wang H, Eyler C, Sathornsumetee S, Shi Q, Cao Y, Lathia J, McLendon RE, Hjelmeland AB & Rich JN. (2009). Hypoxia-inducible factors regulate tumorigenic capacity of glioma stem cells. *Cancer Cell* **15,** 501-513.

Lieb ME, Menzies K, Moschella MC, Ni R & Taubman MB. (2002). Mammalian EGLN genes have distinct patterns of mRNA expression and regulation. *Biochemistry and cell biology = Biochimie et biologie cellulaire* **80,** 421-426.

Lim DA & Alvarez-Buylla A. (2016). The Adult Ventricular-Subventricular Zone (V-SVZ) and Olfactory Bulb (OB) Neurogenesis. *Cold Spring Harbor perspectives in biology* **8**.

Lim J, Kim HI, Bang Y, Seol W, Choi HS & Choi HJ. (2015). Hypoxia-inducible factor-1alpha upregulates tyrosine hydroxylase and dopamine transporter by nuclear receptor ERRgamma in SH-SY5Y cells. *Neuroreport* **26,** 380-386.

Lindeberg J, Usoskin D, Bengtsson H, Gustafsson A, Kylberg A, Soderstrom S & Ebendal T. (2004). Transgenic expression of Cre recombinase from the tyrosine hydroxylase locus. *Genesis (New York, NY : 2000)* **40,** 67-73.

Linnoila RI. (2006). Functional facets of the pulmonary neuroendocrine system. *Laboratory investigation; a journal of technical methods and pathology* **86,** 425-444.

Liu F, You Y, Li X, Ma T, Nie Y, Wei B, Li T, Lin H & Yang Z. (2009). Brain Injury Does Not Alter the Intrinsic Differentiation Potential of Adult Neuroblasts. *The Journal of Neuroscience* **29,** 5075.

Liu Y, Cox SR, Morita T & Kourembanas S. (1995). Hypoxia regulates vascular endothelial growth factor gene expression in endothelial cells. Identification of a 5' enhancer. *Circulation research* **77,** 638-643.

Livermore S, Zhou Y, Pan J, Yeger H, Nurse CA & Cutz E. (2015). Pulmonary neuroepithelial bodies are polymodal airway sensors: evidence for CO2/H+ sensing. *American journal of physiology Lung cellular and molecular physiology* **308,** L807-815.

Llados F & Zapata P. (1978a). Effects of adrenoceptor stimulating and blocking agents on carotid body chemosensory inhibition. *The Journal of physiology* **274,** 501-509.

Llados F & Zapata P. (1978b). Effects of dopamine analogues and antagonists on carotid body chemosensors in situ. *The Journal of physiology* **274,** 487-499.

Logan S, Tobin KE, Fallon SC, Deng KS, McDonough AB & Bavis RW. (2016). Chronic intermittent hyperoxia alters the development of the hypoxic ventilatory response in neonatal rats. *Respiratory physiology & neurobiology* **220,** 69-80.

Lopez-Barneo J, Gonzalez-Rodriguez P, Gao L, Fernandez-Aguera MC, Pardal R & Ortega-Saenz P. (2016). Oxygen sensing by the carotid body: mechanisms and role in adaptation to hypoxia. *American Journal of Physiology-Cell Physiology* **310,** C629-C642.

Lopez-Barneo J, Ortega-Saenz P, Pardal R, Pascual A & Piruat JI. (2008). Carotid body oxygen sensing. *The European respiratory journal* **32,** 1386-1398.

Lopez-Barneo J, Pardal R & Ortega-Saenz P. (2001). Cellular mechanism of oxygen sensing. *Annual review of physiology* **63,** 259-287.

Lussey Lepoutre C, Buffet A, Morin A, Goncalves J & Favier J. (2018). Rodent models of pheochromocytoma, parallels in rodent and human tumorigenesis. *Cell and tissue research* **372,** 379-392.

Macdougall IC, Akizawa T, Berns JS, Bernhardt T & Krueger T. (2019). Effects of Molidustat in the Treatment of Anemia in CKD. *Clinical journal of the American Society of Nephrology : CJASN* **14,** 28-39.

Macias D, Cowburn AS, Torres-Torrelo H, Ortega-Saenz P, Lopez-Barneo J & Johnson RS. (2018). HIF-2alpha is essential for carotid body development and function. *eLife* **7**.

Macias D, Fernandez-Aguera MC, Bonilla-Henao V & Lopez-Barneo J. (2014). Deletion of the von Hippel-Lindau gene causes sympathoadrenal cell death and impairs chemoreceptor-mediated adaptation to hypoxia. *EMBO molecular medicine* **6,** 1577-1592.

Madisen L, Zwingman TA, Sunkin SM, Oh SW, Zariwala HA, Gu H, Ng LL, Palmiter RD, Hawrylycz MJ, Jones AR, Lein ES & Zeng H. (2010). A robust and high-throughput Cre reporting and characterization system for the whole mouse brain. *Nature neuroscience* **13,** 133-140.

Mahmoud AD, Lewis S, Juricic L, Udoh UA, Hartmann S, Jansen MA, Ogunbayo OA, Puggioni P, Holmes AP, Kumar P, Navarro-Dorado J, Foretz M, Viollet B, Dutia MB, Marshall I & Evans AM. (2016). AMP-activated Protein Kinase Deficiency Blocks the Hypoxic Ventilatory Response and Thus Precipitates Hypoventilation and Apnea. *Am J Respir Crit Care Med* **193,** 1032-1043.

Malatesha G, Singh NK, Bharija A, Rehani B & Goel A. (2007). Comparison of arterial and venous pH, bicarbonate, PCO2 and PO2 in initial emergency department assessment. *Emerg Med J* **24,** 569-571.

Malladi P, Xu Y, Chiou M, Giaccia AJ & Longaker MT. (2007). Hypoxia inducible factor-1alpha deficiency affects chondrogenesis of adipose-derived adult stromal cells. *Tissue engineering* **13,** 1159-1171.

Maxwell PH, Pugh CW & Ratcliffe PJ. (1993). Inducible operation of the erythropoietin 3' enhancer in multiple cell lines: evidence for a widespread oxygen-sensing mechanism. *Proc Natl Acad Sci U S A* **90,** 2423-2427.

Maxwell PH, Pugh CW & Ratcliffe PJ. (2001). Activation of the HIF pathway in cancer. *Current opinion in genetics & development* **11,** 293-299.

Maxwell PH, Wiesener MS, Chang GW, Clifford SC, Vaux EC, Cockman ME, Wykoff CC, Pugh CW, Maher ER & Ratcliffe PJ. (1999). The tumour suppressor protein VHL targets hypoxia-inducible factors for oxygen-dependent proteolysis. *Nature* **399,** 271-275.

Mazumdar J, O'Brien WT, Johnson RS, LaManna JC, Chavez JC, Klein PS & Simon MC. (2010). O2 regulates stem cells through Wnt/beta-catenin signalling. *Nature cell biology* **12,** 1007-1013.

Mazzone M, Dettori D, Leite de Oliveira R, Loges S, Schmidt T, Jonckx B, Tian YM, Lanahan AA, Pollard P, Ruiz de Almodovar C, De Smet F, Vinckier S, Aragones J, Debackere K, Luttun A, Wyns S, Jordan B, Pisacane A, Gallez B, Lampugnani MG, Dejana E, Simons M, Ratcliffe P, Maxwell P & Carmeliet P. (2009). Heterozygous deficiency of PHD2 restores tumor oxygenation and inhibits metastasis via endothelial normalization. *Cell* **136,** 839-851.

McDonald D & Mitchell R. (1975a). The innervation of glomus cells, ganglion cells and blood vessels in the rat carotid body: A quantitative ultrastructural analysis. *Journal of neurocytology* **4,** 177-230.

McDonald DM & Mitchell R. (1975b). *A quantitative analysis of synaptic connections in the rat carotid body.* .

McGregor KH, Gil J & Lahiri S. (1984). A morphometric study of the carotid body in chronically hypoxic rats. *Journal of applied physiology: respiratory, environmental and exercise physiology* **57,** 1430-1438.

Mich JK, Signer RA, Nakada D, Pineda A, Burgess RJ, Vue TY, Johnson JE & Morrison SJ. (2014). Prospective identification of functionally distinct stem cells and neurosphere-initiating cells in adult mouse forebrain. *eLife* **3,** e02669.

Millhorn DE, Raymond R, Conforti L, Zhu W, Beitner-Johnson D, Filisko T, Genter MB, Kobayashi S & Peng M. (1997). Regulation of gene expression for tyrosine hydroxylase in oxygen sensitive cells by hypoxia. *Kidney international* **51,** 527-535.

Minamishima YA, Moslehi J, Bardeesy N, Cullen D, Bronson RT & Kaelin WG, Jr. (2008). Somatic inactivation of the PHD2 prolyl hydroxylase causes polycythemia and congestive heart failure. *Blood* **111,** 3236-3244.

Mitchell JA & Yochim JM. (1968). Intrauterine oxygen tension during the estrous cycle in the rat: its relation to uterine respiration and vascular activity. *Endocrinology* **83,** 701-705.

Möglich A, Ayers RA & Moffat K. (2009). Structure and signaling mechanism of Per-ARNT-Sim domains. *Structure* **17,** 1282-1294.

Mohyeldin A, Garzon-Muvdi T & Quinones-Hinojosa A. (2010). Oxygen in stem cell biology: a critical component of the stem cell niche. *Cell stem cell* **7,** 150-161.

Monti-Bloch L, Stensaas LJ & Eyzaguirre C. (1983). Effects of ischemia on the function and structure of the cat carotid body. *Brain research* **270,** 63-76.

Montoro RJ, Urena J, Fernandez-Chacon R, Alvarez de Toledo G & Lopez-Barneo J. (1996). Oxygen sensing by ion channels and chemotransduction in single glomus cells. *The Journal of general physiology* **107,** 133-143.

Morrison SJ, Csete M, Groves AK, Melega W, Wold B & Anderson DJ. (2000). Culture in reduced levels of oxygen promotes clonogenic sympathoadrenal differentiation by isolated neural crest stem cells. *The Journal of neuroscience* **20,** 7370-7376.

Mulligan E, Lahiri S & Storey BT. (1981). Carotid body O2 chemoreception and mitochondrial oxidative phosphorylation. *Journal of applied physiology: respiratory, environmental and exercise physiology* **51,** 438-446.

Myllyharju J. (2009). HIF prolyl 4-hydroxylases and their potential as drug targets. *Current pharmaceutical design* **15,** 3878-3885.

Naeije R. (2010). Physiological adaptation of the cardiovascular system to high altitude. *Progress in cardiovascular diseases* **52,** 456-466.

Nielsen AM, Bisgard GE & Vidruk EH. (1988). Carotid chemoreceptor activity during acute and sustained hypoxia in goats. *J Appl Physiol* **65,** 1796-1802.

Nishi K, Okajima Y, Ito H & Sugahara K. (1981). Alteration of chemoreceptor responses and ultrastructural features of ischemic carotid body of the cat. *The Japanese journal of physiology* **31,** 677-694.

Nurse CA. (2005). Neurotransmission and neuromodulation in the chemosensory carotid body. *Auton Neurosci* **120,** 1-9.

Nurse CA & Fearon IM. (2002). Carotid body chemoreceptors in dissociated cell culture. *Microscopy Research and Technique* **59,** 249-255.

Nurse CA & Vollmer C. (1997). Role of basic FGF and oxygen in control of proliferation, survival, and neuronal differentiation in carotid body chromaffin cells. *Developmental biology* **184,** 197-206.

Ogle ME, Gu X, Espinera AR & Wei L. (2012). Inhibition of prolyl hydroxylases by dimethyloxaloylglycine after stroke reduces ischemic brain injury and requires hypoxia inducible factor-1α. *Neurobiology of Disease* **45,** 733-742.

Oomori Y, Nakaya K, Tanaka H, Iuchi H, Ishikawa K, Satoh Y & Ono K. (1994). Immunohistochemical and histochemical evidence for the presence of noradrenaline, serotonin and gamma-aminobutyric acid in chief cells of the mouse carotid body. *Cell and tissue research* **278,** 249-254.

P. Leichtweiss H, W. Lübbers D, Weiss C, Baumgärtl H & Reschke W. (1969). The oxygen supply of the rat kidney: Measurements of intrarenal pO2. *Pflügers Archiv - European Journal of Physiology* **309,** 328-349.

Pacak K, Jochmanova I, Prodanov T, Yang C, Merino MJ, Fojo T, Prchal JT, Tischler AS, Lechan RM & Zhuang Z. (2013). New syndrome of paraganglioma and somatostatinoma associated with polycythemia. *Journal of clinical oncology : official journal of the American Society of Clinical Oncology* **31,** 1690-1698.

Paciga M, Vollmer C & Nurse C. (1999). Role of ET-1 in hypoxia-induced mitosis of cultured rat carotid body chemoreceptors. *Neuroreport* **10,** 3739-3744.

Palmer TD, Ray J & Gage FH. (1995). FGF-2-responsive neuronal progenitors reside in proliferative and quiescent regions of the adult rodent brain. *Molecular and cellular neurosciences* **6,** 474-486.

Pan J, Bishop T, Ratcliffe PJ, Yeger H & Cutz E. (2016). Hyperplasia and hypertrophy of pulmonary neuroepithelial bodies, presumed airway hypoxia sensors, in hypoxia-inducible factor prolyl hydroxylase-deficient mice. *Hypoxia* **4,** 69-80.

Pan J, Yeger H, Ratcliffe P, Bishop T & Cutz E. (2012). Hyperplasia of pulmonary neuroepithelial bodies (NEB) in lungs of prolyl hydroxylase -1(PHD-1) deficient mice. *Advances in experimental medicine and biology* **758,** 149-155.

Pandini A, Denison MS, Song Y, Soshilov AA & Bonati L. (2007). Structural and functional characterization of the aryl hydrocarbon receptor ligand binding domain by homology modeling and mutational analysis. *Biochemistry* **46,** 696-708.

Pang L & Eyzaguirre C. (1993). Hypoxia affects differently the intracellular pH of clustered and isolated glomus cells of the rat carotid body. *Brain research* **623,** 349-355.

Pang Y, Liu Y, Pacak K & Yang C. (2019). Pheochromocytomas and Paragangliomas: From Genetic Diversity to Targeted Therapies. *Cancers (Basel)* **11,** 436.

Pardal R, Ludewig U, Garcia-Hirschfeld J & Lopez-Barneo J. (2000). Secretory responses of intact glomus cells in thin slices of rat carotid body to hypoxia and tetraethylammonium. *Proceedings of the National Academy of Sciences of the United States of America* **97,** 2361-2366.

Pardal R, Ortega-Saenz P, Duran R & Lopez-Barneo J. (2007). Glia-like stem cells sustain physiologic neurogenesis in the adult mammalian carotid body. *Cell* **131,** 364-377.

Park SK, Dadak AM, Haase VH, Fontana L, Giaccia AJ & Johnson RS. (2003). Hypoxia-induced gene expression occurs solely through the action of hypoxia-inducible factor 1alpha (HIF-1alpha): role of cytoplasmic trapping of HIF-2alpha. *Molecular and cellular biology* **23,** 4959-4971.

Park YM, Chun H, Shin J-I & Lee CJ. (2018). Astrocyte Specificity and Coverage of hGFAP-CreERT2 [Tg(GFAP-Cre/ERT2)13Kdmc] Mouse Line in Various Brain Regions. *Experimental neurobiology* **27,** 508-525.

Pawar A, Nanduri J, Yuan G, Khan SA, Wang N, Kumar GK & Prabhakar NR. (2009). Reactive oxygen species-dependent endothelin signaling is required for augmented hypoxic sensory response of the neonatal carotid body by intermittent hypoxia. *American journal of physiology Regulatory, integrative and comparative physiology* **296,** R735-742.

Paxinos G & Franklin K. (2003). *The Mouse Brain In Stereotaxic Coordinates*, vol. 1.

Pearse AG, Polak JM, Rost FW, Fontaine J, Le Lievre C & Le Douarin N. (1973). Demonstration of the neural crest origin of type I (APUD) cells in the avian carotid body, using a cytochemical marker system. *Histochemie Histochemistry Histochimie* **34,** 191-203.

Pencea V, Bingaman KD, Wiegand SJ & Luskin MB. (2001). Infusion of brain-derived neurotrophic factor into the lateral ventricle of the adult rat leads to new neurons in the parenchyma of the striatum, septum, thalamus, and hypothalamus. *The Journal of neuroscience : the official journal of the Society for Neuroscience* **21,** 6706-6717.

Peng YJ, Nanduri J, Khan SA, Yuan G, Wang N, Kinsman B, Vaddi DR, Kumar GK, Garcia JA, Semenza GL & Prabhakar NR. (2011). Hypoxia-inducible factor 2alpha (HIF-2alpha) heterozygous-null mice exhibit exaggerated carotid body sensitivity

to hypoxia, breathing instability, and hypertension. *Proceedings of the National Academy of Sciences of the United States of America* **108,** 3065-3070.

Percy MJ, Zhao Q, Flores A, Harrison C, Lappin TR, Maxwell PH, McMullin MF & Lee FS. (2006). A family with erythrocytosis establishes a role for prolyl hydroxylase domain protein 2 in oxygen homeostasis. *Proc Natl Acad Sci U S A* **103,** 654-659.

Platero-Luengo A, Gonzalez-Granero S, Duran R, Diaz-Castro B, Piruat JI, Garcia-Verdugo JM, Pardal R & Lopez-Barneo J. (2014). An O2-sensitive glomus cell-stem cell synapse induces carotid body growth in chronic hypoxia. *Cell* **156,** 291-303.

Powell FL, Dwinell MR & Aaron EA. (2000a). Measuring ventilatory acclimatization to hypoxia: comparative aspects. *Respiration physiology* **122,** 271-284.

Powell FL, Huey KA & Dwinell MR. (2000b). Central nervous system mechanisms of ventilatory acclimatization to hypoxia. *Respiration physiology* **121,** 223-236.

Powell FL, Milsom WK & Mitchell GS. (1998). Time domains of the hypoxic ventilatory response. *Respiration physiology* **112,** 123-134.

Prabhakar NR & Jacono FJ. (2005). Cellular and molecular mechanisms associated with carotid body adaptations to chronic hypoxia. *High altitude medicine & biology* **6,** 112-120.

Prabhakar NR, Pieramici SF, Premkumar DR, Kumar GK & Kalaria RN. (1996). Activation of nitric oxide synthase gene expression by hypoxia in central and peripheral neurons. *Brain research Molecular brain research* **43,** 341-346.

Precious SV, Kelly CM, Reddington AE, Vinh NN, Stickland RC, Pekarik V, Scherf C, Jeyasingham R, Glasbey J, Holeiter M, Jones L, Taylor MV & Rosser AE. (2016). FoxP1 marks medium spiny neurons from precursors to maturity and is required for their differentiation. *Experimental neurology* **282,** 9-18.

Rajagopal S, Anderson S, Srajer V, Schmidt M, Pahl R & Moffat K. (2005). A structural pathway for signaling in the E46Q mutant of photoactive yellow protein. *Structure* **13,** 55-63.

Rankin EB, Biju MP, Liu Q, Unger TL, Rha J, Johnson RS, Simon MC, Keith B & Haase VH. (2007). Hypoxia-inducible factor-2 (HIF-2) regulates hepatic erythropoietin in vivo. *The Journal of clinical investigation* **117,** 1068-1077.

Raval RR, Lau KW, Tran MG, Sowter HM, Mandriota SJ, Li JL, Pugh CW, Maxwell PH, Harris AL & Ratcliffe PJ. (2005). Contrasting properties of hypoxia-inducible factor 1 (HIF-1) and HIF-2 in von Hippel-Lindau-associated renal cell carcinoma. *Molecular and cellular biology* **25,** 5675-5686.

Reynolds SD, Giangreco A, Power JH & Stripp BR. (2000a). Neuroepithelial bodies of pulmonary airways serve as a reservoir of progenitor cells capable of epithelial regeneration. *The American journal of pathology* **156,** 269-278.

Reynolds SD, Hong KU, Giangreco A, Mango GW, Guron C, Morimoto Y & Stripp BR. (2000b). Conditional clara cell ablation reveals a self-renewing progenitor function of pulmonary neuroendocrine cells. *American journal of physiology Lung cellular and molecular physiology* **278,** L1256-1263.

Rich PR. (2003). The molecular machinery of Keilin's respiratory chain. *Biochem Soc Trans* **31,** 1095-1105.

Richter S, Qin N, Pacak K & Eisenhofer G. (2013). Role of hypoxia and HIF2α in development of the sympathoadrenal cell lineage and chromaffin cell tumors with distinct catecholamine phenotypic features. *Adv Pharmacol* **68,** 285-317.

Rietze RL, Valcanis H, Brooker GF, Thomas T, Voss AK & Bartlett PF. (2001). Purification of a pluripotent neural stem cell from the adult mouse brain. *Nature* **412,** 736-739.

Robertson DI & Cooney TP. (1980). Malignant carotid body paraganglioma: light and electron microscopic study of the tumor and its metastases. *Cancer* **46,** 2623-2633.

Rogers JL, Bayeh L, Scheuermann TH, Longgood J, Key J, Naidoo J, Melito L, Shokri C, Frantz DE, Bruick RK, Gardner KH, MacMillan JB & Tambar UK. (2013). Development of inhibitors of the PAS-B domain of the HIF-2alpha transcription factor. *Journal of medicinal chemistry* **56,** 1739-1747.

Roitbak T, Surviladze Z & Cunningham LA. (2011). Continuous expression of HIF-1alpha in neural stem/progenitor cells. *Cellular and molecular neurobiology* **31,** 119-133.

Ross HH, Sandhu MS, Cheung TF, Fitzpatrick GM, Sher WJ, Tiemeier AJ, Laywell ED & Fuller DD. (2012). In vivo intermittent hypoxia elicits enhanced expansion and neuronal differentiation in cultured neural progenitors. *Experimental neurology* **235,** 238-245.

Ross LL. (1959). Electron microscopic observations of the carotid body of the cat. *J Biophys Biochem Cytol* **6,** 253-262.

Rotolo T, Smallwood PM, Williams J & Nathans J. (2008). Genetically-directed, cell type-specific sparse labeling for the analysis of neuronal morphology. *PLoS One* **3,** e4099.

Roussis IM, Myers FA & Scarlett GP. (2017). RNA Whole-Mount In Situ Hybridization Proximity Ligation Assay (rISH-PLA), an Assay for Detecting RNA-Protein Complexes in Intact Cells. *Current protocols in cell biology* **74,** 17.20.11-17.20.10.

Roux JC, Peyronnet J, Mamet J, Perrin D, Lagercrantz H, Dalmaz Y & Pequignot JM. (2001). Prenatal hypoxia impairs the early postnatal development of the carotid chemoafferent pathway. *Respiratory Research* **2,** P20.

Rychkov GY, Adams MB, McMillen IC & Roberts ML. (1998). Oxygen-sensing mechanisms are present in the chromaffin cells of the sheep adrenal medulla before birth. *The Journal of physiology* **509,** 887-893.

Rytkonen KT, Williams TA, Renshaw GM, Primmer CR & Nikinmaa M. (2011). Molecular evolution of the metazoan PHD-HIF oxygen-sensing system. *Mol Biol Evol* **28,** 1913-1926.

Sakashita M, Tanaka T & Nangaku M. (2019). Hypoxia-Inducible Factor-Prolyl Hydroxylase Domain Inhibitors to Treat Anemia in Chronic Kidney Disease. *Contributions to nephrology* **198,** 112-123.

Saldana MJ, Salem LE & Travezan R. (1973). High altitude hypoxia and chemodectomas. *Human pathology* **4,** 251-263.

Sato M, Severinghaus JW, Powell FL, Xu FD & Spellman MJ, Jr. (1992). Augmented hypoxic ventilatory response in men at altitude. *Journal of applied physiology (Bethesda, Md : 1985)* **73,** 101-107.

Scadden DT. (2006). The stem-cell niche as an entity of action. *Nature* **441,** 1075-1079.

Scheuermann TH, Li Q, Ma HW, Key J, Zhang L, Chen R, Garcia JA, Naidoo J, Longgood J, Frantz DE, Tambar UK, Gardner KH & Bruick RK. (2013). Allosteric inhibition of hypoxia inducible factor-2 with small molecules. *Nat Chem Biol* **9,** 271-276.

Scheuermann TH, Tomchick DR, Machius M, Guo Y, Bruick RK & Gardner KH. (2009). Artificial ligand binding within the HIF2alpha PAS-B domain of the HIF2 transcription factor. *Proceedings of the National Academy of Sciences of the United States of America* **106,** 450-455.

Schmittgen TD & Livak KJ. (2008). Analyzing real-time PCR data by the comparative C(T) method. *Nature protocols* **3,** 1101-1108.

Schnell PO, Ignacak ML, Bauer AL, Striet JB, Paulding WR & Czyzyk-Krzeska MF. (2003). Regulation of tyrosine hydroxylase promoter activity by the von Hippel-Lindau tumor suppressor protein and hypoxia-inducible transcription factors. *Journal of neurochemistry* **85,** 483-491.

Schofield CJ & Ratcliffe PJ. (2004). Oxygen sensing by HIF hydroxylases. *Nature reviews Molecular cell biology* **5,** 343-354.

Seidl E. (1975). The peripheral arterial chemoreceptors. *Cambridge Univ Press, London and New York* **177,** 230-293.

Semenza GL. (2014). Oxygen sensing, hypoxia-inducible factors, and disease pathophysiology. *Annual review of pathology* **9,** 47-71.

Semenza GL & Wang GL. (1992). A nuclear factor induced by hypoxia via de novo protein synthesis binds to the human erythropoietin gene enhancer at a site required for transcriptional activation. *Molecular and Cellular Biology* **12,** 5447-5454.

Severinghaus JW, Bainton CR & Carcelen A. (1966). Respiratory insensitivity to hypoxia in chronically hypoxic man. *Respiration physiology* **1,** 308-334.

Shojaei F. (2012). Anti-angiogenesis therapy in cancer: current challenges and future perspectives. *Cancer letters* **320,** 130-137.

Slingo ME, Turner PJ, Christian HC, Buckler KJ & Robbins PA. (2014). The von Hippel-Lindau Chuvash mutation in mice causes carotid-body hyperplasia and enhanced ventilatory sensitivity to hypoxia. *Journal of applied physiology (Bethesda, Md : 1985)* **116,** 885-892.

Smith TG, Brooks JT, Balanos GM, Lappin TR, Layton DM, Leedham DL, Liu C, Maxwell PH, McMullin MF, McNamara CJ, Percy MJ, Pugh CW, Ratcliffe PJ, Talbot NP, Treacy M & Robbins PA. (2006). Mutation of von Hippel–Lindau Tumour Suppressor and Human Cardiopulmonary Physiology. *PLOS Medicine* **3,** e290.

Sobrino V, Annese V, Navarro-Guerrero E, Platero-Luengo A & Pardal R. (2019). The carotid body: a physiologically relevant germinal niche in the adult peripheral nervous system. *Cellular and molecular life sciences : CMLS* **76,** 1027-1039.

Sobrino V, González-Rodríguez P, Annese V, López-Barneo J & Pardal R. (2018). Fast neurogenesis from carotid body quiescent neuroblasts accelerates adaptation to hypoxia. *EMBO reports*.

Son JH, Min N & Joh TH. (1996). Early ontogeny of catecholaminergic cell lineage in brain and peripheral neurons monitored by tyrosine hydroxylase-lacZ transgene. *Brain research Molecular brain research* **36,** 300-308.

Soriano P. (1999). Generalized lacZ expression with the ROSA26 Cre reporter strain. *Nature genetics* **21,** 70-71.

Stobdan T, Akbari A, Azad P, Zhou D, Poulsen O, Appenzeller O, Gonzales GF, Telenti A, Wong EHM, Saini S, Kirkness EF, Venter JC, Bafna V & Haddad GG. (2017). New Insights into the Genetic Basis of Monge's Disease and Adaptation to High-Altitude. *Molecular biology and evolution* **34,** 3154-3168.

Takeda K, Aguila HL, Parikh NS, Li X, Lamothe K, Duan LJ, Takeda H, Lee FS & Fong GH. (2008). Regulation of adult erythropoiesis by prolyl hydroxylase domain proteins. *Blood* **111,** 3229-3235.

Takeda K, Cowan A & Fong GH. (2007). Essential role for prolyl hydroxylase domain protein 2 in oxygen homeostasis of the adult vascular system. *Circulation* **116,** 774-781.

Takeda K, Ho VC, Takeda H, Duan LJ, Nagy A & Fong GH. (2006). Placental but not heart defects are associated with elevated hypoxia-inducible factor alpha levels in mice lacking prolyl hydroxylase domain protein 2. *Molecular and cellular biology* **26,** 8336-8346.

Takeda N, Maemura K, Imai Y, Harada T, Kawanami D, Nojiri T, Manabe I & Nagai R. (2004). Endothelial PAS domain protein 1 gene promotes angiogenesis through the transactivation of both vascular endothelial growth factor and its receptor, Flt-1. *Circulation research* **95,** 146-153.

Tan Q, Kerestes H, Percy MJ, Pietrofesa R, Chen L, Khurana TS, Christofidou-Solomidou M, Lappin TR & Lee FS. (2013). Erythrocytosis and pulmonary hypertension in a mouse model of human HIF2A gain of function mutation. *The Journal of biological chemistry* **288,** 17134-17144.

Tank AW & Lee Wong D. (2015). Peripheral and central effects of circulating catecholamines. *Comprehensive Physiology* **5,** 1-15.

Tansley JG, Clar C, Pedersen MEF & Robbins PA. (1997). Human ventilatory response to acute hyperoxia during and after 8 h of both isocapnic and poikilocapnic hypoxia. *Journal of Applied Physiology* **82,** 513-519.

Tatsumi K. (1999). [Effects of female hormones on respiratory and cardiovascular regulation]. *Nihon Kokyuki Gakkai zasshi = the journal of the Japanese Respiratory Society* **37,** 359-367.

Tatsumi K, Pickett CK & Weil JV. (1991). Attenuated carotid body hypoxic sensitivity after prolonged hypoxic exposure. *J Appl Physiol* **70,** 748-755.

Thompson EL, Ray CJ, Holmes AP, Pye RL, Wyatt CN, Coney AM & Kumar P. (2016). Adrenaline release evokes hyperpnoea and an increase in ventilatory CO2 sensitivity during hypoglycaemia: a role for the carotid body. *The Journal of physiology* **594,** 4439-4452.

Thompson RJ, Jackson A & Nurse CA. (1997). Developmental loss of hypoxic chemosensitivity in rat adrenomedullary chromaffin cells. *The Journal of physiology* **498 (2),** 503-510.

Tian H, Hammer RE, Matsumoto AM, Russell DW & McKnight SL. (1998). The hypoxia-responsive transcription factor EPAS1 is essential for catecholamine homeostasis and protection against heart failure during embryonic development. *Genes & development* **12,** 3320-3324.

Toledo RA. (2017). New HIF2alpha inhibitors: potential implications as therapeutics for advanced pheochromocytomas and paragangliomas. *Endocrine-related cancer* **24,** C9-c19.

Toledo RA, Qin Y, Srikantan S, Morales NP, Li Q, Deng Y, Kim SW, Pereira MA, Toledo SP, Su X, Aguiar RC & Dahia PL. (2013). In vivo and in vitro oncogenic effects of

HIF2A mutations in pheochromocytomas and paragangliomas. *Endocrine-related cancer* **20,** 349-359.

Torres-Capelli M, Marsboom G, Li QOY, Tello D, Rodriguez FM, Alonso T, Sanchez-Madrid F, García-Rio F, Ancochea J & Aragonés J. (2016). Role Of Hif2α Oxygen Sensing Pathway In Bronchial Epithelial Club Cell Proliferation. *Scientific Reports* **6,** 25357.

Torres-Torrelo H, Ortega-Saenz P, Macias D, Omura M, Zhou T, Matsunami H, Johnson RS, Mombaerts P & Lopez-Barneo J. (2018). The role of Olfr78 in the breathing circuit of mice. *Nature* **561,** E33-e40.

van Meerbeeck JP, Fennell DA & De Ruysscher DK. (2011). Small-cell lung cancer. *Lancet (London, England)* **378,** 1741-1755.

Verna A. (1979). Ulstrastructure of the carotid body in the mammals. *International review of cytology* **60,** 271-330.

Verna A, Roumy M & Leitner LM. (1975). Loss of chemoreceptive properties of the rabbit carotid body after destruction of the glomus cells. *Brain research* **100,** 13-23.

Vicario I, Rigual R, Obeso A & Gonzalez C. (2000). Characterization of the synthesis and release of catecholamine in the rat carotid body in vitro. *American journal of physiology Cell physiology* **278,** C490-499.

Vidruk EH, Olson EB, Jr., Ling L & Mitchell GS. (2001). Responses of single-unit carotid body chemoreceptors in adult rats. *The Journal of physiology* **531,** 165-170.

Villadiego J, Mendez-Ferrer S, Valdes-Sanchez T, Silos-Santiago I, Farinas I, Lopez-Barneo J & Toledo-Aral JJ. (2005). Selective glial cell line-derived neurotrophic factor production in adult dopaminergic carotid body cells in situ and after intrastriatal transplantation. *The Journal of neuroscience : the official journal of the Society for Neuroscience* **25,** 4091-4098.

Vizek M, Pickett CK & Weil JV. (1987). Increased carotid body hypoxic sensitivity during acclimatization to hypobaric hypoxia. *J Appl Physiol* **63,** 2403-2410.

Vooijs M, Jonkers J & Berns A. (2001). A highly efficient ligand-regulated Cre recombinase mouse line shows that LoxP recombination is position dependent. *EMBO reports* **2,** 292-297.

Wallace EM, Rizzi JP, Han G, Wehn PM, Cao Z, Du X, Cheng T, Czerwinski RM, Dixon DD, Goggin BS, Grina JA, Halfmann MM, Maddie MA, Olive SR, Schlachter ST, Tan H, Wang B, Wang K, Xie S, Xu R, Yang H & Josey JA. (2016). A Small-Molecule Antagonist of HIF2α Is Efficacious in Preclinical Models of Renal Cell Carcinoma. *Cancer Research* **76,** 5491-5500.

Wang ZY & Bisgard GE. (2002). Chronic hypoxia-induced morphological and neurochemical changes in the carotid body. *Microscopy Research and Technique* **59,** 168-177.

Wang ZY, Olson EB, Jr., Bjorling DE, Mitchell GS & Bisgard GE. (2008). Sustained hypoxia-induced proliferation of carotid body type I cells in rats. *J Appl Physiol* **104,** 803-808.

Wang ZZ, Stensaas LJ, Dinger B & Fidone SJ. (1992). The co-existence of biogenic amines and neuropeptides in the type I cells of the cat carotid body. *Neuroscience* **47,** 473-480.

Waypa GB, Smith KA & Schumacker PT. (2016). O2 sensing, mitochondria and ROS signaling: The fog is lifting. *Mol Aspects Med* **47-48,** 76-89.

Weir EK, Lopez-Barneo J, Buckler KJ & Archer SL. (2005). Acute oxygen-sensing mechanisms. *The New England journal of medicine* **353,** 2042-2055.

Wenker IC, Abe C, Viar KE, Stornetta DS, Stornetta RL & Guyenet PG. (2017). Blood Pressure Regulation by the Rostral Ventrolateral Medulla in Conscious Rats: Effects of Hypoxia, Hypercapnia, Baroreceptor Denervation, and Anesthesia. *The Journal of Neuroscience* **37,** 4565.

West JB. (2012). Centenary of the Anglo-American high-altitude expedition to Pikes Peak. *Experimental physiology* **97,** 1-9.

Whalen WJ & Nair P. (1976). PO2 in the carotid body perfused and/or superfused with cell-free media. *J Appl Physiol* **41,** 180-184.

Wieneke JA & Smith A. (2009). Paraganglioma: Carotid Body Tumor. *Head and Neck Pathology* **3,** 303.

Wiener CM, Booth G & Semenza GL. (1996). In vivo expression of mRNAs encoding hypoxia-inducible factor 1. *Biochemical and biophysical research communications* **225,** 485-488.

Wiesener MS, Jurgensen JS, Rosenberger C, Scholze CK, Horstrup JH, Warnecke C, Mandriota S, Bechmann I, Frei UA, Pugh CW, Ratcliffe PJ, Bachmann S, Maxwell PH & Eckardt KU. (2003). Widespread hypoxia-inducible expression of HIF-2alpha in distinct cell populations of different organs. *FASEB journal : official publication of the Federation of American Societies for Experimental Biology* **17,** 271-273.

Willam C, Maxwell PH, Nichols L, Lygate C, Tian YM, Bernhardt W, Wiesener M, Ratcliffe PJ, Eckardt KU & Pugh CW. (2006). HIF prolyl hydroxylases in the rat; organ distribution and changes in expression following hypoxia and coronary artery ligation. *Journal of molecular and cellular cardiology* **41,** 68-77.

Wyatt CN & Buckler KJ. (2004). The effect of mitochondrial inhibitors on membrane currents in isolated neonatal rat carotid body type I cells. *The Journal of physiology* **556,** 175-191.

Wyatt CN, Mustard KJ, Pearson SA, Dallas ML, Atkinson L, Kumar P, Peers C, Hardie DG & Evans AM. (2007). AMP-activated protein kinase mediates carotid body excitation by hypoxia. *The Journal of biological chemistry* **282,** 8092-8098.

Xie C, Gao X, Sun D, Zhang Y, Krausz KW, Qin X & Gonzalez FJ. (2018). Metabolic Profiling of the Novel Hypoxia-Inducible Factor 2α Inhibitor PT2385 In Vivo and In Vitro. *Drug metabolism and disposition: the biological fate of chemicals* **46,** 336-345.

Xu J, Tse FW & Tse A. (2003). ATP triggers intracellular Ca2+ release in type II cells of the rat carotid body. *The Journal of physiology* **549,** 739-747.

Yamashita T, Ninomiya M, Hernandez Acosta P, Garcia-Verdugo JM, Sunabori T, Sakaguchi M, Adachi K, Kojima T, Hirota Y, Kawase T, Araki N, Abe K, Okano H & Sawamoto K. (2006). Subventricular zone-derived neuroblasts migrate and differentiate into mature neurons in the post-stroke adult striatum. *The Journal of neuroscience : the official journal of the Society for Neuroscience* **26,** 6627-6636.

Yang C, Sun MG, Matro J, Huynh TT, Rahimpour S, Prchal JT, Lechan R, Lonser R, Pacak K & Zhuang Z. (2013). Novel HIF2A mutations disrupt oxygen sensing, leading to polycythemia, paragangliomas, and somatostatinomas. *Blood* **121,** 2563-2566.

Yang C, Zhuang Z, Fliedner SM, Shankavaram U, Sun MG, Bullova P, Zhu R, Elkahloun AG, Kourlas PJ, Merino M, Kebebew E & Pacak K. (2015). Germ-line PHD1 and PHD2 mutations detected in patients with pheochromocytoma/paraganglioma-polycythemia. *Journal of molecular medicine* **93,** 93-104.

Yao X, Rosen MK & Gardner KH. (2008). Estimation of the available free energy in a LOV2-J alpha photoswitch. *Nat Chem Biol* **4,** 491-497.

Yi X, Liang Y, Huerta-Sanchez E, Jin X, Cuo ZX, Pool JE, Xu X, Jiang H, Vinckenbosch N, Korneliussen TS, Zheng H, Liu T, He W, Li K, Luo R, Nie X, Wu H, Zhao M, Cao H, Zou J, Shan Y, Li S, Yang Q, Asan, Ni P, Tian G, Xu J, Liu X, Jiang T, Wu R, Zhou G, Tang M, Qin J, Wang T, Feng S, Li G, Huasang, Luosang J, Wang W, Chen F, Wang Y, Zheng X, Li Z, Bianba Z, Yang G, Wang X, Tang S, Gao G, Chen Y, Luo Z, Gusang L, Cao Z, Zhang Q, Ouyang W, Ren X, Liang H, Zheng H, Huang Y, Li J, Bolund L, Kristiansen K, Li Y, Zhang Y, Zhang X, Li R, Li S, Yang H, Nielsen R, Wang J & Wang J. (2010). Sequencing of 50 human exomes reveals adaptation to high altitude. *Science (New York, NY)* **329,** 75-78.

Yoo S, Takikawa S, Geraghty P, Argmann C, Campbell J, Lin L, Huang T, Tu Z, Foronjy RF, Spira A, Schadt EE, Powell CA & Zhu J. (2015). Integrative analysis of DNA methylation and gene expression data identifies EPAS1 as a key regulator of COPD. *PLoS genetics* **11,** e1004898.

Yu AY, Shimoda LA, Iyer NV, Huso DL, Sun X, McWilliams R, Beaty T, Sham JSK, Wiener CM, Sylvester JT & Semenza GL. (1999). Impaired physiological responses to chronic hypoxia in mice partially deficient for hypoxia-inducible factor 1α. *The Journal of clinical investigation* **103,** 691-696.

Zhang M, Zhong H, Vollmer C & Nurse CA. (2000). Co-release of ATP and ACh mediates hypoxic signalling at rat carotid body chemoreceptors. *The Journal of physiology* **525,** 143-158.

Zhang XQ, Pang L & Eyzaguirre C. (1995). Effects of hypoxia on the intracellular K+ of clustered and isolated glomus cells of mice and rats. *Brain research* **676,** 413-420.

Zhao C, Deng W & Gage FH. (2008). Mechanisms and functional implications of adult neurogenesis. *Cell* **132,** 645-660.

Zhou T, Chien MS, Kaleem S & Matsunami H. (2016). Single cell transcriptome analysis of mouse carotid body glomus cells. *The Journal of physiology* **594,** 4225-4251.

Zhu LL, Zhao T, Li HS, Zhao H, Wu LY, Ding AS, Fan WH & Fan M. (2005). Neurogenesis in the adult rat brain after intermittent hypoxia. *Brain research* **1055,** 1-6.

Zhuang Z, Yang C, Lorenzo F, Merino M, Fojo T, Kebebew E, Popovic V, Stratakis CA, Prchal JT & Pacak K. (2012). Somatic HIF2A Gain-of-Function Mutations in Paraganglioma with Polycythemia. *New England Journal of Medicine* **367,** 922-930.

Zimmer M, Doucette D, Siddiqui N & Iliopoulos O. (2004). Inhibition of hypoxia-inducible factor is sufficient for growth suppression of VHL-/- tumors. *Molecular cancer research : MCR* **2,** 89-95.

Zurkirchen L & Sommer L. (2017). Quo vadis: tracing the fate of neural crest cells. *Current opinion in neurobiology* **47,** 16-23.